SÍLVIA DANIELA SARMENTO PIRES

The impact of the oxidative stress response on tacrolimus production by *S.tsukubaensis* NRRL 18488

Tese de Candidatura ao grau de Doutor em Ciências Biomédicas submetida ao Instituto de Ciências Biomédicas Abel Salazar da Universidade do Porto.

Orientadora: Doutora Marta Vaz Mendes
Categoria: Investigadora Auxiliar
Afiliação: IBMC - Instituto de Biologia Molecular e Celular

Co-orientador: Doutor Professor Pedro Moradas-Ferreira
Categoria: Professor Catedrático
Afiliação: ICBAS - Instituto de Ciências Biomédicas Abel Salazar da Universidade do Porto e IBMC - Instituto de Biologia Molecular e Celular

PRECEITOS LEGAIS

De acordo com o disposto no n.º1 do artigo 34.º do Decreto-Lei n.º 74/2006, publicado em Diário da República, 1.ª série, n.º 60 de 24 de Março de 2006, e republicado pelo Decreto-Lei n.º 115/2013, publicado em Diário da República, 1.ª série, n.º 151 de 7 de Agosto de 2013, que procede à terceira alteração ao Decreto-Lei n.º 74/2006, de 24 de Março de 2006, nesta tese foram utilizados os resultados de trabalhos publicados abaixo indicados.

No cumprimento do disposto referido Decreto-Lei, a autora desta tese declara que interveio na concepção e execução do trabalho experimental, na interpretação e redacção dos resultados publicados sob o nome Pires, S. D.

Beites T*, **Pires SD***, Santos CL, Osório H, Moradas-Ferreira P, Mendes MV (2011). " Crosstalk between ROS homeostasis and secondary metabolism in S. natalensis ATCC 27448: modulation of pimaricin production by intracellular ROS." *PLoS One. 2011;**6**(11): e27472*. * These authors contributed equally to this work.

O trabalho apresentado nesta tese foi realizado no IBMC - Instituto de Biologia Molecular e Celular da Universidade do Porto e foi financiado por Fundos FEDER através do Programa Operacional Factores de Competitividade – COMPETE e por Fundos Nacionais através da FCT – Fundação para a Ciência e a Tecnologia no âmbito dos projectos (PTDC/BIO/64682/2006) e ERA-IB/0001/2010 (EIB.10.005) e da da bolsa SFRH/BD/66367/2009.

The most exciting phrase to hear in science, the one that heralds the most discoveries, is not "Eureka!" (I found it!) but "That's funny..."

Isaac Asimov

ACKNOWLEDGMENTS

Apesar de estas serem as últimas palavras que escrevo para a tese, são talvez das mais importantes. Este percurso de quatro anos foi constituído por várias etapas e momentos que de uma forma ou de outra foram partilhados e ajudados a ultrapassar com a contribuição de muitas pessoas que não posso deixar de mencionar e agradecer.

Tenho que começar por agradecer à minha orientadora Marta Vaz Mendes. A tese não é minha, é nossa! Foi um trabalho conjunto, a vários níveis, e apesar de às vezes andarmos “às turras” (in a good way) foi muito enriquecedor tanto a nível profissional como pessoal. Todos os dias aprendo sempre alguma coisa nova contigo e a meu ver isso já diz muito sobre o tipo de pessoa que és. Para além de uma cientista incrível que me ensinou (para além de tudo o resto) a importância de perceber o porquê das coisas, também és um exemplo de força e de perseverança. Tenho mesmo muito orgulho em ti! Tenho muito para te agradecer mas acho que não consigo encontrar palavras que consigam reflectir o quão importante foste (és!) para mim. Ter a certeza de que independentemente do que acontecesse estarias sempre lá para mim, não tem preço! Por isto, pela tua incomensurável dedicação e paciência, por tudo o resto mas principalmente pela tua amizade, Obrigada, vais ser sempre a minha chefinha do coração!

Agradeço também ao Professor Doutor Pedro Moradas-Ferreira, não só por me ter aceite no grupo de Cellular and Applied Microbiology (CAM) mas também pela sua co-orientação nesta tese.

Ao longo dos anos foram várias as pessoas que passaram pelos grupos CAM, RCS e BSM e que de várias maneiras contribuíram para um ambiente incrível! A todos um muito Obrigada! No entanto tenho que fazer agradecimentos especiais a algumas pessoas que foram também igualmente especiais: à Catarina Santos, por seres como uma irmã para mim e me apoiares e ajudares em tudo desde o meu primeiro dia no laboratório! Obrigada pela amizade! Ah e fazes-me falta todos os dias!!! À Pachequinho por ser mega fofa, amiguinha e me dar mega bons conselhos e também por toda a companhia em jantares tardios no Duvália. Ao Dani por toda amizade e companhia, bem como pelos momentos “astrológicos” e musicais! À Drª Amélia por ser um exemplo e por toda a ajuda! À

Rita M, Sara P, Ângela, Professora Paula, Pedro A., Daniela, Meri, Filipe, Zsofia e Zille por todos os momentos bem passados! Ao Paulinho, uma grande aquisição do grupo BSM! Obrigada por toda amizade, ajuda, preocupação, interesse e disponibilidade que continuas a demonstrar todos os dias! Ao pessoal lá de cima passado e presente, principalmente à Sarinha que foi de facto a contratação do ano! Obrigada por todas as gargalhadas e pela amizade que se criou e ficou! Ao Elíso, MJ, Margarida, Nuno, Tony, Professor Vítor, Tânia, Vítor, Vanda, Kalina, Andreia e D. Helena por todos os bons momentos passados no laboratório! À Clara, também uma grande contratação, não fosses tu de Guimarães! Ao Rui pela amizade e companhia aos almoços de sábado no lab! Às minhas amiguinhas do INEB, principalmente à Dani, Caty, Estrelinha, Pipa, Ana Luísa, Aninhas e Bianca por todas as barrigadas de riso e bons momentos que passamos, no qual me tornei membro honorário do INEB, mas principalmente por todo o apoio que me deram nesta recta final! À Catarina Carona pela amizade e partilhas de experiências assim como todas as gargalhadas que me proporcionas. Ao Fred por toda a ajuda e boa disposição! A todos as pessoas dos vários serviços do IBMC que de uma forma ou outra também ajudaram, em especial à Liliana, Paulinha, Antonieta, Senhor Carlos e D. Júlia por me fazerem sentir em casa.

Aos meus amigos membros “daquele grupo secreto que toda a gente falou mas ninguém criou”! A maioria destas amizades nasceram no contexto do laboratório e são para a vida! À Ana, Aidinha, João e Xandinho (“tu és demais!”) por todos os bons momentos que tivemos. Ao Bruno por seres topinho e um exemplo de homem! Ao Lulu Melo por toda a amizade que apesar da distância se manteve forte e muito importante! Aos binos do meu coração: Alfredo (aka Tiggy) e Lodde! As dores de barriga de tanto me rir com vocês no lab e fora dele são intermináveis! Mas acima de tudo obrigada pela amizade! À minha Xuz do coração (aka Bilaça). Estás sempre lá para me apoiar e mostrar realidade seja ela qual for. Fazes-me rir e aceitas-me como sou, pancas incluídas ☺! À minha fofi Joana, foi uma amizade fulminante mas que veio para durar, até porque há coisas que simplesmente não se explicam! Tens um lugar muito especial no meu coração. Obrigada por tudo!

À Soninha, Rute e Marta, já lá vão 10 anos desde a faculdade e apesar de tudo continuamos juntas! Soninha, obrigada pelo teu carinho e preocupação

comigo! À Rute Pati, no nosso caso já lá vão 17 anos de amizade em que nos aturamos uma à outra sempre às turras, mas sempre com carinho e muita cumplicidade! A ti tenho que fazer um agradecimento especial por toda a ajuda que me deste no lab (e fora dele) no último ano, e principalmente nesta recta final! Foste mesmo essencial, se não fosse isso tinha sido o pânico total! Obrigada! À minha Marta Adelina, apesar de estares longe quando estamos juntas é como se nunca tivesses ido. Obrigada por tudo e por me tentares mostrar sempre o lado positivo das coisas!

Aos meus amigos de Guimarães e companheiros na sua maioria já há mais de 20 anos (sinto-me velha a dizer isto!). Um agradecimento especial: ao Peita, Andreia, Litos, Nelo, Gaspar, Maria, Mi e Zeka pelo apoio e amizade em todos os momentos. Pelas férias, “escapadinhas” e jantares de sábado que foram muitas vezes um escape para o “stress” do lab! Mas acima de tudo por terem uma fé inabalável em mim!

Às minhas poms, Nitinha e Pom. É um orgulho quando nos dizem que não conhecem amizade como a nossa. Realmente uma ligação assim é rara e para a vida toda! Vocês são um pedaço de mim e sei que mesmo quando formos velhinhas vamos continuar a ser defs e BFFs como sempre (“Posição de bule”)! *“A true friend is one soul in two bodies." –Aristotle*, no nosso caso são 3!

À minha família, principalmente aos meus pais e ao bolinhas pelo amor incondicional. Nestas alturas por mais rico que seja um vocabulário, não se encontram palavras que consigam transmitir tudo o que vocês são para mim, mas tenho imenso orgulho em ser vossa filha! Vocês são um exemplo e um pilar na minha vida! Ao meu Pai agradeço principalmente por me incutires um sentido de justiça e rectidão e por todo o orgulho que tens em mim. À minha Mãe, por ser o ser humano mais bonito e bondoso que conheço. Obrigada por sempre me ensinares a procurar o melhor das pessoas e acima de tudo por me ensinares que o mais importante na vida é o ser e não o ter.

ABSTRACT

Tacrolimus (FK506) is a macrolide of high market value, widely used to prevent graft rejection in organ transplanted patients. It is produced by several *Streptomyces* strains, which are in fact considered to be small-factories of valuable bioactive compounds. The biosynthesis of tacrolimus in *Streptomyces* submerged cultures is controlled by networks regulated by different factors such as dissolved oxygen (DO). Exposure of microorganisms to high levels of DO increases the formation of reactive oxygen species (ROS) that can damage cellular components. To counteract these effects, microorganisms have developed response mechanisms that operate at different levels, from modulation of gene expression to changes in enzymatic activities in order to sense, detoxify and repair the damage caused by ROS.

We showed a crosstalk between intracellular ROS homeostasis and pimaricin production in *Streptomyces natalensis* ATCC 27448. We were also able to show that in *S. tsukubaensis,* a tacrolimus producer, deletion or over-expression of key genes in the enzymatic anti-oxidant defence system resulted in a modulation of tacrolimus biosynthesis. Furthermore, catalase activity presented a growth dependent profile that differed according to growth medium, i.e, tacrolimus producing or non-producing conditions. Additionally, a perfect overlap between the onset of tacrolimus biosynthesis with catalase induction and the concomitant decrease of H_2O_2 intracellular levels was observed. In fact, we have demonstrated that catalase activity and consequently H_2O_2 intracellular levels play a key role in the production of tacrolimus, which displays antioxidant properties and therefore requires a reduced environment for its biosynthesis.

Putting together our results obtained with *S. natalensis* and *S. tsukubaensis*, we provided further evidence for the role of ROS and the oxidative stress response in the regulation of secondary metabolism in *Streptomyces*.

In silico analysis showed that *S. tsukubaensis* presents a different synteny of the *oxyR-ahpCD* genomic region. In *Streptomyces* the genomic organization of *oxyR-ahpCD* region is much conserved, in which *oxyR,* that codes for a H_2O_2-sensor response regulator, is divergently transcribed form the *ahpCD* genes which code for a H_2O_2 enzymatic detoxification system. In *S. tsukubaensis* OxyR

encoding gene is located 3.9 kb upstream from the *ahpCD* operon. Furthermore three novel genes for this genomic region are present, including *STSU_11560*, which codes for a novel extracytoplasmic function (ECF) sigma factor, SigG that is divergently transcribed from *oxyR*. Transcription analysis of *S. tsukubaensis* wild-type, Δ*sigG*, Δ*oxyR* and Δ*ahpC* strains showed a cross-regulation between OxyR and SigG. Characterization of the OxyR regulon by transcriptional analysis and electrophoretic mobility shift assays demonstrated that OxyR directly regulates its own transcription and *ahpC* in an H_2O_2 dependent manner but also *sigG*, repressing its transcription in oxidative stress conditions The Δ*sigG* strain presented increased sensitivity to H_2O_2 however SigG is not involved in the immediate response to induced oxidative stress by H_2O_2. Further characterization of the Δ*sigG* strain, revealed an hampered ferrous iron uptake with siderophores being produced in iron sufficient conditions.

We were able to establish that *sigG*, coding for a novel ECF sigma factor, regulates the uptake of ferrous iron in *S. tsukubaensis* and that there is a regulatory interplay between ferrous iron uptake and oxidative stress response regulation mediated by SigG and OxyR, respectively.

RESUMO

Tacrolimus (FK506) é um macrólido de grande valor comercial, amplamente utilizado para prevenir a rejeição de órgãos em doentes transplantados. É produzido por várias espécies de *Streptomyces,* bactérias consideradas como pequenas fábricas produtoras de compostos bioactivos. Em *Streptomyces,* a biossíntese de tacrolimus em culturas submersas é controlada por diversos factores, tais como o oxigénio dissolvido (OD). A exposição dos microrganismos a níveis elevados de OD leva a um aumento da formação de espécies reactivas de oxigénio (ERO) capazes de danificar biomoléculas. De maneira a neutralizar esses efeitos, os microorganismos desenvolveram mecanismos de defesa que actuam a diferentes níveis, desde a modulação e regulação a nível transcricional, a alterações em respostas enzimáticas, de modo a detectar, detoxificar e reparar os danos causados pelas ERO.

Foi demostrado um cross-talk entre a homeostasia intracelular de ERO e a produção de pimaricina em *Streptomyces natalensis* ATCC 27448. Também demonstramos que, em *S. tsukubaensis,* um produtor de tacrolimus*,* a deleção e/ou sobre-expressão de genes chave do sistema enzimático de resposta ao stress oxidativo, também levou à modulação da biossíntese de tacrolimus. Além disso, também demonstramos que o perfil de actividade da catalase varia consoante o meio de cultura, ou seja, em condições produtoras ou não produtoras de tacrolimus. Adicionalmente, também se verificou uma perfeita sobreposição temporal entre o início da biossíntese de tacrolimus com uma indução da actividade da catalase e respectiva diminuição dos níveis intracelulares de H_2O_2. De facto, tanto a actividade da catalase como os níveis intracelulares de H_2O_2, desempenham um papel-chave na produção de tacrolimus, que apresenta a capacidade de poder funcionar como um antioxidante, requerendo por isso um ambiente redutor para a sua biossíntese.

Juntando os resultados obtidos em *S. natalensis* e em *S. tsukubaensis,* conseguimos com este trabalho fornecer mais evidências sobre o papel da resposta ao stress oxidativo e das ERO na regulação do metabolismo secundário em *Streptomyces*.

Uma análise *in silico* mostrou que *S. tsukubaensis* apresenta uma organização genómica diferente na região génica *oxyR-ahpCD*. Em *Streptomyces* a organização genómica da região *oxyR-ahpCD* é bastante conservada, com o *oxyR*, que codifica para um regulador sensível ao H_2O_2, sendo transcrito divergentemente dos genes *ahpCD*, que codificam para um sistema enzimático que detoxifica o H_2O_2. Em *S. tsukubaensis* o gene que codifica para o OxyR encontra-se 3.9 kb a montante do operão *ahpCD*. Adicionalmente três novos genes surgem também nesta região, incluindo *STSU_11560* que codifica para um novo factor sigma extracitoplasmático, SigG, que é transcrito divergentemente do *oxyR*.

A análise transcricional às estirpes selvagem, Δ*sigG*, Δ*oxyR* e Δ*ahpC* mostrou a existência de uma regulação cruzada entre o OxyR e o factor sigma SigG em *S. tsukubaensis.* Através da caracterização do regulão do OxyR, foi demonstrado que o OxyR regula directamente a sua própria transcrição e a transcrição da *ahpC*, bem como a transcrição do *sigG*, reprimindo-a em condições de stress oxidativo. A estirpe Δ*sigG* apresenta uma maior sensibilidade ao H_2O_2, no entanto não responde transcricionalmente ao stress oxidativo induzido pelo H_2O_2. A caracterização da estirpe Δ*sigG*, revelou ainda um problema no metabolismo do ferro, nomeadamente na captação de ferro ferroso, com produção de sideróforos em condições suficientes de ferro.

Fomos capazes de demonstrar que o novo factor sigma, SigG, regula a captação de ferro ferroso em *S. tsukubaensis*. Para além disso demonstramos também a existência de uma regulação cruzada entre a captação de ferro ferroso e a resposta ao stress oxidativo em *S. tsukubaensis*, que é mediada pelo SigG e OxyR respectivamente.

TABLE OF CONTENTS

LIST OF FIGURES

LIST OF TABLES

ABBREVIATIONS

2-DE - Two-Dimensional Electrophoresis

3' UTR - Three prime untranslated region

5' UTR - Three prime untranslated region

A – Absorbance

ACP – acyl carrier protein

AT – aminotransferase

ATP - Adenosine-5'-triphosphate

bp - Base pairs

BSA - Bovine serum albumin

CAS – Chrome azurol S

CHAPS - 3-[(3-cholamidopropyl)dimethylammonio]-1-propanesulfonate

CCR – Carbon catabolite repression

DAB – Diaminobenzidine

ddH_2O - double deionized water

DH - dehydratase

DHE - Dihydroethidium

DHR - Dihydrorhodamine 123

DIG – digoxygenin

DNA – Deoxyribonucleic acid

DTT – Dithiothreitol

EDTA – Ethylenediamine tetracetic acid

EMSA – Electrophoretic mobility shift assay

ER – enoylreductase

G6PDH – glucose 6-phosphate dehydrogenase

GAPDH – glyceraldeheyde 3-phosphate dehydrogenase

h – hour

H_2O_2 – Hydrogen peroxide

HTH – helix-turn-helix

IEF - Isoelectric focusing

IPTG – Isopropyl β-D-1-thiogalactopyranoside

KR - ketoreductase

KS - β-ketoacyl-ACP-synthase

LAL – Large ATP-binding regulators of the LuxR family

LB – Luria-Bertani

LMW – low molecular weight

LTTR – LysR-type transcriptional regulators

min – minutes

MS – mass Spectrometry

NRPS – non ribosomal peptide synthetase

nt -nucleotide

O_2 – Molecular oxygen

$O^{2\cdot-}$ – Superoxide anion

$OH^{\cdot}$ – Hydroxyl radical

OD – optical density

PAGE – polyacrylamide gel electrophoresis

PCR – polymerase chain reaction

pI – isoelectric point

Pi – inorganic phosphate

PKS - polyketide synthase

PMFS – phenylmethylsulfonyl fluoride

PPP – pentose phosphate pathway´

RNA - ribonucleic acid

ROS – Reactive oxygen species

rpm – rotations per minute

RT-PCR – Reverse transcriptase-polymerase chain reaction

RT-qPCR – Reverse transcriptase-quantitative polymerase chain reaction

RTT – Relative retention time

SARP – *Streptomyces* antibiotic regulator proteins

SDS – sodium dodecylsulphate

SOD – Superoxide Dismutase

TCA – tricarboxylic acid

Tir – terminal inverted repeats

v/v – volume per volume

vol – volumes

w/v – weight per volume

CHAPTER 1

Introduction

1.1 *STREPTOMYCES* GENUS

1.1.1 *Streptomyces* biology and general characteristics

Members of *Streptomyces* genus are among the most interesting and complex bacteria. Phylogenetically, they belong to the Actinobacteria phylum that includes a vast number of important bacteria, like the human pathogen *Mycobacterium tuberculosis* or the industrially important *Corynebacterium glutamicum*. *Streptomyces* are Gram-positive, filamentous bacteria and obligated aerobes that undergo a complex and unique life cycle including morphological and physiological differentiation. *Streptomyces* inhabit soil, an environment that presents a multitude of challenges to the microbial community. Streptomycetes are important members of this community and due to the many stresses and demanding conditions encountered, they had to adapt and develop responses that enables them to survive and prosper in the soil. In fact their genomic and biologic characteristics are a reflection of such adaptation. Also, *Streptomyces* ability to secrete hydrolytic enzymes, allowing the utilisation of nutrients locked in insoluble polymers, plays an important role in the decomposition of organic matter and is a good reflection of their importance in soil ecosystems (Chater and Chandra 2006, Ventura *et al.* 2007).

Even though *Streptomyces* bacteria are ubiquitous in the soil, they can also be found in marine environments (Pimentel-Elardo *et al.* 2010, Luo *et al.* 2011) and, although rare, as plant pathogens like *Streptomyces scabies* (Lerat *et al.* 2009) or human pathogens like *Streptomyces somaliensis* (Kirby *et al.* 2012). *Streptomyces* genus is also noted for their distinct earthy odor that results from the production of the volatile metabolite geosmin, by several *Streptomyces* species (Gerber 1979). But these bacteria main attributes reside on their developmental complexity and secondary metabolism. They produce a wide range of secondary metabolites, including antibiotics, anti-cancer compounds and immunosuppressors, among others. In fact, about two thirds of antibiotics in clinical use are produced by members of the genus *Streptomyces* (Demain 1999, Hopwood 2007).

Genetic knowledge of the *Streptomyces* genus had a remarkable breakthrough with the complete genome sequencing of *Streptomyces coelicolor*

A3(2) (Bentley *et al.* 2002). In the last few years, the number of *Streptomyces* genomes fully sequenced increased at a very fast pace. The increased number of *Streptomyces* genomes available pointed out that, on average, *Streptomyces* genome harbours more than twenty biosynthetic gene clusters with potential to produce new secondary metabolites, also known as specialized metabolites, making of them a natural factory of bioactive compounds.

The *Streptomyces* genus is characterized for having one of the highest GC content in DNA found in bacteria, with approximately 70-74% (Ventura *et al.* 2007). Another peculiar feature presented by the members of *Streptomyces* genus is the linearity of its chromosome, that was first described in 1993 for *S. lividans* 66 (Lin *et al.* 1993). They also present one of the largest genomes that can be found among bacteria, with a size that ranges from 7 to 12 Mb [10]. *Streptomyces* linear chromosome presents terminal inverted repeat (TIR) regions on the chromosome ends and a terminal protein (TP) bound to their free 5'-ends. Chromosome replication is bidirectional from the internal region *oriC*. This topology is common to *Streptomyces* species (Lin *et al.* 1993, Lezhava *et al.* 1995, Leblond *et al.* 1996, Pandza *et al.* 1997). Furthermore in the vicinity regions of the chromosomal extremities it can also be found a high number of direct repeats, insertions and transposable elements (Kieser *et al.* 2000). All together, these genetic characteristics are thought to be the cause of the high genetic instability displayed by many *Streptomyces* strains. This genomic instability can be reflected in phenotypical changes, alterations in development, primary and secondary metabolism. Given the continuous challenges presented by their main habitat, the soil, this genomic instability could be responsible for providing to *Streptomyces* the ability to adapt (Volff and Altenbuchner 1998). It is also frequent to encounter extra chromosomal elements in *Streptomyces*, in particular plasmids (Toyama *et al.* 1982). Plasmids can be either linear, with associated proteins in the ends (Kinashi and Shimaji 1987), or circular like pSNA1, a 9367-bp plasmid present in *Streptomyces natalensis* ATCC 27448 (Mendes *et al.* 2000).

1.1.2 *Streptomyces* life cycle

For a period of time, it was believed that streptomycetes were intermediate microorganisms between bacteria and fungi. Although they are in fact classified as bacteria, they present characteristics that resemble fungi, particularly concerning its life cycle. *Streptomyces* complex life cycle includes differentiation processes and programmed cell death phenomena (PCD). The life cycle of *Streptomyces* (Fig.1.1) begins with the germination of a spore when the environment conditions are favourable. At this point protein biosynthesis occurs (Mikulik *et al.* 1984) and when the germ tube emerges DNA biosynthesis begins (Hardisson *et al.* 1978). The germ tube originates branching hyphae that grow by tip extension into the substrate to form a dense filamentous network, designated by first vegetative mycelium (MI). MI is characterized by highly septated hyphae and an active primary metabolism. When the appropriate signals occur, namely nutrient starvation, part of the MI mycelium undergoes PCD. Afterwards viable MI compartments give rise to a multinucleated secondary vegetative mycelium (MII). This process is accompanied by the onset of secondary metabolism and the activation of the developmental program through the transcription of proteins involved in the formation aerial mycelium. During morphological differentiation the superficial layer of MII differentiates into aerial mycelium while the inner part of MII mycelium undergoes a second round of PCD. When aerial growth ceases, the aerial hyphae undergo massive septation giving rise to unigenomic spores (Chater 1993, Flardh and Buttner 2009).

Although *Streptomyces* spores are less resistant, when compared to endospores produced by *Bacillus* species, they can still survive in dry conditions for long periods. In the past few years the classical model for *Streptomyces* development/differentiation has been refined with additional features being added, including two rounds of programmed cell death. In this recent developmental model differentiation is described both in solid and liquid media with the absence of MII hydrophobic layers in liquid medium. In liquid cultures MI corresponds to the *Streptomyces* vegetative mycelium and MII to the *Streptomyces* differentiated mycelium producing secondary metabolites (Manteca *et al.* 2007, Manteca *et al.* 2008, Yague *et al.* 2012).

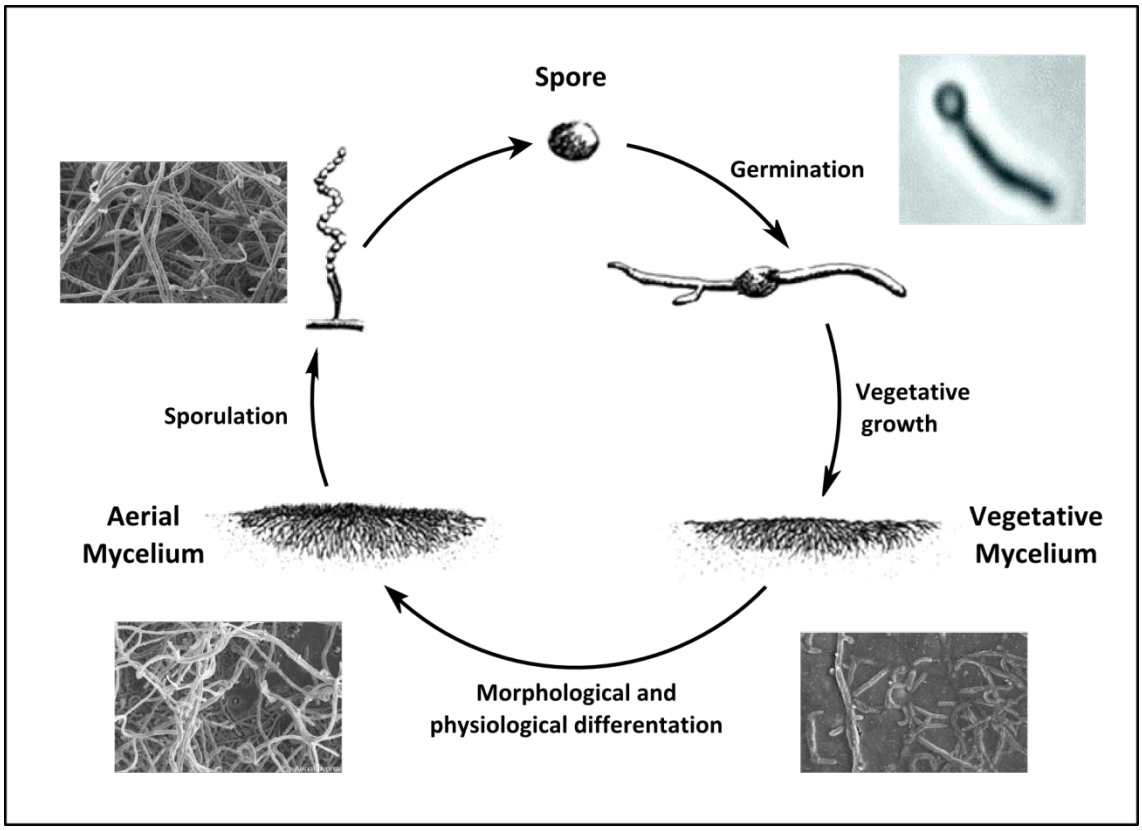

Figure 1.1 - Life cycle of *Streptomyces* sp.. Figure adapted from Mendes, MV *et al.* (Aparicio *et al.* 2002). Microscopy images from Claessen *et al.* (Claessen *et al.* 2006) and Piette *et al*. (Piette *et al.* 2005).

1.1.3 *Streptomyces* primary metabolism: C, N and P at the interface between primary and secondary metabolism

Control and regulation of *Streptomyces* primary metabolism plays an essential role on secondary metabolism since primary metabolism is the main supply of precursors and cofactors for secondary metabolite production. The ability of secondary metabolic pathways to drain precursors from primary metabolism involves not only a coordinated regulation between these two systems but also precursors' intracellular concentration. The supply of cofactors also needs to be taken into account in secondary metabolites production, given that for some metabolites biosynthesis, like the case of polyketides, a considerable large amount of reducing power from NADPH is required. In the central carbon metabolism NAPDH is mainly generated in the oxidative branch of the pentose phosphate pathway (PPP) via NADP+ regeneration, but it can also be regenerated by the isocitrate dehydrogenase from the tricarboxylic acid cycle (TCA).

Carbon is probably one of the most important medium component since in most cases is also used as energy source. Even though *Streptomyces* can grow on different carbon sources, in the presence of a readily usable carbon source, like glucose, a repression of other carbon utilisation pathways occurs in a phenomenon known as carbon catabolite repression (CCR) (Paulsen 1996). The availability of the carbon source affects antibiotic production (Ruiz *et al.* 2010), with glucose blocking the production of several secondary metabolites, like the case of actinorhodin production in *S. coelicolor* and *S. avermitilis* (Kim *et al.* 2001).

Glycolysis is one of the main metabolic pathways that allow an efficient utilisation of carbon that besides generating two pyruvate molecules also originates two ATP and two NADH molecules. From this pathway it is important to highlight two enzymes: the phosphofructokinase (Pfk) and glyceraldehyde-3-phosphate dehydrogenase (GAPDH). In the case of the first, it was reported in *S. coelicolor* that the deletion of *pfkA2* (in *S. coelicolor* three *pfkA* encoding genes are present) led to an actinorhodin and undecylprodigiosin overproducing strain (Borodina *et al.* 2008). In the case of GAPDH, it is known to be susceptible to oxidative stress (Dastoor and Dreyer 2001, Ralser *et al.* 2007). Either by phosphofructokinase deletion or GAPDH inactivation by oxidative stress, the consequence could be a redirection of the carbon flux to PPP increasing the NADPH intracellular and providing this way reducing power to enzymes not only involved in oxidative stress response (Godon *et al.* 1998, Pollak *et al.* 2007) but also in secondary metabolites production. This redirection of the flux to PPP is directly linked with PPP enzyme glucose-6-phosphate dehydrogenase (G6PDH). In fact studies already demonstrated the influence of this enzyme on *Streptomyces* secondary metabolism like the case of *S. tsukubaensis* where an overexpression of the G6PDH encoding gene (*zwf2*) led to an increase of 35% in tacrolimus production (Huang *et al.* 2013). Also in *S. natalensis* Δ*ahpC*D, a strain defective on the alkyl hydroperoxide system responsible for hydrogen peroxide detoxification, and also a pimaricin overproducing strain, it was shown a re-direction of carbon flux through PPP with increase in both transcription and activity of G6PDH (Beites *et al.* 2014).

Together with the carbon source, nitrogen is also an essential nutrient that can also influence secondary metabolism outcome. Both positive and negative

effects have been reported such as the increase of 150% in rapamycin production in *S. hygroscopicus* with the addition of lysine to the culture medium (Cheng *et al.* 1995). On the other hand a decrease in secondary metabolites production was also demonstrated when in the presence of nitrogen sources that were more favourable for growth (Aharonowitz 1980, Sanchez and Demain 2008). The assimilation and utilisation of nitrogen is under the control of the global transcriptional regulator GlnR (Wray and Fisher 1993). GlnR regulates in a nitrogen-dependent manner several targets such as the glutamine-synthetase I (GSI) and glutamine-synthetase II (GSI) enconding genes, *glnA* and *glnII* respectively, the ammonium transporter encoding gene, *amtB,* PII family protein encoding gene *glnK* and the uridylyltransferase encoding gene *glnD* (Hesketh *et al.* 2002, Reuther and Wohlleben 2007). However, another regulator appears in this metabolic picture, *glnrII*, which can also regulate several nitrogen metabolism genes at the transcriptional level. It is interesting to see that in *S. coelicolor* nitrogen metabolism is regulated by mechanisms that involve a doubling of some structural and regulatory genes (Reuther and Wohlleben 2007). Besides regulating nitrogen related genes, GlnR can also bind to the promoter regions of several secondary metabolites pathway specific regulators such as *actII*-ORF4, *redZ* and *cdaR* (Wang *et al.* 2013). Also deletion of g*lnK*, resulted in loss of antibiotic production in a medium-dependent manner (Waldvogel *et al.* 2011). Interestingly, a phosphate control over nitrogen metabolism has recently been described, with PhoP (the phosphate metabolism major regulator) directly repressing *glnR* transcription in phosphate limiting conditions (Rodriguez-Garcia *et al.* 2009).

Phosphate is an essential component that plays an important role in cell metabolism as a component of many molecules, including DNA, RNA and ATP and also in post-translational regulation of proteins by phosphorylation /dephosphorylation processes. The preferred source of phosphorus in *Streptomyces*, as in the majority of bacteria, is inorganic phosphate (Pi), which can enter the cell mainly by two different transport systems: Pst, an ABC transporter that has an ATP-driven high-affinity Pi uptake and the Pit system, a low-affinity phosphate inorganic transporter, which transport Pi coupled with divalent metals (Santos-Beneit *et al.* 2008). Pi uptake is tightly regulated by a two-component system (TCS): the PhoRP, which controls the response to Pi scarcity in *Streptomyces*. In *Streptomyces* Pi is one of the most important nutritional factors,

affecting both primary and secondary metabolism (Martin 2004, Allenby *et al.* 2012). Pi control over secondary metabolism is present in the production of many *Streptomyces* secondary metabolites and is accompanied by changes at the transcriptional level of genes involved in the metabolite biosynthetic pathway (Santos-Beneit *et al.* 2009). Phosphate control in secondary metabolism mediated by the TCS PhoRP was first described in actinorhodin and undecylprodigiosin production in *S. lividans* (Sola-Landa *et al.* 2003). In the majority of the situations the excess of Pi exerts a negative effect in secondary metabolism, with a low concentration of phosphate being required for secondary metabolism onset. Such effects have already been demonstrated in several *Streptomyces* species, including pimaricin production in *S. natalensis* that in the presence of high Pi concentrations is fully repressed (Mendes *et al.* 2007).

1.2 *STREPTOMYCES* SECONDARY METABOLISM

A major feature of *Streptomyces* is their ability to produce a variety of secondary metabolites that are chemically and structurally diverse presenting a wide range of applicability, including antibiotics, anticancer, immunosuppressors and antifungals just to name a few. Their biosynthesis occurs in a growth-phase dependent manner and is intrinsically connected with morphological differentiation (Bibb 2005). The production of these compounds is regulated in response to an altered nutritional status and to a variety of environmental conditions and signals. Secondary metabolites production was probably established during evolution as a way to respond to all the competitive pressures present in *Streptomyces* habitat. In fact the incredible high number of biosynthetic gene clusters with the capacity to produce secondary metabolites found in *Streptomyces* genomes, points out to their role in acquiring advantages in such a harsh natural environment. The designation of secondary lays on the fact that their absence does not result in immediate death, unlike what would happen for primary metabolism. However there is a thin line between these two metabolic systems that makes it hard to dissociate them, given that secondary metabolites derive from primary metabolites (Rokem *et al.* 2007). This is the reason why their regulation is so tightly related with growth and development. *Streptomyces* constitute a paradigm of secondary metabolites producing microorganisms, with a

plethora of diversified factors described to participate on their onset and regulation that constitute a complex network with many different levels of regulation, which can go from a high pleiotropic level to a pathway-specific one. In the next section it will be described the regulators more important/relevant for this work.

1.2.1 The players in the regulation network: from pathway specific to pleiotropic regulators

1.2.1.1 Cluster situated regulators

Usually, genes involved in the synthesis of secondary metabolites are grouped in biosynthetic gene clusters that can vary in size going form a few kb to 100 kb (Ohnishi *et al.* 2008). The common pattern found in these biosynthetic gene clusters consists in the presence of genes encoding proteins responsible for the biosynthesis of the compound structural backbone, proteins responsible for the tailoring of the structural backbone, i.e, that add modifications to the chemical structure, proteins involved in the export of the molecule, proteins that confer resistance and also proteins that directly regulate and control the transcription of the gene cluster (Kelemen *et al.* 1998, Aparicio *et al.* 1999, Aparicio *et al.* 2000). These cluster situated regulators (CSRs) function like a bridge between the biosynthetic gene cluster and pleiotropic regulators that monitor the organism's physiology. The signals received by CSRs will have an impact on both the onset of the metabolite production as well as in the obtained yields. Although CSRs action has been described as limited to the genes from the clusters were they are located, recent data suggest that they can also regulate the expression of distant genes (Huang *et al.* 2005).

In *Streptomyces* a large number of CSRs belong to the SARP (*Streptomyces* antibiotic regulatory protein) family. They are characterized by the presence of a helix-turn-helix (HTH) DNA binding domain in the N-terminus, that resembles both in amino acidic sequence and predicted secondary structure to the OmpR-family (Wietzorrek and Bibb 1997). Among the most well studied SARPs are the *S. coelicolor* ActII-Orf4 and RedD that regulate, respectively, the biosynthesis of actinorhodin (Fujii *et al.* 1996) and undecylprodigiosin (Narva and Feitelson 1990) by *S. coelicolor* and CcaR that regulates cephamycin production in *S. clavuligerus* (Perez-Llarena *et al.* 1997).

The regulation of biosynthetic gene cluster has also been assigned to the members of the Large ATP-binding regulators of the LuxR family (LAL). They are characterized by their unusual big size (872–1159 amino acids) and the presence of a LuxR-like DNA-binding domain containing the HTH motif in the C-terminal and an ATP/GTP-binding domain easily identified by the presence of the conserved Walker A motif in the N-terminal (Walker *et al.* 1982). These type of regulators can be found in several biosynthetic genes including PikD that regulates pikromycin production in *Streptomyces venezuelae* (Wilson *et al.* 2001), RapH that regulates rapamycin production in *Streptomyces hygroscopicus* (Kuscer *et al.* 2007) and FkbN that regulates tacrolimus production in *S. tsukubaensis* (Goranovic *et al.* 2012).

Beyond SARP and LAL regulators, a number of additional protein families have been described as CSRs (e.g. TetR, MarR). Within this work it is worth mention the LysR-type transcriptional regulators (LTTR). Despite their diversity, LTTR present important structural regions that are highly conserved and that include a HTH DNA-binding domain in the N-terminus and a co-inducer binding domain at the C-terminus (Maddocks and Oyston 2008). LysR regulators are usually sensitive to the levels of different types of ligands, including products of the pathway they are regulating; in fact they normally require the binding of a small molecule (co-inducer) for activation (Schell 1993). Their presence in secondary metabolites biosynthetic gene clusters include the ClaR located in the clavulanic acid biosynthetic gene cluster of *S clavuligerus* (Perez-Redondo *et al.* 1998), FkbR1 located in the ascomycin biosynthetic gene cluster of *S. hygroscopicus* var. *ascomyceticus* (Wu *et al.* 2000) and its ortholog FkbR present in tacrolimus biosynthetic gene cluster of *S. tsukubaensis* (Goranovic *et al.* 2012)

1.2.1.2 Pleiotropic regulators

Different regulatory strategies are found not only when looking at different biosynthetic pathways, but also in the same biosynthetic pathway, when subjected to different stimuli and conditions. These so called “higher level” regulators perceive those signals and changes, and their cognate response leads to a modulation, normally in an indirect way, that is reflected in secondary metabolite biosynthesis.

Two-component system regulators

Two-component signal regulatory transduction systems (TCS) are very abundant and common in bacteria allowing them to adapt and respond quickly to environmental changes. A typical TCS is composed by two proteins, a sensor histidine kinase (HK) that senses specific environmental stimuli and its cognate response regulator (RR) that mediates the response at the transcriptional level via activation/repression of its target genes (Hakenbeck and Stock 1996). Since TCS have the ability to sense and quickly respond to alterations and given the challenging environment that *Streptomyces* species face, it is understandable that the members of this genus have more TCS when compared to other bacteria; e.g. *S. coelicolor* harbours 100 HK and 87 RR (Rodriguez *et al.* 2013). In *Streptomyces* a very significant number of the TCS are involved in secondary metabolism regulation. They can exert their effect in a direct way by binding to CSRs promoters or indirectly, through intermediate regulatory pathways.

One of the most studied TCS in *Streptomyces* is the PhoRP system. In *Streptomyces* phosphate depletion is one of the signals that triggers secondary metabolism. In fact, pimaricin production in *S. natalensis* is extremely sensitive to the phosphate concentration in the medium being abolished when Pi is present at a concentration of 2 mM. Also the deletion of *phoP* increased the production of pimaricin in a phosphate rich medium (Mendes *et al.* 2007). The determination of the PhoP regulon has demonstrated the multicity of targets that are under the regulation of the PhoRP system. They include genes related with phosphate uptake and phosphate metabolism but also genes related with nitrogen metabolism, carbon metabolism, with a direct link to secondary metabolism. Recently, it was demonstrated PhoP direct binding to *afsS* promoter region, a regulator that among others, regulates the CSR *actII*-ORF4 (Santos-Beneit *et al.* 2009, Allenby *et al.* 2012).

Hormone like molecules

γ-butyrolactones are a family of small molecules, with big structural diversity, designated as microbial hormones that can regulate at different levels secondary metabolism. Although they are present at low concentrations they can be effective at nanomolar concentrations. They bind to specific receptor proteins, thereby preventing them from binding to their target promoter region, modulating in

an indirect way gene transcription (Horinouchi and Beppu 1994). Since in the majority of the cases the specific receptors they bind are repressors, this molecules activate transcription of the cognate target genes. Probably the most characterized γ-butyrolactone in *Streptomyces* is *S. griseus* A-factor that controls both secondary metabolism and morphological differentiation (Horinouchi 2002). The A-factor intracellular concentration gradually accumulates in a growth-dependent manner; when it reaches a critical concentration it binds to the receptor protein, the transcriptional repressor ArpA that, by its turn, can no longer repress its target gene *adpA*. AdpA is transcriptional regulator that activates the transcription of several genes including the streptomycin CSRs, *strR* (Higo *et al.* 2011).

1.2.1.3 Sigma factors

Streptomyces bacteria present an astonishing number of genes encoding for sigma factors (σ) in their genomes. In *S. coelicolor,* 65 sigma factors encoding genes have been described, whilst in *E. coli*, *Mycobacterium tuberculosis* and *Bacillus subtilis* are reported to harbour 7, 13 and 18 sigma factors, respectively (Cho *et al.* 2001). Sigma factors are essential components of RNA polymerase that bind reversibly to RNA polymerase catalytically active core recruiting it to the promoter region of the target genes. Even though the bacterial RNA polymerase complex, which consists of five subunits, is sufficient for transcription elongation and termination, without the presence of its dissociable subunit, the sigma factor, it cannot initiate transcription. Cells harbour primary sigma factors that are responsible for the transcription of housekeeping genes and a variable number of alternative sigma factors that can respond to different signals. Each sigma factor confers specificity to transcription, by recognizing specific promoters, allowing them to switch on specific regulons, enabling the cell to respond to its needs by modulating gene transcription (Helmann and Chamberlin 1988). Regarding sequence similarity, sigma factors can be grouped into two classes, the σ^{54} and σ^{70} families. The σ^{54} family members are required for the transcription of promoters that have a -24 and -12 consensus recognition element instead of the typical -10, -35 sequence. The σ^{70} family includes factors that are related in sequence and domain organization to the primary *E. coli* σ^{70}. Furthermore σ^{70} family members can be further divided into three groups with different functions.

The sigma members belonging to the first group are designated as primary sigmas, which are essential for cell survival and present high homology among its members. Members of the group 2, even though they present sequence similarity with the primary sigma factors, they are not considered to be essential for growth. Members of the group 3, also known as alternative sigmas, are responsible for the transcription of specific regulons. Furthermore they also differ in sequence from the members of the group 1 and 2 (Lonetto *et al.* 1992). Sigma factor activity is normally regulated by anti-sigma factor proteins that prevent them from interacting with RNA polymerase. By its turn anti-sigma factors can also be themselves regulated by sequestration through the action of anti-anti-sigma factors (Helmann 1999).

Extracytoplasmic function sigma factors

In *S. coelicolor* among the 65 sigma factors present, 51 code for extracytoplasmic function (ECF) sigma factors. ECF sigma factors represent a diverse family of alternative sigma factors and based on their structure and sequence homology, they have been included within the σ^{70} family (Lonetto *et al.* 1994, Staron *et al.* 2009). ECF sigma factors are capable of responding to a number of signals including cell envelope stress, oxidation state and iron levels (Helmann 2002); for example σ^{E} and σ^{R} from *S. coelicolor* that play a role in cell wall homeostasis and oxidative stress response, respectively (Paget *et al.* 1998, Paget *et al.* 1999). The majority of sigma factors can autoregulate their own transcription, by a positive feed-back loop. Also they are usually co-transcribed with their cognate anti-sigma factor, which is normally located immediately downstream of the corresponding ECF sigma factor encoding gene (Li *et al.* 2002). Anti-sigma factors bind to sigma factors and inhibit their transcriptional activity. They sense and respond to different signals and in the presence of a proper stimulus anti-sigma factors are inactivated, usually by proteolytic degradation, allowing the sigma factor to bind RNA polymerase. Among the most well studied sigma factors, besides *S. coelicolor* σ^{R}, we find *E. coli* σ^{E}, involved in heat shock response, *E. coli* FecI, involved in ferric citrate transport system, and *Bacillus subtilis* σ^{W} involved in cell envelope stress response. The regulons affected by ECF sigma factors are very diverse, covering different cell processes. Still there is a tremendous knowledge scarcity regarding ECF sigma factors role in

bacteria, especially in *Streptomyces* given the high number of ECF sigma factors they harbour.

Sigma factors and secondary metabolism

The high number of sigma factors present in *Streptomyces* genomes suggests an important role in transcriptional regulation. Indeed, sigma factors regulate different cell processes and secondary metabolism is no exception. It was described for *S. antibioticus* that σ^E deletion blocked actinomycin production (Jones *et al.* 1997). Recently, more work describing sigma factors impact on secondary metabolism has been done. In *S. avermitilis* deletion of the ECF sigma factor Sig6 led to an increase of almost 3-fold in avermictin production, when compared to the wild-type strain, with no major impact on growth and stress responses being observed. Sig6 negative role on avermictin production is mediated through the CSRs *aveR* from avermictin biosynthetic gene cluster (Jiang *et al.* 2011). In *S. coelicolor* the ECF sigma factor SigT was demonstrated to regulate actinorhodin production in response to nitrogen stress. Upon nitrogen stress the production of actinorhodin was practically abolished in a *sigT* knock-out mutant. In this case, SigT controls the expression of *relA*, which code for 5'-diphosphate 3'-diphosphate (ppGpp) a known signal involved in the onset of secondary metabolism (Chakraburtty and Bibb 1997), affecting in this way secondary metabolism in *S. coelicolor* (Feng *et al.* 2011). In *S. albus* an ECF sigma factor, σ^{AntA}, was found to be present in antimycin biosynthetic gene cluster. σ^{AntA} controls the production of a precursor required for antimycin production by directly regulating at the transcriptional level two genes from antimycin biosynthetic gene cluster, *antG* and *antH* (Seipke *et al.* 2014). In a recent study performed in *Streptomyces* sp. strain KCCM 11116P, a producer of tacrolimus, it was proposed the inclusion in tacrolimus biosynthetic gene cluster of a ECF sigma factor FujE, since *fujE* overexpression led to a 3-fold increase in tacrolimus production, even though the deletion did not had impact on tacrolimus biosynthesis (Lee *et al.* 2014).

1.3 TACROLIMUS

Tacrolimus (Tsukuba macrolide immunosuppressant) also known as FK506 or Fujimycin, is a 23-membered polyketide macrolide with immunosuppressant

activity. It was isolated for the first time in 1984 from the fermentation broth of *S. tsukubaensis* No 9993 by the pharmaceutical company Fujisawa Pharmaceutical Co and was first described in 1987 (Kino *et al.* 1987). Nowadays tacrolimus production is also assigned to 17 more *Streptomyces* strains (Hatanaka *et al.* 1989, Garrity *et al.* 1993, Sigmund *et al.* 2003, Kim and Park 2008).

The initial tacrolimus characterization revealed that this macrolide presented a superior potency and fewer side effects in preventing graft rejection, when compared to the immunosuppressor cyclosporine A. Currently, tacrolimus is used in the clinical practice as immunosuppressor to prevent transplant rejection. The immunosuppressant activity of tacrolimus (FK506) relies in its ability to induce with very high affinity, a ternary complex between FK-506 binding protein 12 (FKBP12) and the phosphatase calcineurin, thereby inhibiting a key signal transduction cascade required for T cell proliferation.

Although tacrolimus is mainly used as immunosuppressant, it has shown promising therapeutic potential for other clinical applications due to its ability to bind to other FK-506 binding proteins. Given its properties and broaden applicability tacrolimus became a very important and valuable compound, reaching in 2010, the year this PhD project was initiated, $2,340 million USD in profits.

1.3.1 Tacrolimus producing strain: *S. tsukubaensis* NRRL 18488

S. tsukubaensis, isolated from a soil sample from Tsukuba (Japan) was the first strain described as a tacrolimus producer. It was deposited in 1985 as strain no. 9993 in the Fermentation Research Institute, Agency of Industrial Science and Technology (Japan), and later it was redeposited in the Agricultural Research Culture Collection International Depository (U.S.) under the accession number NRRL 18488. *S. tsukubaensis* genome has been recently sequenced and is publicly available (Barreiro *et al.* 2012). Besides tacrolimus, *S. tsukubaensis* also produces two tacrolimus analogues: FK520 (ascomycin) and FK506D. Structurally they differ at the C-21 side chain. The allyl side chain present in tacrolimus at C-21 is replaced by an ethyl group in FK520 and by a propyl group in FK506D (Fig 1.2).

The size of *S. tsukubaensis* draft genome is 7.62 Mbp with a GC content of 71.52% and is estimated to have 6623 protein-coding genes; 6 rRNA operons, 68 tRNAs and 52 sigma factors encoding genes. It also harbours two plasmids:

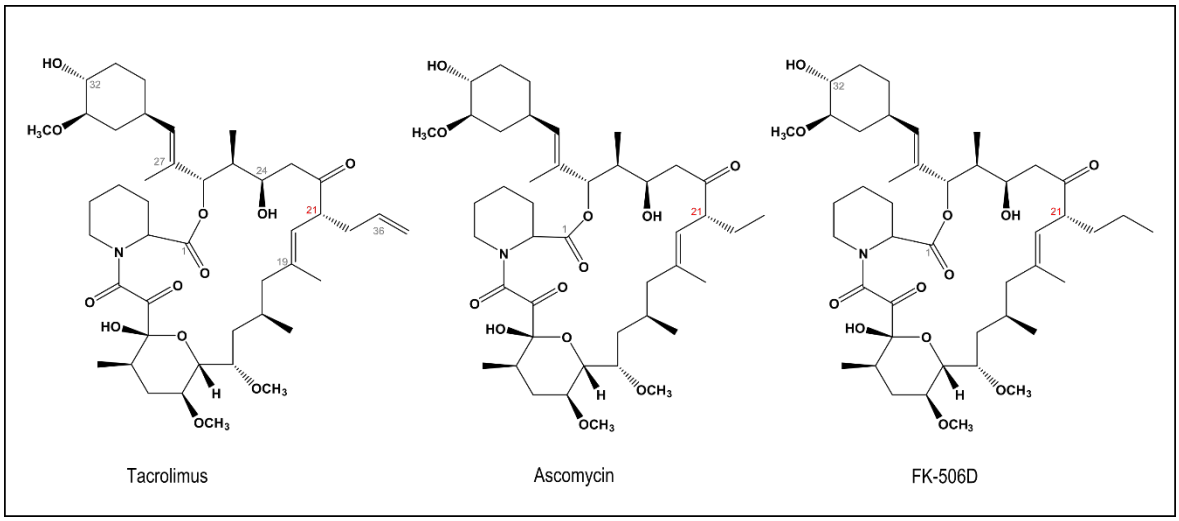

Figure 1.2 - Chemical structures of tacrolimus, ascomycin and FK-560D.

pSTS1 of 24.7 kb and pSTS2 of 31.1 kb. By genome mining of *S. tsukubaensis* genome 30 secondary metabolite clusters were identified: four type I polyketide synthase (PKS), two type II PKS, one type III PKS, three non ribosomal peptide synthetase (NRPS), three hybrid PKS/NRPS, eight terpene, six lantibiotic, and three siderophore gene clusters (Barreiro *et al.* 2012).

1.3.2 Tacrolimus biosynthetic pathway

Tacrolimus is produced by a hybrid PKS/NRPS system (for a review on PKS/NRPS mechanisms see that catalyzes the assembly of the polyketide by the sequential condensation of twelve precursors units (Fig 1.3).

Tacrolimus biosynthesis begins with the FkbO catalysed hydrolysis of chorismate, derived from the shikimate pathway that originates the starter unit DHCHC [(4R,5R)-4,5-dihidrociclohex-1-enecarboxylic acid] (Andexer *et al.* 2011). Next, the PKS FkbA, FkbB and FkbC incorporate the starter unit and catalyse ten successive polyketide chain elongation cycles, with the incorporation and assembling of two malonylCoA, five methylmalonyl-CoA, two methoxymalonyl-ACP and an allylmalonyl-CoA unit. The lysine cyclodeaminase FkbL catalyzes the α-deamination and cyclization of the lysine into pipecolate that is incorporated into the acyl chain. FkbP is a NRPS that activates and incorporates the pipecolate moiety into the completed acyl chain, through the formation of an amide bond, originating the closed macrocycle ring (Motamedi and Shafiee 1998). The macrocycle ring then suffers post PKS modifications, including methylation of the

hydroxyl group at C31 catalysed by the methyltransferase FkbM and the C9 oxidation by cytochrome P450 FkbD (Motamedi *et al.* 1996). These post-PKS modifications are required for tacrolimus full biological activity (Chen *et al.* 2013). During formation of the macrolide the PKSs incorporate two unusual extender units for polyketides, methoxymalonyl-ACP that is also common for ascomycin and allylmalonyl-CoA, which is unique for tacrolimus. Methoxymalonyl-ACP is generated through the action of the *fkbGHIJK* encoding genes that share the same organisation in the ascomycin biosynthetic cluster from *S. hygroscopicus*. FkbH, with acyltransferase and phosphatase activities, loads the substrate glycerate-1,3-bisphosphate, into the ACP protein, FkbJ, originating glyceroyl-ACP, which will suffer further modifications by the actions of two dehydrogenases, FkbH and FkbI and one O- methyltransferase, FkbG, originating the methoxymalonyl-ACP unit (Wu *et al.* 2000). The origin of allymalonyl extender unit, unique for tacrolimus, was recently described simultaneously by Goranovic *et al* in *S. tsukubaensis*, who named the genes involved as *allAKRD* (Goranovic *et al.* 2010) and by Mo *et al* in *Streptomyces* sp. KCTC 11604BP, who named the genes involved as *tcsABCD* (Mo *et al.* 2011). However there is a difference among them with the AllR (TscC in *Streptomyces* sp. KCTC 11604BP) participating in the biosynthetic pathways for both allylmalonyl-CoA (whose incorporation leads to tacrolimus) and ethylmalonyl-CoA (whose incorporation leads to ascomycin), unlike TcsC that was only related with allylmalonyl-CoA. This way AllR constitutes a convergence point for tacrolimus and ascomycin biosynthesis in *S. tsukubaensis* (Kosec *et al.* 2012).

1.3.3 Regulation of tacrolimus biosynthesis

As mentioned in section 1.2, regulation of secondary metabolism in *Streptomyces* is complex and contains many different layers, with the production of secondary metabolites being linked to many environmental and physiological signals. In addition to numerous pleiotropic regulatory genes present, most of *Streptomyces* biosynthetic gene clusters contain clustered situated regulatory genes (CSRs).

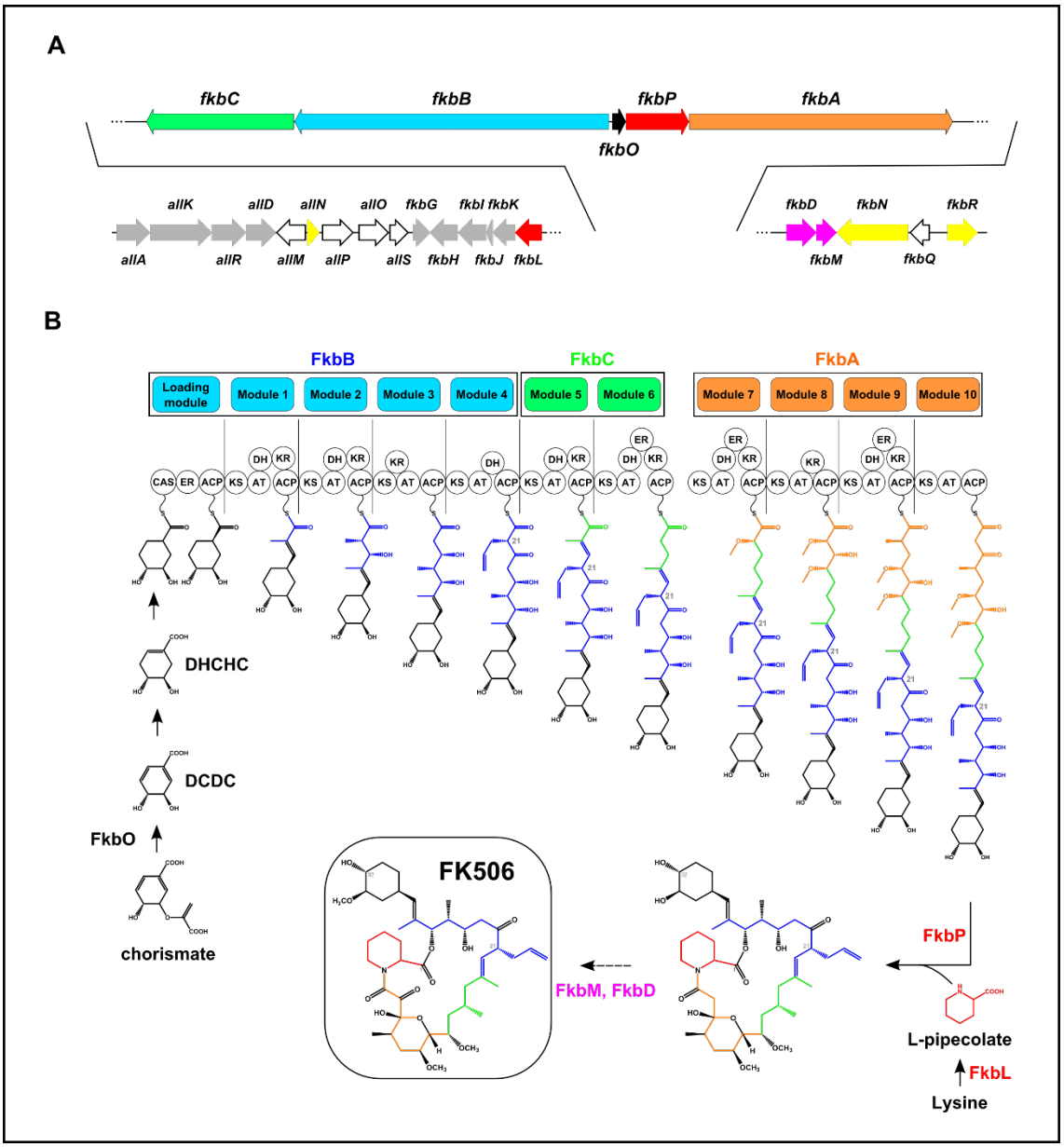

Figure 1.3 – Tacrolimus biosynthetic gene cluster and biosynthetic pathway in *S. tsukubaensis*. Image adapted from Barreiro and Martínez-Castro (Barreiro and Martinez-Castro 2014). (A) Schematic representation of tacrolimus biosynthetic gene cluster. The gene colour is in accordance with their role in the biosynthetic pathway (B). Gene responsible for starter unit biosynthesis is in black (*fkbO*); PKS genes are in orange, blue and green (*fkbA*, *fkbB*, *fkbC*); genes involved in post-PKS modifications are in pink (*fkbM*, *fkbD*); genes involved in allylmalonyl-CoA biosynthesis are in grey (*allAKRD*); genes involved in methoxymalonyl-ACP biosynthesis are in grey (*fkbGHIJK*); genes with unknown function are in white (*allMPOS* and *fkbQ*); NPRS gene is in red (*fkbP*); gene responsible for pipecolate biosynthesis is in red (*fkbL*); cluster transcriptional regulators are in yellow (*fkbN*, *fkbR*, *allN*). (B) Schematic representation of tacrolimus biosynthetic pathway. The different modules of PKSs comprise the following domains: CAS - CoA synthetase; ER - enoyl reductase; ACP - acyl carrier protein; KS - ketoacyl synthase; AT - acyl transferase; DH - dehydratase; KR - keto reductase. The central squared panel corresponds to the final structure of tacrolimus.

Three CSR encoding genes have been recently identified and characterised in *S. tsukubaensis* tacrolimus biosynthetic cluster (Fig 1.3 A): *fkbN* coding for a transcriptional regulator belonging to the LAL family of transcriptional regulators; *fkbR* coding for a transcriptional regulator belonging to the LysR family of transcriptional regulators and *allN* coding for a transcriptional regulator from the AsnC family regulatory proteins (Goranovic *et al.* 2012). Bioinformatic analysis showed that *S. tsukubaensis* FkbN shares 69.9% amino acid identity with FkbN from the ascomycin biosynthetic gene cluster of *S. hygroscopicus* var. *ascomyceticus* and 57.4% amino acid identity with RapH from the rapamycin biosynthetic gene cluster of *S. hygroscopicus*. Conversely, no orthologue for FkbR was found in those strains. The functional characterization of these regulatory genes through gene-deletion and overexpression showed that in *S. tsukubaensis,* FkbN functions as a positive regulator that is essential for tacrolimus production, since its deletion abolished tacrolimus biosynthesis (Goranovic *et al.* 2012).

Interestingly, transcription of the structural genes tested (*fkbB* and *fkbG*) was still observed in Δ*fkbN* strain, indicating that post-transcriptional regulation of tacrolimus biosynthesis may be an important mechanism. With FkbN overexpression it was also observed an increase of 55% in tacrolimus production. Moreover, it was shown that *fkbN* transcription is first detected at the same time as the onset of tacrolimus production. FkbR also functions as a positive regulator, however in this case this transcriptional regulator is not essential for tacrolimus production, since Δ*fkbR* still retained approximately 20% of the wild-type production. As observed for Δ*fkbN,* transcription of the structural genes tested was also observed in Δ*fkbR.* With FkbR overexpression it was also observed an increase in tacrolimus production, however not as high as the one observed for fkbN overexpression (Goranovic *et al.* 2012). Unlike *fkbN* transcription profile, transcription of *fkbR* begins at early stages of growth and continues throughout the entire fermentation process. In the case of AllN, neither the overexpression nor deletion of the *allN* gene showed any influence on tacrolimus production (Goranovic *et al.* 2012).

At the same time three regulatory genes have also been identified and characterised in *Streptomyces* sp. KCTC 11604BP tacrolimus biosynthetic cluster: *fkbN*, *tcs7* (orthologue of *S. tsukubaensis fkbR*) and *tcs2* (orthologue of *S.*

tsukubaensis allN). Curiously, in this strain and unlike what was observed for *S. tsukubaensis*, *tcs7* was described as a negative regulator of tacrolimus production (Mo *et al.* 2012). This was surprising considering the high degree of similarity that both tacrolimus biosynthetic gene clusters share. In fact two types of tacrolimus biosynthetic gene clusters are present in different tacrolimus producing strains, with the first group comprising the two strains mentioned above. The second group comprises *S. tacrolimicus* (formerly known as *Streptomyces* sp. ATCC 55098) (Martinez-Castro *et al.* 2011) and *S. kanamyceticus* KCTC 9225. In this case, a shorter version of the tacrolimus biosynthetic gene cluster is present, with several *all* genes missing. Also *S. tacrolimicus*, a low tacrolimus producer, does not contain *fkbR* encoding gene. Interestingly, when *fkbR1*, a distant homologue of *fkbR* (sharing only 24% identity with *S. tsukubaensis fkbR*) was overexpressed in *S. tacrolimicus* a three-fold in tacrolimus production was observed, suggesting that the absence of *fkbR* in *S. tacrolimicus* could also explain the low yields in tacrolimus production in this strain.

As previously described (section 1.3) the autoregulators gamma-butyrolactones function as signals that influence secondary metabolism. Recently the *bul* regulatory cluster was studied in *S. tsukubaensis* (Salehi-Najafabadi *et al.* 2014). The *bul* regulatory cluster is involved in the synthesis and control of a gamma-butyrolactone and contains two SARP regulators (*bulY* and *bulZ*); two γ-butyrolactone receptors (*bulR1* and *bulR2*) and two γ-butyrolactone synthetases (*bulS1* and *bulS2*). Deletion of the γ-butyrolactone receptor *bulR1* resulted in decreased tacrolimus production as well as changes in strain morphology with a delay in sporulation being observed. This result suggest that BulR1 functions as a tacrolimus positive regulator (Salehi-Najafabadi *et al.* 2014).

1.4 OXIDATIVE STRESS

Microbial life first developed in an anaerobic atmosphere, but the arising of photosynthesis, led to an increase of oxygen levels in the atmosphere. This change was responsible for the introduction of a more efficient form of respiration with molecular oxygen (O_2) as the terminal electron accepter. However this oxygenation also created a strong selective pressure on organisms that either had to become restricted to niches free of O_2 or had to develop protective

mechanisms in order to cope with its deleterious presence. Even though molecular oxygen is a rather stable molecule, its ability to abstract electrons from electron-transfer enzymes, generating reactive oxygen species (ROS), is what makes oxic environments so dangerous. The presence of O_2 in the atmosphere resulted in what is commonly known as the "oxygen paradox": oxygen is as essential as it is toxic for life. During normal aerobic metabolism ROS such as superoxide anion ($O_2^{\cdot -}$), hydrogen peroxide (H_2O_2) and hydroxyl radical ($HO^{\cdot}$) are continuously produced (Fig. 1.4). These reactive by-products of oxygen reduction have a harmful biological effect through the damage of vital cellular components like proteins, nucleic acids and lipids (Storz and Imlay 1999). In order to overcome the toxic effects of ROS, organisms had to develop response mechanisms at different levels, from modulation of gene expression to changes in enzymatic and non-enzymatic activities.

1.4.1 Reactive oxygen species: origin and molecular targets

ROS indissociability with respiratory metabolism resides in the fact that any enzyme capable of metabolizing molecular oxygen also have the capability of generating these harmful species. Given molecular oxygen negative reduction potential (-0.16 V), its affinity for the first electron is low and it can only accept one electron at a time from univalent electron donors such as metal centres, flavins and respiratory quinones (Imlay 2013). But the observation that *E. coli* mutants defective in respiratory enzymes still produced a significant amount of both $O_2^{\cdot -}$ and H_2O_2 indicate that in fact autoxidation of non-respiratory flavoproteins was the primarily source of $O_2^{\cdot -}$ and H_2O_2 (Messner and Imlay 2002). When the balance between oxidants/antioxidants is disrupted a situation of oxidative stress is created. Different ROS have different reduction potentials thus causing different cellular damages.

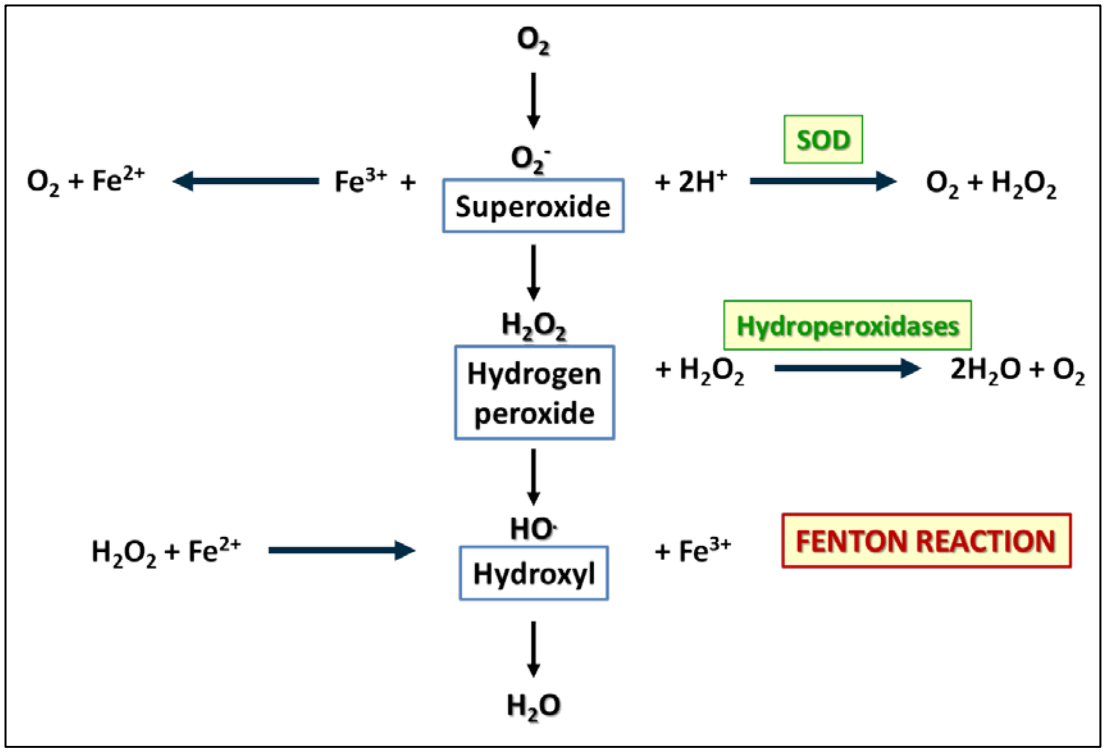

Figure 1.4 – Schematic representation of reactive oxygen species generation and the enzymatic scavenging system. Image adapted from Imlay (Imlay 2003).Representation of the reactive oxygen species (ROS) generated during oxygen incomplete reduction as well as the reactions catalysed by the enzymes required for ROS scavenging, namely the superoxide dismutases (SOD) and hydroperoxidases. The Fenton reaction is also represented.

1.4.1.1 Superoxide anion - $O_2^{\cdot -}$

Superoxide anion is a highly unstable molecule unable to diffuse through biological membranes. It is mainly known for attacking and destroying iron-sulfer clusters, namely dehydratases, which are a widespread class of proteins that include key catabolic and biosynthetic enzymes such as fumarase or aconitase from the TCA cycle. It has also been implicated in the disruption of some amino acid biosynthetic pathways in *E. coli* (Benov and Fridovich 1999). Another way of $O_2^{\cdot -}$ toxicity is through the Haber-Weiss reaction in which $O_2^{\cdot -}$ oxidation of iron-sulfur clusters, increases the intracellular pool of ferrous iron (Keyer and Imlay 1996) . In its reduced form, iron is highly toxic since it reacts with H_2O_2 generating the hydroxyl radical through the well-known Fenton reaction (Imlay *et al.* 1988).

1.4.1.2 Hydrogen peroxide – H_2O_2

Hydrogen peroxide is an uncharged compound that can easily diffuse through biological membranes. Like $O_2^{\cdot -}$, H_2O_2 also oxidizes iron sulfer clusters, but at a slower rate. H_2O_2 can also oxidized intracellular unincorporated ferrous iron, including iron associated with DNA. In fact it was shown in *E. coli* that 1 µM of H_2O_2 could lead to DNA damage (Imlay 2008). It was also discovered that the negative effect of H_2O_2 addition in *E. coli* on the PPP was through the inactivation of ribulose-5-phosphate 3-epimerase, an enzyme that contains ferrous iron as a solvent-exposed cofactor (Sobota and Imlay 2011). Also mononuclear iron enzymes have been described as the primary target of H_2O_2 (Anjem and Imlay 2012). H_2O_2 oxidizes specific amino acid residues, namely cysteines and methionines. The oxidation of cysteine residues transforms the thiol groups (-SH) into sulphenic acid (-SOH) that can either form disulphide bonds with other cysteine residues or be further oxidised to sulphinic acid (-SOOH), which is considered to be in an irreversibly oxidised state. Proteins with thiol-based redox switches can be found in both prokaryotes and eukaryotes and are involved in the regulation of different cell processes, such as the antioxidant response. However, the oxidation rate constant of protein thiols differs. While H_2O_2 can oxidize thiols on OxyR and AhpC proteins with rate constants that exceed 10^7 m^{-1} s^{-1}, the oxidation rate constants of other protein thiols do not exceed 60 m^{-1} s^{-1} (Aslund *et al.* 1999, Peskin *et al.* 2007).

1.4.1.3 Hydroxyl radical - $HO^{\cdot}$

The hydroxyl radical is a highly reactive molecule that in biological systems derives in its majority from ferrous iron oxidation by H_2O_2 through the Fenton reaction (Imlay *et al.* 1988). This molecule is considered to be the most harmful and toxic form of ROS, being able to directly damage most biomolecules.

1.4.2 Reactive oxygen species detoxification: sensors and effectors in *Streptomyces*

Throughout evolution the need to counteract the damaging effects derived from the exposure to ROS lead to the development of a set of adaptive and protective responses, with the development of both sensors and effectors that together give an appropriate response towards oxidative stress (Imlay 2008). In

Streptomyces field, the oxidative stress response systems and mechanisms were in their majority described in *S. coelicolor*, with the exception of the catalase-peroxidase system which was mainly characterized in *S. reticuli*. *Streptomyces* oxidative stress response is mainly governed by the transcriptional regulators OxyR, CatR, FurS and Nur as well as the sigma factor SigR, which control the expression of different antioxidant systems, namely the alkylhydroperoxide reductase system AhpCD, the monofunctional catalase KatA1, the catalase peroxidase CpeB, the superoxide dismutases SodF and SodN and the thioredoxin system TrxAB, respectively (Paget *et al.* 1998, Hahn *et al.* 2000, Hahn *et al.* 2002).

1.4.2.1 ROS Sensors

Fur (ferric uptake regulator) protein was initially characterised in *E. coli* as an iron-sensing transcriptional factor, involved in the regulation of iron metabolism, namely siderophore biosynthesis and iron transport (Hantke 1981). Currently, it is considered to be a global transcriptional factor regulating many cellular processes including the oxidative stress response (da Silva Neto *et al.* 2009). The Fur superfamily consists of DNA binding proteins that can act as sensors of iron (Fur), zinc (Zur), nickel (Nur) and peroxide (PerR) (Bsat *et al.* 1998, Gaballa and Helmann 1998, Escolar *et al.* 1999, Ahn *et al.* 2006). *S. coelicolor* CatR, an orthologue of the *Bacillus subtilis* inducible peroxide stress response regulator PerR, represses its own transcription as well as the transcription of the H_2O_2 inducible monofunctional catalase CatA. When exposed to H_2O_2 CatR is irreversible oxidized in an iron depend way, and loses DNA binding affinity thus derepressing *catR* and *catA* transcription (Fig. 1.5) (Hahn *et al.* 2000).

The ECF sigma factor SigR is a key regulator of the oxidative stress response in *Streptomyces.* It has already been described that in *Streptomyces* the control of intracellular thiol-disulphide balance is made by the thioredoxin system (Cohen *et al.* 1993), which is under the control and regulation of SigR (Paget *et al.* 1998). *S. coelicolor* SigR regulon includes a plethora of genes most of them involved in thiol metabolism (Paget *et al.* 2001).

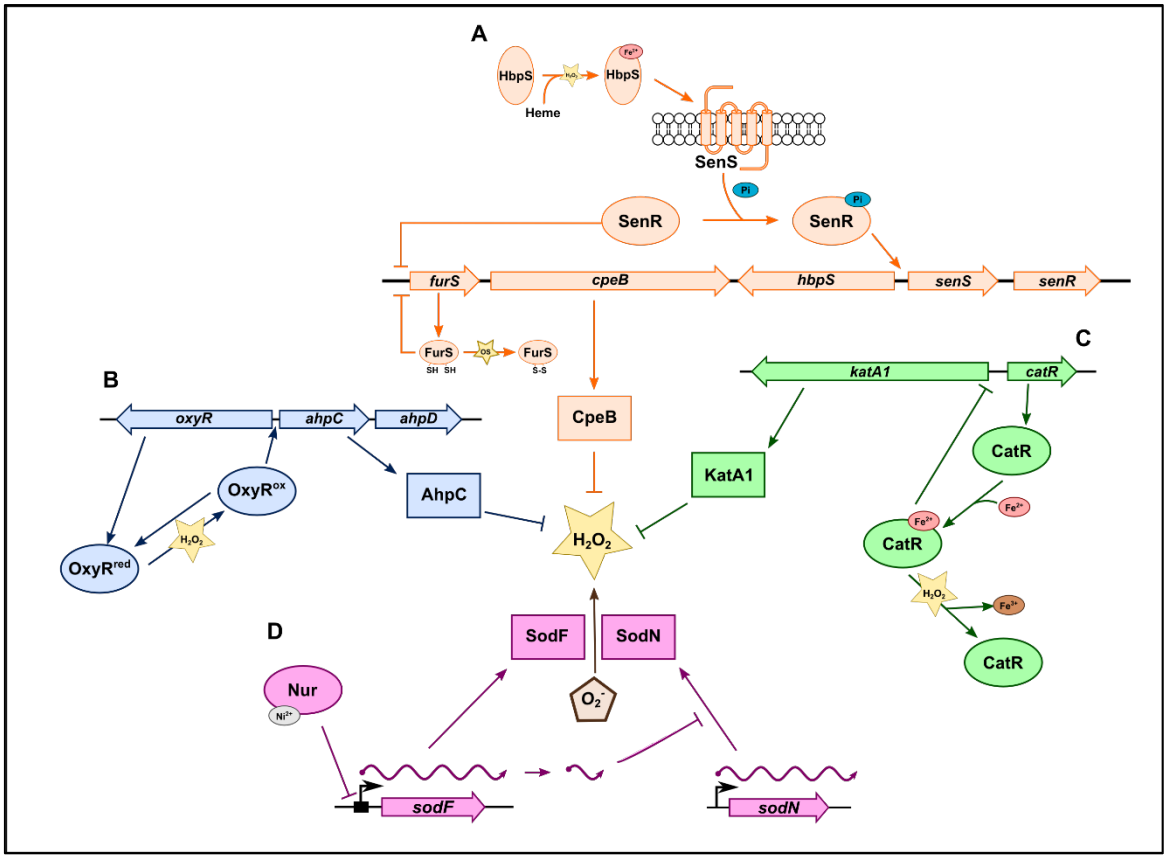

Figure 1.5 – Schematic representation of *Streptomyces* enzymatic H_2O_2 and $O_2^{\cdot-}$ scavenging systems. (A) *S. reticuli* H_2O_2 detoxification via *furS-cpeB* under the regulation of the HbpS-SenS-SenR redox system. (B) *S. coelicolor* H_2O_2 detoxification through the alkylhydroperoxide system (AhpCD), which is under the control of the H_2O_2 sensor regulator OxyR. (C) *S. coelicolor* H_2O_2 detoxification through the monofunctional catalase KatA1, which is under the negative regulation of the Fur-like protein CatR in an iron and H_2O_2 dependent manner. (D) $O_2^{\cdot-}$ dismutation through the action of superoxide dismutases, which are under the control of the Fur-like regulator Nur, in a nickel dependent manner.

The most studied anion superoxide sensor and regulatory system is *E. coli* SoxRS regulon. It is composed by two regulators: SoxR, a MerR-family transcription regulator that presents iron-sulfur clusters, and SoxS an AraC family regulator, whose transcription is regulated by SoxR. Many genes are under this regulon control including superoxide dismutases (Hidalgo *et al.* 1995, Pomposiello and Demple 2001). Even though an iron-sulfur cluster is present in SoxR, a known target of $O_2^{\cdot-}$, it is believed that it does not sense $O_2^{\cdot-}$ directly. This was supported with the results obtained with an *E. coli* SOD-null mutant strain, where low level of induction in the SoxRS regulon was achieved (Gort and Imlay 1998). In fact this regulon seems to be induce by redox-cycling agents, such as, menadione, plumbagin or paraquat (Gu and Imlay 2011). In *S. coelicolor* genome it was only

found a *soxR* orthologue (Bentley *et al.* 2002). In the case of *S. coelicolor*, unlike *E. coli*, no superoxide dismutase encoding gene was under SoxR control. It was however demonstrated that SoxR was sensitive to the benzoisochromanequinone polyketide antibiotic actinorhodin, which resembles the ring structures of phenazine (Shin *et al.* 2011). Therefore, it was suggested that *S. coelicolor* SoxR regulon can be involved in secretion of potentially harmful redox-active compounds, like actinorhodin.

1.4.2.2 H_2O_2 sensor: a special look into OxyR

In bacteria, the presence of oxidative stress sensors, whose activation relies on reactive proteins able to sense the signals and rapidly activate the appropriate response, constitutes a major advantage in stressful situations where a fast response is required. OxyR is a hydrogen peroxide sensing transcriptional factor (TF) that regulates bacterial response to oxidative stress. It belongs to the LysR-type transcriptional regulator (LTTR) family of proteins (see section 1.2.1.1). LTTR present at the C-terminus a co-inducer binding domain, that upon binding changes the tertiary conformation of the protein and also their ability to bind DNA (Maddocks and Oyston 2008). In the case of OxyR, activation is not achieved by the binding of a co-inducer, but by disulfide bond formation between the reactive cysteines (Cys) present in the C-terminal domain (Zheng *et al.* 1998, Aslund *et al.* 1999). The unique properties of the sulfur chemistry in Cys residues is utilized by OxyR to reversibly switch from an inactive to an active state in response to H_2O_2, making the H_2O_2-mediated activation of OxyR a very sensitive, fast and transient regulation, that relies on the intracellular redox status. OxyR is a tetramer which binds to the promoter of target genes before and after stress sensing. It can act as an activator but also as a repressor. Upon H_2O_2 treatment, the conformation of the OxyR tetramer changes and becomes in most cases an activator of RNA polymerase. Even though several models have been proposed for the activation mechanism of OxyR, in *E. coli* sensing of H_2O_2 seems to occur as follows: the thiol of Cys residue 199 becomes oxidized by H_2O_2 to an unstable SOH, which rapidly reacts with Cys 208 to form an intramolecular disulfide bond [8-10]. Regarding OxyR binding to DNA in its oxidized form it is achieved by four contacts, with the four subunits of the oxidized homotetrameric protein binding to four adjacent major DNA grooves on one side of the DNA helix. In the reduced form it binds DNA but

in an extended motif, resulting in a binding of two pairs of major grooves (Toledano *et al.* 1994). The two modes of binding allow OxyR to regulate different promoters under oxidizing and reducing conditions.

OxyR-dependent regulation of enzymatic antioxidant genes is conserved among bacteria, but there is much more to OxyR than meets the eye. Recent genome-wide analyses in several bacteria have expanded the OxyR regulon indicating not only new OxyR targets but also other modes of OxyR-dependent regulation of gene expression that cross path with other regulatory pathways [11-12]. Among the roles and responses in which OxyR is implicated, one can also find this transcriptional factor to be involved in metal ion homeostasis as a response and adaptation to peroxide stress [10, 13-15]. In fact, in *E. coli* where OxyR has been extensively studied, the active form of OxyR regulates almost 40 genes involved not only directly in oxidative stress response, like *katG* (catalase/hydroperoxidase I) or *ahpCF* (alkyl hydroperoxide reductase system), but also genes related to iron metabolism, in a way to prevent intracellular iron toxicity, by positively regulating genes like the *dps* (iron-binding and storage protein involved in DNA protection), *fur* (iron related transcriptional regulator), *mntH* (manganese/divalent cation transporter) and the *sufABCDSE* cluster (Fe–S cluster assembly protein) and also by negative regulating genes involved in iron transport by siderophores, like *fhuF* (ferric iron reductase involved in ferric hydroximate transport) (Chiang and Schellhorn 2012).

In *S. coelicolor*, OxyR was shown to function as a positive transcriptional regulator of the *ahpCD* operon (Fig. 1.5). However, unlike what was observed for *E. coli* where OxyR negatively regulates its own transcription, in *S. coelicolor* OxyR works as an activator of *oxyR* (Hahn *et al.* 2002). Regarding the genomic organization of the *oxyR-ahpCD* region, *Streptomyces* present a much conserved synteny, with *ahpC* and *ahpD* genes being transcribed in an operon divergently from the OxyR encoding gene (Hahn *et al.* 2002). This genomic organization is also conserved in several *Mycobacterium* species (Dhandayuthapani *et al.* 1997).

1.4.2.3 Effectors

Superoxide dismutase

Superoxide anion dismutation is catalysed by metalloenzymes named superoxide dismutases (SOD), through the sequential reduction and oxidation of the metal active centre, giving rise to molecular oxygen and hydrogen peroxide (Abreu and Cabelli 2010, Miller 2012). There are three different families of SODs that even though distinct, they all present the ability to dismutate $O_2^{\cdot-}$ using different catalytic active metals: the Fe/MnSOD, the CuSOD and the NiSOD. The most ancient SOD is the FeSOD that uses iron as prosthetic group. However during evolution new forms appeared with the ability to use Mn^{2+} as the active metal. Some forms of SODs also have the ability to use both metals, Fe/MnSOD, known as cambialistics. Due to the d-electronic configuration, manganese is less prone to oxidation by H_2O_2 than iron, thus MnSOD is considered safer than FeSOD upon oxidative stress conditions. Concerning the distribution across life domains, FeSOD are found in both aerobic and anaerobic bacteria, whilst MnSOD is mainly found in aerobic bacteria (Miller 2012). CuSOD is in most cases a dimeric enzyme, where each monomer contains an active site with one copper ion and one zinc ion bridged by a histidine imidazole (Abreu and Cabelli 2010, Miller 2012). The distribution of this enzyme spans all life domains. In bacteria, it is present in the periplasmic space of Gram-negative bacteria, especially in infectious organisms (Miller 2012). Moreover, this family of SODs is also found in Gram-positive bacteria like *Mycobacterium tuberculosis* (Wu *et al.* 1998). NiSODs were first described in *Streptomyces* and are characterized by the presence of nickel in its active center, and a homohexameric structure with one nickel per subunit (Youn *et al.* 1996). *Streptomyces* NiSOD require processing with the first amino acids being cleaved from the N-terminus in order to become active (Barondeau *et al.* 2004, Wuerges *et al.* 2004). The first 9–12 amino acids of the mature NiSOD, known as the nickel hook, have been shown to bind nickel and form the active site (Tietze *et al.* 2009). As far as it is currently known, NiSOD family members display a very restricted distribution: actinobacteria, proteobacteria, chlamydiae and eukaryotic green algae (Schmidt *et al.* 2009). The SOD activity profile in *Streptomyces* was first addressed in *S. coelicolor*, where two FeSOD encoded by *sodF* and *sodF2* and one NiSOD encoded by *sodN* were

identified (Kim *et al.* 1996, Kim *et al.* 1998). Furthermore, it was also described that, in the presence of nickel in the media, the expression of *sodF* and *sodF2* was repressed, whereas *sodN* transcription was induced (Chung *et al.* 1999). In *S. griseus*, two proteins SrnR and SrnQ were implicated in the nickel repression of *sodF* transcription. These two proteins form a complex that suffers a conformational change upon nickel binding thus binding to *sodF* promoter region and repressing its transcription (Kim *et al.* 2003). The same nickel repression was reported for *S. coelicolor sodF* and *sodF2* transcription, however in this strain no SrnRQ orthologues were found, suggesting the presence of another nickel-responsive regulatory system. It was later discovered, a Fur-like protein - nickel uptake repressor (Nur) – responsible for the regulation of the iron-containing SOD encoding genes in *S. coelicolor* through repression of *sodF* transcription in the presence of nickel (Ahn *et al.* 2006). Recently, this FeSOD/NiSOD inverse regulation was explored in *S. coelicolor* where it was observed that a small regulatory RNA of about 90 nt produced from *sodF* mRNA 3' UTR (s-sodF), matched exactly the 5' UTR of *sodN* mRNA. By pairing with this region, s-sodF blocks its translation decreasing *sodN* mRNA half-life (Fig. 1.5) (Kim *et al.* 2014).

Alkylhydroperoxide reductase system

Alkylhydroperoxide reductase C (AhpC) belongs to the family of 2-Cys-peroxiredoxins whose enzymatic mechanism of peroxide detoxification relies on a conserved cysteine residue known as peroxidatic cysteins (Cp) that reduces peroxide substrates, namely H_2O_2, organic hydroperoxides and peroxynitrite. During catalysis a second free thiol, known as the resolving cysteine (Cr), forms a disulphide with Cp (Hall *et al.* 2009). In *E. coli* AhpC is reactivated through the action of AhpF, a flavoprotein with NADH:disulfide oxidoreductase activity that restores AhpC to its reduced form (Poole and Ellis 1996). In the majority of the cases *ahpF* is co-transcribed with *aphC.* In *Mycobacterium tuberculosis*, AhpF is absent and AhpC is reduced by the alkylhydroperoxidase AhpD (Hillas *et al.* 2000).

AhpC ability to detoxify different peroxides is impacted by its substrate specificity. It was already demonstrated that AhpC displays approximately 100-fold preference for H_2O_2 over cumene hydroperoxide (Parsonage *et al.* 2008). In *E. coli* AhpC is described as the primary scavenger of endogenous hydrogen peroxide

being kinetically a more efficient scavenger of trace H_2O_2 than catalase (Seaver and Imlay 2001). However other roles for AhpC have also been appointed in *E. coli*. It was observed that an *ahpC* mutant presented a reduction of total intracellular iron content and a decrease in the siderophore enterobactin production when growing in low-iron medium. It was proposed that AhpC participation in the first step of enterobactin biosynthesis was either by facilitating the delivery of chorismate, a precursor of enterobactin, to the enterobactin biosynthetic pathway or by maintaining an optimal chorismate pool inside the cells (Ma and Payne 2012). Also in *Streptococcus agalactiae* AhpC was shown to work as an intracellular chaperone for heme, optimizing its trafficking and transfer to cellular targets including catalase (Lechardeur *et al.* 2010). In *S. coelicolor* a functional AhpCD system was also described and it was demonstrated that AhpC was maximally produced during early exponential phase and could be induced by exogenous H_2O_2 under the control of OxyR (Fig. 1.5) (Hahn *et al.* 2002).

Hydroperoxidases

Hydroperoxidases, commonly known as catalases, catalyse the disproportion of two molecules of hydrogen peroxide into water and molecular oxygen. This reaction can be performed by monofunctional catalases in the absence of an external reductant (heme catalases and non-heme catalases), or by bifunctional-peroxidases in the presence of an electron donor (catalase-peroxidases).

Monofunctional catalases are ubiquitous across kingdoms. They are incredibly resistant to stresses including heat and proteolysis and they only follow the Michaelis-Menten curve in the presence of small amounts of substrate, only reaching inhibition above 3 M H_2O_2 in some cases (Chelikani *et al.* 2004). Catalase activity is predominant only when H_2O_2 reaches higher doses and peroxidases, like AhpC, reach saturation, a profile that has been observed in several bacteria (Seaver and Imlay 2001). Monofunctional catalases can be distinguished in two types: heme catalases and non-heme catalases, also known as manganese catalases. They differ on the nature of their prosthetic group, with iron being present in the first and manganese present in the latter. While heme-catalases are widespread, non-heme catalases constitute a smaller group with a distribution restricted to Eubacteria. The heme-catalases can be further divided in

clades according to their phylogeny. Catalases from clade 1, are mostly present in plants, although representatives from this clade were identified in bacteria, clade 2 are widespread among bacteria and fungus and clade 3 present in all life domains that are characterized by the ability to bind NADPH (Chelikani *et al.* 2004).

Catalase-peroxidases or bifunctional-catalases can also catalyse the disproportion of H_2O_2 but are characterized by a bifunctional behavior, requiring organic reductants as electron donors, hence the name peroxidase.(Chelikani *et al.* 2004).

Streptomyces strains usually harbour multiple catalase encoding genes. *S. coelicolor* harbours at least three monofunctional-catalases and one catalase-peroxidase. CatA is the major monofunctional catalase required for efficient growth and resistance towards H_2O_2 (Cho and Roe 1997) being negatively regulated by CatR in a H_2O_2 and iron dependent manner (Fig. 1.5). CatB is required for osmoprotection and proper differentiation and is regulated by σ^B. However, post-translational control is exerted on CatB expression during the development, which includes proteolytic cleavage and extracellular secretion (Cho *et al.* 2000). CatC is a catalase-peroxidase expressed transiently at late exponential to early stationary phase under the control of a Fur regulator, FurA (Hahn *et al.* 2000). However this system was mainly characterized in *S. reticuli* where the Fur regulator (FurS), besides its autoregulation in a redox-dependent fashion, is also under the control of a TCS constituted by SenS (SK) and SenR (RR) (Lucana *et al.* 2003). SenS-SenR system acts in coordination with HbpS, a heme binding protein, and function as a redox sensor. In vitro studies have shown that SenS and HpbS interact, and in fact HbpS in the presence of iron and/or oxidative-stress conditions stimulates SenS autokinase activity, increasing the phosphorylated form of SenR and thus de-repressing *furS –cpbE* transcription (Fig. 1.5) (Lucana *et al.* 2004, Lucana *et al.* 2005, Ortiz de Orue Lucana and Groves 2009).

Non-enzymatic defenses

Glutathione is considered to be the major thiol buffer among kingdoms. However that is not the case for Actinobacteria that instead uses a structurally unrelated, sugar-containing monothiol compound called mycothiol that functions in an analogous way to glutathione, coping with stress from thiol reactive toxins. (Newton *et al.* 1996). Although mycothiol regulation and biosynthesis are still not

fully disclosed it has been reported that the σ^R anti-sigma factor RsrA of *S. coelicolor* controls key elements of mycothiol metabolism (Newton and Fahey 2008).

1.4.3 Iron and ROS: partners in crime

Iron plays a vital role on bacteria survival since cells rely on iron for a wide range of metabolic and signaling functions. Iron is one of the most abundant elements on Earth and it occurs in two different forms: the ferrous iron (Fe^{2+}) which is soluble in aqueous solutions at neutral pH and the ferric iron (Fe^{3+}) which is highly insoluble at neutral pH and is the predominant form in oxic environments [21]. To cope with the insolubility of ferric iron many bacteria have developed an iron acquisition system that utilizes siderophores, which are small and low weight molecules that are secreted into the environment and binding ferric iron with high affinity (Andrews *et al.* 2003). After siderophore-ferric iron complex internalization, iron is released upon a reduction reaction that usually takes place in the cytoplasm [4]. Siderophores can be divided in sub-classes according to the chemical nature of ferric iron coordination: hydroxamates, catecholates, carboxylates, heterocyclic compounds, and mixed types (Winkelmann and Drechsel, 1997) and its biosynthesis is commonly achieved through a NRPS–dependent pathway (Barry and Challis 2009). In Gram-negative bacteria the Fur regulator and OxyR protein are partners in regulating iron uptake by siderophores and iron metabolism (Zheng *et al.* 1999). In most Gram-positive bacteria the iron repressor DtxR seems to regulate siderophore biosynthesis and iron uptake [25]. DtxR-like proteins have already been described in *Mycobacteria* (Dussurget *et al.* 1996) and *Streptomyces,* namely in *S. coelicolor* (DmdR1 and DmdR2) [26-28]. In *S. coelicolor,* DmdR1 is the major iron regulator repressing in the presence of iron, the biosynthesis of the siderophore desferrioxamine (Flores *et al.* 2005, Tunca *et al.* 2007).

Even though cells have a demand for iron there is a need to have a strict control over iron uptake because iron overload can be toxic for the cells; in fact the generation of the hydroxyl radical via the oxidation of Fe^{2+} by H_2O_2 (Fenton reaction) is still the most deleterious iron-mediated mechanism known (Touati 2000). Given the linkage between oxygen and iron it is understandable that

bacteria developed a strict and cross-linked response regulatory mechanism to cope with both iron and oxygen levels in order to maximize growth and minimize the damaging effects. One common response in bacteria towards peroxide stress consists in altering the intracellular metal pool by repressing iron uptake, increasing transcription of proteins that incorporate iron and/or proteins that have the ability to sequester and storage iron (e.g. bacterioferritins and ferritins) or even by increasing intracellular levels of other divalent metals, especially manganese (Mn^{2+}), in order to replace ferrous iron as a target of peroxide stress in iron containing proteins (Faulkner and Helmann 2011).

Several different types of mechanisms for iron uptake and its cross-regulation with oxidative stress have been extensively described in Gram-negative and some Gram-positive bacteria, however there is still a scarcity of information regarding *Streptomyces* related mechanisms, especially on ferrous iron uptake and regulation. Understanding iron metabolism is important for *Streptomyces* since some reports have already stated that increased iron content, beyond optimal growth conditions, have a positive effect in secondary metabolite production, although the pathways remain unknown (Cheng *et al.* 1995). Also it was reported that secondary metabolite production was triggered in certain species when they were grown in proximity to isolates producing siderophores such as desferrioxamine E (Yamanaka *et al.* 2005). Additionally reports have also supported the hypothesis that siderophores may play a much more complex role in triggering a wide range of cellular processes such as secondary metabolite production or morphological development in *Streptomyces* (Traxler *et al.* 2013, Lambert *et al.* 2014).

1.4.4 Oxygen and secondary metabolism in *Streptomyces*

From an industrial point of view, oxygen supply is a key parameter on the production of secondary metabolites. While low O_2 concentrations limit growth and product formation, increased O_2 concentration usually can improve secondary metabolite production (Yegneswaran *et al.* 1991, Song *et al.* 2006). However above a certain threshold, O_2 may have regulatory and toxic effects on microbial cultures mainly due to oxidative stress. The influence of Dissolved Oxygen (DO) levels on the secondary metabolism has been studied in *Streptomyces* cultures, although the molecular mechanisms by which DO influences secondary metabolite

production are not fully understood. However it has been proved that high DO levels have a positive regulatory role in secondary metabolism. In fact it has already been confirmed the influence of DO in tacrolimus fermentation (Singh and Behera 2009).

Like other environment-induced responses, the oxidative stress related mechanisms are embedded in global networks that extend the effect of the oxidative stress response into secondary metabolism. Thus, it is reasonable to assume that oxygen, or the by-products of its reduction, may have a regulatory effect on the *Streptomyces* secondary metabolism. Some studies have already point out the correlation between the oxidative stress response and secondary metabolism in *Streptomyces.* Recently it was demonstrated for the pimaricin producer *S. natalensis* an important role of H_2O_2 intracellular levels in regulating secondary metabolism, presumably through redox-based mechanisms (Beites *et al.* 2011).

1.5 OBJECTIVES

This PhD project proposal was prepared within the frame of the funded ERA-IB (www.era-ib.net) project IMMUNOTEC (ERA-IB/0001/2010; EIB.10.005). IMMUNOTEC integrated the complementary efforts of five European research groups. The objective of the project was to develop a robust *Streptomyces*-based fermentation process for the production of the immunosuppressant tacrolimus, whose production yields, even in industrial strains, are low. Thus, to achieve IMMUNOTEC goals we needed to understand first the basic molecular mechanisms that affect the biosynthesis of tacrolimus in *S. tsukubaensis*. One of the factors known to have a significant role in tacrolimus fermentation yields is dissolved oxygen (Singh and Behera 2009). In our work-package we addressed the molecular events that relate oxygen levels and tacrolimus yields in order to unveil the molecular mechanisms associated with oxygen-related regulation in aerated submerged cultures.

Integrated in the IMMUNOTEC consortium the objectives for this PhD project were:

- To characterize the oxidative-stress response in *Streptomyces tsukubaensis* NRRL 18488

- To evaluate the influence of intracellular ROS homeostasis in the production of tacrolimus.

- To functionally characterize, through the construction of mutant strains, oxidative-stress related genes in *Streptomyces tsukubaensis* NRRL 18488.

CHAPTER 2

Material & Methods

2.1 BACTERIAL STRAINS, VECTORS, MEDIA AND GROWTH CONDITIONS

2.1.1 Bacterial strains

The bacterial strains used in this work were:

***Escherichia coli* DH5α** (Hanahan 1983) is a strain commonly used to transform and replicate plasmid DNA, due to the high transformation efficiency of its competent cells (up to 5 x 10^8 transformants per mg of plasmid DNA) and its low recombination rates. Genotype: *F*⁻ (φ80d *lacZ*Δ*M15*) Δ(*lacZYA-argF*)U169 *thi*-1 *rec*A1 *rel*A1 *end*A1 *hsd*R17 (r^{-k}, m^{+k}) *gyr*A96 *sup*E44 λ⁻.

***Escherichia coli* BW25113 [pIJ790]** (Datsenko and Wanner 2000) is a strain containing the plasmid pIJ790 that includes a cloramphenicol resistance gene and a L-arabinose inducible operon that codes for the λ RED recombinase system. Plasmid pIJ790 contains a temperature sensitive origin of replication that requires 30ºC for replication. Genotype: Δ*(araD-araB)567*, *ΔlacZ4787(::rrnB-4)*, *lacIp-4000(lacIQ)*, λ⁻, *rpoS369(Am), rph-1*, Δ*(rhaD-rhaB)568, hsdR514*.

***Escherichia coli* ET12567 [pUZ8002]** (Bierman *et al.* 1992) displays cloramphenicol resistance and it is used as a donor strain in the DNA transfer by intergeneric conjugation. Furthermore, it is a *dam*⁻ strain, i.e. it does not methylate DNA, which is an advantage to circumvent the methylspecific restriction system present in *Streptomyces*. The plasmid pUZ8002 contains a kanamycin resistance gene and the necessary genes to perform conjugation (*tra* genes). Even though it is not a mobile DNA plasmid *per se* (it does not possess an origin of transference), it is necessary for the mobilization of other vectors. Genotype: *dam*⁻ 13:Tn9, *dcm*⁻ [6], *hsd*M.

***Saccharomyces cerevisiae* BY4741** (Euroscarf) is the *Saccharomyces cerevisiae* strain used for growth inhibition bioassays. Genotype: MATa, *his3*Δ1, *leu2*Δ0, *met15*Δ0, *ura3*Δ0.

***Saccharomyces cerevisiae* TB23** (Breuder *et al.* 1994) is the *Saccharomyces cerevisiae* strain sensitive to tacrolimus used to confirm tacrolimus production.

Genotype: MATα *ilv5*Δ *ura3*Δ *leu2*::*hisG* [*rho*^{0}].

***Streptomyces tsukubaensis* NRRL 18488** (Kino *et al.* 1987) is the tacrolimus producing strain used as our working model to construct knock-out mutants on antioxidant related genes.

***Streptomyces natalensis* ATCC 27448** (Struyk *et al.* 1957) is the pimaricin producing strain also used as a work model to construct knock-out mutants on antioxidant related genes.

***Streptomyces avermitilis* MA-4680** (Burg *et al.* 1979) is an avermectin and filipin producing strain whose genome is completely sequenced and available.

***Streptomyces coelicolor* M145** (Bentley *et al.* 2002) is a derivative of *S. coelicolor* A(3)2 lacking its two plasmids: SCP1 and SCP2. It is an actinorhodin and undecylprodigiosin producer.

2.1.2 Vectors

All the plasmid vectors and cosmids used in this work as well as their purpose and characteristics are listed in Table 2.1

Table 2. 1 - Vectors and cosmids used in this work.

Plasmid or cosmid	Description	Reference or source
pGEM®-T Easy	High copy number plasmid used for general cloning. Size: 3 kb. *Amp*^{r}	PROMEGA
pIB139	Conjugative, integrative vector derived from pSET152, containing the strong constitutive promoter *ermE**p. Size: 5.9 kb Apra^r	(Wilkinson *et al.* 2002)
pET-30a	Cloning vector carrying a N-terminal/C- terminal His-tag used for protein overexpression in *E. coli* – vector size*:* 5.4 kb. Kan^r	Novagen
cos10B10	Cosmid vector 10B10 containing the *katA1* coding sequence from *S. tsukubaensis*, used for PCR-targeting mutagenesis. Kan^r, Amp^r	This work
cos1C4	Cosmid vector 1C4 containing the *katA1* coding sequence from *S. tsukubaensis*, used for PCR-targeting mutagenesis. Kan^r, Amp^r	
cos4D4	Cosmid vector 4D4 containing the *katA1* coding sequence from *S. tsukubaensis*, used for PCR-targeting mutagenesis. Kan^r, Amp^r	
cos18F2	Cosmid vector 18F2 containing the *katA1* coding sequence from *S. tsukubaensis*, used for PCR-targeting mutagenesis. Kan^r, Amp^r	
cos15C1	Cosmid vector 15C1 containing the *ahpC, oxyR and sigG* coding sequences from *S. tsukubaensis*, used for PCR-targeting mutagenesis. Kan^r, Amp^r	
cos6E6	Cosmid vector 6E6 containing the *sodA* coding sequence from *S. tsukubaensis*, used for PCR-targeting mutagenesis. Kan^r, Amp^r	

2.1.3 Culture media

When the use of antibiotics was required, their addition to the media was done after sterilisation in autoclave. Antibiotics were sterilised by filtration using 0.2 µm pore filters (Whatman), with the exception of antibiotics solubilised in organic solvents.

2.1.3.1 Escherichia coli *culture media*

All media were sterilised for 20 min at 121 ºC. For solid media 2 % (w/v) agar was added.

LB (Sambrook and Russell 2001): 1 % (w/v) tryptone, 0.5 % (w/v) yeast extract and 0.5 % (w/v) NaCl. pH was adjusted to 7.

SOB (Hanahan 1983): 2 % (w/v) bacto-tryptone, 0.5 % (w/v) yeast extract, 10 mM NaCl, 2.5 mM KCl. The pH was adjusted to 7.0 and before use $MgCl_2$ and $MgSO_4$ were added at a final concentration of 10 mM.

2.1.3.2 Saccharomyces cerevisiae *culture media*

Media were sterilised for 20 min at 110 ºC. For solid media 2 % (w/v) agar was added.

YPD : 1 % (w/v) yeast extract, 2 % (w/v) bactopeptone, 2 % (w/v) glucose.

2.1.3.3 Streptomyces *culture media*

All media were sterilised for 20 min at 121 ºC, unless stated otherwise.

MG modified (MGm) (Doull and Vining 1989)**:** 5% (w/v) Difco soluble starch, 60 mM glutamic acid, 100mM MOPS, 0.8 mM $MgSO_4 \cdot 7H_2O$, 9 µM $CaCl_2$, 17 µM NaCl, 100x concentrated trace elements solution (70 µM $CuSO_4 \cdot 5H_2O$, 40 µM H_3BO_3, 13 µM $(NH_4)_6Mo_7O_{24} \cdot 4H_2O$, 1.63 µM $MnSO_4 \cdot 1H_2O$, 1400 µM $ZnSO_4 \cdot 7H_2O$) is added to the medium at a final concentration of 1x. The pH is adjusted with NaOH to 6.5. Media was sterilised for 15min at 121ºC, after which is supplemented with $FeSO_4$ to a final concentration of 32 µM and with potassium phosphate to a final concentration of 2.5mM.

ISP4 (ref. 277210 difco™ ISP Medium 4): For 100 mL of medium dissolve 3.7 g of Difco™ ISP Medium 4 in water with agitation, boiled for 1min and then sterilised for 15 min at 121ºC.

YED (Gil *et al.* 1985): 1 % (w/v) yeast extract, 1 % (w/v) glucose. The pH was adjusted to 7.0. Media was sterilised for 20 min at 110 ºC.

TBO (Higgens *et al.* 1974): 2% (w/v) tomato paste, 2% (w/v) oat flakes and 2.5% (w/v) agar. The pH was adjusted to 6.5.

YEME (Chater *et al.* 1982): 0.3 % (w/v) yeast extract, 0.5 % (w/v) peptone, 0.3 % (w/v) malt extract, 1 % (w/v) glucose and 5 mM $MgCl_2$. The pH was adjusted to 7.0. Media was sterilised for 20 min at 110 ºC.

2XTY (Sambrook and Russell 2001): 2 % (w/v) tryptone, 1 % (w/v) yeast extract, 86 mM NaCl.

2.1.4 Growth conditions

E. coli strains were grown at 37ºC or 30ºC according to strain requirements. Orbital agitation at 100-200 rpm was used to culture *E. coli* in liquid media. For long term storage, *E.coli* strains were stored at -80 ºC as cell suspensions in 20 % (w/v) glycerol. *Saccharomyces cerevisiae* strains were grown at 30ºC with orbital agitation at 150 rpm. For long term storage, *Saccharomyces cerevisiae* strains were stored at -80ºC as cell suspensions in 50 % (w/v) glycerol.

Streptomyces strains were grown at 28 ºC. Spores from *S. tsukubaensis* were obtained by growing in ISP4 solid medium for 8-10 days. Given the genomic instability of *S. tsukubaensis* strains, it was very important to assure that the spore stocks were prepared from one “good” isolated colony. For that a dilution of spores were spread on ISP4 solid medium in order to isolate a colony. After 4-8 days, the selected colony was spread on ISP4 solid medium. After 8-10 days spores are overlaid with 8 mL 30 % (w/v) glycerol and 0.025 % (v/v) Triton X-100, scraped from the plate and filtered. Spores from *S. natalensis* were obtained by growing in TBO solid medium for 8-12 days. The quantification of *S. tsukubaensis* spores was performed by measuring the optical density at 450 nm and using the formula: 1 OD_{450} = $3.15x10^8$ cfu mL^{-1}. Quantification of *S. natalensis* spores was performed by measuring the optical density at 600 nm and using the formula established for *S. coelicolor* (Kieser *et al.* 2000). For *S. tsukubaensis* liquid cultures 100 mL of MGm medium in 500 mL unbaffled flasks was inoculated with 10^7 spores (with a ratio of flask volume *vs* medium culture of 5). Cultures were incubated with an orbital agitation at 220 rpm, at 28ºC for 8 days. *S. natalensis* cultures were

inoculated in 100 mL YEME media in 1 L baffled flasks with $3x10^8$ spores (with a ratio of flask volume *vs* medium culture of 10), with an orbital agitation at 250 rpm, at 28ºC for 3 days.

2.2 DNA PROCEDURES

2.2.1 *Streptomyces* genomic DNA extraction

Streptomyces genomic DNA was obtained with the "Master™ pure Gram-positive DNA purification kit" (Epicentre). The protocol provided by the manufacturer was subjected to minor modifications namely: 1) the RNase A treatment was performed during the last 30 min of the 2h incubation of *Streptomyces* pellets with lysozyme; 2) after protein purification samples were treated with 1 vol of phenol-CIA (25 phenol: 24 chloroform: 1 isoamyl alcohol) saturated with 10 mM Tris pH 8.0 and 1 mM EDTA.

2.2.2 Polymerase chain reaction - PCR

The polymerase chain reaction (PCR) was used to obtain a high number of copies of a certain DNA fragment. PCR reactions with DNA template from *Streptomyces* included dimethyl sulphoxide (DMSO) at a final concentration of 5 % (v/v) due to the high G+C content typical of actinobacterial genomes. In the course of the laboratorial work two DNA polymerases were used: GoTaq® (Promega) and *Pfu* (Fermentas). All primers were designed using the computer software Vector NTI Advance™ 11 (Invitrogen) and are listed on Tables 2.2 and 2.3.

Table 2. 2 – List of primers used in this work.

Primer name	Primer sequence (5'→3')	Purpose
catA_F	CGACCTSACCAAGGTSTG	Probe generation for cosmid library screening
catA_R	TTGAYGCCGASGCGGTAG	
sodF_F	RYCCSSAGATCATCGAGC	
sodF_R	TGSAGRTAGAAGGCGTGC	
ahpC_F	CTGTCGGTGACAAGTTCCCC	
ahpC_R	GSTCCAGTTGCACGGGCA	
Tsodfish_F	CCGGTGACGCTTATTGCACATCC	
Tsodfish_R	GAACCTGGTGCTGACACCGC	
TahpC_F	GTGGATTTGTCCAACC	
TahpC_R	GGACTTGTGGTTGATG	
RED_ahpC_F	TTGATCAATTTCACCGGCGATCGCGGGTATGACAGGGT GATTCCGGGGATCCGTCGACC	*aac(3)IV-oriT* cassette amplification
RED_ahpC_R	CGGTATGGCGGACTTCAGCGCGTCGAGCGACACGGGT CATGTAGGCTGGAGCTGCTTC	
RED_oxyR_F	ATTAACATCAAGGGGAACGATAGGGAGAAGGAATCAAT GATTCCGGGGATCCGTCGACC	
RED_oxyR_R	GCGCGCCCCGCAGCGACCGCGCGACTAGCTAGCTAGC TATGTAGGCTGGAGCTGCTTC	
RED_sigG_F	GTGTTTCCCGGTGGTGCTGCTGATACGAAGAGAGGTAT GATTCCGGGGATCCGTCGACC	
RED_sigG_R	CACGGGAAAGGAATCGGCGGACTGTTGTGACCCGGGT CATGTAGGCTGGAGCTGCTTC	
RED_sodA_F	TGTGCAATAAGCGTCACCGGAGGGACCGGACACACCAT GATTCCGGGGATCCGTCGACC	
RED_sodA_R	CGGGGCCACCGGCCCCGGCCGTACCGGTTCACCCGGT CATGTAGGCTGGAGCTGCTTC	
T_ahpC_F	GTGGATTTGTCCAACC	Gene deletion confirmation
T_ahpC_R	GGACTTGTGGTTGATG	
RED_conf_oxyR_F	ACCTCTCTTCGTATCAGCAGCA	
RED_conf_oxyR_R	TAGCACCGAGTAGCCGCGAA	
aac(3)_IV_R	CGGAAGTGCAGATGCTCGGC	
oxyR_R	AACCGAGCAAAGGCATGACC	
RED_conf_sodA_F	ATAAGCGTCACCGGAGGGA	
RED_conf_sodA_R	ACGATCACGAGCAGGACGA	
tsku_erm_katA1_F	CGGGATCCGACCAAAGGAGGCGGACATATGACGCAGG GACCGCTCACCA	Amplification for gene overexpression
tsku_erm_katA1_R	CCTCTAGATCAGCCGCGCAGGGCCTGGAC	
tsku_erm_sodA_F	GACATATGGCCATCTACACGCTGCCC	
tsku_erm_sodA_R	CCTCTAGAGGTCAGGGGGCGATCAGCGAAGT	
tsku_erm_sodN_F	GACATATGCTCTCCCGCCTGTTCGCA	
tsku_erm_sodN_R	CCTCTAGAGGTCAGGCCTTCTTGGTCTCCCA	
pIB_U_F	GGCTTGCGCCCGATGCTAGT	Confirmation of pIB139 integration
pIB_U_R	CCGGCTCGTATGTTGTGTGG	
SP_pIBkatA1R	TCCACTGCGACACGTCCCTG	
SP_pIBsodAR	TATGGCCGGAGAGGTGGAAC	
SP_pIBsodNR	CGCTCCACAGCACCGAGATG	
STSU_attB_F	GTGTCCGTCCAGCTCACCG	
oxyR_GSP1	ACAGCGGGATCTCGGTGACC	RACE
oxyR_GSP2	ATTACGCCGAGCCGCAGGAC	

Primer name	Primer sequence (5'→3')	Purpose
oxyR_GSP3	AGCAGCCCAGCCTGTCGCAA	
ahpC_GSP1	CGGTCACCATCGTGAACTGG	
ahpC_GSP2	TTGGAGTCGGCCAGCATCG	
ahpC_GSP3	CCACCTTCGAACTGACGGC	
Adapter Primer	GGCCACGCGTCGACTAGTACTTTTTTTTTTTTTTTT	
STSU_his_oxyR_F	GAATCATATGGCTACGGCGAACCG	OxyR amplification for OxyR-His_6 construction
STSU_his_oxyR_R	GGGTCGACTCCGGGGGCGGAATCCGT	
Ctg_348_F	ATGGCTACGGCGAACG	OxyR sequencing
Ctg_349_R	CTGGTCGGGGCGCGGG	
EMSA_padR1_F	ACCGATGGACATGGTCCGAC	EMSA
EMSA_padR_IR1_F	GCACAGCGCGGAGCGCCCGC	
EMSA_ahpC1_R	GCCGACAGTGAGCACAGTGT	
EMSA_sigG_F	CGCCACCCTGGTCGCTCATA	
EMSA_oxyR_R	CGGTTCGCCGTAGCCATTGA	
EMSA_katA1_F	CTCCTGCGTCATCCCTGCTT	
EMSA_katA1_R	CAGGTCACTCATAAGGGCCA	
EMSA_katA2_F	CAGCGGAGTGGCGAGCAGTT	
EMSA_katA2_R	GGGTATCGGACACGAGCGTC	
EMSA_dtxR_F	AGATGCTCCGGGAGCCCGTT	
EMSA_dtxR_R	CGTGGTGTCGATCAAACCGG	
EMSA_phoR_F	TGGTACGCGTCCCGCATGGA	
EMSA_phoR_R	GCGTTCACGTCCATGCCTCA	
EMSA_SCO_F	GCAGGCGGTCAGGTCGAACT	
EMSA_SCO_R	TCACGGAAGTGCAGGTGCTC	

Table 2. 3 - **Primers used for RT-PCR and RT-qPCR**

Primer name	Primer sequence (5´→3´)	Amplicon length (bp)	Target
Tsu_hrdB_F	GCGGCACTGACCATCAGCGT	87	Reference genes
Tsu_hrdB_R	GATTCCGCCAACCCAGTGGA		
Tsu_rpsP_F	GCGCCGACGGAAAGCCAGTA	94	
Tsu_rpsP_R	CCATCGAGGAGATCGGCCTG		
Tsu_fkbR_F	CTTGGGAACGTCCTGCCTTC	90	Tacrolimus biosynthetic gene cluster
Tsu_fkbR_R	GTCTTGACGTTGAAGTGCCG		
Tsu_fkbN_F	TGAACTGATCGCTCGTGACG	127	
Tsu_fkbN_R	CTCCAGCAGTGCCGTCTTGC		
Tsu_allN_F	GTTGTCCTGGATTCGATAGA	153	
Tsu_allN_R	ACCTCTGATCACACCTGCCT		
RT_fkbL_F	TCAGCGCGATATCAAGCAGA	174	
RT_fkbL_R	ATGAACTCGATGACGCCGGG		
RT_fkbO_F	CGAACGCCTCCTCCTCGAAGGT	138	
RT_fkbO_R	TCGTGCCGTCGGACCTCGAA		
RT_fkbB_F	TCGGCCTGTGCACGAATTGCTG	178	
RT_fkbB_R	TCCGAGCAGCAGCGCGATAC		
RT_fkbG_F	CCGGTCAACCGCACCAGGAA	125	
RT_fkbG_R	TCACTGCGGGACGACAGGGT		
RT_fkbK_F	GGAACGGAACGGCGGATCCT	160	
RT_fkbK_R	CGGACGTGTCGACGAGTGTG		
RT_allA_F	TCGTGATCGGATTCGAGCAG	86	
RT_allA_R	GAGGAGTTCCGGCTGAAGCC		
RT_allP_F	CGGGAAGGCGGGCCAGTGTT	100	
RT_allP_R	CGTGGAGGCGTGGTCGGTCA		
Tsu_katA1_F	CTCCGGTCGCCGACAACCAGAA	100	Oxidative stress related genes
Tsu_katA1_R	CGGTTGAAGTGCGCGAGCTT		
Tsu_katA2_F	GTGTCGGCGGCGTTGACTGA	104	
Tsu_katA2_R	GCGTTGTTGGTGGTGTAGGGG		
Tsu_sodN_F	ATGCTCTCCCGCCTGTTCGC	121	
Tsu_sodN_R	TCTCCTGGACGGCCTTGACC		
Tsu_sodA_F	GCCATCTACACGCTGCCCGA	121	
Tsu_sodA_R	TAGGCGGCGTGGTGCTTGTC		
Tsu_ahpC_F	TCAGCACCATGGAGTGACACTG	95	
Tsu_ahpC_R	AACTCCTTGCCGCTCTCGAG		
Tsu_oxyR_F	CAGCCCAGCCTGTCGCAACT	100	
Tsu_oxyR_R	AGAGCGCGGGCTGACTCATG		
Tsu_catR_F	TGTTGGAACGACTCCGTGGA	103	
Tsu_catR_R	ACCTCGTCGGCGGTCAGATG		
RT_Nur_F	ACCACCGACTGGCAGAGCGA	99	
RT_Nur_R	AGTGGCGTGCTCCAGGGTGT		
RT_dps_F	CCCAGCGCGTCCACCATGAT	187	
RT_dps_R	TCCAGCTCGACGAGGTCGTC		
stsu_11555_F	CCGAACTGCTCCAGGGCGAT	114	*oxyR* and *ahpCD* genomic region
stsu_11555_R	GGACAGGCTGATCGGCACCT		
RT_sigG_F	GACGGTCATATCGAGGGCGT	102	
RT_sigG_R	GTGATCCAGCATCTGCCGCC		

Primer name	Primer sequence (5´→3´)	Amplicon length (bp)	Target
stsu_11580_F	GTCGACCTCGACGAGTCCGTTCTT	137	
stsu_11580_R	TCGAATCCGGCCCTCGTCAC		
stsu_11595_F	CGACGACACCTTGCCGAGGA	122	
stsu_11595_R	TGTTCGCGTACCAGGCCACC		
Tsu_phoP_F	GAGTGCTCGTCGTCGAGGAC	146	Phosphate metabolism
Tsu_phoP_R	GAGAAGGACGAGATCGGCGC		
Tsu_phoR_F	GGTCTGCTGACCGGCGTCTT	137	
Tsu_phoR_R	AGCGCAGTACGGAGAGGACC		
Tsu_phoU_F	CCAGATCGTGCTGGAGATCGTCGA	174	
Tsu_phoU_R	GGGACGCGTACCACGAGGAA		
Tsu_pstS_F	GAACCGGACGCCAGGAGCTT	102	
Tsu_pstS_R	GGACGACAACACGAGCAGCA		
RT_pitH1_F	AGGGAGACGAGCTTCTACGA	176	
RT_pitH1_R	AGCTGGTGGAAGATGGCATG		
RT_pitH2_F	GCCGGGATCAGGACCTTGGT	105	
RT_pitH2_R	TTCCTCGCACGCCCTCATGG		
RT_glnD_F	TCCCAGACCGGGTACCAGATGC	151	Nitrogen metabolism
RT_glnD_R	TAACCGGCTCCGCACTGGTC		
RT_glnK_F	TCCTCGGCGAGGACTTCGAT	155	
RT_glnK_R	ATCAAAGAGGCGCTCCAGGC		
RT_glnR_F	CCCGTCGACCAGGATCACGT	80	
RT_glnR_R	TGCACAACGTACGGGTGGCT		
RT_glnII_F	GGGCAGGAGTACACCGGCTT	122	
RT_glnII_R	TCCAAGACCCGGATCCTTCC		
RT_glnA_F	CAGCGCCATGTCGGACTCGT	96	
RT_glnA_R	ATCCCGGCGAGCGTCTTCGA		

2.2.3 Southern blot hybridization

In Southern blotting analysis, DNA was first digested by restriction endonucleases and the resulting fragments were separated by electrophoresis in a 0.8 % (w/v) agarose gel. DIG labelled λ phage DNA digested with *Hind*III was used as a ladder. DNA transfer from the agarose gel to a nylon membrane was carried out in a vacuum system (Bio-Rad) and following the manufacturer's instructions. DNA probes were labelled with digoxygenin using “DIG-High prime” kit (Roche) and following the protocol provided by the manufacturer. Generally, 500 ng of DNA probe were used in the digoxigenin labelling procedure. Hybridisation and detection were performed following the manufacture’s instructions using the alkaline phosphatase substrate CPD-Star (Roche).

2.2.4 Gene deletion in *Streptomyces* using the Redirect technology

Redirect© technology is a two-step PCR-based method in which a target gene is replaced by a resistance cassette through double recombination (Sambrook and Russell 2001). In the first step, the target gene present in a cosmid is replaced by a resistance cassette through homologous recombination. In the second step, the mutated cosmid is transferred to *Streptomyces* (intergeneric conjugation) and the target gene chromosomal loci is replaced by the resistance cassette also through homologous recombination.

For *Streptomyces* mutants construction, it was used an apramycin resistance cassette from plasmid pIJ773 - *aac(3)IV-oriT*. This resistance cassette was amplified using primers listed in Table 2.2 and *Pfu* DNA polymerase. The amplification product was purified and introduced in *E. coli* BW25113 [pIJ790] harbouring the cosmid with the target gene. The induction of λ RED recombination system catalysed the replacement of the target gene by *aac(3)IV-oriT*. The mutated cosmid was then purified, transformed in *E. coli* ET12567 [pUZ8002] and transferred to *Streptomyces* by intergeneric conjugation. Double recombinant exconjugants were resistant to apramycin (selective marker of the resistance cassette) and sensitive to kanamycin (due to the loss of the cosmid). Double recombinants were confirmed by PCR and Southern Blot hybridisation.

2.3 RNA PROCEDURES

2.3.1 RNA isolation

Samples for gene transcription studies were taken at 72 h, 96 h and 120 h of growth. For H_2O_2 induced stress experiments, samples were taken at 72h (t0) and 15 min after the addition of 5 mM H_2O_2 (t1). Culture aliquots were mixed with two volumes of “RNA Protect Bacteria Reagent” (Quiagen) and maintained for 5 min at room temperature. Cells were harvested by centrifugation and immediately frozen by immersion in liquid nitrogen. RNeasy® Mini kit (Quiagen) was used for RNA isolation according to manufacture instructions with modifications described elsewhere (Beites *et al.* 2011). Total RNA concentration was determined with a NanoDrop ND-1000 spectrophotometer (Thermo Scientific) and RNA quality and

integrity were checked in an Experion™ Automated Electrophoresis System (Bio-Rad).

2.3.2 RT-qPCR and RT-PCR

For cDNA synthesis, 1µg of DNase I-treated total RNA was transcribed with the iScript™ Select cDNA synthesis kit (Bio-Rad), using the random primers supplied in a final volume of 20 µL and following the manufacturer's instructions.

qPCR amplifications were performed in an iCycler iQ5 Real-Time PCR Detection System (Bio-Rad) using the primer pairs listed in Table 2.3 and using 0.2 µM of each primer, 10 µL of KAPA SYBR FAST® qPCR Master Mix (KAPA Biosystems) and 2 µL of template cDNA (dilution 1/4). qPCR conditions were as follows: 95ºC for 3 min; 40 cycles of 95ºC for 3 sec, 60ºC or 65ºC (depending on the set of primers used) for 30 sec and 72ºC for 30 sec. Standard dilutions (1/2, 1/4, 1/8, 1/16) of the cDNA were used to check the relative efficiency and quality of each primer pair. Negative controls (non-template control) were included in all qPCR. A melting curve analysis was performed at the end of each qPCR to exclude the formation of nonspecific products. RT-qPCR analysis included three biological replicates and technical triplicates for each cDNA. The data obtained was analysed using the method described by PfaffI (Pfaffl 2001). For each analysis 16S rRNA and *hrdB* were used for normalization. The identity of each amplified product was corroborated by sequencing the PCR product.

RT-PCR amplifications were performed using GoTaq (Promega) with the primers listed in table 2.3. Primers were designed to generate PCR amplicons in the range of 80-200 bp and an annealing temperature of 61ºC, exception for primer pair Tsu_phoP_F+Tsu_phoP_F R that required an annealing temperature of 65ºC. The cycle number for each gene was tested and optimize. For each analysis 16S rRNA and *hrdB* were used as control.

2.3.3 Transcriptional Start Point identification by Rapid Amplification of cDNA Ends (5' RACE):

The 5'-ends of *oxyR* and *ahpC* transcripts was identified using the 5'-RACE system (Invitrogen), following the manufacturer's instructions (version 2.0). First strand cDNA synthesis was carried out using 4 µg of RNA, SuperScript™II reverse

transcriptase, and the gene-specific primer GSP1 (Table 2.2). cDNA was purified using the SNAP columns provided in the kit, and poly(dC) tails were added to the 3'-ends using terminal deoxynucleotidyl transferase. PCR amplification of the tailed cDNA was carried out using the 5'-RACE abridged anchor primer with the first nested primer GSP2 (Table 2.2). A dilution of the PCR mixture then was subjected to reamplification using a third nested primer GSP3 (Table 2.2) and GSP2 to confirm specificity. The PCR products were gel-purified, cloned into pGEM®-T Easy and sequenced. When cDNA tailing with poly(dC) did not permit the correct identification of the transcription start point, poly(dA) tails were added to the 3'-ends of cDNA. All primers used in RACE experiment are listed in Table 2.2.

2.4 PROTEIN PROCEDURES

2.4.1 Protein crude extracts and protein quantification

Protein crude extracts were obtained from 1 mL of culture broth which were washed once with 50 mM potassium-phosphate buffer, pH 6.8 and resuspended in the same buffer containing 25% (v/v) of protease inhibitor (Roche). Cell lysis was achieved by sonication (Branson Sonifier, Model B-15) using 3 cycles of 10 sec, duty cycle 50 % and an output of 3. The lysate was centrifuged and the supernatant was recovered. Protein content of cellular extracts was determined by the BCA™ Protein Assay Kit (Pierce) and bovine serum albumin was used to determine standard curves.

2.4.2 Enzymatic activities determination

2.4.1.1 Catalase activity

Catalase activity was measured spectrophotometrically (Shimadzu UV-240) by following the rate of decrease in absorbance at 240 nm caused by the disappearance of H_2O_2 (Beers and Sizer 1952). Assays were carried out at 25 ºC. Catalase activity was expressed in units per mg of total protein (U mg^{-1}) in which one unit of enzyme activity is defined as the amount required for the conversion of 1 µmol substrate into product min^{-1}.

Catalase activity was also monitored on native-PAGE gels, using a specific negative staining (Clare *et al.* 1984). Gels are soaked into a solution of horseradish peroxidase, which catalyses the conversion of diaminobenzidine into a brown compound, using H_2O_2 as a co-factor. In the area(s) of the gel corresponding to proteins displaying catalase activity, the H_2O_2 is degraded and therby an uncoloured band becomes visible. Electrophoresis was performed on 7.5% (w/v) native polyacrylamide gel.

2.4.1.2 SOD activity

The spectrophotometric measurement of SOD activity is based on the inhibition of the reduction of cytochrome c by the superoxide anion (Beauchamp and Fridovich 1971). The degradation of xanthine by xanthine oxidase generates superoxide anion, which reduces cytochrome c. The rate at which cytochrome c is reduced is measured in a spectrophotometer at 550 nm (Shimadzu UV-240) and at 25 ºC. The addition of protein extracts containing SOD in the reaction will destroy some of the superoxide anion generated by the action of the xantine oxidase, which will decrease the cytochrome c reduction rate. Thus, 1 Unit of SOD activity corresponds to a 50 % decrease in the cytochrome c reduction rate in 1 min. The final SOD specific activity was expressed in SOD activity units per mg of protein.

SOD activity was also monitored in native-PAGE gels by a negative specific staining (Beauchamp and Fridovich 1971). The light induced reduction of riboflavin by TEMED was used to generate superoxide anion. This particular ROS reacts with nitroblue tetrazolium (NBT) forming a blue precipitate. Proteins with SOD activity detoxify the superoxide anion and hence no NBT is reduced, leaving that gel area colourless. Electrophoresis was performed on 10% (w/v) native polyacrylamide gel.

2.4.3 Western-blotting

Cell-free protein crude extracts (10 µg of total protein) were loaded into the gel and electrophoresis was performed on a 10% (w/v) denaturing SDS-PAGE. Proteins were then transferred to a nitrocellulose membrane “HybondTM–C Extra” (Amersham). Briefly, the protein transference process was carried out in a “V20 Semi-Dry Blotter” (Scie-Plas Ltd.), in a semi-dry transference with the following

solution [60 mM Tris, 35 mM glycine and 0.05 % (w/v) SDS] and applying an electric current intensity of 0.8 mA per cm^2 of nitrocellulose membrane, for 1 h. Next, the membrane was blocked 16-18h at 4ºC with 5 % (w/v) dry milk in TPBS [137 mM NaCl, 2.7 mM KCl, 4.3 mM Na_2HPO_4, 1.47 mM KH_2PO_4 and 1 % (v/v) Tween-80], rinsed twice in TPBS, incubated with anti-cpeB, in a 1:10000 dilution for 2 h, rinsed twice in TPBS and incubated with the secondary antibody goat anti-rabbit IgG-peroxidase (SIGMA) in a 1:5000 dilution for 1.5h. In the case of the Western blot using an antibody raised against His tag, His-probe (Santa Cruz Biotechnology) the membrane was blocked for 1h and incubation with anti-His, in a 1:500 dilution was performed ON at 4ºC. Incubation with the secondary antibody anti-mouse, in a 1:3000 dilution was performed for 1h. Washing steps and incubation processes were performed at room temperature for the anti-His antibody, however for the anti-CpeB they were performed at 37ºC, following the instructions described elsewhere (Zou *et al.* 1999). Detection was performed using the "ECL plus Western Blotting system" (Amersham) and following the instructions provided by the manufacturer.

2.4.4 Two dimensional Electrophoresis (2-DE)

In order to remove nucleic acids, 100 µg of total protein extract was incubated with 3 % (v/v) of Benzonase Nuclease (SIGMA) at 37 ºC for 30 min. Afterwards the sample had an additional cleaning step with "2-D clean up Kit" (GE Healthcare) following the instructions provided by the manufacturer. The pellet obtained after the clean-up step was resuspended in 350 µl of 8 M urea, 0.5 % (w/v) CHAPS, 0.5 % (w/v) Triton X-100, 0.2 % (w/v) DTT and 0.25 % (v/v) IPG Buffer 3-10 (Bio-Rad). The resulting homogenised solution was used for isoelectric focusing (IEF) in 17 cm precast IPG strips (Bio-Rad) with a pH gradient of 4-7. Rehydration of the IPG strips occurred for 16-18h at room temperature. IEF was performed in a "PROTEAN IEF Cell" (Bio-Rad). After positioning the strips in the focusing tray, two paper electrode pads per strip were moist, one with ddH_2O, for the pad to the anode, and other with 10 mM DTT, to the cathode. Finally, the strips were covered with mineral oil, to avoid evaporation and carbamylation, due to the presence of urea. Isoelectric focusing was performed using the following conditions: (i) a conditioning step of 250 V for 15 minutes, to remove salt ions and charged contaminants; (ii) a voltage ramping step that increases the voltage to the

maximum voltage, without exceeding the current limit of 50 μA/strip; (iii) a time of 60 000 V/h is programmed to complete the focusing process once the maximum voltage of 10 000 V is reached and (iv) a final hold step at 500 V is maintained until the run is stopped, to prevent diffusion of focused proteins or over-focusing artefacts. To solubilise focused proteins and to allow SDS binding for the second dimension, it was necessary to equilibrate focused IPG strips in the SDS equilibration buffer [6 M urea, 2 % (w/v) SDS, 0.1 mM EDTA, 30% (v/v) glycerol, 0.01% (w/v) bromophenol blue and 50 mM Tris-HCl pH 6.8]. The equilibration process is divided in two steps: a reduction of the sulphydryl groups, by incubation of the strips in the equilibration buffer with 1% (w/v) DTT for 20 min with gentle agitation and an alkylation of the sulphydryl groups where the strips are incubate in the equilibration buffer with 2.5% (w/v) iodoacetamide for another 20 min with gentle agitation. Second dimension was performed in a 12.5 % (w/v) SDS-PAGE gel using the "Ettan™ DALTsix Large Vertical System" (GE Healthcare). Electrophoresis conditions were: 25 mA per gel for 1 h and 350 mA for 6-8 h at 4ºC. IPG strips were positioned directly on top of the gel and to secure the strips, they were overlaid with melted 0.5 % (w/v) agarose prepared in SDS-PAGE running buffer. Gel staining was performed recurring to the silver staining method compatible with mass-spectrometry [Goromova 2006]. After electrophoresis, the gel was placed into a tray containing appropriate volume of fixation solution [50 % (v/v) ethanol, 12 % (v/v) acetic acid, 0.05 % (v/v) formalin]. The proteins were left to fixate ON at room temperature with gentle shaking. The fixation solution is removed and the gel was rinsed twice with 20 % (v/v) ethanol for 10 min each wash. Afterwards the gel was incubated with the sensitizing solution [0.02 % (w/v) $Na_2S_2O_3$] for 2 min, with gentle agitation. The sensitising solution was removed and the gels washed twice for 1 min with ddH2O. The water was removed and the gel was incubated with the silver staining solution [2 % (w/v) $AgNO_3$ and 0.076 % (v/v) formalin] for 20 min. After staining is complete, the gel is washed twice, briefly, with ddH_2O and then with the developing solution [6% (w/v) Na_2CO_3, 0.0004 % (w/v) $Na_2S_2O_3$ and 0.05 % (v/v) formalin]. The developing reaction is stopped as soon as the desired intensity of the spots is reached, with the terminating solution [12 % (v/v) acetic acid]. Gels can be kept in ddH_2O at 4 ºC in sealed plastic bags.

2D gels were scanned using the GS-800 densitometer (Bio-Rad). 2D gels were analysed with "PDQuest" software, version 8.0.1 (Bio-Rad CA). Data were normalised using the local regression model (LOESS) which is the most sophisticated normalisation method available in PDQuest. We performed an A-B analysis which is commonly used for experiments control *vs* treated. This method allowed the quantitative identification of differences between protein extracts from wild-type and mutant strains. A 2-fold change was defined as the threshold value. To complement this study the student t-test method was used (significance level of 90%). After the analysis, the spots of interest were cutted from the gels with a spot picker of 3.0 mm diameter. Protein identification was performed at the "Proteomic Unit" (IPATIMUP). Briefly, the gel pieces were digested with trypsin and the proteins digests were desalted and concentrated using ZipTips (Millipore). Samples were analysed in the "4700 Proteomics Analyser MALDI-TOF/TOF" (Applied Biosystems). Peptide mass fingerprint data was collected in MS reflector mode in the range of 700–4000 m/z and was calibrated internally using trypsin autolysis peaks.

2.4.5 Expression and purification of OxyR-His$_6$ protein

The *oxyR* gene from *S. tsukubaensis* (*STSU_11565*) was amplified by PCR using the primer pair STSU_his_oxyR_F/STSU_his_oxyR_R (Table 2.2) that introduced unique *Nde*I and *Sal*I sites at the 5'- and 3'-end of the gene, respectively. The amplified DNA fragment was digested with *Nde*I and *Sal*I, cloned into *Nde*I-*Sal*I-cut pET-30a vector (Novagen) generating pEToxyR$_{STSU}$ plasmid and confirmed by DNA sequencing. pEToxyR$_{STSU}$ was introduced into *E. coli* BL21-CodonPlus^{TM} (DE3) for protein expression.

E. coli BL21-CodonPlus^{TM} (DE3) cell carrying pEToxyR$_{STSU}$ were grown at 30ºC to an OD_{600} of 0.65 and, after induction with 0.5 mM IPTG, cultures were grown for additional 17h. Cells were harvested at 4000 g for 20 min, ressuspended in lysis buffer [20 mM Tris-HCl pH 7.9, 0.5 M NaCl, 20 mM imidazole, 1 mM $MgCl_2$, 1 mM PMSF, 0.2 mg mL^{-1} lysozyme and 10 µg mL^{-1} DNase] and lysed by sonication (Branson Sonifier, Model B-15). The insoluble material was removed by centrifugation (13 000 g for 20 min at 4ºC) and the supernatant was recovered and loaded on a His-Trap HP column (GE Healthcare). C- terminally His-tagged OxyR

was eluted using a 20 mM to 500 mM imidazole gradient in elution buffer [20 mM Tris-HCl pH 7.9 and 0.5 M NaCl] and monitored at 280 m. Fractions containing OxyR-His_6 protein were pooled, dialysed against storage buffer [20 mM Tris-HCl pH 7.9, 50 mM NaCl, 2.5 mM $MgCl_2$, 0.45 mM EDTA, 0.5mM DTT and 10% (v/v) glycerol] and concentrated by ultrafiltration (Millipore, 3kDa cut-off size). OxyR-His_6 protein was checked by 10% SDS-PAGE and Western analysis using a mouse monoclonal anti-His-tag antibody (Santa Cruz Biotechnology, Inc.). Protein concentration was determined with a NanoDrop ND-1000 spectrophotometer (Thermo Scientific) and protein was stored at – 80ºC.

2.4.6 Electrophoretic mobility shift assay (EMSA)

DNA fragments used as probes were obtained by PCR using the primers listed in Table 2.2; for the *oxyR* upstream region primers EMSA_sigG_F/EMSA_oxyR_R were used, for the *STSU_11580-ahpC* intergenic region two pair of primers were used, EMSA_padR__F/EMSA_ahpC_R and EMSA_padR_IR1_F/EMSA_ahpC_R, for the *katA1* upstream region primers EMSA_katA1_F/EMSA_katA1_R were used, for the *katA2* upstream region primers EMSA_katA2_F/EMSA_katA2_R were used, for the *dtxR* upstream region primers EMSA_dtxR_F/EMSA_dtxR_R were used and for the *S.coelicolor oxyR* upstream region primers EMSA_SCO_F/EMSA_SCO_R were used. DNA fragments obtained were confirmed by DNA sequencing. DNA fragments were labelled at both ends with digoxigenin with the DIG Oligonucleotide 3'-End labelling kit, 2nd Generation (Roche Applied Science). The purified OxyR-His_6 protein was incubated with 2 ng of labelled DNA probe in 20 µL of binding buffer [25 mM Tris-HCl pH7.9, 50 mM KCl, 5 mM $MgCl_2$, 0.5 mM DTT, 0.1 mg mL^{-1} herring sperm DNA, 2 µg mL^{-1} BSA and 10% (v/v) glycerol]. The reaction was incubated for 10 min at 30ºC and loaded onto a 4% polyacrylamide gel (29:1) native gel in 0.5X TBE (Tris-Borate-EDTA) buffer. After electrophoresis (90 V for 1h45 at 4ºC) DNA was electroblotted onto a nylon membrane (HyBond™-N, GE Healthcare) in 0.5X TBE buffer (45 min, 200 mA). The DNA was fixed by UV cross-linking, detected with anti-digoxigenin antibody and developed by chemiluminiscence with the CDP-Star™ reagent (Roche Applied Science).

2.4.7 Quantification of intracellular ROS levels

Intracellular H_2O_2 and $O_2^{\cdot -}$ levels were detected with dihydrorhodamine 123 (DHR) and Dihydroethidium (DHE) (Invitrogen) respectively. DHR is a non-fluorescent molecule that upon oxidation is transformed into a fluorescent molecule - rhodamine 123 (Royall and Ischiropoulos 1993). The ability to easily cross biological membranes makes DHR a powerful tool to measure the intracellular H_2O_2 levels. Dihydroethidium is a superoxide anion indicator that changes from blue-fluorescence to red- fluorescence upon oxidation. Aliquots of 1 mL from the culture broth were taken at selected time points, pellets were ressuspended in 500 µL 50 mM potassium phosphate buffer pH 6.8 and DHR and DHE were added to a final concentration of 15 µg mL^{-1} and 5 µg mL^{-1} respectively. Cells were incubated in the dark at 30 ºC for 60 min in the case of DHR and for 30 min in the case of the DHE probe. Mycelium samples were then washed twice in 50 mM potassium phosphate buffer pH 6.8 and cells were lysed by sonication. The amount of ROS was quantified with a spectrofluorometer (Fluoromax-4, Horiba) emiting at 504 nm and measurig at 534 nm for DHR and emiting at 355 nm and measuring at 420 nm for DHE. Total protein content of crude extracts was used as normalisation factor.

2.5 QUANTIFICATION OF IRON CONTENT

2.5.1 Chrome azurol S (CAS) assay for siderophore detection and quantification

Chrome azurol S medium was prepared as previously described (Bagg and Neilands 1987), without the addition of nutrients. The medium for 1 L of CAS was as follows: 60.5 mg CAS, 72.9 mg hexadecyltrimethyl ammonium bromide (HDTMA), 30.24 g piperazine-1,4-bis-(2-ethanesulfonic acid) (PIPES) and 1 mM $FeCl_3.6H_2O$ in 10 mM HCl. 1%(w/v) agarose was used as gelling agent. 1 mL of culture broth was centrifuged for 10 min and the supernatant was 5-fold concentrated using speed vacuum. Wells were performed in the CAS media and filled with 100 µL of the extracts. For the liquid CAS assay 1 mL of culture broth was centrifuged for 20 min to remove cells, 500 µL of supernatant was mixed with the same volume of CAS solution and 10 µl of 0.2 M sulfosalicylic acid. After 60

min of incubation at 30ºC absorbance was determined at 630 nm (Calugay *et al.* 2003).

2.5.2 Quantitative colorimetric iron determination

Aliquots of 1 mL were taken from the culture broth throughout growth to determine extracellular iron levels. Cells were centrifuged for 10 min and the supernatant was recovered and used to determine total extracellular iron content, using the kit QuantiChrom™ Iron Assay Kit (DIFE-250) and following the manufacturer's instructions. Briefly, 50 µL of supernatant were incubated with 200 µL of working reagent for 40 min at room temperature and absorbance was determined at 590 nm.

2.5.3 Flame atomic absorption spectrophotometry

Total intracellular iron content was determined by flame atomic absorption spectrophotometry. Briefly, 2.5 mL of cells were harvested by centrifugation at 13.400 rpm for 5min at 4ºC. The pellets were then washed three times with TE buffer (20 mM Tris-HCl, 5 mM EDTA, pH 7.7) and once with metal-free double distilled water to remove salts, resuspended in 100 µl of 65% HNO_3 (AAS grade), and heated at 75°C for 10min until cells were completely lysed. Finally 1mL of metal-free double distilled water was mixed with the lysed cells, centrifuged at 13400 rpm for 5 min and analyse the supernatant for iron content by flame atomic absorption (Philips, PU 9200X). 0.1 mg/L of iron equals 1.79 µM. Iron content was normalized to the protein concentration.

2.6 TACROLIMUS QUANTIFICATION

Tacrolimus production by *S. tsukubaensis* strains was quantified by HPLC. Briefly, 1 mL of culture broth was mixed with an equal volume of methanol and incubated for 1h at 30ºC. The mixture was centrifuged for 10 min. The supernatant was recovered and analysed in a HPLC system (Merck-Hitachi) equipped with UV detector set at 210 nm, with a SunFire™ C18 column (4.6 x 150 mm, 3.5 µm; Waters) and the oven set at 55ºC. Elution was performed with a gradient of a mobile phase composed of 0.1% (v/v) trifluoroacetic acid and 20% (v/v) MTBE in acetonitrile according to the following program (acetonitrile-MTBE concentration):

40% 0-5 min, up to 80% 5-35 min, up to 90% 35-36 min, 90% 36-39 min down to 40% 39-40 min and 40% 40-43 min. Flow rate was maintained at 0.5 mL min^{-1}. Chromatographic peaks corresponding to tacrolimus and ascomycin were identified using external standards (Sigma). To confirm peaks identification Relative Retention Time (RRT) was used. Unlike what happens with the Retention Time of compound (RT), which varies from system to system, the RRT of a compound is constant among systems. In the case of our compound of interest its RRT towards purified tacrolimus is 1 (RT/RTstd =1). If the RRT is <1 it elutes before our main peak; if the RRT is >1 it elutes after our main peak. In this case RRT of ascomycin was 0.96.

2.7 PIMARICIN QUANTIFICATION

Pimaricin in liquid cultures was routinely quantified by spectrophotometric determination at 304 nm. A 100 μL aliquot of culture was extracted with 8 vol of water-saturated butanol, and the organic phase was diluted in water-saturated butanol to bring the absorbance at 304 nm in the range of 0.1–0.8 absorbance units. Pimaricin volumetric concentration was quantified using a solution of pure pimaricin (Calbiochem) as standard. The specific pimaricin concentration of *S. natalensis* cultures was calculated by normalizing the volumetric pimaricin production with the protein concentration or dry weight. To confirm the identity of pimaricin, a UV–visible absorption spectrum (absorption peaks at 319, 304, 291 and 281 nm) was routinely determined.

2.8 OXYGEN CONSUMPTION

Oxygen consumption rate was assessed in mycelium samples grown in MGm medium using an oxygen electrode (Oxygraph, Hansatech). Experimental data was analyzed using the Oxyg32 V2.25 software and normalized by dry weight.

2.9 GROWTH INHIBITION ASSAYS

Agar-diffusion growth inhibition assays were performed to assess *Streptomyces* strains sensitivity to H_2O_2; 10^7 spores were inoculated into YED medium and disks containing 9 M of H_2O_2 were placed on top. The plates were

incubated at 30ºC and the growth was monitored for three days. The growth inhibition halo was measured for each strain using a Vernier caliper. For the bioassays to test tacrolimus role as an antioxidant the same procedures were applied with the addition of 1 M of H_2O_2, 1 µg of tacrolimus (Sigma) and 50 mM of ascorbic acid to the disks.

CHAPTER 3

The oxidative stress response and secondary metabolism in Streptomyces

3.1 THE OXIDATIVE STRESS RESPONSE AND SECONDARY METABOLISM IN *STREPTOMYCES*

Streptomyces bacteria are a prolific source of biologically active secondary metabolites, whose biosynthesis occurs in response to a wide variety of environmental and physiological conditions. The regulatory mechanisms that control secondary metabolism operate at different levels, from a high pleiotropic level to a pathway-specific one. Even though secondary metabolism regulatory networks have been widely studied in *Streptomyces* (for a review see Liu *et al* 2013) not much is known about the molecular mechanisms by which oxygen influences secondary metabolite production. Being an aerobic process, *Streptomyces* secondary metabolism is highly dependent on oxygen availability. However, high levels of oxygen can lead to the formation of reactive oxygen species (ROS) that can damage cell components. To counteract the toxic effects of ROS, microorganisms have developed an adaptive response that extends from the modulation of gene expression to changes in enzymatic and non-enzymatic activities. One example is catalase, a key enzyme in H_2O_2 detoxification.

The catalase activity profile of *S. natalensis, S. coelicolor, S. avermitilis* and *S. tsukubaensis* was monitored throughout the growth curve (EE-early exponential; LE-late exponential; S-stationary; LS-late stationary) in YEME liquid medium (Fig. 3.1). Two different growth-dependent catalase profiles could be observed. In *S. coelicolor* and *S. avermitilis* there was an induction of catalase activity in stationary phase. Note that it has already been described, for the conditions tested, that *S. coelicolor* produces actinorhodin and undecylprodigiosin, whereas *S. avermitilis* does not produce avermictin. The second profile was that of *S. natalensis* and *S. tsukubaensis* in which catalase activity gradually decreased during exponential phase until mid-stationary phase and then it was induced in late stationary phase. Again, one should note that under these conditions *S. natalensis* produces pimaricin while *S. tsukubaensis* does not produce tacrolimus. *S. tsukubaensis* catalase activity was also monitored in tacrolimus producing conditions (MGm medium). Interestingly, in these conditions, catalase activity profile radically changed and presented a dramatic increase of total catalase levels

during growth and an induction of catalase activity in late exponential phase (Fig. 3.1), temporally overlapping with tacrolimus production onset.

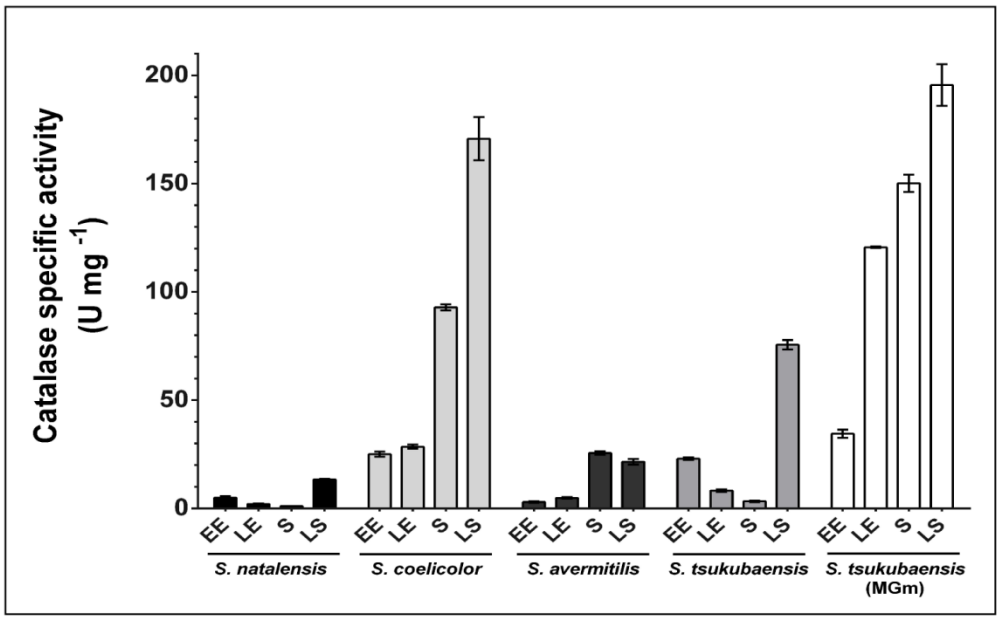

Figure 3.1 - Total catalase activity of *Streptomyces* strains. *S. natalensis*, *S. coelicolor*, *S. avermitilis* and *S. tsukubaensis* cultures were grown in YEME medium and in the case of the latter strain also in MGm medium. Catalase activity was determined spectrophotometrically at the four defined growth phases: EE - early exponential; LE - late exponential; S - stationary; LS - late stationary. Results (average of triplicates and standard deviation) are representative of three independent experiments.

A *S. natalensis* knock-out mutant on the monofunctional catalase, KatA1, was generated originating the strain *S. natalensis* CAM.05. The mutation led to a deregulation of H_2O_2 intracellular levels and to a modulation of pimaricin production. The *S. natalensis* mutant defective on the H_2O_2-detoxifying enzyme catalase, behaved as a pimaricin overproducer strain, reaching 156% of the pimaricin produced by the wild-type strain. It is worth noting that the pimaricin overproducer behaviour of the mutant strain CAM.05, was enhanced by the addition of H_2O_2 to the culture broths during late exponential phase, reaching 204% of the pimaricin produced by the wild-type strain (Fig. 3.2).

The results obtained suggested that H_2O_2 intracellular levels interplay with the regulation of *S. natalensis* secondary metabolism, since a deregulation of H_2O_2 intracellular levels resulted in a modulation of pimaricin production. In fact, the construction and characterization of additional *S. natalensis* knock-out mutants defective on other proteins involved in the oxidative stress response, showed that

maintaining H_2O_2 homeostasis is key to the onset and regulation of secondary metabolism in *S. natalensis* (Beites *et al.* 2011). Particularly, we showed that there is a positive correlation between H_2O_2 intracellular levels during late exponential/early stationary phases and pimaricin biosynthesis in *S. natalensis*.

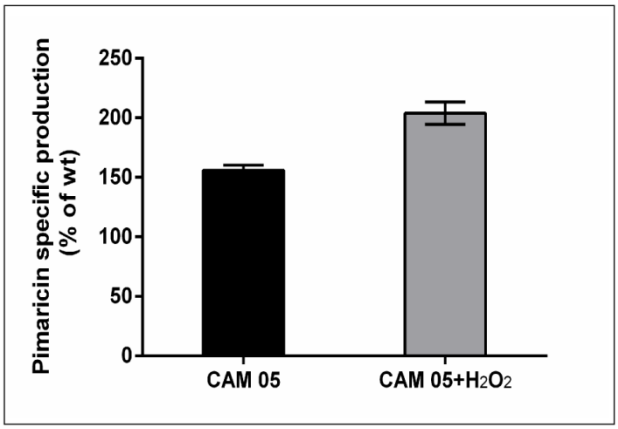

Figure 3.2 – Pimaricin specific production of **CAM.05 (Δ*katA1*)**. Pimaricin specific production of CAM.05 (Δ*katA1*) cultures grown in YEME medium. 1mM of H_2O_2 was added at late exponential phase. Pimaricin specific production was expressed as percentage of the wild-type. Results (average of triplicates and standard deviation) are representative of three independent experiments.

The results obtained for *S. natalensis* and the catalase activity profile in *S. tsukubaensis* in tacrolimus non-producing and producing-conditions, led us to question whether the modulation effect observed in knock-out mutants of *S. natalensis* is a general effect on *Streptomyces* secondary metabolism or is a strain or even metabolite specific phenomena. Due to the economic impact of tacrolimus, recently out of patent, and the growing interest of the pharmaceutical industry to increase production yields an effort to improve the tacrolimus production processes has been made. The majority of the studies rely on feeding strategies and in some cases on the generation of mutant strains in target genes involved in tacrolimus biosynthesis or in tacrolimus precursor supply. However there is still a lot of knowledge scarcity regarding tacrolimus biosynthetic regulation. Given the vital role of oxygen in *Streptomyces* physiology and the results obtained for *S. natalensis*, where a modulation of pimaricin biosynthesis was achieved through a redox regulation, we focused on the study of the oxidative stress related regulatory mechanisms that affect tacrolimus production in *S. tsukubaensis*.

3.2 PHYSIOLOGICAL CHARACTERIZATION OF *S. TSUKUBAENSIS* NRRL 18488

S. tsukubaensis was the first *Streptomyces* strain described as a tacrolimus producer (Kino *et al.* 1987). Nowadays the production of tacrolimus is also assigned to seventeen more strains (Barreiro and Martinez-Castro 2014). By the time this work started only a few sequences of *S. tsukubaensis* NRRL 18488 were available at the database, namely 16S RNA and part of the tacrolimus biosynthetic cluster (Goranovic *et al.* 2010). However this PhD project was integrated in a European consortium - IMMUNOTEC - in which *S. tsukubaensis* NRRL 18488 genome had been sequence and was available. This represented a major advantage and the main reason to choose *S. tsukubaensis* NRRL 18488 as our working model. In 2012 a draft genome of *Streptomyces tsukubaensis* NRRL 18488 was published (Barreiro *et al.* 2012). To simplify strain denomination, from now on we will be referring to *S. tsukubaensis* NRRL 18488 as *S. tsukubaensis.*

A physiological characterization of the antioxidant defenses as well as tacrolimus production was assessed at the shake flasks level in *S. tsukubaensis. S. tsukubaensis* growth and tacrolimus conditions were defined within the frame of the IMMUNOTEC project in order to standardize experiments between project partners. Therefore MG modified medium (MGm) was chosen for liquid cultures and ISP4 medium for sporulation. *S. tsukubaensis* cultures were grown in an orbital incubator shaker at 28ºC and 220 rpm, with a ratio of flask volume *vs* medium culture of 5 (500 mL shake flasks and 100 mL medium), unless stated otherwise.

3.2.1 Tacrolimus production

In MGm medium, *S. tsukubaensis* presented the typical bacterial growth kinetics where it could be distinguished the exponential phase and stationary phase (Fig. 3.3. A). For experimental purposes we divided the exponential phase in early exponential and late exponential. Under the conditions tested tacrolimus was first detected during late exponential phase (120 h) and maximum production occurred at 168 h, during stationary phase, with a production of approximately 23 mg L^{-1} on average. Tacrolimus production was quantified by HPLC but it was also routinely monitored by bioassays using *Saccharomyces cerevisiae* TB23, a strain

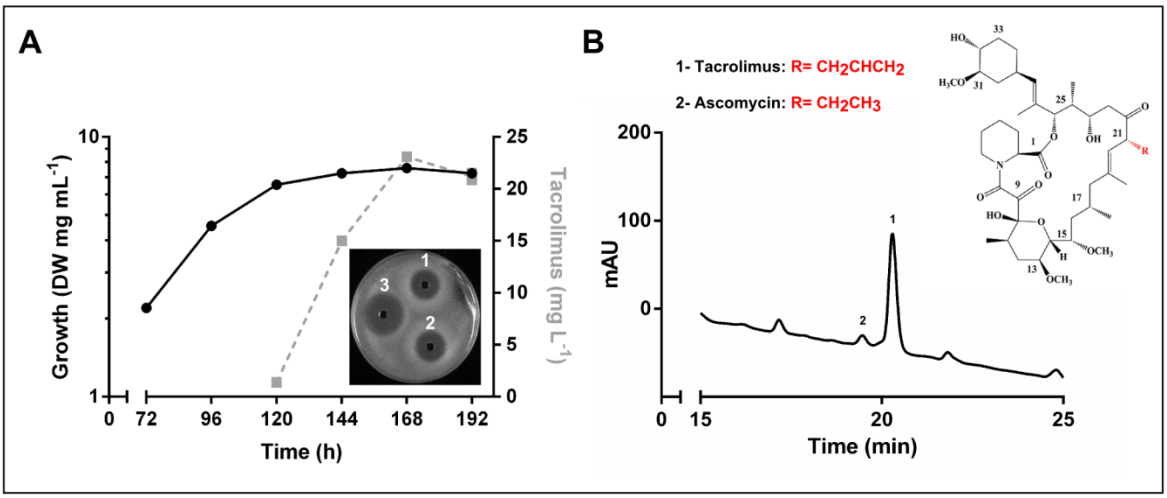

Figure 3.3 – *S. tsukubaensis* growth curve, tacrolimus and ascomycin production. (A) Growth and tacrolimus production of *S. tsukubaensis* in MGm medium. Growth was assessed by dry weight measurements. Tacrolimus production was assessed by HPLC. Growth inhibition assay with *Saccharomyces cerevisiae* TB23 strain in YPD medium, using 50 µL of methanol extracts from *S. tsukubaensis* cultures at 120 h (2) and 144 h (3) of growth was also used to confirm tacrolimus production, purified tacrolimus was used as positive control (1). Vertical bars indicate standard deviation of the mean values. Results (average of triplicates and standard deviation) are representative of three independent experiments. (B) Chromatogram of tacrolimus and ascomycin production in *S. tsukubaensis* at 168 h of growth; chemical structure of tacrolimus (1) and ascomycin (2).

sensitive to tacrolimus, as test organism (Breuder *et al.* 1994) (Fig. 3.3 A). Similar to most tacrolimus producing strains, *S. tsukubaensis* also produces trace amounts of ascomycin (FK520) as a by-product of tacrolimus biosynthesis (Hatanaka *et al.* 1989). Ascomycin and tacrolimus have closely related structures. They differ at the C21 side chain of the macrolide ring, presenting either an allyl group (tacrolimus) or an ethyl group (ascomycin). Both compounds are distinguishable by HPLC with ascomycin presenting a relative retention time (RRT) of 0.96 (Fig. 3.3 B). In the conditions tested *S. tsukubaensis* produced on average 1.1 mg L^{-1} of ascomycin (Fig. 3.3 B).

3.2.2 Enzymatic antioxidant defences

Bacteria had to develop defence mechanisms to cope with oxidative stress, including enzymatic antioxidant defences. Among those we found catalases, enzymes that scavenge H_2O_2. The catalase activity profile of *S. tsukubaensis* was monitored during growth both by measuring spectrophotometrically total catalase activity levels and by native-PAGE analysis (Fig. 3.4). In tacrolimus producing conditions *S. tsukubaensis* displayed high catalase activity levels during growth,

especially when comparing with *S. natalensis*, reaching more than 300 U mg^{-1} of catalase activity during stationary phase (Fig.3.4 A). Worth noting that overlapping with the transition from early exponential phase (96 h) to late exponential phase (120 h) an induction of catalase activity is observed. The native-PAGE analysis of cell free protein extracts showed the existence of two bands that displayed catalase-like activity (Fig.3.4 B). The fastest migrating band is present throughout growth, increasing its intensity during stationary phase. The second band that displayed catalase activity and migrates slower in the gel, is induced from early exponential phase to late exponential phase (96 h – 120 h).

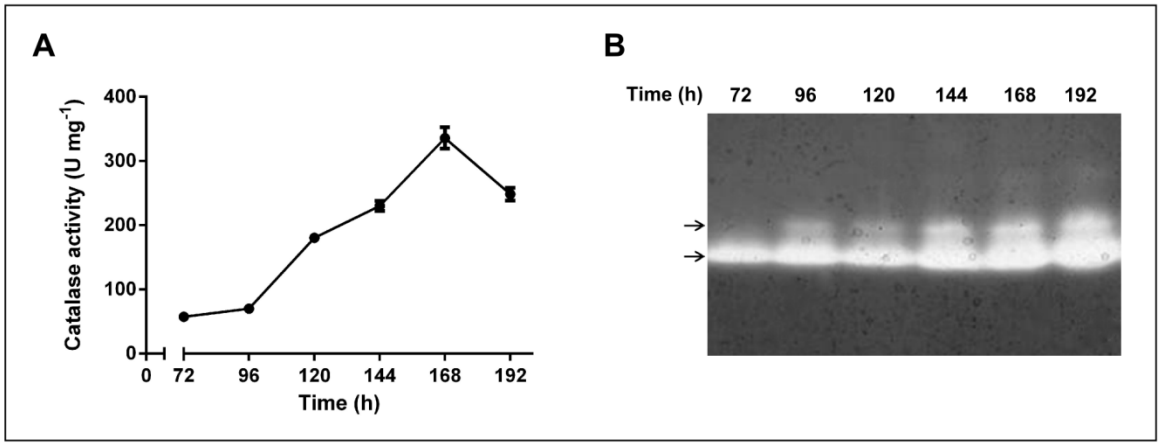

Figure 3.4 – *S. tsukubaensis* catalase activity. (A) Total catalase activity was measured spectrophotometrically in samples collected throughout growth from *S. tsukubaensis* cultures. Vertical bars indicate standard deviation of the mean values. Results (average of triplicates and standard deviation) are representative of three independent experiments. (B) Native-PAGE of cell-free protein extracts (1 µg of total protein per lane) from *S. tsukubaensis* stained for catalase activity. Samples were collected throughout growth.

Streptomyces strains usually harbour multiple catalase encoding genes, but only one is inducible by H_2O_2 (Cho and Roe 1997). In order to identify the H_2O_2-inducible monofunctional catalase, a test was performed where H_2O_2 was added to the cultures, samples were taken and analysed by native-PAGE stained for catalase activity, similarly to what we had previously performed for *S. natalensis* (Beites *et al.* 2011). However the high catalase activity levels displayed by *S. tsukubaensis* hampered this task by masking the activity induction. Note that in Fig. 3.4 B only 1 µg of total protein extracts were loaded into the native-PAGE. Although we were not able to identify the H_2O_2-inducible monofunctional catalase in the native-PAGE, genome analysis identified two catalase encoding genes (see section 3.3.1) confirming the native-PAGE results.

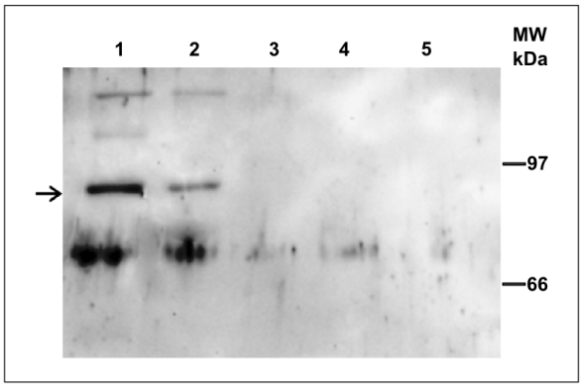

Figure 3.5 – Immunoblot detection of catalase-peroxidase. Protein samples from *S. tsukubaensis* were collected throughout growth from cultures grown as standard. *S. natalensis* and *S. coelicolor* were grown in YEME medium and samples collected at 48 h of growth. Cell-free protein extracts (10 µg protein per lane) were loaded into an SDS-PAGE and transferred to a membrane. Immunoblot detection was performed using an antibody raised against the catalase-peroxidase CpeB from *S. reticuli*. The arrow indicates the band that corresponds to *S. coelicolor* and *S. natalensis* catalase-peroxidase with a molecular weight of 83kDa.

It is also common to find among *Streptomyces* the presence of a bifunctional catalase. In order to analyse the presence of a catalase-peroxidase in *S. tsukubaensis* a western-blot was performed using a primary antibody raised against a catalase-peroxidase purified from *S. reticuli* (Zou *et al.* 1999). The western-blot showed no signal for *S. tsukubaensis* (lanes 3, 4 and 5 Fig. 3.5), suggesting the absence of a bifunctional catalase-peroxidase. Protein extracts from *S. natalensis* and *S. coelicolor* were used as positive control (lanes 1 and 2 Fig. 3.5). This result was also confirmed by the genome analysis where no catalase-peroxidase was found (see section 3.3.1).

The SOD activity profile of *S. tsukubaensis* was also monitored throughout growth both by measuring spectrophotometrically total SOD activity levels and by native-PAGE stained for SOD activity. *S. tsukubaensis* SOD specific activity levels were kept fairly constant throughout growth varying between 15 U mg^{-1} and 25 U mg^{-1} (Fig. 3.6 A). Regarding SODs distribution in *Streptomyces*, the common pattern is the presence of two genes coding for two different SODs: a nickel containing SOD and an iron containing SOD. However there are exceptions. For instance, *S. coelicolor* and *S. fradiae* have an additional gene coding for another FeSOD that displays SOD activity (Chung *et al.* 1999). The native-PAGE performed with cell-free protein extracts from *S. tsukubaensis* grown in MGm medium showed two bands with SOD activity (Fig. 3.6 B). Furthermore, it has

been reported a nickel dependent regulatory system that controls the expression of either the NiSOD or the FeSOD in *S. coelicolor* and *S. griseus*, i.e., in the presence of nickel ions NiSOD is preferentially expressed whereas FeSOD expression is down-regulated (Kim *et al.* 1996). Although MGm medium contains nickel (see section 2.1.3.3) we could not rule out the possibility that the two bands corresponded to two FeSODs. To verify the presence of a second FeSOD or a NiSOD, MGm medium was supplemented with 20 µM of $NiSO_4$, samples were collected and a new native-PAGE analysis was performed. With these conditions we were able to identify that the first band displaying SOD activity corresponded to a NiSOD, as its intensity increased with the addition of nickel, and the fastest migrating band corresponded to a FeSOD (Fig.3.6 B).

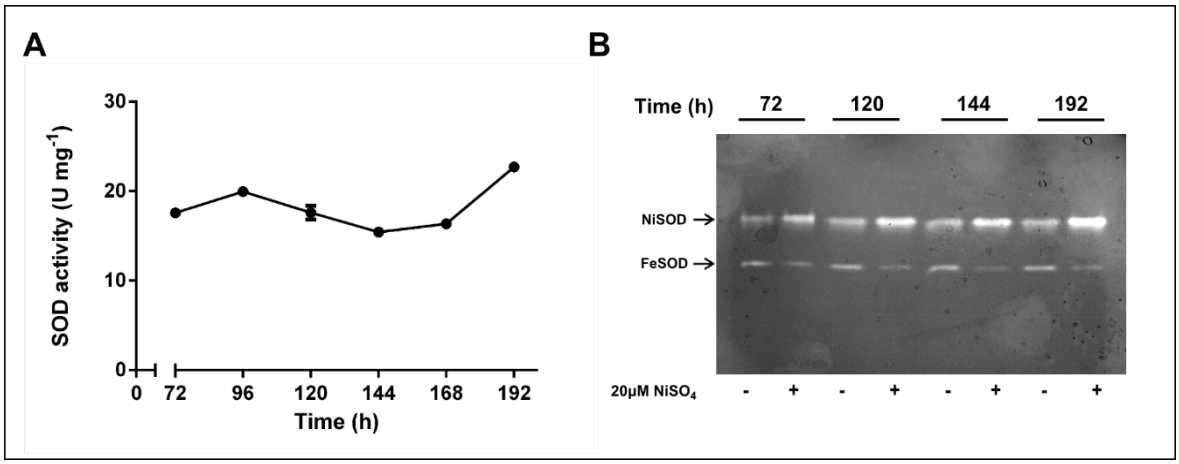

Figure 3.6 – *S. tsukubaensis* SOD activity. (A) SOD activity was measured spectrophotometrically in samples collected throughout growth from *S. tsukubaensis* cultures. Results (average of triplicates and standard deviation) are representative of three independent experiments. Vertical bars indicate standard deviation of the mean values. (B) Native-PAGE of cell-free protein extracts (50 µg of total protein per lane) from *S. tsukubaensis* stained for SOD activity. Samples were collected throughout growth from *S. tsukubaensis* cultures grown in two conditions: in standard conditions (-) or in MGm medium supplemented with 20 µM $NiSO_4$ (+).

3.2.3 Intracellular ROS levels

Intracellular levels of H_2O_2 and $O_2^{\cdot-}$ were monitored with dihydrorhodamine 123 (DHR) and dihydroethidium (DHE), respectively. While intracellular levels of superoxide anion were kept fairly constant throughout growth (Fig. 3.7 A), the same was not true for H_2O_2 intracellular levels (Fig. 3.7 B). H_2O_2 intracellular levels were high during early exponential phase and then a marked decreased

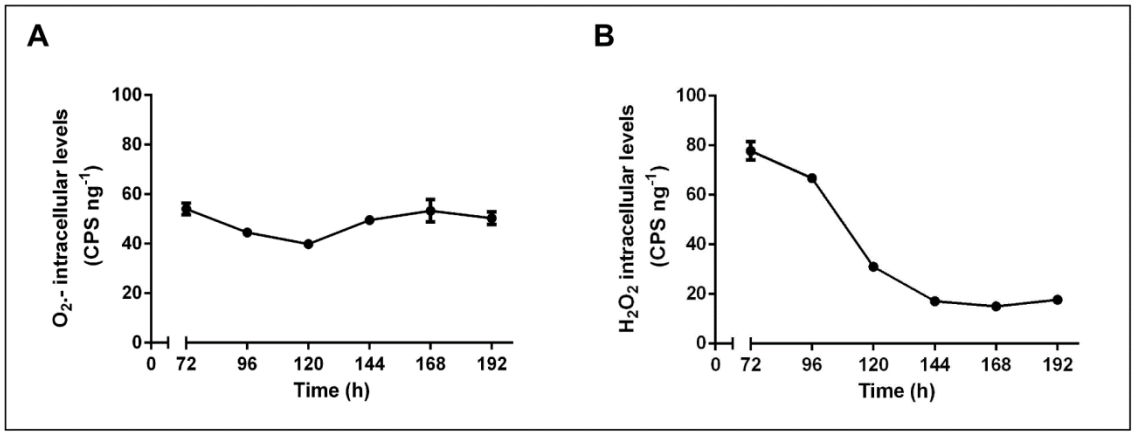

Figure 3.7 – *S. tsukubaensis* ROS intracellular levels. (A) DHE oxidation levels were used as a measure of O_{2^-} intracellular levels. (B) DHR oxidation levels were used as a measure of H_2O_2 intracellular levels. Samples were collected throughout growth curve. Growth conditions were as standard. Vertical bars indicate standard deviation of the mean values. Results (average of triplicates and standard deviation) are representative of three independent experiments.

occurred during the transition from early exponential to late exponential phase (96 h - 120 h) (Fig. 3.7 B). Note that the decrease of H_2O_2 intracellular levels overlaps with the increase in catalase activity and also with the onset of tacrolimus production.

3.2.4 Dissolved oxygen and tacrolimus production

Dissolved Oxygen (DO) is a key parameter on the industrial production of secondary metabolites by submerged cultures fermentations (Yegneswaran *et al.* 1991, Dick *et al.* 1994, Regentin *et al.* 2002). The O_2 demand by microorganisms is counteracted by its low solubility and limitations in gas-liquid mass transfer. Also, while low O_2 concentrations will limit growth and product formations, increased O_2 concentrations may have regulating and toxic effects on microbial cultures. In order to study the effect of DO in *S. tsukubaensis* growth and tacrolimus production we changed the ratio of flask volume *vs* medium culture from 5 to 10, increasing oxygen availability.

S. tsukubaensis cultures were grown in MGm medium, in an orbital incubator shaker at 28ºC and 220 rpm, decreasing media volume to 50 mL. Changing oxygen availability led to an apparent early entry of the cultures into late exponential phase, 96 h *vs* 120 h, i.e. an anticipation of the metabolic switch (Fig. 3.8 A). This anticipation led to an early induction of catalase activity (Fig. 3.8 B)

and an early onset of tacrolimus production (Fig. 3.8 C). Furthermore tacrolimus production increased 44% when compared to the standard conditions (35 mg mL^{-1} instead of 23 mg mL^{-1}) and the peak of production was achieved 24 h earlier, at

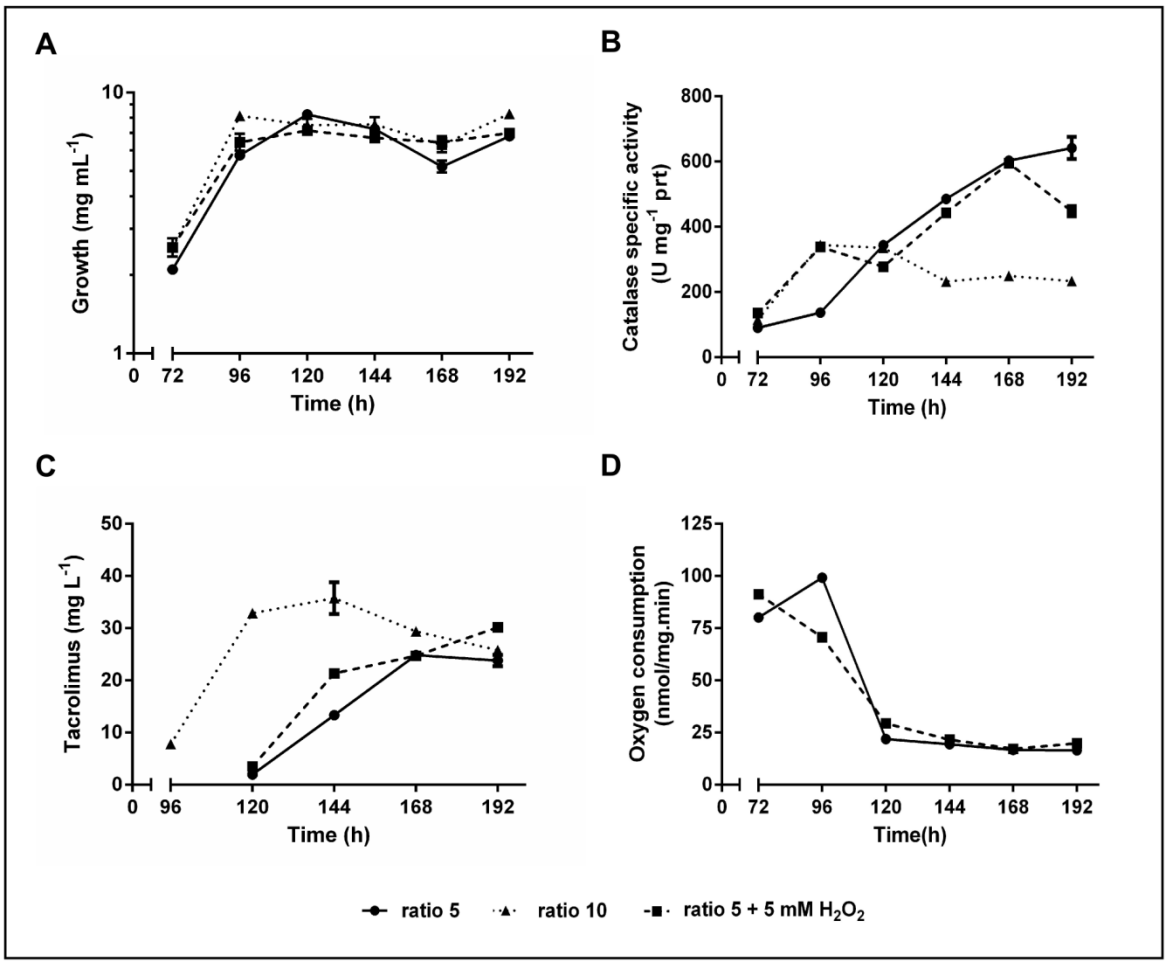

Figure 3.8 – Physiological characterization of *S. tsukubaensis* in different DO conditions. (A) Growth of *S. tsukubaensis* in different DO conditions. Growth was assessed by dry weight. (B) Total catalase activity was measured spectrophotometrically in samples collected throughout growth from *S. tsukubaensis* cultures. (C) Tacrolimus production was assessed by HPLC. (D) Oxygen consumption rate was determined throughout growth in cultures grown in standard conditions (ratio 1:5) and in cultures treated with H_2O_2. Values correspond to the oxygen consumption during a time period of 1 min. Vertical bars indicate standard deviation of the mean values. Results (average of triplicates and standard deviation) are representative of three independent experiments.

144 h of growth (Fig. 3.8 C).

It has also been suggested that adding H_2O_2 to the culture broth could function as a source of dissolved oxygen levels given that H_2O_2 disproportion by catalase originates water and oxygen (Tusseau-Vuillemin *et al.* 2002).

In order to see if the addition of H_2O_2 could have an effect in tacrolimus production, 5 mM of H_2O_2 was added to *S. tsukubaensis* cultures at 72 h of growth. Although the addition of H_2O_2 had no apparent effect on growth (Fig. 3.8 A), the same was not observed regarding other physiological parameters. The induction of catalase activity observed in standard conditions, from 96 h to 120 h was anticipated by 24 h in H_2O_2 supplementation conditions, similarly to the cultures with a 10 ratio (Fig. 3.8 B). The addition of H_2O_2 also led to a modulation of tacrolimus biosynthesis, by increasing total production to approximately 30 mg mL^{-1} on average. Additionally, tacrolimus production at 120 h in *S. tsukubaensis* cultures grown in standard conditions was 1.99 mg ml^{-1}, while in *S. tsukubaensis* cultures grown with H_2O_2 supplementation tacrolimus production was already 3.51 mg ml^{-1} (Fig. 3.8 C). Oxygen consumption rate was also assessed using mycelium samples taken every 24 h, from *S. tsukubaensis* cultures grown in standard conditions and in *S. tsukubaensis* cultures supplemented with H_2O_2. Unlike what happened to the control culture, where an increase in oxygen consumption during early exponential phase occurred, suggesting that the cultures still undergo a primary metabolism, the addition of H_2O_2 led to a decrease in oxygen consumption (Fig. 3.8 D).

Even though it was achieved a modulation of *S. tsukubaensis* physiology, especially regarding tacrolimus production, with the addition of 5 mM of H_2O_2, the constant supply of increased DO, by changing the ratio of flask volume *vs* medium culture from 5 to 10 was proven to be more efficient in altering tacrolimus titters.

3.2.5 Tacrolimus as an antioxidant compound

Although tacrolimus is best known for its imunossupressive properties (Kino *et al.* 1987), in the past few years additional activities have been appointed to this compound (Guo *et al.* 2001, Akimoto *et al.* 2008, Benson *et al.* 2008). In the context of oxidative stress we analysed the antioxidant activity of tacrolimus. For that purpose we tested the sensitivity of *Saccharomyces cerevisiae* BY4741 and *S. natalensis* ATCC 27448 to H_2O_2 in the presence of tacrolimus, by evaluating growth inhibition around disks containing 1 M of H_2O_2 and 1.5 mM of tacrolimus (Fig. 3.9); 50 mM of ascorbic acid was used as control. Both the addition of ascorbic acid and tacrolimus had no impact neither in *Saccharomyces cerevisiae*

BY4741 growth nor in *S. natalensis* ATCC 27448 growth (Fig. 3.9). The addition of H_2O_2 led to growth inhibition in both strains that could be easily visualized by the formation of a growth inhibition halo. The addition of the antioxidant ascorbic acid led to a decrease of the inhibition halo (Fig. 3.9 A). Interestingly, the addition of tacrolimus also led to a decrease in the inhibition halo in both *Saccharomyces cerevisiae* BY4741 and S. *natalensis* ATCC 27448 (Fig. 3.9), suggesting that tacrolimus can act as an antioxidant compound.

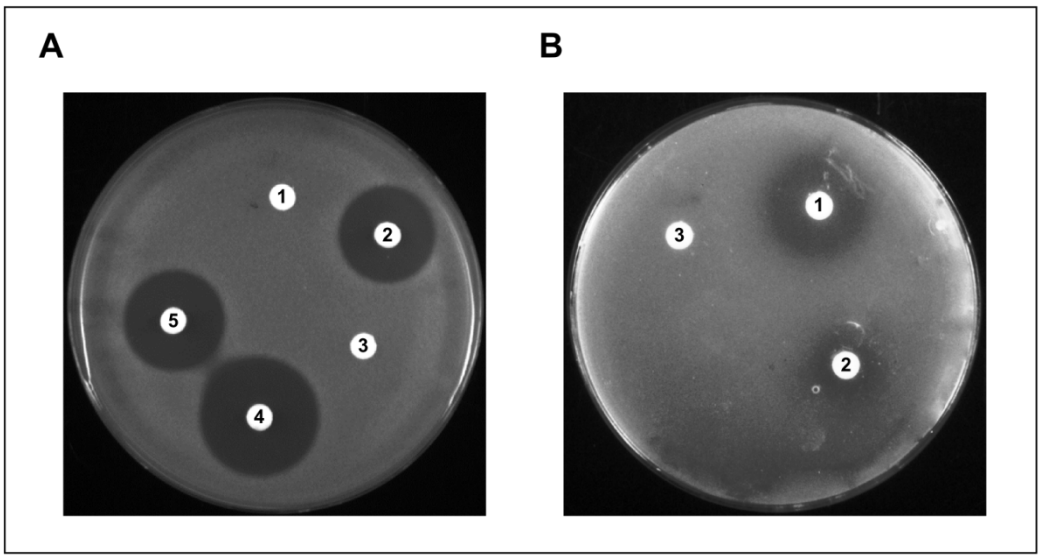

Figure 3.9 – Growth inhibitions assays. (A) Growth inhibition bioassay using *Saccharomyces cerevisiae* BY4741 in YPD medium. 1 - 50 mM ascorbic acid; 2 – 1 M of H_2O_2 + 1.5 mM of tacrolimus; 3 – 1.5 mM of tacrolimus; 4 - 1 M of H_2O_2; 5 - 1 M of H_2O_2 + 50 mM ascorbic acid. (B) Growth inhibition bioassay using *S. natalensis* ATCC 27448 in YED medium. 1 - 1 M of H_2O_2; 2 - 1 M of H_2O_2 + 1.5 mM of tacrolimus; 3 – 1.5 mM of tacrolimus.

The addition of H_2O_2 to tacrolimus was also analysed by HPLC. Different concentrations of purified tacrolimus were mixed with H_2O_2 and samples were analysed by HPLC. The HPLC chromatogram revealed not only a change in tacrolimus quantification when compared to the purified compound in the absence of H_2O_2 but also the appearance of a new peak with a RRT of 0,95 suggesting a modification of the tacrolimus structure by H_2O_2 (Fig. 3.10).

Moreover, analysis of the chemical structure of tacrolimus identified five functional groups that could be oxidized by H_2O_2. The C32 and C24 secondary alcohol groups can be susceptible to H_2O_2 oxidation to its corresponding ketone. Additionally the double bonds at C36, C27 and C19 can also be susceptible to

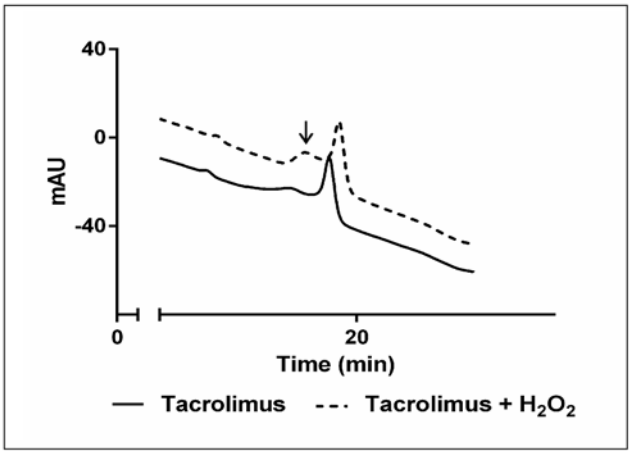

Figure 3.10 – Chromatogram of purified tacrolimus. 1 µg of purified tacrolimus was injected in HPLC in the absence (solid line) and in the presence of H_2O_2 (dashed line). Tacrolimus modification by H_2O_2 is indicated by an arrow.

oxidation by H_2O_2 to epoxy groups, particularly the double bond at the C21 side chain (Fig 3.3 B).

3.3 OXIDATIVE STRESS RELATED GENES IN *S. TSUKUBAENSIS*: IDENTIFICATION, SCREENING AND MUTANT GENERATION

Further characterization of the oxidative stress response in *S. tsukubaensis* was performed based on the construction of mutant strains on oxidative-stress related genes, namely knock-out mutant and/or strains overexpressing the selected genes (section 3.3.3 and section 3.3.4). Knock-out mutants were generated using a PCR targeting strategy where the target gene was replaced by a cassette containing the apramycin resistance gene - a*ac(3)IV* and an origin of transfer - *oriT* (Gust *et al.* 2003). This strategy requires the use of a cosmid that harbours the target gene. The complete genome sequence of *S. tsukubaensis* was available scattered over 960 contigs, as well as an ordered genomic library (Martinez-Castro *et al.* 2009). For the identification of cosmids harbouring oxidative stress related genes, we first analysed the genome searching for *Streptomyces* orthologue genes that code for the H_2O_2 inducible monofunctional catalase, *katA1*, the iron containing superoxide dismutase, *sodF* and the alkyl hydroperoxide reductase, *ahpC,* using as reference *S. coelicolor* genome. Afterwards the genomic library was screened by blot hybridization using internal probes as described elsewhere (Martinez-Castro *et al.* 2009).

3.3.1 Genome mining for antioxidant encoding genes

For the identification of antioxidant encoding genes in *S. tsukubaensis* genome (Barreiro *et al.* 2012) (accession number AJSZ01000000), we performed BLASTp analysis limited to *S. tsukubaensis* genome, using as query the protein sequences from *S. coelicolor* for the monofunctional catalases KatA1 (SCO0379), KatA2 (SCO7590) and KatA3 (SCO6204), the catalase-peroxidase (SCO0560), the superoxide dismutases SodF (SCO2633), SodF2 (SCO0999) and SodN (SCO5254) and the alkyl hydroperoxide reductase AhpC (SCO5032). The results obtained are summarized in Table 3.1.

Table 3. 1 - *S. tsukubaensis* orthologues of *S. coelicolor* oxidative-stress related proteins.

S. coelicolor	***S. tsukubaensis* ortholog protein**	**E-value**	**Accession number**
SCO0379 - CatA1	STSU_10876	0	EIF92400
SCO7590 - CatA2	STSU_11535	0	EIF92263
SCO6204 - CatA3	STSU_10876	0	EIF92400
SCO0666	STSU_11535	$8e^{-104}$	EIF92263
SCO0560 - CpeB	Not found	na	na
SCO2633 - SodF	STSU_24238	$6e^{-144}$	EIF89738
SCO0999 - SodF2	STSU_24238	$7e^{-135}$	EIF89738
SCO5254 - SodN	STSU_10666	$6e^{-86}$	EIF92449
SCO5032 - AhpC	STSU_11585	$3e^{-123}$	EIF92260

Two clade 3 monofunctional catalase encoding genes were identified in *S. tsukubaensis, STSU_10876* (1470 bp) and *STSU_11535* (1452 bp). *STSU_10876* codes for a protein with 489 amino acid and a deduced molecular mass of 54 kDa; *STSU_11535* codes for a protein with 483 amino acid and a deduced molecular mass of 54 kDa. Both proteins presented the two conserved domains displayed by clade 3 monofunctional catalases: the N-terminal catalase active site motif (between amino acid 49-65 in STSU_10876 and between amino acid 44-60 in STSU_11535) and the C-terminal heme-ligand motif (between amino acid 339-347 in STSU_10876 and between amino acid 333-341 in STSU_11535). In both proteins the catalase active site harbours a conserved histidine residue known to be important for the catalytic mechanism of the enzyme (Mate *et al.* 1999). Further *in silico* analysis of the *STSU_10876* genomic region unveiled the presence of *STSU_10881* divergently transcribed from *STSU_10876*. *STSU_10881* codes for a Fur-like repressor and is an orthologue of *S. coelicolor* Fur-like repressor *catR*.

In *S. coelicolor, catR* is also divergently transcribed from *katA1* and regulates its transcription in a H_2O_2-dependent manner (Hahn *et al.* 2000).

Regarding catalase-peroxidase, no orthologues of *cpeB* were found on *S. tsukubaensis* by the genome-wide *in silico* analysis. This result confirms the western-blot analysis (Fig. 3.5).

Two genes coding for superoxide dismutases were identified in *S. tsukubaensis, STSU_24238* (636 bp) and *STSU_10666* (396 bp). *STSU_24238* codes for a protein with 211 amino acid and a deduced molecular mass of 23 kDa that has been annotated as SodA; *STSU_10666* codes for a protein with 131 amino acid and a deduced molecular mass of 14.6 kDa, annotated as SodN. The analysis of the amino acid sequence of STSU_24238 revealed the presence of the four conserved residues involved in binding to the metal cofactor: H^{28}, H^{76}, D^{165} and H^{169} two of them are included in the SOD conserved motif: D^{165}AWEHAFY^{172} (Parker and Blake 1988). Furthermore, analysis of the upstream genomic region of *STSU_24238* revealed the presence of the Ni-responsive regulatory motif (TTGCAN_7TGCAA) recognized by the Fur like transcriptional regulator Nur, a repressor of *sodF* in *S. coelicolor* (Ahn *et al.* 2006, An *et al.* 2009).The analysis of the amino acid sequence of STSU_10666 revealed the presence in the N-terminal of the nickel responsive motif: His-Cys-X-X-Pro-Cys-Gly-X-Tyr that chelates nickel ions.

Finally, *STSU_11585* was identified as coding for AhpC, a typical 2-Cysteine Peroxiredoxin. Peroxiredoxin are thiol-specific antioxidant (TSA) proteins that reduce hydrogen peroxide, peroxynitrite, and organic hydroperoxides. AhpC contains two invariant cysteine residues, each followed immediately by a proline residue, one at the N-terminus and one at the C-terminus. The three conserved catalytic cysteine residues described to be involved in the peroxidatic activity of *M. tuberculosis* AhpC (Hillas *et al.* 2000) were identified in STSU_11585: C^{51}, C^{164} and C^{166}. Further *in silico* analysis of the *STSU_11585* genome region unveiled the presence of *STSU_11590* coding for alkyl hydroperoxidase reductase (AhpD). The amino acid sequence of STSU_11590 showed the conserved C-terminal motif: C^{132}XXC^{134}, typical of the AhpD protein family and that has been reported to be important for reducing AhpC (Nunn *et al.* 2002). The common genomic synteny found in *Streptomyces* for this genomic region, already described for *S. coelicolor,*

is characterized by the presence of the H_2O_2 inducible regulator coding gene *oxyR,* divergently transcribed form the *ahpCD* operon (Hahn *et al.* 2002). Interestingly, this is not the case for *S. tsukubaensis* with OxyR encoding gene (*STSU_11565*) located 3.9 kb upstream from the *ahpCD* operon. Also three novel genes are present in this genomic region, including *STSU_11560* that codes for a novel extracellular sigma factor that shares 67% homology with *S. clavuligerus* extracytoplasmic function (ECF) sigma factor SigG and is divergently transcribed from *oxyR.* This genomic organization will be further addressed and explored in chapter 4.

3.2.2 Screening of *S. tsukubaensis* genomic library

An ordered cosmid library of the immunosuppressant tacrolimus-producer strain *S. tsukubaensis* was screened by blot-hybridization as described elsewhere (Martinez-Castro *et al.* 2009). Briefly 1656 individual clones were organized in a pyramidal arrangement following three stages. In the final stage all clones are present in a total master plate, which is then used for the *in situ* blot hybridization. Internal probes for *katA1* (*STSU_10876*), *ahpC* (*STSU_11585*) and *sodA* (*STSU_24238*) were obtained by PCR using the primers listed on Table 2.2

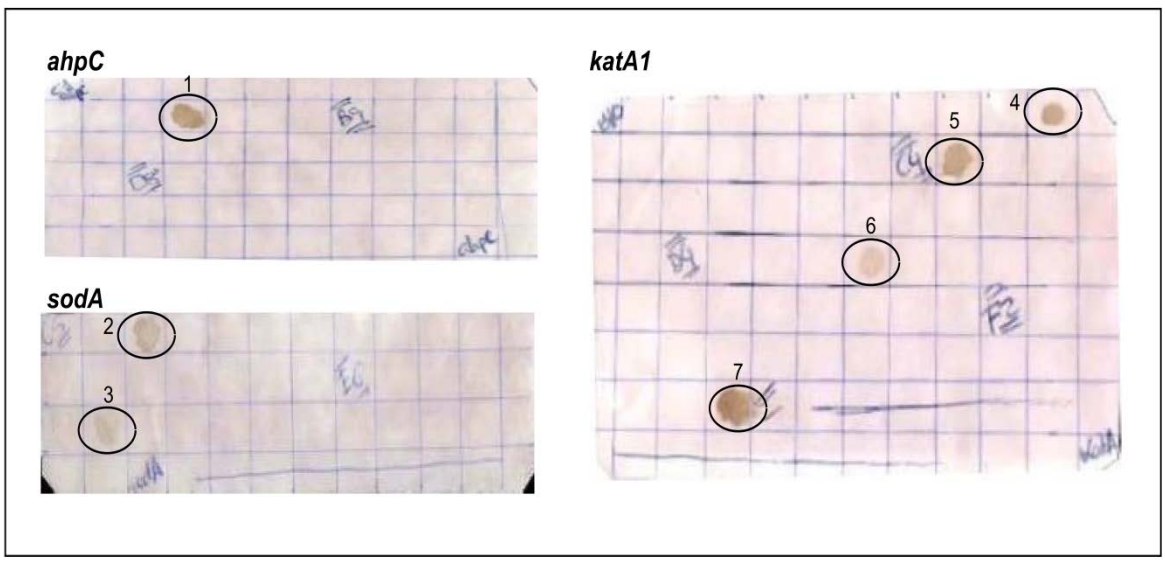

Figure 3.11 – Blot-Hybridization of *S. tsukubaensis* cosmid library for gene identification. 1- Positive identification of *ahpC* containing cosmid: cos15C1; 2- Positive identification of s*odA* containing cosmid: cos2C5; 3- Positive identification of s*odA* containing cosmid: cos6E6; 4- Positive identification of *katA1* containing cosmid: cos10B10; 5- Positive identification of *katA1* containing cosmid: cos1C4; 6- Positive identification of *katA1* containing cosmid: cos4D4; 7- Positive identification of *katA1* containing cosmid: cos18F2.

(section 2.2.2). Blot hybridization of the cosmid library identified seven cosmids: four harbouring *katA1*, cos10B10, cos1C4, cos4D4 and cos18F2; two harbouring *sodA,* cos2C5 and cos6E6 and one harbouring *ahpC*, cos15C1 (Fig. 3.11). Cosmid identity was further confirmed by Southern blot hybridization of purified cosmids.

Cosmids extremities were sequenced with primer pair T3/T7. For cosmids 1C4, 18F2 and 2C5 we were not able to identify at least one of the extremities, suggesting cosmid reorganization. With the sequence of the cosmids we were able to determine the length of the fragment cloned in each cosmid (Table 3.2) as well as the relative position of our gene of interest in the cosmids (Fig. 3.12). Note that the cosmid containing *ahpC* is scattered in eight contigs and *oxyR* is located between contig 348 and contig 349, which led to an incorrect annotation of the gene. This will be also further explored in Chapter 4.

Table 3. 2 - Identified cosmids**.**

Target gene	Cosmid	Cosmid size
katA1	COS10B10	36025 bp
	COS1C4	na
	COS4D4	42972 bp
	COS18F2	na
sodA	COS2C5	na
	COS6E6	39166 bp
ahpC	COS15C1	37442 bp

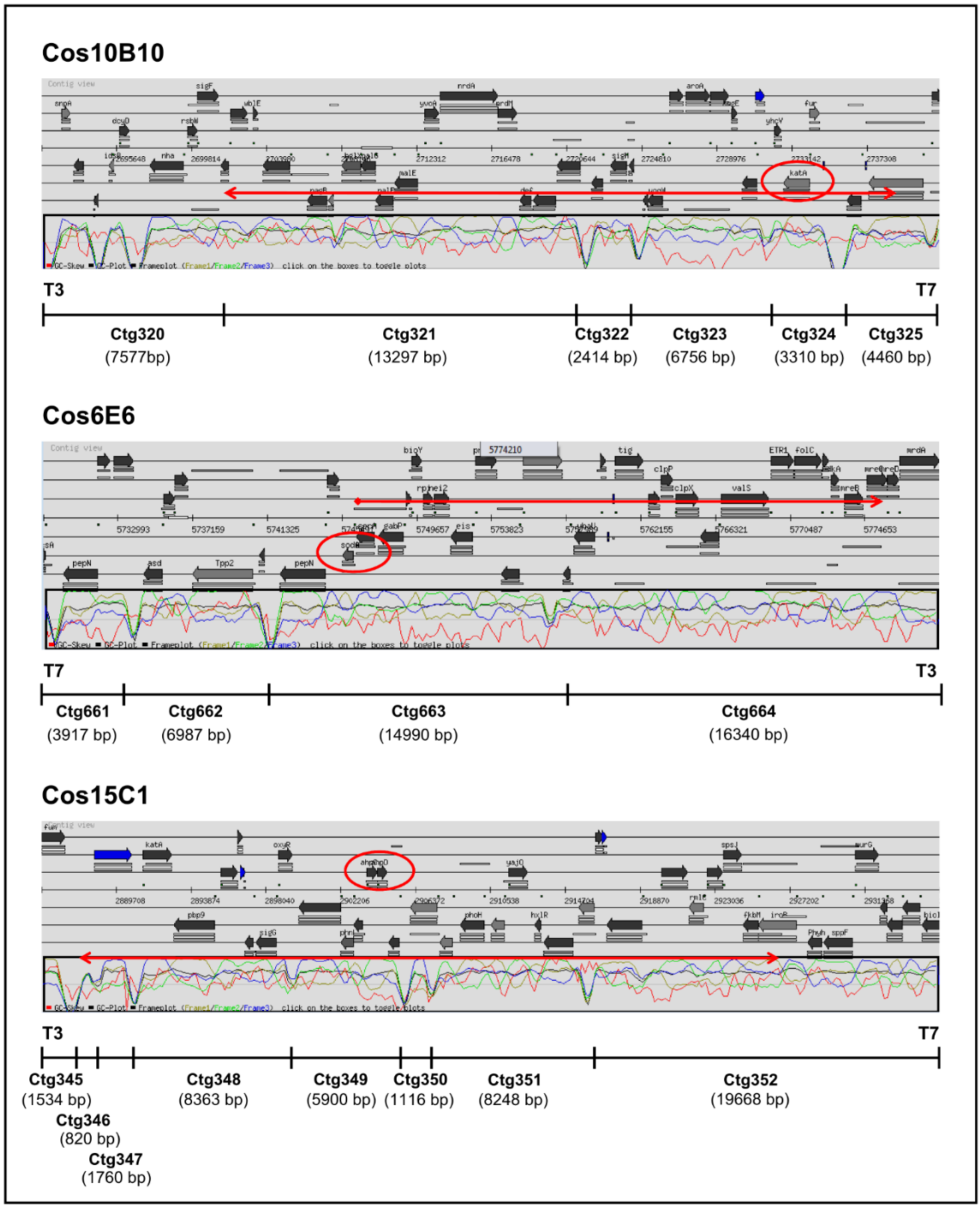

Figure 3.12 – Identified cosmids used for knock-out mutant constructions. Organization of the identified cosmids containing our genes of interest: cos10B10 containing *katA1*; cos6E6 containing *sodA* and cos15c1 containing *ahpC*. The genes of interest are identified with a red circle. *S. tsukubaensis* genome contigs for each cosmid, and their length, is indicated by black lines.

3.3.3 Construction of mutant strains defective in oxidative related genes

Four *S. tsukubaensis* knock-out mutants defective on OxyR, AhpC, SigG and SodA were generated using a PCR targeting strategy (Gust *et al.* 2003). Briefly, the coding sequences of *oxyR*, *ahpC*, *sigG* and *sodA* were replaced by a cassette containing the apramycin resistance gene, *aac(3)IV*, and *oriT*. The primers used for amplifying the *aac(3)IV-oriT* cassette from plasmid pIJ773 are listed on Table 2.2 (section 2.2.2). Gene replacement of the target genes for the *aac(3)IV-oriT* cassette was performed by homologous recombination within the cosmids harbouring the genes i.e. cos15C1 for *oxyR*, *ahpC* and *sigG* and cos6E6 for *sodA*. Four mutant cosmids cos15C1Δ*oxyR*::*aac(3)IV-oriT*, cos15C1Δ*ahpC*::*aac(3)IV-oriT*, cos15C1Δ*sigG*:: *aac(3)IV-oriT* and cos6E6Δ*sodA*:: *aac(3)IV-oriT* lacking *oxyR*, *ahpC*, *sigG* and *sodA* respectively were generated. Each mutant cosmid was introduced in non-methylating *E. coli* ET12567 containing pUZ8002 and transferred to *S. tsukubaensis* by intergeneric conjugation. Double recombinants were selected by screening for apramycin-resistant and kanamycin-sensitive colonies.

The identity of all mutants was confirmed by Southern blot hybridization and PCR. In Fig. 3.13, Fig. 3.14, Fig. 3.15 and Fig. 3.16 is summarized the construction of *S. tsukubaensis* Δ*oxyR*, *S. tsukubaensis* Δ*ahpC, S. tsukubaensis* Δ*sigG* and *S. tsukubaensis* Δ*sodA* strains, respectively.

Construction of a *katA1* knock-out mutant was also intended. However we were not able to obtain double recombinants.

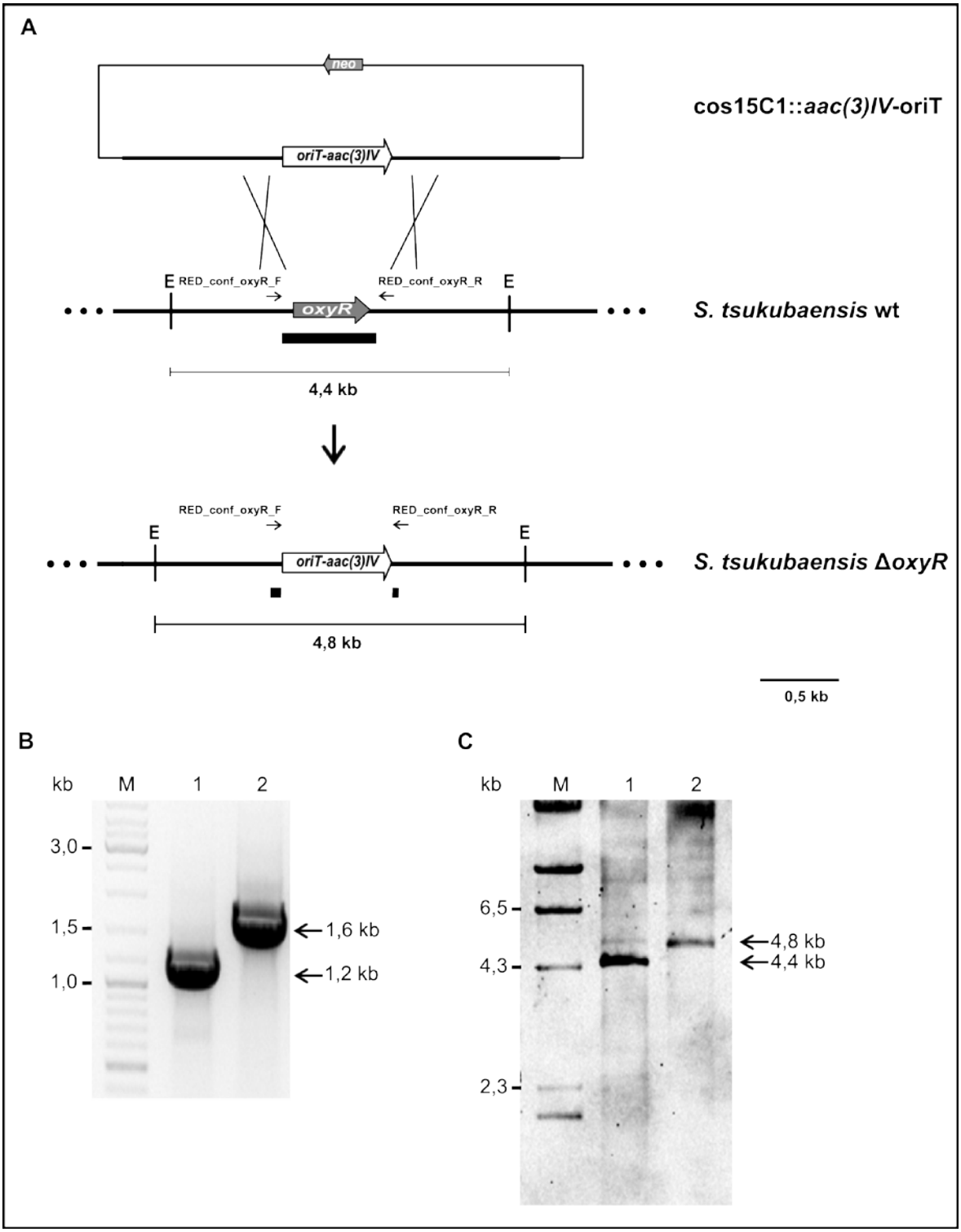

Figure 3.13 – Construction of *S. tsukubaensis* Δ*oxyR* strain. (A) Predicted restriction enzyme polymorphism caused by gene replacement. The *Eco*RV (E) restriction pattern before and after replacement is shown. The probe used for Southern hybridization is indicated by black thick line. (B) Confirmation of gene deletion by PCR. Primers RED_conf_oxyR_F and RED_conf_oxyR_R (Table 2.2) that amplify a 1.2 kb in the wild-type (lane 1) and a 1.6 kb fragment in Δ*oxyR* (lane 2) were used to identify double crossover mutants (C) Confirmation of gene deletion by Southern hybridization of the *Eco*RV digested chromosomal DNA of the wild-type (lane 1) and the mutant Δ*oxyR* (lane 2). M: Molecular weight marker.

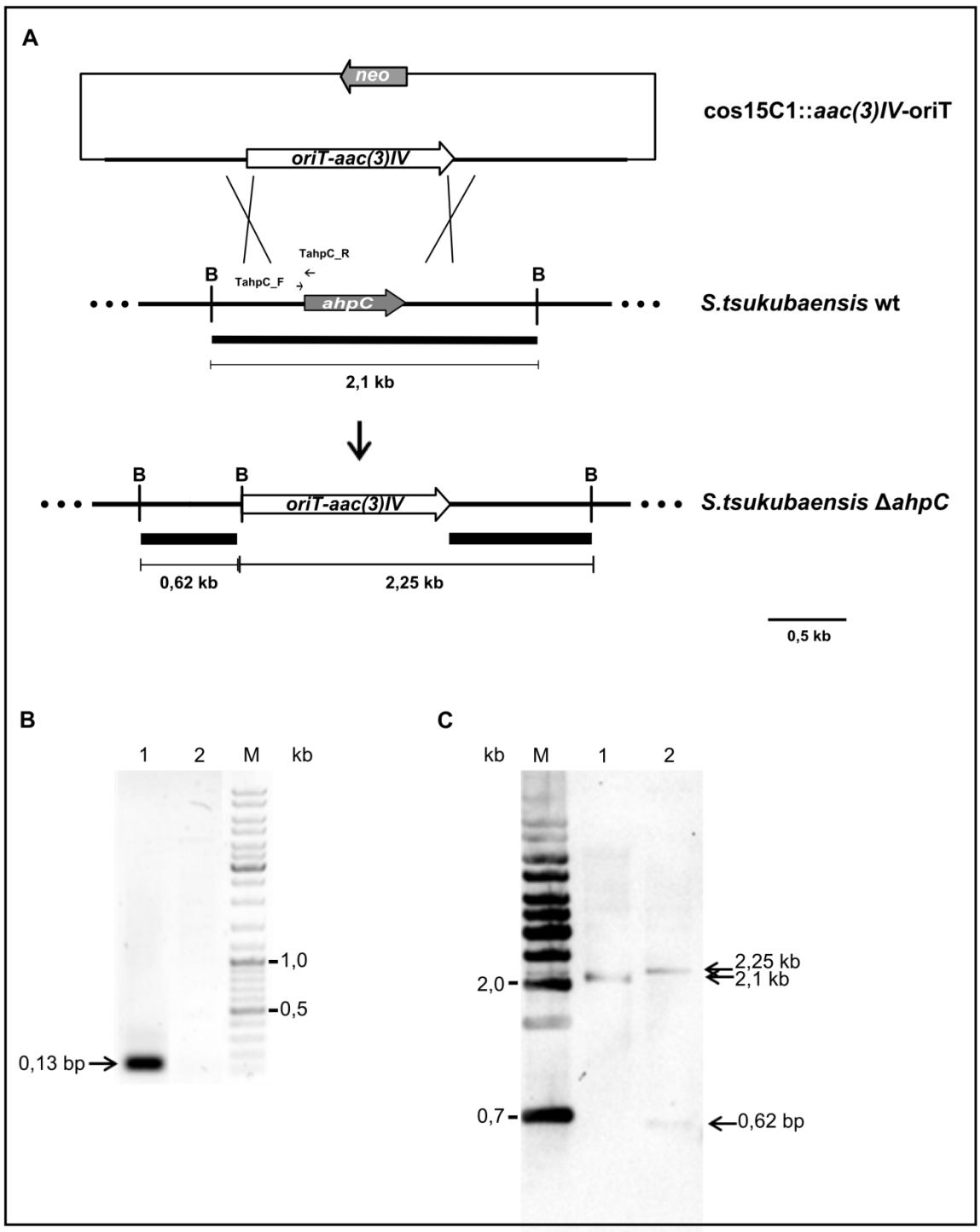

Figure 3.14 – Construction of *S. tsukubaensis* Δ*ahpC* strain. (A) Predicted restriction enzyme polymorphism caused by gene replacement. The *Bam*HI (B) restriction pattern before and after replacement is shown. The probe used for Southern hybridization is indicated by black thick line. (B) Confirmation of gene deletion by PCR. Primers TahpC_F and TahpC_R (Table 2.2) that amplify a 130 bp internal fragment of the *ahpC* gene from wild-type (lane 1) were used to identify double crossover mutant (lane 2). (C) Confirmation of gene deletion by Southern hybridization of the *Bam*HI digested chromosomal DNA of the wild-type (lane 1) and the mutant Δ*ahpC* (lane 2). M: Molecular weight marker.

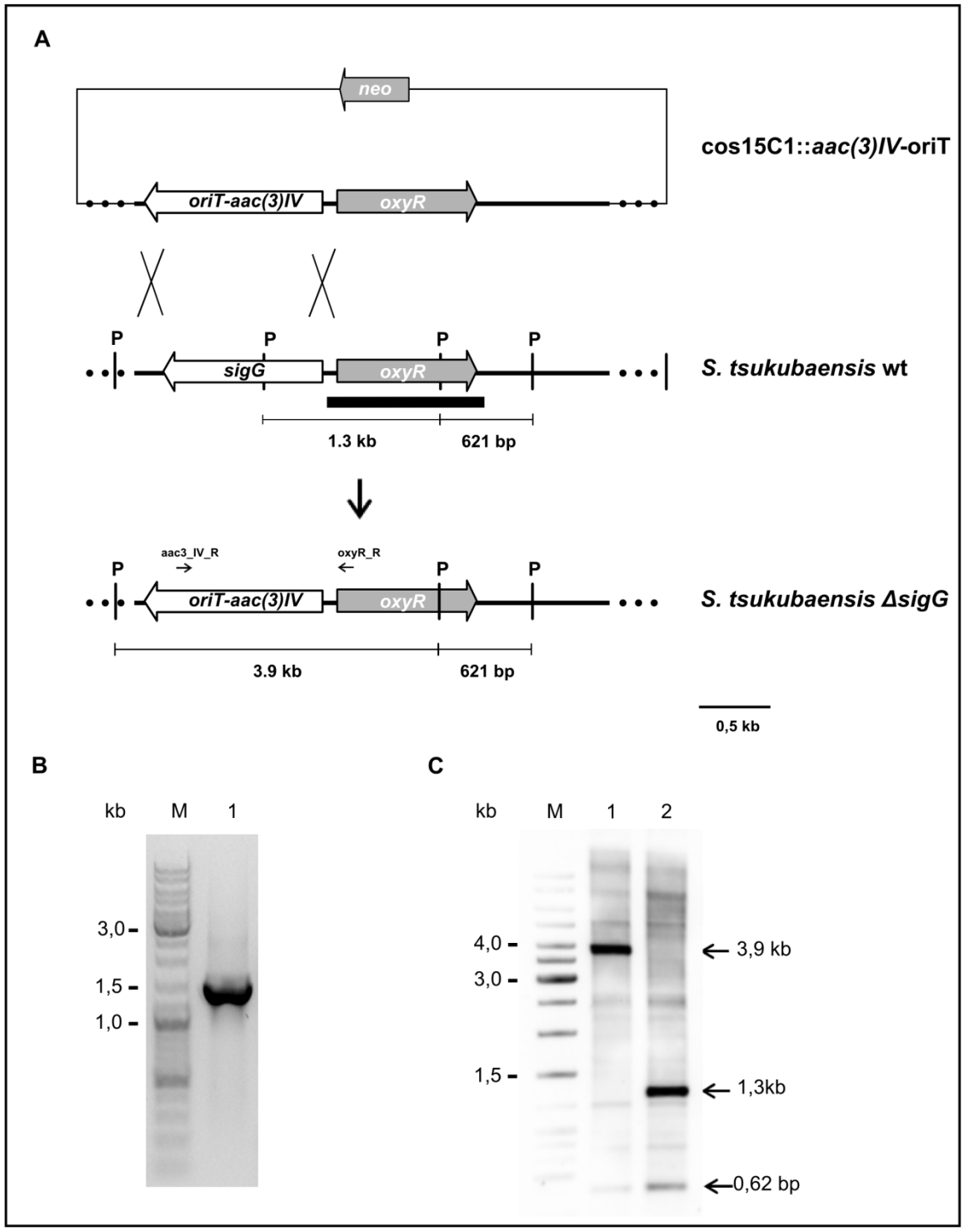

Figure 3.15 – Construction of *S. tsukubaensis* **Δ***sigG* strain. (A) Predicted restriction enzyme polymorphism caused by gene replacement. The *Pvu*II (P) restriction pattern before and after replacement is shown. The probe used for Southern hybridization is indicated by black thick line. (B) Confirmation of gene deletion by PCR. Primers aac3_IV_R and oxyR_R (Table 2.2) that amplify 1.3 kb fragment in Δ*sigG* (lane 1) were used to identify double crossover mutants by absence of the amplicon in the wt. (C) Confirmation of gene deletion by Southern hybridization of the *Pvu*II digested chromosomal DNA of the wild-type (lane 2) and the mutant Δ*sigG* (lane 1). M: Molecular weight marker.

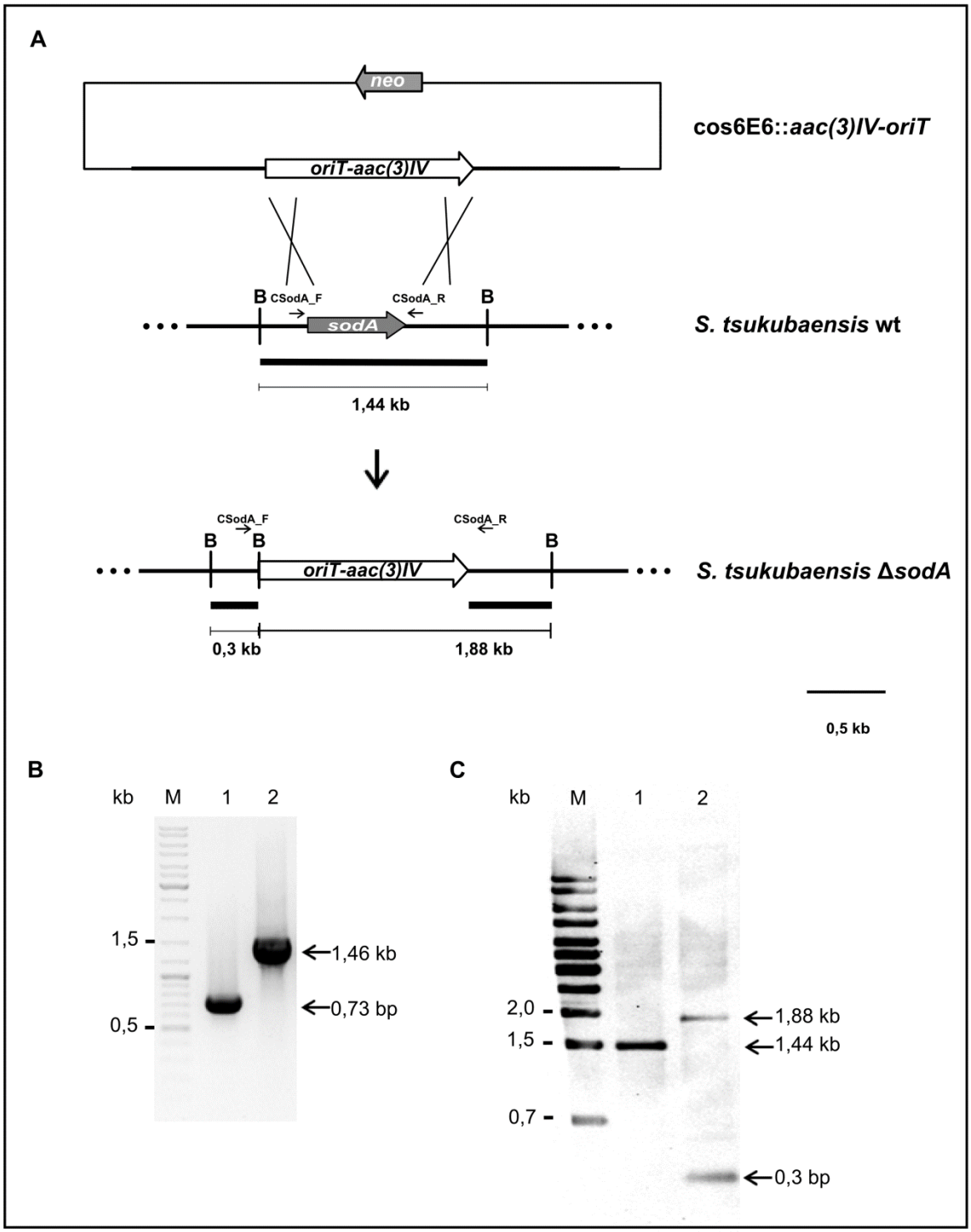

Figure 3.16 – Construction of *S. tsukubaensis* Δ*sodA* strain. (A) Predicted restriction enzyme polymorphism caused by gene replacement. The *Bam*HI (B) restriction pattern before and after replacement is shown. The probe used for Southern hybridization is indicated by black thick line. (B) Confirmation of gene deletion by PCR. Primers CsodA_F and CsodA_R (Table 2.2) that amplify a 0.73 kb in the wild-type (lane 1) and a 1.46 kb fragment in Δ*sodA* (lane 2) were used to identify double crossover mutants (C) Confirmation of gene deletion by Southern hybridization of the *Bam*HI digested chromosomal DNA of the wild-type (lane 1) and the mutant Δ*sodA* (lane 2). M: Molecular weight marker.

3.3.4 Construction of mutant strains overexpressing oxidative stress related genes

Three *S. tsukubaensis* strains overexpressing *sodA*, *sodN* or *katA1* were generated. DNA fragments containing the *sodA*, *sodN* or *katA1* were generated by PCR using primer pairs, tsku_erm_sodA_F/tsku_erm_sodA_R, tsku_erm_sodN_F/tsku_erm_sodN_R and tsku_erm_katA1_F/tsku_erm_katA1_R (Table 2.2) respectively. DNA fragments were inserted into the integrative vector pIB139 (Wilkinson *et al.* 2002) downstream the constitutive promoter *ermE**p (Bibb *et al.* 1985), generating pIB*sodA*, pIB*sodN* and pIB*katA1* respectively. Plasmids were transferred to *S. tsukubaensis* by intergeneric conjugation, generating the strains *S. tsukubaensis* [pIB*sodA*], *S. tsukubaensis* [pIB*sodN*] and *S. tsukubaensis* [pIB*katA1*]. Integration in *S. tsukubaensis* genome was confirmed by southern blot hybridization and/or PCR (Fig. 3.17, Fig. 3. 18 and Fig. 3.19 respectively).

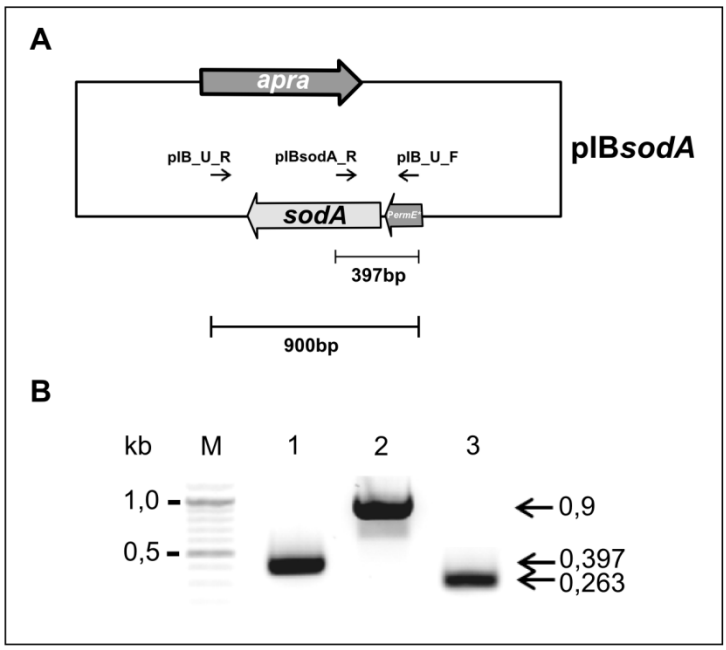

Figure 3.17 – *S. tsukubaensis* [pIB*sodA*] strain. (A) Hybridization regions of the primer pairs, used to confirmation vector integration in the chromosome by PCR, are indicated by arrows. (B) pIB*sodA* integration was confirmed by PCR, using as template genomic DNA of *S. tsukubaensis* [pIB*sodA*] and *S. tsukubaensis* [pIB139] and primer pairs pIB_U_F and pIB*sodA*_R and pIB_U_F and pIB_U_R (Table 2.2) for pIB*sodA* integration confirmation (lane 1 and 2 respectively) and primer pair pIB_U_F and pIB_U_R for pIB139 integration (lane 3). M: Molecular weight marker

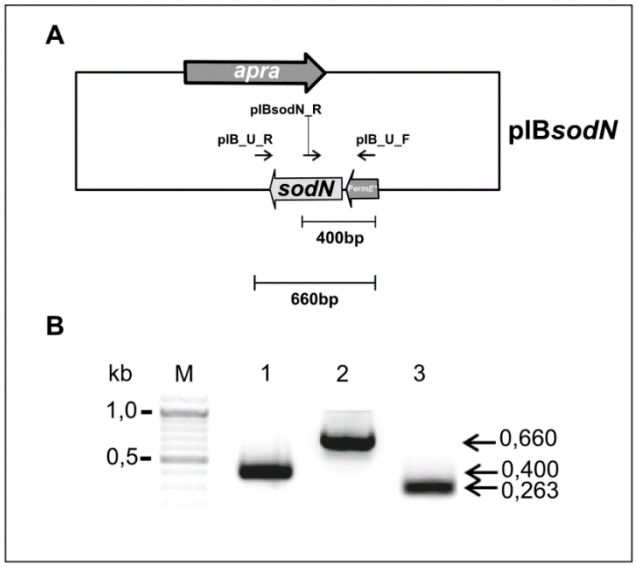

Figure 3.18 – *S. tsukubaensis* [pIB*sodN*] strain. (A) Hybridization regions of the primer pairs, used to confirm vector integration in the chromosome by PCR, are indicated by arrows. (B) pIB*sodN* integration was confirmed by PCR, using as template genomic DNA of *S. tsukubaensis* [pIB*sodN*] and *S. tsukubaensis* [pIB139] and primer pairs pIB_U_F and pIB*sodN*_R and pIB_U_F and pIB_U_R (Table 2.2) for pIB*sodN* integration confirmation (lane 1 and 2 respectively) and primer pair pIB_U_F and pIB_U_R for pIB139 integration (lane 3). M: Molecular weight marker

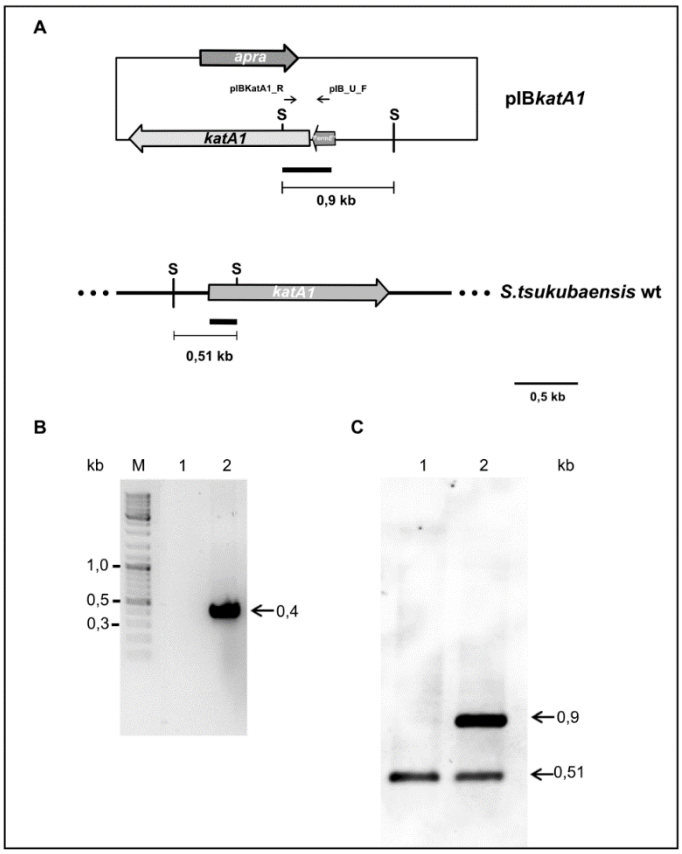

Figure 3.19 – *S. tsukubaensis* [pIB*katA1*] strain. (A) Predicted restriction enzyme polymorphism by pIB*katA1* integration. The *Sma*I (S) restriction pattern is shown. The probe used for Southern hybridization is indicated by black thick line and primer pair hybridization region is indicated by arrows. (B) Confirmation of gene integration by PCR. Primers pIBkatA1_R and pIB_U_F (Table 2.2) were used to identify mutants (lane 1 wild-type; lane 2 *S. tsukubaensis* [pIB*katA1*]). (C) Confirmation of vector integration by Southern hybridization of the *Sma*I digested chromosomal DNA of wild-type (lane 1) and the mutant *S. tsukubaensis* [pIB*katA1*] (lane 2). M: Molecular weight marker

3.4 – DISCUSSION

In *S. natalensis* ATCC 27448, maintaining H_2O_2 intracellular levels at a certain threshold, particularly during late exponential and early stationary phases, proved to be important to elicit pimaricin biosynthesis and to change its final yield. Although the punctual H_2O_2 modulation achieved by the addition of exogenous H_2O_2 suggested such a crosstalk, the correlation between H_2O_2 and secondary metabolism was clearly shown by the characterization of the H_2O_2-related enzymes defective mutants, in which a long-term modulation of H_2O_2 levels was achieved (Beites *et al.* 2011). In specific, *S. natalensis* Δ*katA1* strain behaved as a pimaricin overproducer, reaching 156% of the pimaricin produced by the wild-type.

The *in silico* analysis performed for *S. tsukubaensis* showed that this strain presents two genes coding for monofunctional catalases, *katA1* and *katA2*, whereas no catalase-peroxidase was detected. It also showed the presence of two superoxide dismutase encoding genes, *sodA* coding for an iron-containing SOD and *sodN* coding for a nickel containing SOD. The alkyl hydroperoxidase system was also identified but, interestingly, a difference in the common *Streptomyces oxyR-ahpCD* genomic region organization was found in *S. tsukubaensis*. This peculiarity will be further explored in chapter 4. The results obtained with the *in silico* analysis were in accordance with the ones obtained with the physiological characterization of *S. tsukubaensis*.

In *S. tsukubaensis*, total SOD activity was maintained at a constant level throughout the growth curve with the activation of both an iron and a nickel containing SOD. The same pattern was observed for $O_2^{\cdot -}$ intracellular levels. However, regarding catalase activity, a growth dependent profile was observed that differs according to growth conditions, i.e., in tacrolimus producing and non-producing conditions. In many microorganisms induction of catalase activity is observed not only as a response to oxidative stress, but it can also be modulated by internal developmental events (Loewen and Switala 1988, Chary and Natvig 1989) as previously described for *S. coelicolor* (Walker *et al.* 1995). In the case of *S. tsukubaensis* growing in tacrolimus-producing conditions, total catalase activity profile showed a growth-dependent behaviour with a marked induction of catalase activity during the transition from early to late exponential phase overlapping with the onset of tacrolimus production. Conversely, H_2O_2 intracellular levels decreased

and were maintained low during tacrolimus production (Fig. 3.20). This behaviour is different from the one observed in *S. natalensis* ATCC 27448 in pimaricin producing conditions (Beites *et al.* 2011) which suggests a different redox-based regulation of tacrolimus biosynthesis in *S. tsukubaensis*.

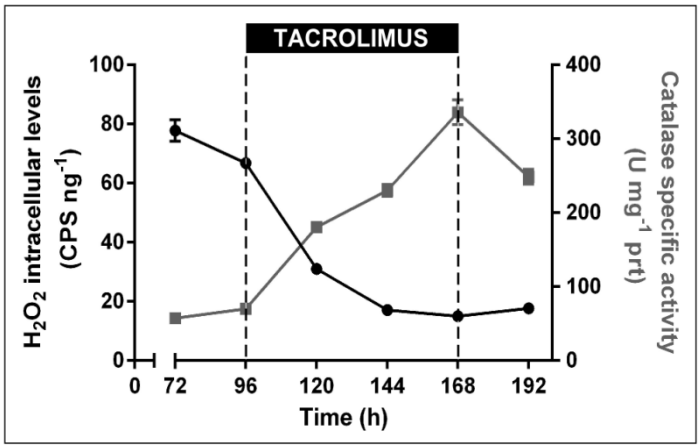

Figure 3.20 – Overlapping between H_2O_2 intracellular levels, catalase activity and tacrolimus production in *S. tsukubaensis*. In the transition from early (96 h) to late exponential phase (120 h) and overlapping with the onset of tacrolimus production, a marked decrease of H_2O_2 as well as an induction of catalase activity occurs. Tacrolimus production time range is indicated on top of the graph by a thick black line.

The fact that the onset of tacrolimus production overlaps with the decrease of H_2O_2 intracellular levels and increase in catalase activity, raises the possibility that tacrolimus production may require a very controlled intracellular redox environment. Moreover the putative role of tacrolimus as an antioxidant compound combined with the fact that the molecule can be susceptible to oxidation points out the importance of maintaining low H_2O_2 intracellular levels in order to protect tacrolimus from oxidative damage during its biosynthesis and before secretion. Furthermore, the increase of O_2 availability, as well as the addition of H_2O_2 to the medium led to an induction of catalase activity and increase in tacrolimus production. Catalase induction resulted in a decrease in H_2O_2 intracellular levels given that catalase presents a high catalytic efficiency regarding H_2O_2 decomposition, being inactivated in some cases, only with 3 M of H_2O_2 (Chelikani *et al.* 2004). Considering the resulting increase in ROS intracellular levels, a redirection of the carbon flux to the PPP could be occurring in order to increase intracellular reducing power, through an increase in NAPDH pool. Given that NAPDH is also required for tacrolimus biosynthesis, this hypothesis could help

explain the increased observed for tacrolimus production. Interestingly, a *S. tsukubaensis* strain overexpressing G6PDH, presented an increase of 35% in tacrolimus production (Huang *et al.* 2013). Another possibility is that the metabolic switch, from primary metabolism to secondary metabolism, can be anticipated with these conditions given that the metabolic shift is intrinsically associated with metabolic stress. Understanding the switch to secondary metabolism is of major importance in biotechnology, since it can contribute to improve secondary metabolites production.

Adaptation to conditions known to increase ROS production resulted in a decrease of intracellular oxic conditions that favoured tacrolimus production. Finally, the fact that we were never able to generate a Δ*katA1* strain can suggest a crucial role of the monofunctional catalase. All this together reinforces the idea that the molecular mechanisms behind tacrolimus production have a redox-dependent regulation.

CHAPTER 4

Interplay between oxidative stress response, iron metabolism and tacrolimus production

4.1 GENOMIC ORGANIZATION OF THE *OXYR-AHPCD* REGION IN *S. TSUKUBAENSIS*

In silico analysis of *S. tsukubaensis oxyR* genomic region (Chapter 3) revealed a different genomic organization when compared to other *Streptomyces* strains. In order to study this peculiar feature an *in silico* analysis of this genomic region in other *Streptomyces* strains was performed, as well as the functional characterization of *S. tsukubaensis oxyR*, *ahpC* and *sigG*.

4.1.1 *S. tsukubaensis* displays an unique genomic organization of the *oxyR-ahpCD* region

BLASTp analysis of the *S. tsukubaensis* NRRL 18488 draft genome [accession number AJSZ01000000; Barreiro et al. (2012)] using the *S. coelicolor* OxyR protein sequence (SCO5033) as query, identified STSU_11565 as the orthologous OxyR protein in *S. tsukubaensis* (83% of sequence identity). Automatic annotation identified the protein coded by *STSU_11565* as a LysR family transcriptional regulator although with a predicted size (257 aa) considerable smaller than that of SCO5033 (312 aa). The smaller size of the expected protein and the location of *STSU_11565* at the 3'-end of contig 348 (AJSZ01000348) suggested a sequence gap between adjacent contigs 348 and 349 that could have led to an incorrect *STSU_11565* ORF annotation. Sequencing of a 1,17 kb PCR-generated fragment using primers ctg348_F and ctg349_R (located at the 3'- and 5'-extremities of contigs 348 and 349, respectively; (Table 2.2) allowed to assemble the two contigs into one sequence (sequence to be submitted to the GenBank database; Appendix I) and to correct *STSU_11565* annotation. *STSU_11565* codes for a 326 aa-long protein that presents high sequence identities with hydrogen peroxide sensing regulators of the LysR-family (best hit: sequence identity of 86% with SCLAV_3936 from *S. clavuligerus*). STSU_11565 displays the typical OxyR protein domain architecture: an N-terminal HTH bacterial regulatory domain (12 – 71 aa; PF00126) and a C-terminal LysR substrate binding domain (95 – 305 aa; PF03466). Hereafter we will designate STSU_11565 by OxyR.

Synteny analysis of *oxyR* genomic region in 71 *Streptomyces* strains that presented an OxyR orthologous protein revealed that *S. tsukubaensis* presents a unique genomic organization of the *oxyR-ahpCD* region (Fig. 4.1). The common *Streptomyces* genomic organization is typified by *S. coelicolor* where *oxyR* is divergently transcribed from the *ahpCD* operon encoding the alkyl hydroperoxide reductase system (Hahn *et al.* 2002). Downstream from *oxyR* and also divergently transcribed, is the operon formed by *SCO5036*, *SCO5035* and *SCO5034* genes that are presumably involved in resistance to vancomycin (Hesketh *et al.* 2011, Santos-Beneit *et al.* 2014). In *S. tsukubaensis* the *ahpCD* operon is located 3,9 kbp downstream from *oxyR*, and is divergently transcribed from the conserved operon formed *by STSU_11580*, *STSU_11575* and *STSU_11570* genes, homologous to the *SCO5036-SCO5034* operon (Fig. 4.1). Three additional genes are found in the *oxyR* genomic region of *S. tsukubaensis*: *STSU_11555*, *STSU_11560* and *STSU_11595*. Regarding *STSU_11555* and *STSU_11595* no conserved domains were found in these proteins, which have been annotated as hypothetical proteins.

Due to its uniqueness and to discard any sequencing and/or sequence

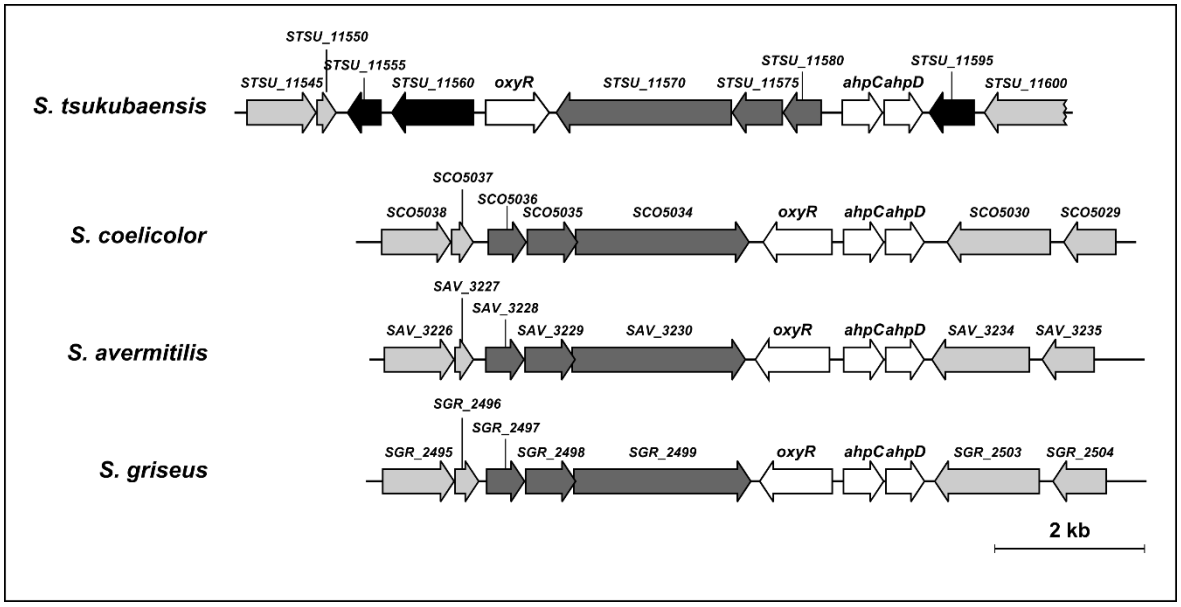

Figure 4.1 – Genomic organization of the *oxyR-ahpCD* region in *Streptomyces* sp. *S. tsukubaensis* unique *oxyR-ahpCD* genomic region with *ahpC* found 3.9 kb apart from *oxyR* (white arrows); the three novel genes are indicated by black arrows. The common *Streptomyces oxyR-ahpCD* genomic region here typified by *S. coelicolor*, *S. avermitilis* and *S. griseus* strains with *oxyR* being divergently transcribed from *ahpCD*.

assembling errors, we further confirmed the *S. tsukubaensis oxyR* genomic region organization by Southern-blot analysis using a 1.2 kb probe, covering the *oxyR* gene plus its upstream and downstream regions (Fig. 4.2 A). The corrected

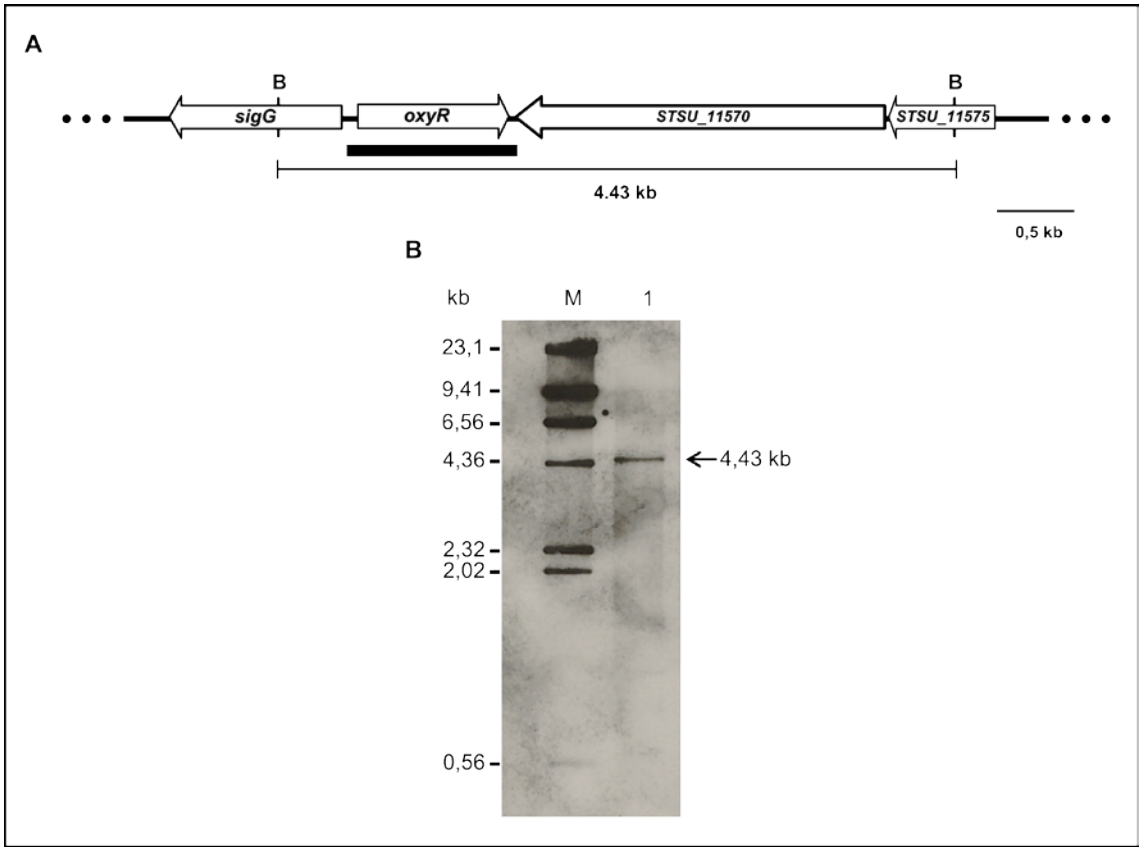

Figure 4.2 – Genomic organization confirmation by Southern-blot hybridization. (A) Predicted *Bam*HI (B) restriction pattern of the *oxyR* genomic region. The probe used for Southern hybridization is indicated by black thick line. (B) Confirmation of *S. tsukubaensis oxyR* genomic gene organization by Southern hybridization of the *Bam*HI digested chromosomal DNA of the wild-type (lane 1). M: Molecular weight marker.

organization was confirmed by Southern blot (Fig. 4.2 B).

Studies performed on OxyR from several bacteria have identified two conserved cysteines in the C-terminus region that provide the redox-sensing domain and are responsible for the thiol based redox switch of OxyR (Lee *et al.* 2004). OxyR from *S. tsukubaensis* harbours two cysteines at a homologous position (C^{208} and C^{217}) likely to be responsible for providing the free thiol-groups for redox sensing. This redox sensing motif is conserved amongst *Streptomyces*; however in *S. tsukubaensis* a point mutation is present with a substitution of an isoleucine for a valine in position 216 (Fig. 4.3). Interestingly, the analysis of the OxyR sequence in the 71 *Streptomyces* strains with an OxyR orthologous protein

revealed the presence of this point mutation in 12 more strains (Fig 4.3), all of which have already been described as pathogenic. Taking into consideration the importance of OxyR in the virulence of the infectious processes (Flores-Cruz and Allen 2011), this point mutation found in OxyR could be related with these *Streptomyces* strains pathogenicity. Further structural and mechanistic studies on OxyR will help to clarify this putative relation.

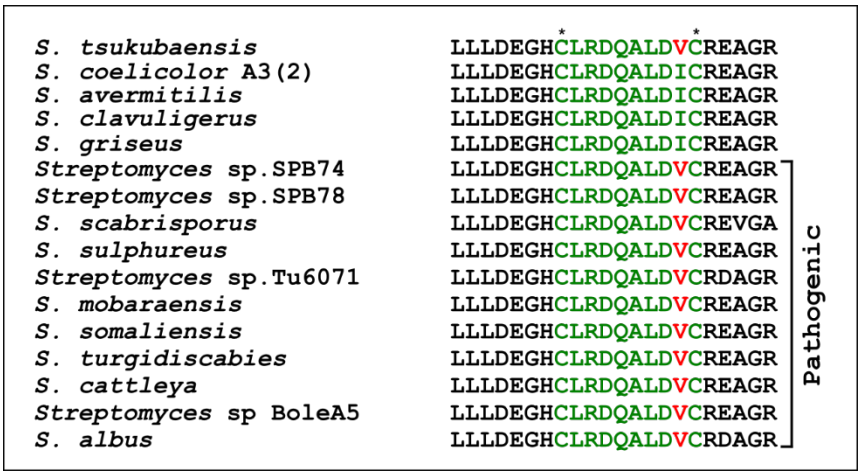

Figure 4.3 – OxyR redox sensing-motif in *Streptomyces*. The conserved *Streptomyces* OxyR redox-sensing motif is indicated in green. The point mutation of an isoleucine for a valine is indicated in red and the redox active cysteines are indicated with an *.

4.1.2 A novel Extracytoplasmic function (ECF) sigma factor in *S. tsukubaensis*

In *S. tsukubaensis*, *oxyR* is divergently transcribed from *STSU_11560* that showed sequence identity with *Streptomyces* RNA polymerase σ^{70} factors such as SRIM_16270 from *S. rimosus* subsp. *rimosus* ATCC 10970 (71% sequence identity) and SSCG_00713 from *S. clavuligerus* (67% sequence identity). *In silico* analysis of the 369 aa long STSU_11560 protein revealed the presence of three conserved domains: region σ_2 of σ^{70} proteins between 53 and 120 aa (Sigma70_r2; PF04542; E-value 3.8e-20), region σ_4 of σ^{70} proteins between 174 and 227 aa (Sigma70_r4_2; PF08281; E-value 1e-17) and a polyketide cyclase SnoaL-like domain between 252 and 352 aa (SnoaL_2; PF12680; E-value 8e-10). The presence of the conserved regions σ_2 and σ_4 of the σ^{70} protein family suggests that STSU_11560 is a member of the extracytoplasmic function (ECF) subfamily of bacterial sigma factors. Based on a phylogenetic analysis, ECF

proteins have been classified into 43 groups (Staron *et al.* 2009). However the criteria used led to the exclusion of proteins with more than 50 amino acids between regions σ_2 and σ_4 and proteins with domains other than Sigma70_r2 and Sigma70_r4/Sigma70_r4_2; STSU_11560 has 53 amino acids between σ_2 and σ_4 regions and harbours a C-terminal polyketide cyclase SnoaL-like domain (Fig 4.4). BLASTp analysis of STSU_11560 restricted to the *Mycobacterium* genus showed sequence identities (best hit 43% identity) with the alternative ECF sigma factor SigG that also harbours the Sigma70_r2, Sigma70_r4_2 and SnoaL_2 domains. Previous studies in *M. tuberculosis* have shown that SigG is regulated as part of the DNA damage response controlling genes putatively involved in the detoxification of DNA damaging agents (Smollett *et al.* 2011, Gaudion *et al.* 2013). Henceforward we will refer to STSU_11560 as SigG.

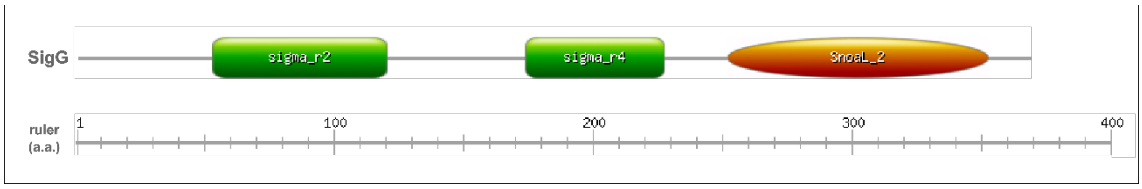

Figure 4.4 – Domain structure of *S. tsukubaensis* SigG protein. SigG harbours three conserved motifs: region σ^2 and σ^4 indicating that SigG belongs to the extracytoplasmic function ECF sigma factor as well as a SnoaL_like domain.

4.2 FUNCTIONAL CHARACTERIZATION OF *SIGG*, *OXYR*, AND *AHPC* IN *S. TSUKUBAENSIS*

To characterize the OxyR-mediated oxidative stress response in *S. tsukubaensis* we constructed three mutants defective on OxyR, AhpC or SigG by replacing the target encoding gene with an apramycin resistance cassette using the PCR targeting procedure (Gust *et al.* 2003). Gene replacements were performed within cosmid 15C1 and the obtained mutant cosmids where introduced into *S. tsukubaensis* NRRL 18488 by intergeneric conjugation. The generated Δ*oxyR*, Δ*ahpC* and Δ*sigG* mutants were confirmed by PCR and Southern blot hybridization (Chapter 3).

All three mutants grew normally in liquid and solid media (Fig. 4.5 A), nevertheless in liquid cultures Δ*sigG* mutant displayed a slight growth delay and also required more incubation time to reach sporulation in solid cultures.

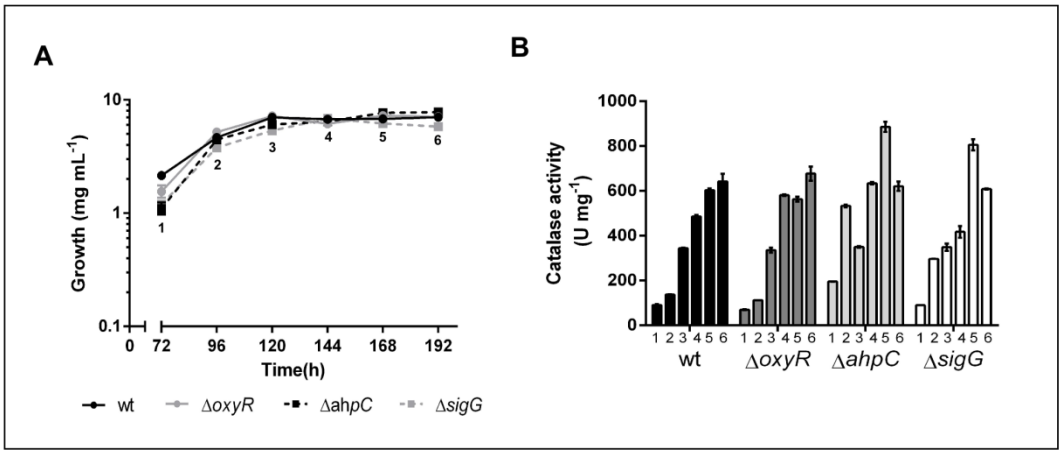

Figure 4.5 – Growth curve and catalase activity of *S. tsukubaensis*, **Δ***oxyR*, **Δ***ahpC* **and Δ***sigG* strains. (A) *S. tsukubaensis* wild-type and mutant strains growth. Strains were grown in MGm medium and growth was assessed by dry weight measurements. (B) Total catalase activity was measured spectrophotometrically in samples collected throughout growth in all strains – time points 1 to 6. Vertical bars indicate standard deviation of the mean values. Results (average of triplicates and standard deviation) are representative of three independent experiments.

4.2.1 *S. tsukubaensis* Δ*sigG*, Δ*oxyR* and Δ*ahpC* ROS sensitivity bioassays

We tested the sensitivity of the three mutant strains to H_2O_2 induced oxidative stress by evaluating growth inhibition around disks containing 9 M H_2O_2 (Fig. 4.6). Under the conditions tested, *S. tsukubaensis* Δ*oxyR* (inhibition halo 4,65 ± 0.07 cm) and Δ*sigG* (4,86 ± 0,13 cm) strains displayed higher sensitivity than the wild-type (3,47 ± 0,23 cm) to exogenous H_2O_2 whilst Δ*ahpC* (2,73 ± 0.07 cm) was more resistant. The results showed that in *S. tsukubaensis* OxyR is involved in H_2O_2-induced stress response. Interestingly, they also indicated an involvement of SigG in the oxidative stress response of *S. tsukubaensis*.

To determine if strain sensibility to H_2O_2 could be attributed to a modulation of catalase activity, we monitored total catalase activity of the mutant strains throughout the growth curve (Fig. 4.5 B). The increase of catalase activity in Δ*ahpC* strain when compared to the wild-type, could partially explain the increased resistance to H_2O_2 induced stress. However, Δ*sigG* strain also presented higher

levels of catalase activity then the wild-type even though it was more sensible to H_2O_2.

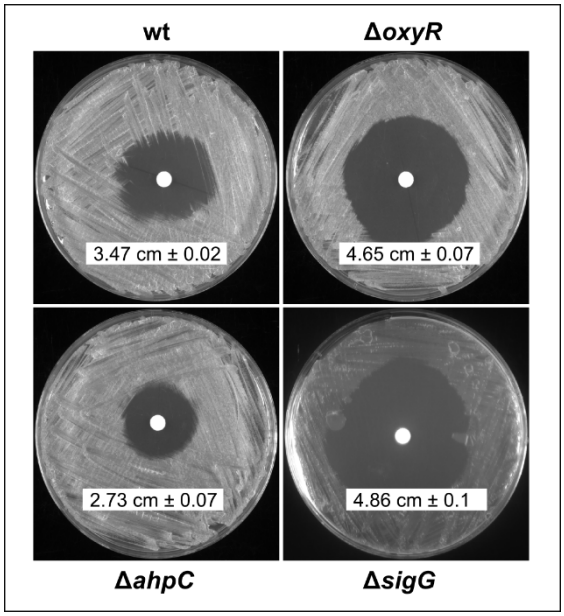

Figure 4.6 – Growth inhibitions assays in *S. tsukubaensis* wild-**type, Δ***oxyR,* **Δ***ahpC* **and Δ***sigG* strains. For oxidative stress growth inhibition bioassays *S. tsukubaensis* wild-type and mutant strains were grown in YED medium. Sensitivity to H_2O_2 was tested with the addition of 9M of H_2O_2 to sterile discs.

4.2.2 SigG and iron metabolism

Iron plays a key role in the bacterial oxidative stress response either as a cofactor in ROS-sensing proteins or by the generation of hydroxyl radical via the Fenton reaction (Cornelis *et al.* 2011). In *E. coli*, in addition to genes directly involved in H_2O_2 detoxification, the OxyR regulon includes genes involved in iron uptake and storage (Zheng *et al.* 2001), in order to maintain a strict and cross-regulated control of iron levels, to avoid iron toxicity. To elucidate whether the SigG-OxyR-AhpC system could be involved in iron uptake in *S. tsukubaensis* we monitored total iron content of the wild-type and mutant strains culture broths throughout the growth curve (Fig. 4.7). The results showed higher levels of total iron in the culture supernatant of the Δ*sigG* strain throughout the growth curve when compared to the wild-type, suggesting a hampered iron uptake in this mutant strain. The extracellular total iron content was a reflection of the intracellular total iron content as confirmed by atomic absorption spectrophotometry at 120 h (8,0 ± 0,6 μM in wild-type *vs* 5,2 ± 0,5 μM in Δ*sigG*).

Even though there is a knowledge scarcity regarding ferrous iron uptake in *Streptomyces*, ferric iron uptake has been elucidated and it is mediated by high affinity iron chelators known as siderophores. To evaluate siderophore production

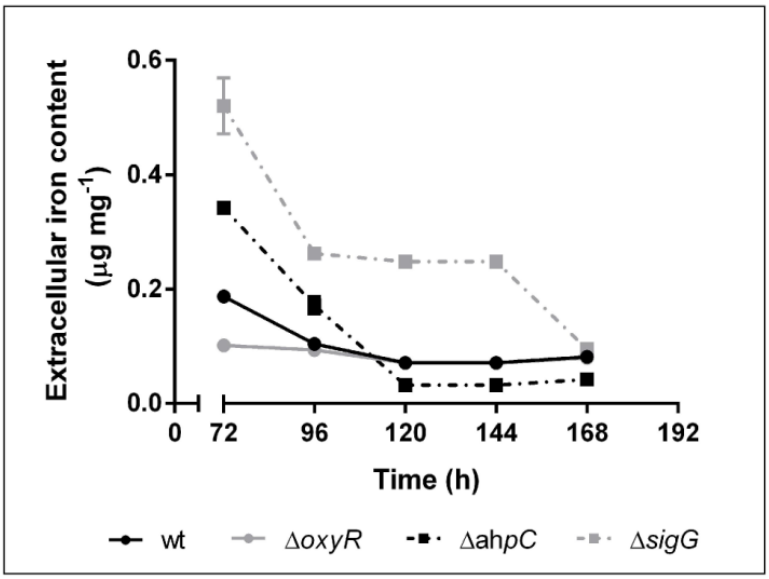

Figure 4.7 – Extracellular iron content of *S. tsukubaensis* wild-**type, Δ***oxyR,* **Δ***ahpC* **and Δ***sigG* strains. Extracellular iron content was determined in all *S. tsukubaensis* strains throughout growth. Strains were grown in MGm medium as standard. Vertical bars indicate standard deviation of the mean values. Results (average of triplicates and standard deviation) are representative of three independent experiments.

in *S. tsukubaensis* strains we performed CAS agar diffusion assays with culture broths grown in iron sufficient (32 μM) or iron limitation conditions (MG medium not

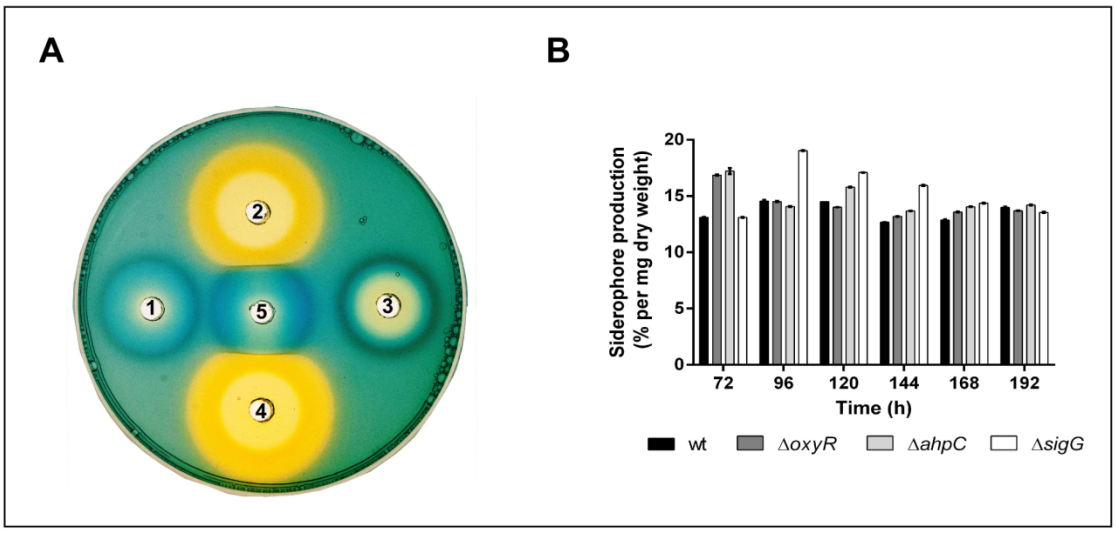

Figure 4.8 –*S. tsukubaensis* wild-**type, Δ***oxyR,* **Δ***ahpC* **and Δ***sigG* strains siderophore production. (A) CAS assay to determine siderophore production in wild type and Δ*sigG* strains grown in MGm medium with and without ferrous iron supplementation. 1- Supernatant of the wild-type grown in MGm; 2- Supernatant of the wild-type grown in MGm medium without Fe^{2+} supplementation. 3- Supernatant of the Δ*sigG* grown in MGm; 4- Supernatant of the Δ*sigG* grown in MGm without Fe^{2+} supplementation; 5 – MGm medium. (B) Siderophore production in wild-type, Δ*oxyR*, Δ*ahpC* and Δ*sigG* strains grown in MGm medium without ferrous iron supplementation. Siderophore production was assessed using liquid CAS assay in samples collected throughout growth. Vertical bars indicate standard deviation of the mean values. Results (average of triplicates and standard deviation) are representative of three independent experiments.

supplemented with iron; initial iron concentration below 5 μM) that favour siderophore production in *Streptomyces* (Tunca *et al.* 2007). Detection of siderophores in non-limiting iron conditions was hardly visible, particularly for the wild-type, Δ*oxyR* and Δ*ahpC* strains. However, for Δ*sigG* strain it was clearly visible at 96 h a yellowish halo indicative of siderophore production (Fig. 4.8 A). Conversely, all strains displayed high siderophore production in iron limiting conditions; however from 96 h to 144 h of growth Δ*sigG* presented increased total siderophore production (Fig. 4.8 B).

In *E. coli*, OxyR is well studied and it has been shown to be not only implicated in regulating the H_2O_2-induced stress response but also iron metabolism, regulating, among others, the ferritin like proteins called Dps. Dps proteins bind DNA to protect it from oxidative damage; they can also function as iron reservoir and use H_2O_2 to oxidize ferrous iron to ferric iron, avoiding this way iron toxicity (Almiron *et al.* 1992). *S. coelicolor* presents three *dps* encoding genes *dpsA*, *dpsB* and *dpsC* but none has been described as directly involved in oxidative stress response in *S. coelicolor* (Facey *et al.* 2009). One Dps-like encoding gene is present in *S. tsukubaensis* genome - *STSU_08138* (77%

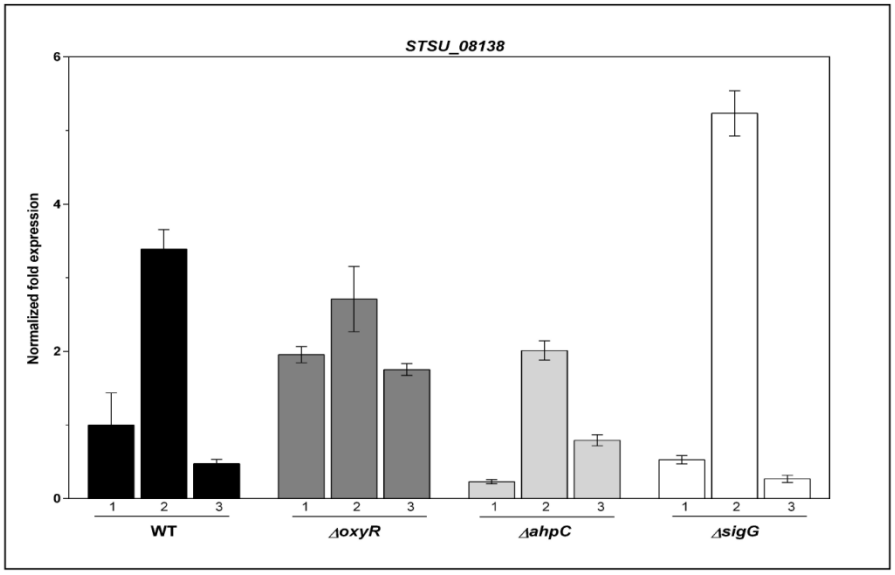

Figure 4.9 – Transcription profile of *STSU_08138* in *S. tsukubaensis* wild-**type, Δ***oxyR,* **Δ***ahpC* **and Δ***sigG* strains. Samples were collected at 72 h (1), 96 h (2) and 120 h (3). Transcription was assessed by RT-qPCR. The Mean Normalised Fold Expression (± standard errors) of the target genes was calculated relative to the transcription of the reference genes (16 S rDNA and *hrdB*) and the reaction of internal normalisation was performed using wild-type as the control situation.

sequence identity with *S. coelicolor* DpsB). We analysed *S. tsukubaensis STSU_08138* transcription during exponential phase (72 h, 96 h and 120 h) (Fig. 4.9). *STSU_08138* transcription was induced at 96 h in all strains, although at different extents. In the case of Δ*oxyR* strain total transcriptional levels were increased during the tested time-points, especially at 72 h and 120 h of growth when compared to the wild-type. As for Δ*ahpC* strain the transcriptional induction observed at 96 h was lower when compared to the wild-type strain while for Δ*sigG* higher transcriptional induction was achieved. Interestingly, this transcriptional profile follows the strains sensitivity towards H_2O_2, suggesting elevated stress conditions in Δ*oxyR* and Δ*sigG* mutants.

4.2.3 Cross-regulation between OxyR and SigG but response to H_2O_2 is SigG-independent

Gene expression of *sigG*, *oxyR*, *STSU_11580* and *ahpC* was assessed in the wild-type and the three mutant strains throughout the exponential growth phase at 72 h, 96 h and 120 h (Fig. 4. 10). The results revealed a negative cross-regulation between OxyR and SigG, i.e., transcription of *oxyR* increased at all time points in the Δ*sigG* mutant and *sigG* expression was up-regulated in the Δ*oxyR* mutant when compared to the wild-type. It should be also highlight the up-regulation of *STSU_11580* expression observed in the Δ*ahpC* mutant and the consistent decrease at 96 h of *ahpC* transcription in the Δ*sigG* mutant. Finally, the positive regulation of *ahpC* transcription by OxyR at mid and late exponential phase is confirmed by the down-regulation of *ahpC* expression in the Δ*oxyR* mutant, however we were able to observe that an OxyR-independent transcription of *ahpC* was also occurring in *S. tsukubaensis*.

The transcriptional response to H_2O_2 induced stress was investigated in RNA samples collected 15 min after the addition of 5 mM H_2O_2 to exponentially *S. tsukubaensis* growing cultures (72 h) (Fig. 4.11). H_2O_2 induction of *ahpC* transcription was clearly observed in the wild-type (6-fold) and Δ*sigG* (5,8-fold) mutant. On the other hand, expression of *ahpC* was not induced in Δ*oxyR* despite the up-regulation of *sigG* transcription in this mutant. Taken together, these results show that the H_2O_2 induction of *ahpC* transcription is mediated by OxyR but not by SigG. Moreover, in the absence of OxyR, *sigG* transcription was induced by H_2O_2,

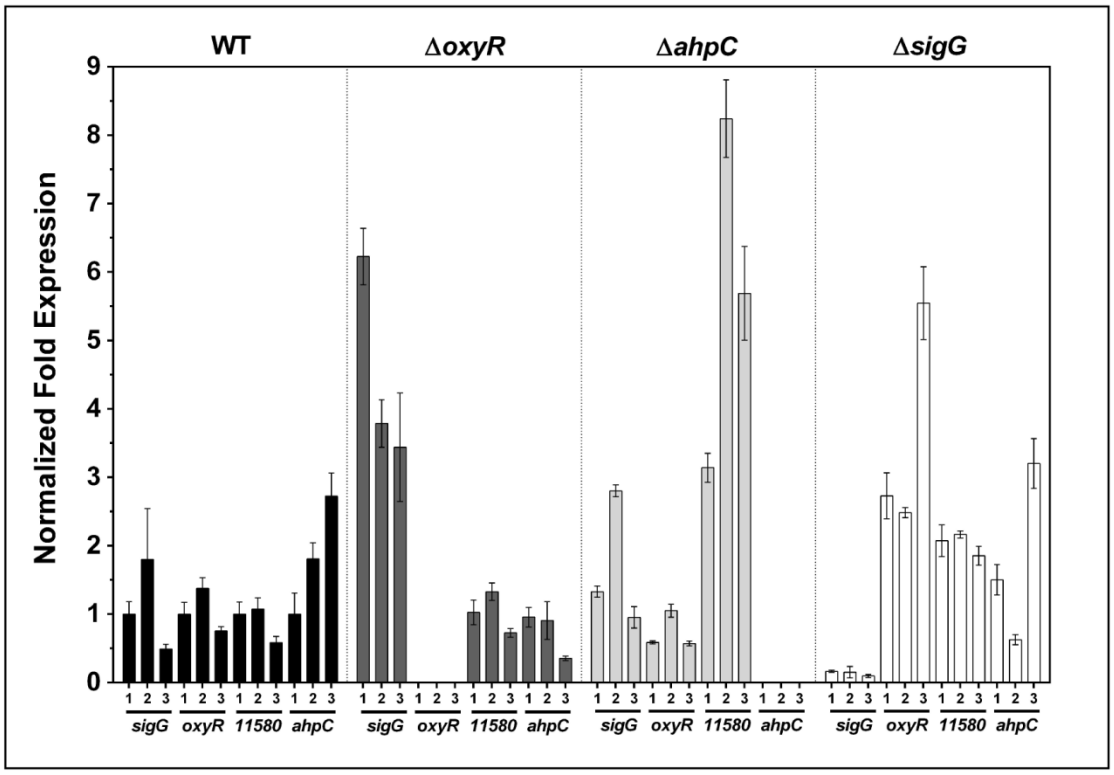

Figure 4.10 – Transcription profile of *sigG*, *oxyR*, *STSU_11580* and *ahpC* in *S. tsukubaensis* wild-type, **Δ***oxyR,* **Δ***ahpC* **and Δ***sigG* strains. Samples were collected at 72 h (1), 96 h (2) and 120 h (3). Transcription was assessed by RT-qPCR. The Mean Normalised Fold Expression (± standard errors) of the target genes was calculated relative to the transcription of the reference genes (16 S rDNA and *hrdB*) and the reaction of internal normalisation was performed using wild-type as the control situation.

however no induction of *sigG* was achieved in the wild-type strain, indicating that in H_2O_2-stress conditions OxyR could be repressing *sigG* transcription and if so SigG is not directly involved in the H_2O_2-induced oxidative-stress response in *S. tsukubaensis*. Finally, the non-responsive transcription of *STSU_11580* to H_2O_2 suggests that this gene is not involved in the H_2O_2-induced oxidative stress response.

In addition, the transcription of *katA1* and its putative regulator *catR* was assessed in the same conditions (Fig. 4.12). As expected, the monofunctional catalase *katA1* and *catR* responded to H_2O_2 insult in all strains suggesting that neither OxyR nor SigG are directly involved in *katA1* regulation and that similar to what was described for *S. coelicolor,* CatR regulates *katA1* transcription in *S. tsukubaensis*.

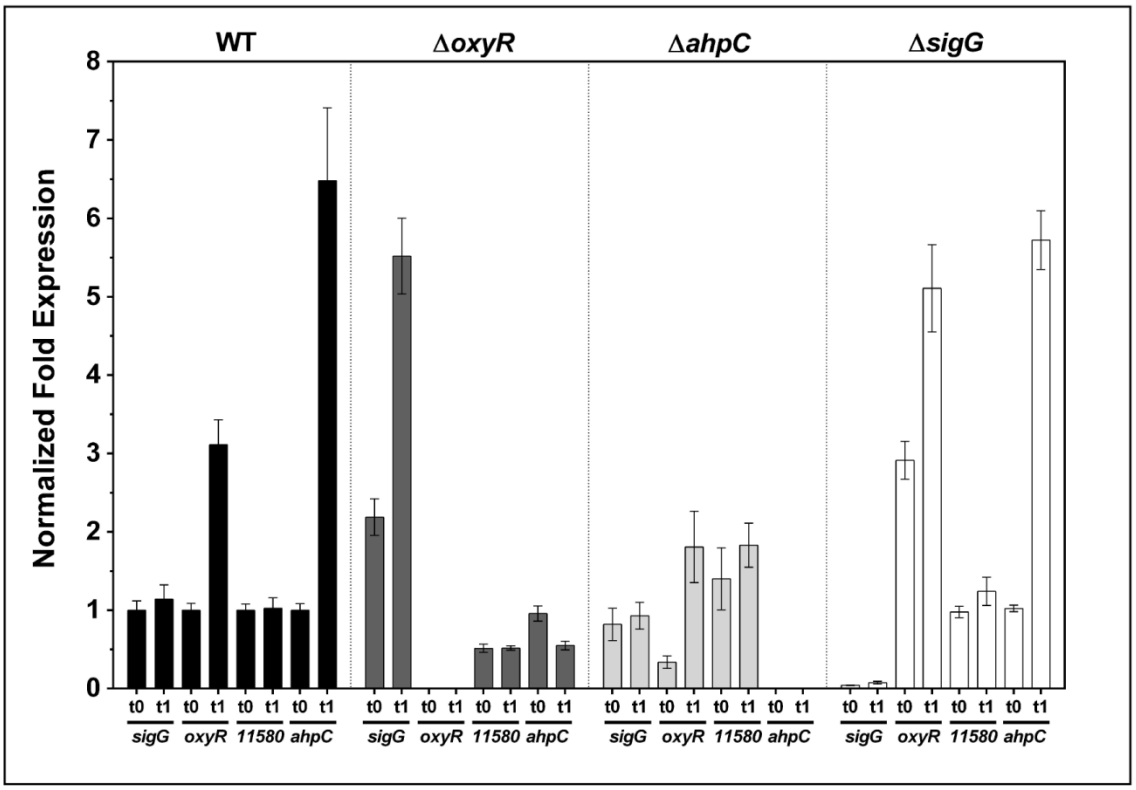

Figure 4.11 – Transcription profile of *sigG*, *oxyR*, *STSU_11580* and *ahpC* in *S. tsukubaensis* wild-type, **Δ***oxyR*, **Δ***ahpC* **and Δ***sigG* strains submitted to H_2O_2 induced stress. Addition of 5 mM H_2O_2 was performed at 72 h of growth. Samples were collected before the addition (t0) and 15 min after (t1). Transcription was assessed by RT-qPCR. The Mean Normalised Fold Expression (± standard errors) of the target genes was calculated relative to the transcription of the reference genes (16 S rDNA and *hrdB*) and the reaction of internal normalisation was performed using wild-type as the control situation.

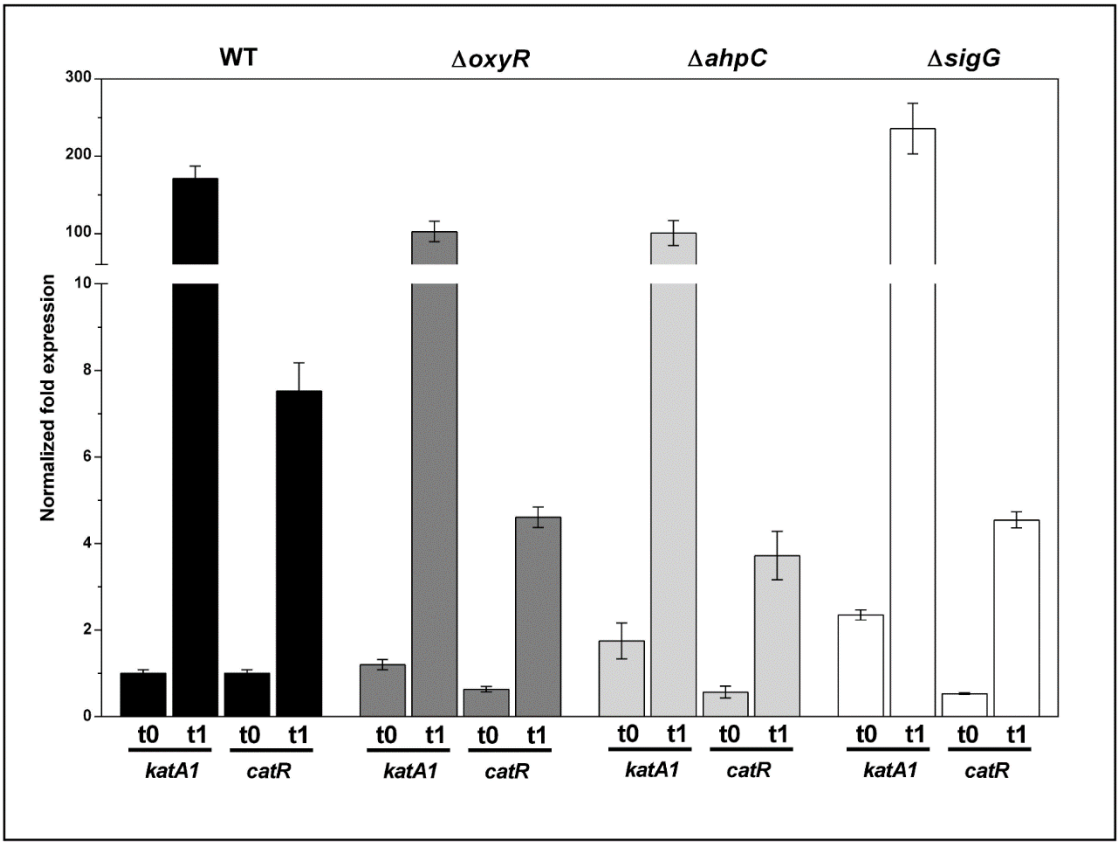

Figure 4.12 – Transcription profile of *katA1* and *catR* in *S. tsukubaensis* wild-**type, Δ***oxyR*, **Δ***ahpC* **and Δ***sigG* strains submitted to H_2O_2-induced oxidative stress. Addition of 5 mM H_2O_2 was performed at 72 h of growth. Samples were collected before the addition (t0) and 15 min after (t1). Transcription was assessed by RT-qPCR. The Mean Normalised Fold Expression (± standard errors) of the target genes was calculated relative to the transcription of the reference genes (16 S rDNA and *hrdB*) and the reaction of internal normalisation was performed using wild-type the control situation.

4.2.4 OxyR binding activity and direct regulatory regulon

In order to investigate the in vitro DNA-binding activity of OxyR from *S. tsukubaensis*, electrophoretic mobility shift assays (EMSAs) were performed with purified C-terminal His-tagged OxyR protein. $OxyR_{STSU}$-His6 was expressed in *E. coli* and purified to near homogeneity (Fig. 4.13).

$OxyR_{STSU}$-His6 binding activity to the *sigG-oxyR* (-167 to +17 relative to the *oxyR* start codon) and *STSU11580-ahpC* (-278 to +15 relative to the *ahpC* start codon) intergenic regions was examined (Fig. 4.14 A and B). With both regions, strong shifted bands were observed and in the case of the *sigG-oxyR* several shifted bands could be detected suggesting multiple binding sites for $OxyR_{STSU}$-His6. We have also analysed the DNA-binding activity of $OxyR_{STSU}$-His6 to the

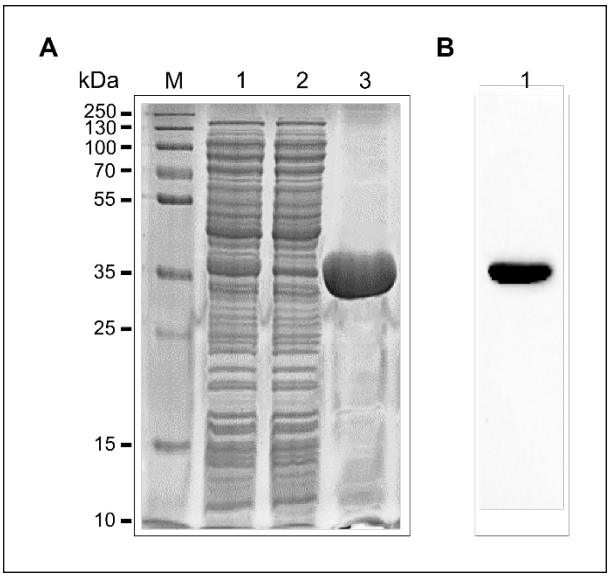

Figure 4.13 – SDS-PAGE of purified $OxyR_{STSU}$-His6 and immunoblot detection. (A) SDS-PAGE (10% polyacrylamide) of total lysate protein crude extracts (1); flow through (2); purified $OxyR_{STSU}$-His6 (3); M – Molecular weight marker. (B) Immunoblot detection of $OxyR_{STSU}$-His6 was performed using an antibody raised against His-Tag. $OxyR_{STSU}$-His6 expected size is approximately 35 kDa.

oxyR-ahpCD intergenic region from *S. coelicolor* (Fig. 4.14 D). The probe used was the same as the one previously used by (Hahn *et al.* 2002) (position -182 to +79 relative to the *oxyR* start codon). A shifted band was also detected showing that $OxyR_{STSU}$-His6 is able to recognize the *S. coelicolor ahpC-oxyR* intergenic region. In all cases, specific binding was confirmed by the increase of free DNA band intensity when un-labelled probe was added (lane S) and the lack of band mobility when non-specific DNA was added to the binding reaction mixture (lane NS). The promoter region of *katA1* was also tested, however, no shift was observed, indicating that OxyR does not bind to this promoter region (Fig. 4.14 C).

To test the DNA-binding activity of reduced *vs* oxidized OxyR, 200 mM DTT or 100 mM H_2O_2 respectively, was added to the binding reaction performed with 10 pmol $OxyR_{STSU}$-His6. The addition of H_2O_2 led to an increase of free DNA band intensity in the three probes tested. This result shows that although $OxyR_{STSU}$-His6 can bind to the probes in both forms, oxidized OxyR presents lower DNA-binding activity to the regions tested.

Furthermore, other promoter regions were tested including the *S. coelicolor* orthologue in *S. tsukubaensis* of the iron repressor encoding gene *dtxR*, the monofunctional catalase *katA2* and the *phoR-phoP* intergenic region. In the promoter regions tested no band shifts were observed, suggesting that OxyR does not bind to these promoter regions (Fig. 4.15).

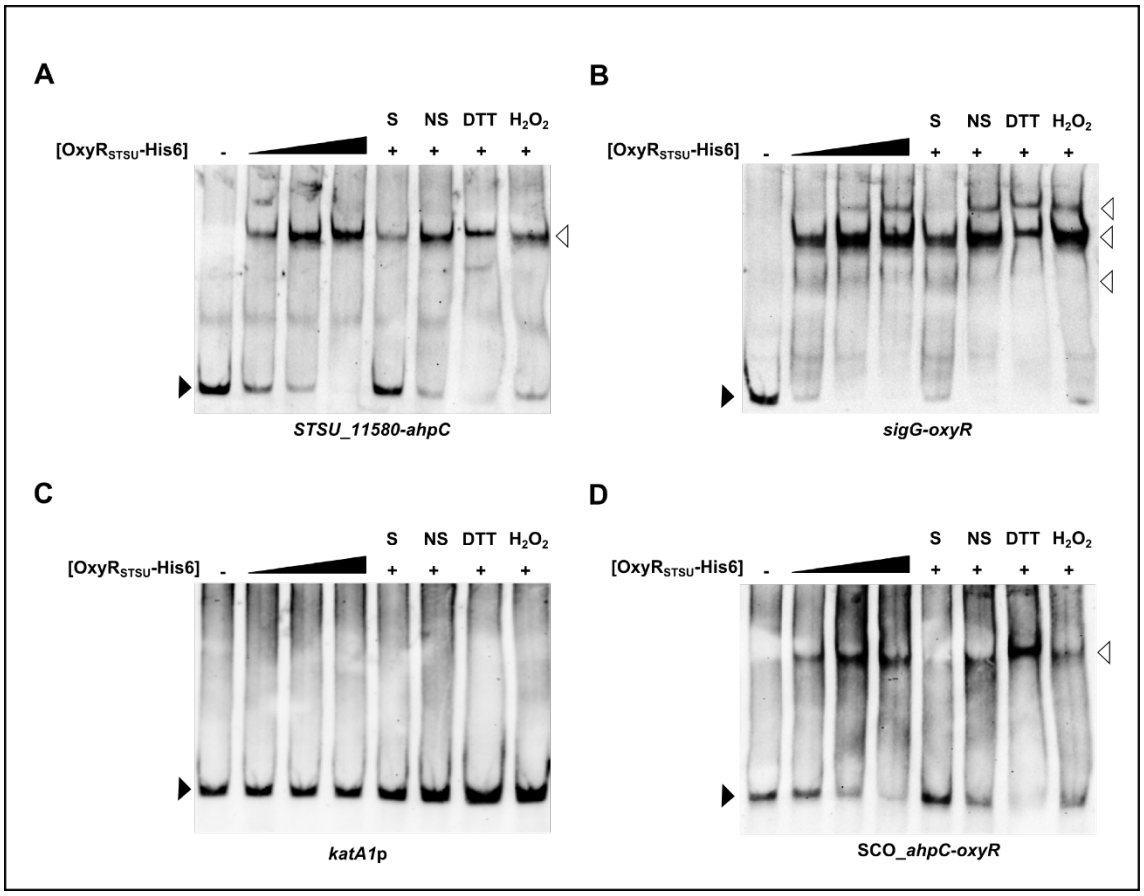

Figure 4.14 – Electrophoretic mobility shift assays (EMSAs) of purified OxyR$_{STSU}$-His6. (A) EMSA using *STSU_11580-ahpC* promoter region. (B) EMSA using *sigG-oxyR* promoter region; (C) EMSA using *katA1* promoter region; (D) EMSA using *S. coelicolor ahpC-oxyR* promoter region. In all EMSAs a gradient of protein concentration was used, namely 0, 1, 5 and 10 pmol. S – Specific un-labelled probe; NS – non-specific un-labelled probe; DTT – 200 mM of DTT were added to the binding reaction; H_2O_2 – 100 mM of H_2O_2 were added to the binding reaction.

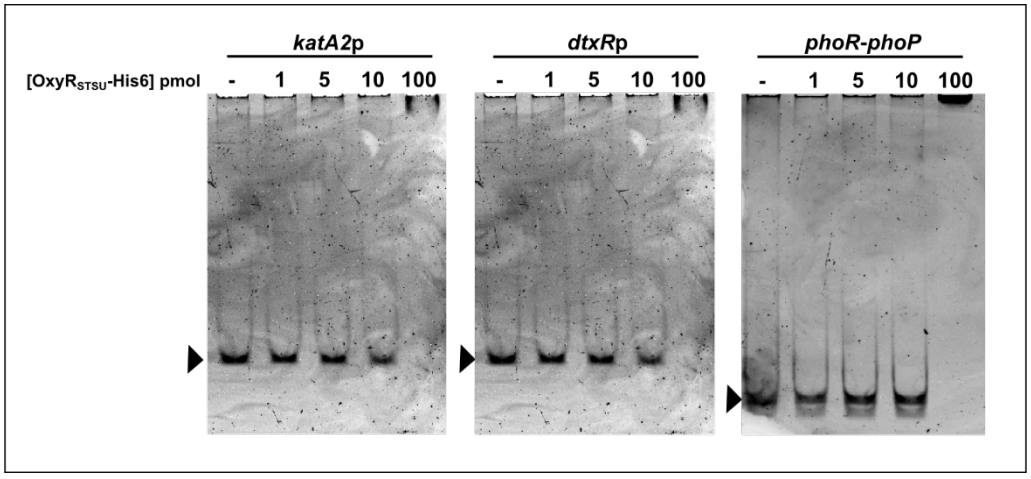

Figure 4.15 – Electrophoretic mobility shift assays (EMSAs) of purified OxyR$_{STSU}$-His6. EMSAs using *katA2*, *dtxR* and *phoR-phoP* promoter regions, respectively All EMSAs were stained with ethidium bromide. Increased protein concentrations were used (0, 1, 5, 10 and 100 pmol).

4.2.5 Characterization of *oxyR* and *ahpC* promoters

The transcription start point (TSP) of *oxyR* and *ahpC* was determined by the rapid amplification of cDNA ends (RACE) method. Two transcription start points were identified for *oxyR*, located at the A and G residues 17 and 21 bp upstream from the ATG start codon, respectively. Noteworthy that in *S. coelicolor* it was also identified two TSP for *oxyR* (Hahn *et al.* 2002). Analysis of the region upstream of *oxyR* TSP with BPROM tool revealed the presence of putative -10 (GATTAACAT; BPROM score 51) and -35 (TCGCCG; BPROM score 18) promoter elements (Fig 4.16 A). The identified -10 box matches the TANNNT hexamer identified by Bourn and Babb (1995) as the consensus sequence for the -10 region recognized by *Streptomyces* principal sigma factor σ^{hrdB}.

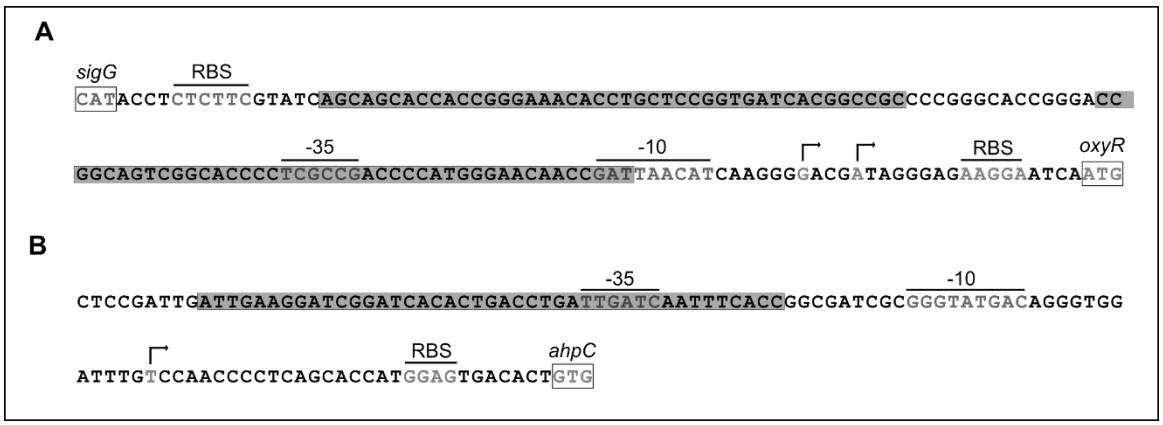

Figure 4.16 – Transcriptional start sites of *oxyR* and *ahpC.* (A) *sigG* and *oxyR* promoter region. (B) *ahpC* promoter region. The position of the transcriptional start site was determined by 5' RACE. The putative −10 and −35 hexanucleotides are in grey and marked with a black line; The TSP is indicated by a bent arrow and grey letter. Nucleotides showing homology with the 16S RNA, which could form a ribosome-binding site, are in grey and labelled RBS with a black thick line on top. The start codon is framed within a box. OxyR predicted binding motifs are framed with a grey box.

In the case of *ahpC*, the TSP was mapped in a T residue located 30 bp upstream of the GTG start codon and -10 (GGGTATGAC; BPROM score 37) and -35 (TTGATC; BPROM score 36) promoter elements were identified 13 bp and 40 bp upstream from the TSP site, respectively (Fig 4.16 B). Although RACE experiments were also performed to identify *sigG* TSP they were unsuccessful. Moreover, no -10 and -35 regions were identified for *sigG* using BPROM software. Putative ribosome-binding sites that showed homology with the 3´-end of *S.*

tsukubaensis 16S RNA were identified (Fig 4.16 A). In an attempt to predict a putative OxyR binding site we aligned the sequence of the EMSA probes (*sigG-oxyR* and *STSU_11580-ahpC* intergenic regions from *S. tsukubaensis* and *oxyR-ahpC* intergenic region from *S. coelicolor*) with the promoter regions of 30 $OxyR_{STSUK}$ orthologous proteins (30 best BLASTp hits) (see Appendix II) and searched for common DNA motifs using MEME algorithm from the MEME suite (http://meme.nbcr.net/meme/) (Bailey *et al.* 2009). We set the search parameters to allow "any number of repetitions" and a maximum motif width of 60 to allow the detection of extended sites typical of OxyR binding motifs (Toledano *et al.* 1994). A 60-nucleotide motif, common to 29 sequences (including *S. coelicolor oxyR-ahpC* intergenic region), was identified with P-values ranging from $1.52e^{-34}$ to $4.95e^{-25}$ (Fig. 4. 17). Using TOMTOM algorithm, the identified motif showed significant similarity to the *E. coli* OxyR binding motif position-specific weight matrix MX000155 (P-value 0.00482) from the PRODORIC Database Release 8.9 (Munch *et al.* 2003), a matrix constructed based on the work of Toledano *et al.* (1994). Between position 7 and 43 the identified motif matches partially the consensus OxyR binding motif $ATAGN_7CTATN_7ATAGN_7CTAT$ identified in the same study (Toledano *et al.* 1994).

Curiously, MEME algorithm failed to align both *S. tsukubaensis* sequences as well as the *oxyR* promoter regions of *S. clavuligerus* and *S. pristinaespirales* ATCC 25486. Search of the *sigG-oxyR* and *STSU_11580-ahpC* intergenic regions from *S. tsukubaensis* for matches to the MEME derived motif retrieved two putative motifs in the *sigG-oxyR* region (P values $1.07e^{-3}$ and $1.04e^{-3}$) and one putative motif in the *ahpC* promoter region (P value $4.9e^{-5}$) that overlaps with the *ahpC* -35 box (Fig. 4. 16). Although the P values are considerable higher than those from the MEME alignment, EMSA experiments do show that OxyR from *S. tsukubaensis* is able to bind these regions as well as the *ahpC-oxyR* region from *S. coelicolor*. These results suggest a different mechanism for OxyR from *S. tsukubaensis* and that will likely recognize a different binding sequence.

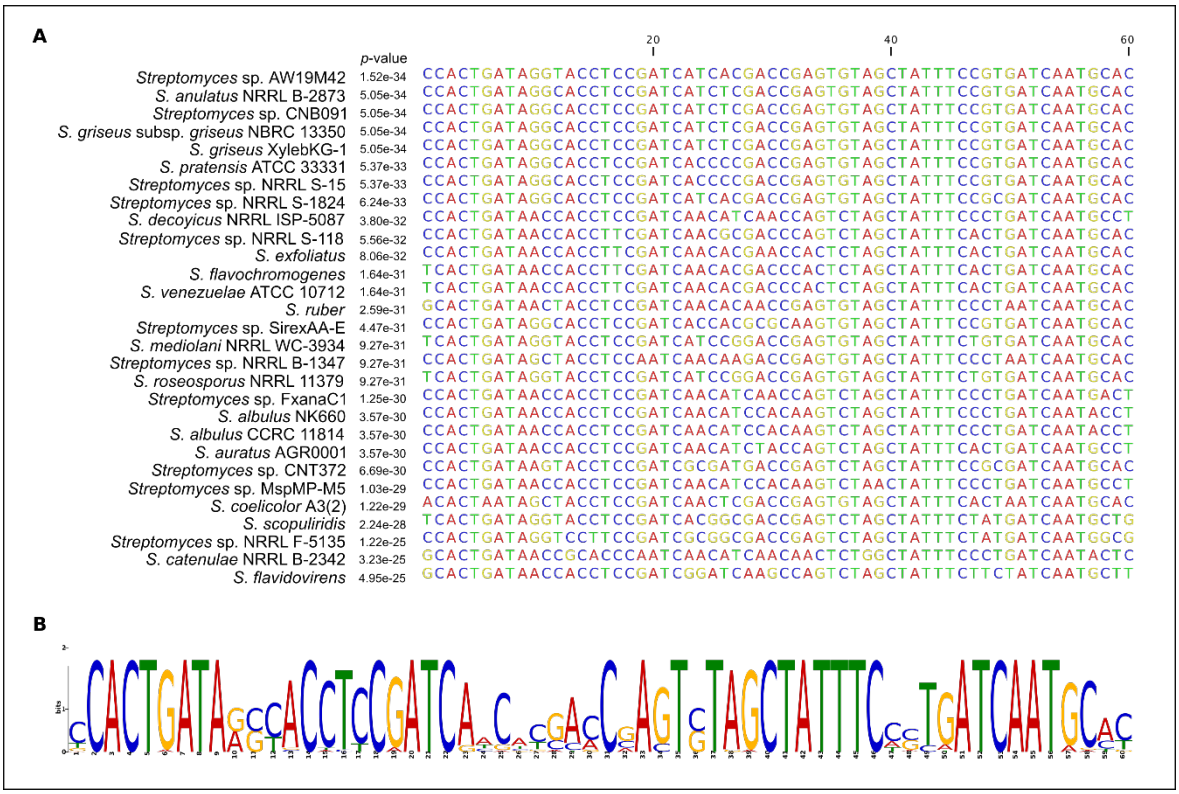

Figure 4.17 – Determination of OxyR consensus DNA binding motif in *Streptomyces* strains. (A) Prediction of the OxyR DNA binding motif, using MEME algorithm, from the 28 *Streptomyces* strains that gave best BLASTp hit with $OxyR_{STSUK}$ as well as the *S. coelicolor oxyR-ahpCD* promoter region, whose binding was verified by EMSAs. (B) DNA sequence logo representing the predicted 60-nucleotide OxyR DNA binding motif, showing the relative frequency of each nucleotide at each position (the height of each base is proportional to the percentage of its occurrence at each position).

4.3 TACROLIMUS PRODUCTION

Regarding tacrolimus production, two different production profiles were observed in the three mutant strains (Fig. 4.18 A). The first, presented by Δ*ahpC* and Δ*oxyR* strains, was similar to the wild-type production profile with the onset of production in the transition from late exponential phase to stationary phase, with tacrolimus being actively produced during stationary phase (144 h - 168 h). In both mutant strains a tacrolimus overproducing phenotype was observed, with Δ*ahpC* reaching a production maximum at 168 h of growth, with an increase on tacrolimus production of 37% on average, when compared to the wild-type, and Δ*oxyR*, reaching a maximum of production at 192 h, with an increase on tacrolimus production of 9% on average, when compared to the wild-type. Conversely, Δ*sigG* mutant strain displayed a different tacrolimus production profile, with the onset of

tacrolimus production occurring during stationary phase and only being actively produced at late stationary phase, reaching maximum of production, normally, at 240 h of growth.

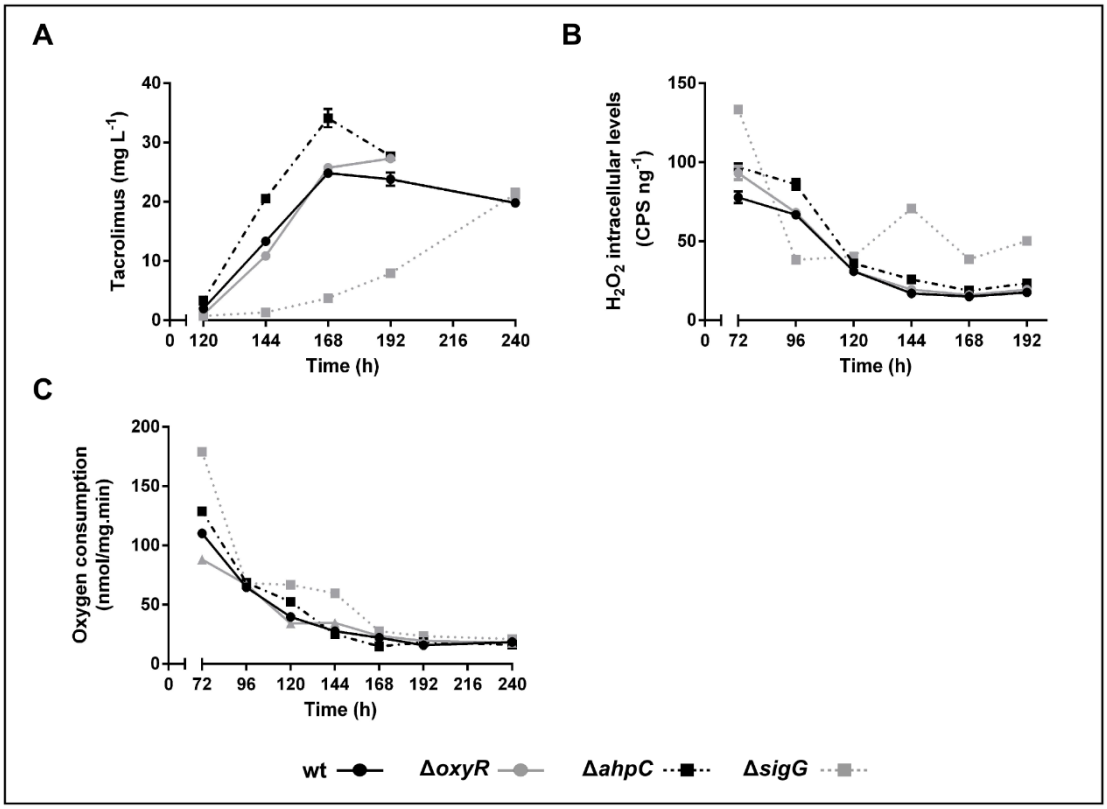

Figure 4.18 – Tacrolimus production, H_2O_2 intracellular levels and oxygen consumption of *S. tsukubaensis* wild-type, Δ*oxyR*, Δ*ahpC* and Δ*sigG* strains. (A) Tacrolimus production of wild-type, Δ*oxyR*, Δ*ahpC* and Δ*sigG* strains throughout growth. Tacrolimus production was assessed by HPLC. (B) DHR oxidation levels were used as a measure of H_2O_2 intracellular levels throughout grwoth in all *S. tsukubaensis* strains. (C) Oxygen consumption rate was determined throughout growth in cultures grown in standard conditions. Vertical bars indicate standard deviation of the mean values. Results (average of triplicates and standard deviation) are representative of three independent experiments.

As previously shown in Chapter 3, keeping a controlled intracellular redox homeostasis is important for tacrolimus biosynthesis in *S. tsukubaensis*. We monitored H_2O_2 intracellular levels in all mutant strains throughout growth (Fig. 4.18 B). At 72 h, the intracellular H_2O_2 levels were higher in all mutant strains when compared to the wild-type, particularly in Δ*sigG* strain. Afterwards, Δ*oxyR* was able to adapt displaying similar H_2O_2 intracellular levels as the wild-type. Regarding Δ*ahpC,* a similar profile was presented although intracellular H_2O_2 levels were kept slightly higher than those presented by the wild-type. Even

though catalase activity was increased in Δ*ahpC* when compared to the wild-type strain (Fig. 4.5 B) (2-fold increase at 72 h and 4-fold increase at 96 h), it was not enough to keep H_2O_2 intracellular levels at lower levels than the ones presented by the wild-type, indicating an important role of AhpC in detoxifying H_2O_2 during exponential growth. Finally, Δ*sigG* strain presented an erratic profile of the H_2O_2 intracellular levels that were kept higher than the wild-type during stationary phase. Even though total levels of catalase activity were higher in Δ*sigG* (Fig. 4.5 B), they were not enough to keep H_2O_2 intracellular levels low, whose increase could also be a result of a higher respiratory rate presented by Δ*sigG* (Fig. 4.18 C). This behaviour resulted in a delay on the onset of tacrolimus production in Δ*sigG* strain.

4.3.1 Iron and tacrolimus production

Iron has been appointed as an important factor on *Streptomyces* secondary metabolism, namely on rapamycin production by *S. hygroscopicus* (Cheng *et al.* 1995). In order to understand if the hampered iron uptake displayed by Δ*sigG* strain could be related to the tacrolimus under-producing phenotype, we monitored tacrolimus production in the wild-type and Δ*sigG* strains grown in MGm medium supplemented with 32 μM Fe^{2+} (standard growing conditions) and without iron supplementation (iron-limiting conditions). Both strains presented a slight decrease on growth in iron-limiting conditions particularly regarding biomass at late stationary phase (Fig 4.19 A). Interestingly, the wild-type strain grown without iron supplementation presented the same tacrolimus production profile as the one observed for Δ*sigG* strain grown in standard conditions i.e., iron supplemented conditions (Fig 4.19 B). This result suggests that the low tacrolimus production titres observed in Δ*sigG* could be ascribed to the hampered ferrous iron uptake.

4.3.2 Oxygen availability

As shown in Chapter 3, altering oxygen availability can modulate tacrolimus production in *S. tsukubaensis*. In order to study the effect of DO in tacrolimus production by the mutant strains Δ*ahpC,* Δ*oxyR* and Δ*sigG* we monitored tacrolimus production in cultures with a ratio of flask volume *vs* medium culture of 10 (in standard growth conditions the ratio of flask volume *vs* medium culture is 5), thus increasing oxygen availability.

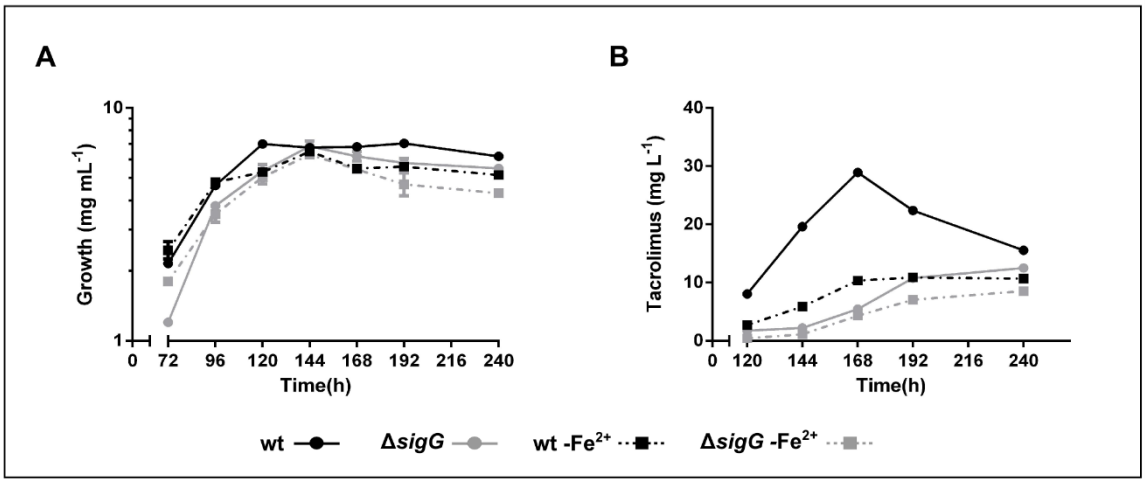

Figure 4.19 – Growth and tacrolimus production of *S. tsukubaensis* wild-type and Δ*sigG* strains grown in different iron conditions. (A) Growth of *S. tsukubaensis* wild-type and Δ*sigG* strains grown in MGm medium with (solid lines) and without iron (Fe^{2+}) supplementation (dashed lines). Growth was assessed by dry weight. (B) Tacrolimus production of wild-type and Δ*sigG* strains throughout growth. Tacrolimus production was assessed by HPLC. Vertical bars indicate standard deviation of the mean values. Results (average of triplicates and standard deviation) are representative of three independent experiments.

Changing oxygen availability led to major growth defects in Δ*sigG* strain, while in Δ*ahpC* and Δ*oxyR* growth was similar to the wild-type (Fig. 4.20 A). Regarding catalase activity an anticipation of 24 h of the typical catalase induction, which in standard conditions already occurred in Δ*ahpC* and Δ*sigG* strains, was also observed for wild-type and Δ*oxyR* strains (Fig. 4.20 B). Curiously, in Δ*sigG* another induction of catalase activity was observed at 120 h that represented a 4-fold increase in total catalase activity when compared to the other three strains. Regarding tacrolimus production a 44% (25 mg mL^{-1} *vs* 36 mg mL^{-1}), 46% (26 mg mL^{-1} *vs* 38 mg mL^{-1}) and 31% (34 mg mL^{-1} *vs* 46 mg mL^{-1}) increase was observed for the wild-type, Δ*oxyR* and Δ*ahpC*, respectively. Also the peak of production was achieved earlier, at 144 h of growth for wild-type and Δ*oxyR* and 120 h of growth for Δ*ahpC* (Fig. 4. 20 C). In opposition, Δ*sigG* did not produce tacrolimus. In this mutant strain the increase of oxygen availability led to growth defects and even though catalase activity was induced, given this strain sensitivity to H_2O_2, one can assume that the intracellular levels of ROS were very high leading to increased oxidative stress and consequently an abolishment of tacrolimus production. Conversely, Δ*ahpC* increased resistance to H_2O_2 was beneficial to help this strain to cope with the increased oxygen availability.

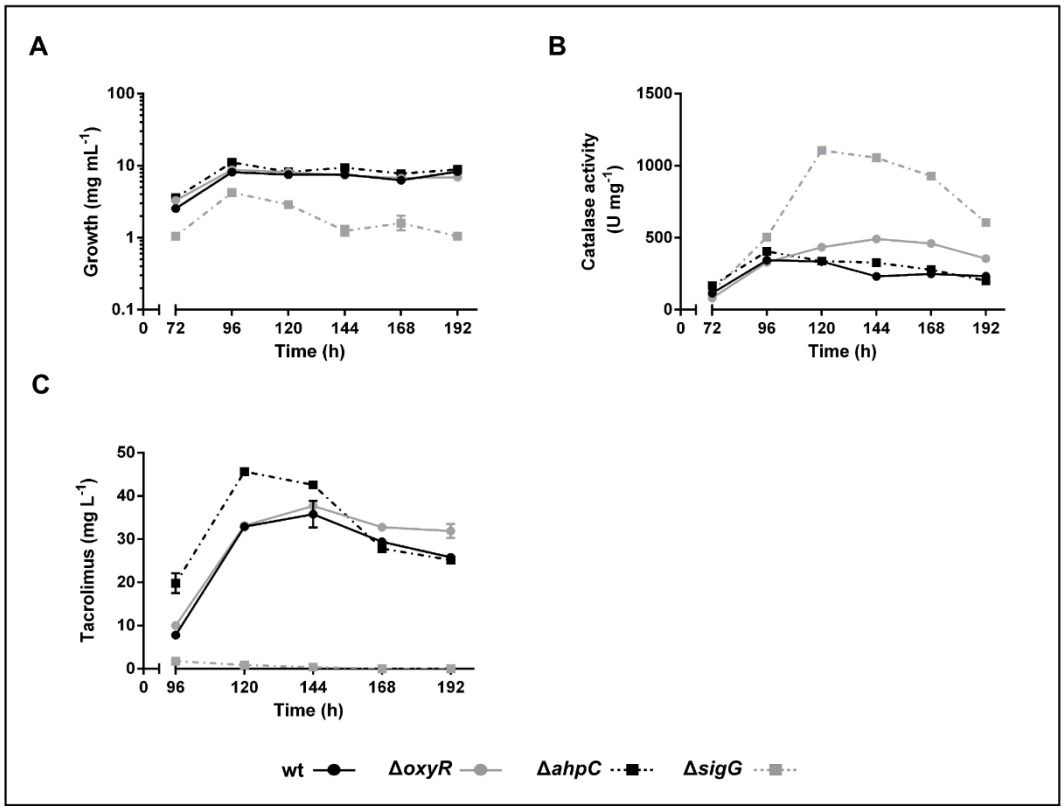

Figure 4.20 – Growth, catalase activity and tacrolimus production of *S. tsukubaensis* wild-type, Δ*oxyR*, Δ*ahpC* and Δ*sigG* strains grown in different DO conditions. (A) Growth of *S. tsukubaensis* strains in MGm medium with a ratio of flask volume *vs* medium culture of 10. Growth was assessed by dry weight. (B) Total catalase activity was measured spectrophotometrically in samples collected throughout growth in all strains (C) Tacrolimus production of wild-type, Δ*oxyR*, Δ*ahpC* and Δ*sigG* strains throughout growth. Tacrolimus production was assessed by HPLC Vertical bars indicate standard deviation of the mean values. Results (average of triplicates and standard deviation) are representative of three independent experiments.

4.3.3 Transcriptional analysis of the tacrolimus biosynthetic cluster

Gene expression of the cluster situated regulators (CSRs) *fkbN* and *fkbR* as well as some structural genes, including *fkbB, fkbL* and *fkbO,* was assessed in the wild-type and the three mutant strains throughout the exponential growth phase, namely at 72 h, 96 h and 120 h (Fig. 4. 21).

Regarding transcription of tacrolimus CSR *fkbN,* both overproducing strains presented increased transcriptional levels. Noteworthy that Δ*ahpC* strain already presented a 10-fold increase at 96 h of growth when compared to the wild-type. As for Δ*sigG* strain *fkbN* transcriptional levels were kept constant and low during the three time-points tested. Regarding the other CSR, *fkbR*, both Δ*oxyR* and Δ*ahpC*

presented increased transcriptional levels at 96 h and 120 h, while in Δ*sigG* strain an up-regulation only occurred at 120 h, when compared to the wild-type. It is interesting to note that in Δ*ahpC*, which presented the most significant increase in tacrolimus production, both CSRs presented higher transcriptional levels at earlier stages of growth (96 h).

Regarding the transcription of the PKS encoding gene *fkbB*, the overproducing strains Δ*ahpC* and Δ*oxyR* presented an up-regulation when compared to the wild-type (Fig. 4.21).

As for the transcription of the lysine cyclodeaminase encoding gene, *fkbL,* and the chorismatase encoding gene, *fkbO,* significant transcriptional changes were observed in all mutant strains. At 96 h Δ*ahpC* already presented a 9.5-fold increase in *fkbL* expression while in Δ*oxyR* strain an up-regulation was achieved at 120 h (Fig. 4.21). This up-regulation of *fkbL* transcription in both overproducing mutants suggests an increase in lysine availability for tacrolimus biosynthesis. Regarding *fkbO* transcription, no transcription was detected at 72 h for Δ*sigG* strain however, at 96 h a 5-fold increase occurred both in Δ*sigG* and Δ*ahpC*, when compared to the wild-type. At 120 h all strains presented an induction of *fkbO* transcription with the exception of Δ*sigG* (Fig. 4.21). Given that chorismate availability has been suggested to play a regulatory effect on *fkbO* transcription (Huang *et al.* 2013), one can assume that this transcription profile could be a reflection of chorismate intracellular availability for tacrolimus production, which seems to be increased in both overproducing mutants, especially in Δ*ahpC*.

Overall, the transcriptional results of tacrolimus biosynthetic genes are in accordance with the tacrolimus production profiles presented by the mutant strains.

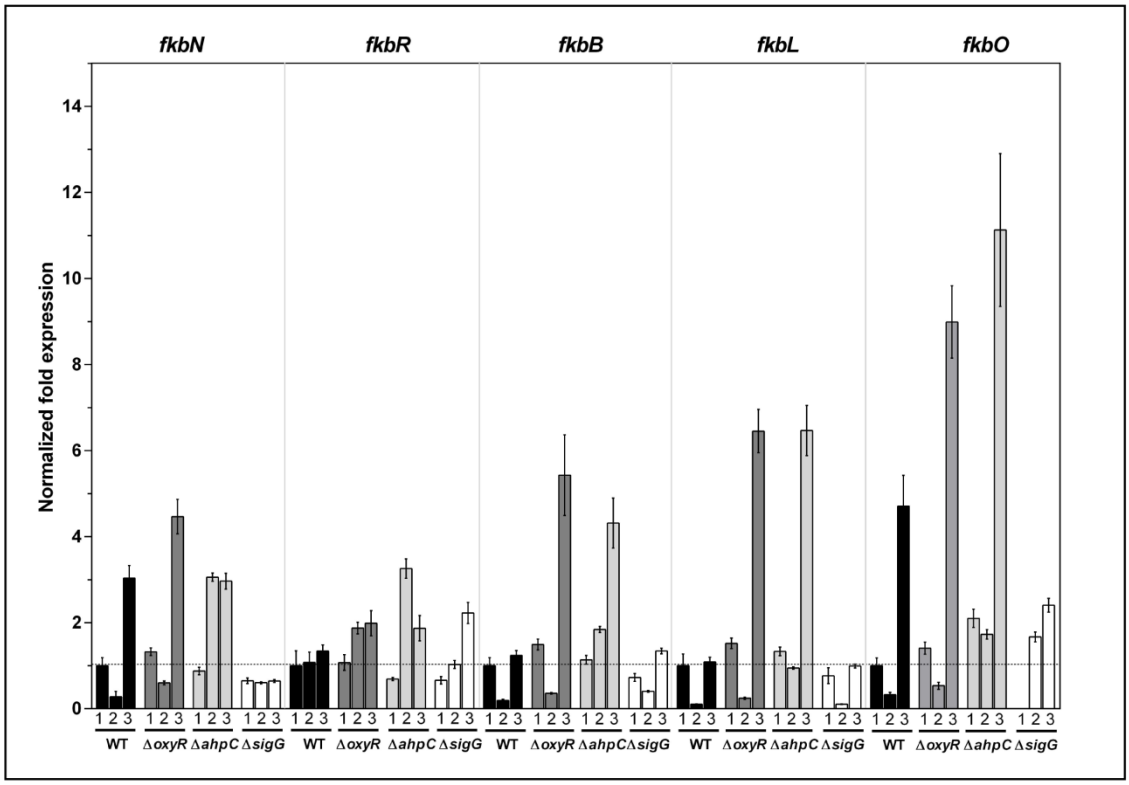

Figure 4.21 – Transcription profile of *fkbN*, *fkbR*, *fkbB, fkbL* and *fkbO* in *S. tsukubaensis* wild-**type, Δ***oxyR,* **Δ***ahpC* **and Δ***sigG* strains. Samples were collected at 72 h (1), 96 h (2) and 120 h (3). Transcription was assessed by RT-qPCR. The Mean Normalised Fold Expression (± standard errors) of the target genes was calculated relative to the transcription of the reference genes (16 S rDNA and *hrdB*) and the reaction of internal normalisation was performed using wild-type the control situation.

4.4 PROTEOMIC ANALYSIS OF Δ*OXYR* AND Δ*AHPC* STRAINS

A proteomic analysis of the wild-type, Δ*oxyR* and Δ*ahpC* strains at 72 h of growth was performed through two-dimensional electrophoresis (2-DE) of protein crude extracts. Biological triplicates were performed for each strain. PDQuest software (Bio-Rad, USA) was used for quantitative analysis of the differences amongst 2-DE gels (Fig. 4.22). A total of 436 protein spots were match between the different 2-DE gels / strains and in their majority, the changes observed in protein expression took the form of up/down regulation although on/off regulation was also observed. A two-fold change was defined as the threshold value for the analysis.

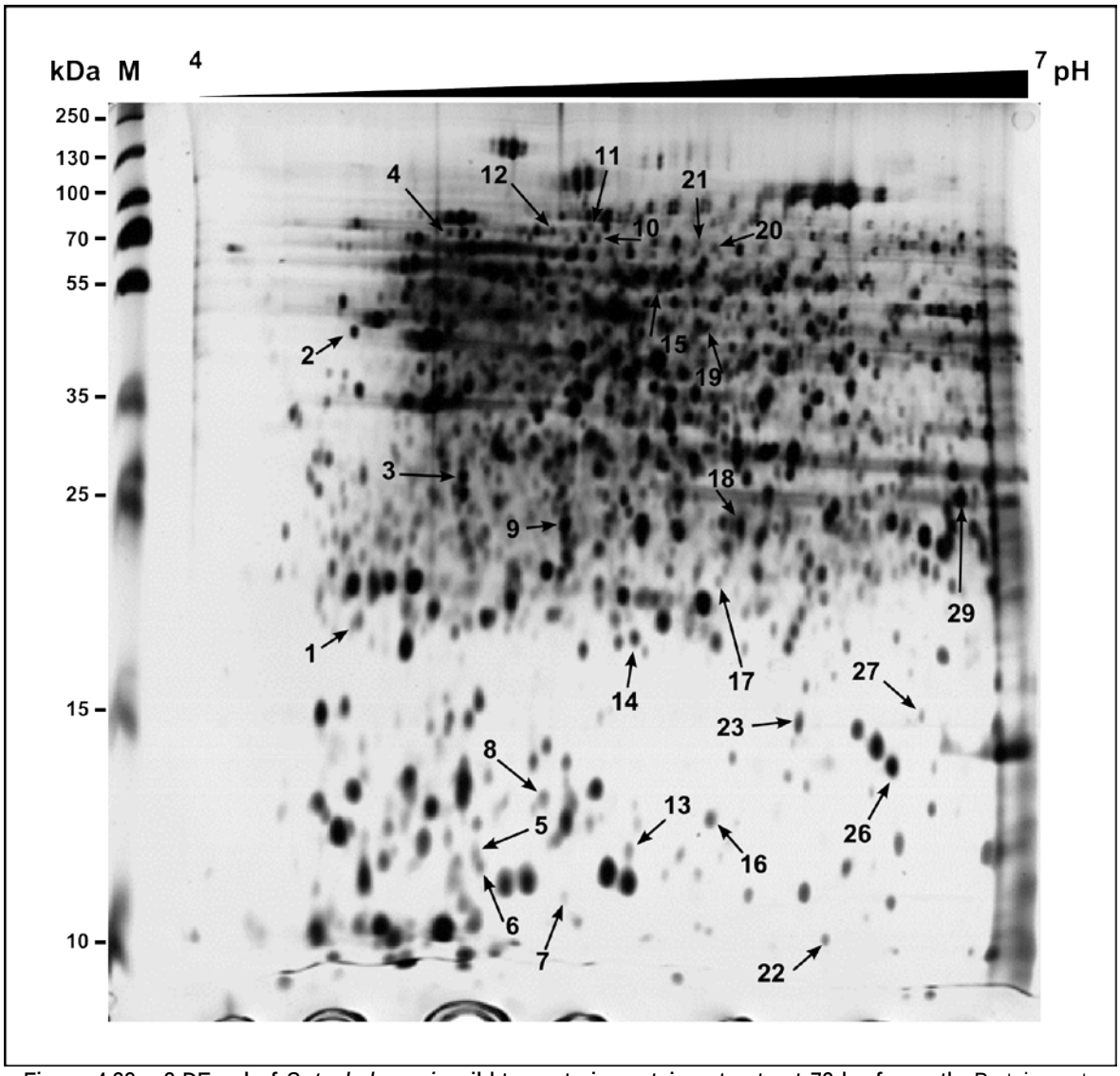

Figure 4.22 – 2-DE gel of *S. tsukubaensis* wild-type strain protein extracts at 72 h of growth. Protein spots send for identification are indicated by an arrow and numbered using the same order presented on table 4.1. pH range is indicated on top of the gel. M - molecular weight. Protein extracts were analysed by comparative 2D gel electrophoresis to assess the expression profile of the *S. tsukubaensis* wild-type, Δ*ahpC* and Δ*oxyR* strains proteome at 72 h of growth. Fold variations reflect the 2D-gel analysis of three independent experiments.

The quantitative analysis revealed a total of 47 differences between the wild type and Δ*oxyR* and 66 differences between the wild-type and Δ*ahpC.* A comparison between Δ*oxyR* and Δ*ahpC* was also performed and a total of 46 differences were identified, most of which coincided with those obtained by the comparison with the wild-type strain. From the analysis, 29 protein spots were selected for identification. Proteins were identified by peptide mass fingerprinting (PMF) and in those cases that no confident identification was obtained by PMF, protein spots were submitted to tandem MS (MS/MS). Spectra were submitted to MASCOT

software (Perkins *et al.* 1999) using the UniProt protein database restricted to *Streptomyces tsukubaensis* or extended to Actinobacteria; protein MASCOT scores greater than 51 or 77, respectively, were significant ($p<0.05$). MASCOT protein identification results were further sieved taking into consideration the equivalence between identified protein predicted theoretical molecular weight / pI and the experimental protein spot molecular weight / pI. Protein spots number 24, 25 and 28 that were present only in the mutant strains, were excluded from further analysis because were identified as the apramycin resistant protein originated by the introduction of the apramycin resistance cassette in the mutant generation process. A summary of identified proteins is presented in Table 4.1. For protein spots number 4, 6, 10, 11, 23, 26 and 29 more than one protein was identified with statistical significance.

Identified proteins were grouped according to the functional categorization available for *S. coelicolor* genome (ftp://ftp.sanger.ac.uk/pub/S_coelicolor/) followed by in-house curation (Table 4.2). Note that the fold-change presented in Table 4.2 represents the ratio between the mutant strains and the wild-type. Some protein spots were identified based on the fold-change between Δ*oxyR* and Δ*ahpC*.

The majority of the differences identified reflected a decrease of protein spots intensity in the mutant strains when compared to the wild-type. In particular proteins involved in protein metabolism and translation were decreased in both mutants (Table 4.2). These results suggest an anticipation of the metabolic shift towards secondary metabolism in *S. tsukubaensis* mutant strains.

Table 4. 1 - Identified proteins by PMF-MS/MS.

Spot ID	Nº of hits	UniProt ID	MASCOT score	Nº of matched peptides	STSU ID
1	1	I2N5G3	113	13	STSU_11585
2	1	I2MU68	145	4	STSU_31495
3	1	I2N4D9	281	10	STSU_13455
4	2	(a) I2MUZ9	214	20	STSU_30056
		(b) I2MWJ0	199	13	STSU_27281
5	1	I2N4C9	383	12	STSU_13630
6	2	(a) I2N4C9	158	6	STSU_13630
		(b) I2N569	84	5	STSU_11935
7	1	I2N697	71	8	STSU_10154
8	1	I2N6B0	168	14	STSU_10084
9	1	I2N4D9	369	16	STSU_13455
10	2	(a) I2N500	942	41	STSU_12400
		(b) I2MUE0	75	11	STSU_31120
11	3	(a) I2N795	473	29	STSU_08394
		(b) I2MXY7	170	18	STSU_24776
		(c) I2N2N9	106	12	STSU_16472
12	1	I2MVR2	94	16	STSU_28812
13	1	I2N5A6	285	18	STSU_11830
14	1	I2N4D9	551	18	STSU_13455
15	1	I2MX63	464	26	STSU_26189
16	1	I2N3Y4	121	17	STSU_14128
17	1	I2MUY0	283	18	STSU_30145
18	1	I2MWV7	197	14	STSU_26704
19	1	I2MY97	149	15	STSU_24268
20	1	I2N5I2	517	35	STSU_11515
21	1	I2N3S0	283	26	STSU_14552
22	1	I2N1Y7	289	16	STSU_17678
23	2	I2N5G4	190	17	STSU_11590
		I2MXE8	124	9	STSU_25689
26	2	(a) I2N4D9	458	18	STSU_13455
		(b) I2N7H0	72	3	STSU_07948
27	1	I2N2W5	123	16	STSU_15993
29	2	(a) I2MT61	558	24	STSU_33250
		(b) I2N4U0	112	12	STSU_12680

Table 4. 2 - Functional characterization of the identified proteins.

Protein	Description	Δ*oxyR vs* wt (fold change)	Δ*ahpC vs* wt (fold change)
Stress response			
STSU_07948	LexA repressor	0.27*	0.33*
STSU_11585	Alkyl hydroperoxide reductase - AhpC	1.22	na
STSU_11590	Alkyl hydroperoxide reductase – AhpD	2.00*	0.54*
STSU_33250	Universal stress protein - UspA	1.14*	0.52*
Protein metabolism & translation			
STSU_08394	Proline-tRNA ligase - ProS	0.88*	0.21*
STSU_13455	Elongation factor Tu	0.23	0.37
STSU_17678	30S ribosomal protein S6 – RpsF	0.35	0.32
STSU_27281	30S ribosomal protein S1 – RpsA	1.03*	0.45*
STSU_28812	Proteasome-assocated ATPase	1.27	0.59
STSU_31120	Methionine--tRNA ligase – MetG	0.52*	0.09*
Energy and carbon metabolism			
STSU_10154	ATP synthase epsilon chain – AtpC	0.42	0.42
STSU_11515	Fumarate hydratase – FumB	0.79	0.38
STSU_12680	Succinate dehydrogenase iron-sulfur subunit – SdhB	1.14*	0.52*
STSU_30056	Phosphoenolpyruvate-protein phosphotransferase	1.03*	0.45*
Nitrogen metabolism			
STSU_12400	Carbamoyl-phosphate synthase L chain ATP-binding protein	0.52*	0.09*
STSU_15993	Putative nucleoside diphosphate kinase	2.17	0.86
STSU_26189	Glutamine synthetase I	0.24	0.23
Amino acid metabolism			
STSU_14552	Dihydroxy-acid dehydratase – IlvD	0.79	0.29
STSU_24776	2-isopropylmalate synthase – LeuA	0.88*	0.21*
Iron metabolism			
STSU_16475	IucA/IucC family protein	0.88*	0.21*
Regulatory proteins			
STSU_14128	AsnC family transcriptional regulator	0.36	0.71
Hypothetical / uncharacterized proteins			
STSU_10084	Hypothetical protein	2.07	1.99
STSU_11830	Nuclear transport factor 2	0.50	1.23
STSU_11935	Hypothetical protein	0.30*	0.36*
STSU_13630	Hypothetical protein (COG2030 Acyl dehydratase)	0.40	0.44

Protein	Description	Δ*oxyR vs* wt (fold change)	Δ*ahpC vs* wt (fold change)
STSU_24268	Hypothetical protein	0.69	1.63
STSU_25689	Hypothetical protein	2.01*	0.54*
STSU_30145	Hypothetical protein	2.26	3.08
STSU_31495	Hypothetical protein	1.24	2.01

Characterization of *S. coelicolor* metabolic switch showed that transcription of genes involved in protein biosynthesis and translation were down-regulated during the transition phase (Nieselt *et al.* 2010), mimicking the pattern observed during the stringent response. The stringent response in *Streptomyces* is mediated by guanosine 5'-diphosphate 3'-diphosphate (ppGpp) that has a key signalling role in *Streptomyces* secondary metabolism (Chakraburtty and Bibb 1997). ppGpp production is induced when the supply of amino acids becomes rate limiting for protein synthesis. Both *S. tsukubaensis* mutant strains, particularly Δ*ahpC* strain, presented a decrease of two proteins involved in the biosynthesis of leucine and valine: 2-isopropylmalate synthase encoded by *leuA* and dihydroxy-acid dehydratase encoded by *ilvD*, respectively (Table 4.2). Furthermore, leucine and valine are branched chain amino acids (BCAA) whose metabolism interplays with *Streptomyces* secondary metabolism: the BCAA biosynthetic and catabolic pathways use or originate biosynthetic precursors for secondary metabolites. A down-regulation of BCAA biosynthesis in the mutant strains, suggests an accumulation of pyruvate that can be re-directed towards the generation of acetyl-CoA, phosphoenolpyruvate (PEP) or oxaloacetate. Accumulation of the last two metabolites can lead to the increase of chorismate availability through the shikimate pathway and lysine through the conversion of oxaloacetate and glutamate into aspartate, respectively. Interestingly, a decrease of glutamine synthetase (GSI) protein levels was also observed in both mutants. GSI is an enzyme that utilizes glutamate as substrate; its down-regulation can lead to an accumulation of glutamate that can generate more aspartate and consequently more lysine.

Furthermore, Δ*ahpC* mutant strain presented a decrease in the protein levels of phosphoenolpyruvate-protein phosphotransferase (EPI) from the phosphotransferase system (PTS) (STSU_30056). Even though the majority of

bacteria use the PTS to transport glucose into the cells, in the case of *Streptomyces* the utilization of N-acetylglucosamine is favoured. In both cases, *Streptomyces* uses PEP as the phosphoryl donor (Wang *et al.* 2002). The decrease of EPI protein levels also contributes to the increased availability of PEP to enter the shikimate pathway.

Also in Δ*ahpC* mutant strain, a two-fold decrease in a protein from the IucA/IucC family (STSU_16475) was also identified. This protein is a siderophore synthase involved in siderophore biosynthesis and transport. Analysis of the genomic region of STSU_16475 encoding gene using the antiSMASH software (http://antismash.secondarymetabolites.org/), suggest that it encodes for a hydroxamate siderophore that requires lysine for its biosynthesis.

Exogenous feeding studies have shown that the addition of chorismate or lysine/pipecolate to *S. tsukubaensis* culture broth leads to an increase of tacrolimus production similar to the one obtained by overexpressing *fkbO* or *fkb*L (Huang *et al.* 2013) The increased availability of tacrolimus biosynthetic precursors (chorismate and lysine) in the mutant strains, particularly in Δ*ahpC* strain, through a metabolic flux redirection as inferred by the 2-DE gel analysis, has certainly contributed to the tacrolimus overproduction profile observed. Moreover, the up-regulation of *fkbO* and *fkbL* transcription further supports the increased availability of tacrolimus biosynthetic precursors.

Interestingly, it was also identified in both mutant strains a decrease in the protein levels of an uncharacterized protein (STSU_13630) that has been functionally annotated as involved in the fatty acid biosynthetic process (COG2030: Acyl dehydratase). A down-regulation of fatty acid biosynthesis can lead to an accumulation of acetyl-CoA and/or malonyl-CoA which are also tacrolimus biosynthetic precursors. Proteins involved in central carbon metabolism including the fumarate hydratase FumB and the succinate dehydrogenase iron-sulfur subunit – SdhB have been also identified. Both protein levels were decreased in Δ*ahpC* strain and given their sequential role in the TCA cycle, one can hypothesize an accumulation of succinate in this mutant strain. However, and given the reversibility of succinate into succinyl-CoA and the generation of methylmalonyl-CoA through succinyl-CoA isomerization, the impairment of the

TCA cycle can lead to an increased availability of methylmalonyl-CoA, also a tacrolimus biosynthetic precursor.

In the cases of LeuA, IucA/IucC and SdhB proteins, more than one protein have been identified per spot. Even though they presented high identification scores and their predicted pI and MW was in accordance with the 2-DE gel, further confirmation of these results either by enzymatic assays or transcriptional analysis will be required in order to validate these results.

4.5. DISCUSSION

In bacteria, genes are not located along genomes in a random manner; in fact, their genomic synteny is a reflection of selective events that occurred throughout evolution. The organization of these clustered genes is much conserved and normally constitutes a reflection of their biological role in the cells. In the case of *Streptomyces oxyR-ahpCD* operon synteny, in the 71 *Streptomyces* strains analysed, only 9 exceptions were found, including *S. tsukubaensis*. Those exceptions did not reflect any phylogenetic proximity between strains, suggesting that those differences were acquired in order to improve cell survival/fitness or another kind of selective advantage. Furthermore, none of the other 8 exceptions found presented a similar synteny as the one presented by *S. tsukubaensis*, making of this a unique genomic region among *Streptomyces* strains. Interestingly, a novel ECF sigma factor encoding gene, *sigG*, being divergently transcribed from *oxyR,* was present in this unique genomic region. Through characterization of Δ*sigG* we were able to notice that this mutant strain presented an increased sensitivity to H_2O_2. Additionally, when grown with increased DO availability, Δ*sigG* presented growth defects and tacrolimus production was abolished. All these suggested a role for SigG in *S. tsukubaensis* oxidative stress response, however its transcription was not induced by H_2O_2 insult. Further characterization of Δ*sigG* strain showed that this mutant presented an hampered ferrous iron uptake, which led to siderophore production of Δ*sigG* in iron sufficient conditions, indicating a regulatory role of SigG in iron metabolism, more specifically in ferrous iron uptake. Even though siderophore production and regulation has begun to be uncovered in the past few years in *Streptomyces* field, to our knowledge, this is the first time

that a ferrous iron regulator has been described. Additionally, we also demonstrated a regulatory cross-talk between SigG and OxyR in *S. tsukubaensis*.

OxyR role in bacteria can vary according to bacterial strains, reason why in some strains including *E. coli* and *S. coelicolor*, deletion of *oxyR* leads to increased sensitivity to H_2O_2 (Mukhopadhyay and Schellhorn 1997, Hahn *et al.* 2002), whereas in others like *C. glutamicum,* an opposite behavior is observed (Teramoto *et al.* 2013). In the case of *S. tsukubaensis, oxyR* deletion presented a H_2O_2-sensitivity phenotype. Interestingly, both *E. coli* and *S. coelicolor* Δ*oxyR* strains presented growth defects (Gonzalez-Flecha and Demple 1997, Hahn *et al.* 2002) and in *Pseudomonas aeruginosa* PAO1, inactivation of *oxyR* impaired iron uptake, mediated by the siderophore pyoverdine, and growth, particularly in low-iron conditions (Vinckx *et al.* 2011). Different siderophores have been shown to promote growth of many microorganisms (Kingsley *et al.* 1999, Yamanaka *et al.* 2005). In fact it has been described that siderophore production and *Streptomyces* developmental processes are tightly connected (Tierrafria *et al.* 2011) and that iron concentrations influence developmental gene expression (Traxler *et al.* 2013). *S. coelicolor* Δ*oxyR* presented growth defects in liquid and solid medium; and in R2YE solid medium it presented a bald phenotype, i.e., inability to produce aerial hyphae (Hahn *et al.* 2002). The presented developmental impairment could be related with an altered iron metabolism since OxyR role in iron metabolism regulation has been well established in other bacteria. In the case of *S. tsukubaensis,* at least in the conditions tested, Δ*oxyR* strain did not present any growth defect. In fact our results showed that neither ferrous iron nor siderophore mediated iron uptake was hampered in this strain. However that was not the case for Δ*sigG*, where growth defects both in liquid and in solid medium were observed. In solid medium, the problem was not in forming aerial mycelium *per se* but it was in the time that this mutant strain required to form aerial mycelium as well as to achieve full sporulation, which was longer than the one presented by the wild-type strain. We believe that Δ*sigG* hampered ferrous iron uptake can explain this developmental problem, which is not severe and is surpassed by the increased siderophore production. Curiously, all the strains that presented the Ile216Val point mutation in OxyR, also presented in the genome an ECF sigma factor harbouring the three domains presented in SigG. Even though we cannot affirm that they are SigG orthologues and display the same biological function, it would

still be something very interesting to pursue in order to understand if it is related with *Streptomyces* pathogenicity. OxyR role in pathogenicity has been described in some bacterial strains, in fact *P. aeruginosa* Δ*oxyR* showed decreased virulence in animal models (Lau *et al.* 2005, Melstrom *et al.* 2007). Furthermore it has been suggested that the decreased in virulence observed for this strain could be due to an hampered siderophore uptake (Vinckx *et al.* 2008).

Regarding OxyR direct regulon, shift assays combined with transcriptional analysis allowed us to determine that OxyR directly binds and regulates the transcription of *ahpC* and *sigG* as well as its own transcription. Through shift assays we were able to determine that OxyR could bind to these promoter regions both in its reduced and oxidized state and that in the case of *sigG-oxyR* promoter region multiple shift bands were observed, suggesting more than one OxyR binding site, which was confirmed by bioinformatic analysis. Moreover, we were able to demonstrate an interplay between iron metabolism and oxidative stress response mediated by SigG and OxyR: in oxidative stress conditions OxyR activates *ahpC* transcription as well as its own while it represses *sigG*

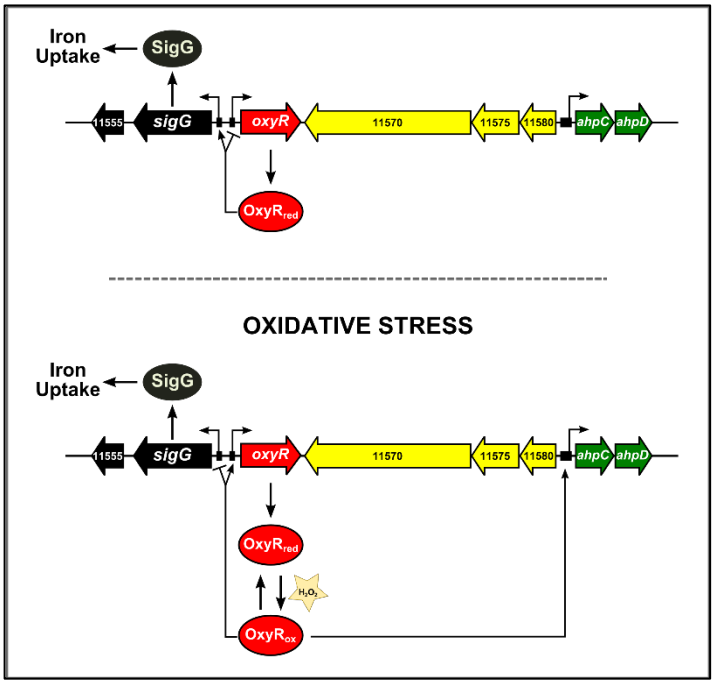

Figure 4.23 – Schematic representation of OxyR and SigG proposed regulatory model. Genes are indicated by arrows and the cognate proteins in circles. Small boxes upstream the genes indicate OxyR predicted binding motifs. Bend arrows indicate transcription initiation.

transcription, probably as a way to avoid iron overload and toxicity (Fig. 4.23).

Regarding transcriptional regulation of the Dps-like encoding gene *STSU_08138*, EMSAs will have to be performed in order to determine if OxyR can be directly involved, similar to what is observed for other bacteria such as *E. coli* (Altuvia *et al.* 1994). Nevertheless, our transcriptional results showed that in Δ*oxyR* strain, *dps* transcription was increased in all time-points. Interestingly the observed induction of *STSU_08138* transcription at 96 h overlaps with the mid-exponential increased ferrous iron uptake, suggesting that this dps-like protein could function as an iron binding protein being regulated in an oxidative-stress controlled manner.

Remarkably, when testing *S. tsukubaensis* OxyR binding to *S. coelicolor oxyR-ahpCD* promoter region we saw an increased binding affinity in its reduced form, which also seem to be the case for the *S. tsukubaensis* promoter regions tested. Different binding activities for OxyR according to its redox state had already been described; for example in *Xantomonas campestris* reduced OxyR presented higher affinity for the *ahpC* promoter than oxidized OxyR (Loprasert *et al.* 2000). Additionally, we also found two TSP in *oxyR* which are also indicative of different regulatory mechanisms.

We also have demonstrated that *ahpC* transcription is SigG independent and that, even though the response to H_2O_2 induced stress requires OxyR regulation and activation, an OxyR-independent *ahpC* transcription is also present in *S. tsukubaensis*. While analyzing *ahpC* promoter region we found a putative Crp biding motif. Curiously, when looking into other *ahpC* promoter regions of other *Streptomyces* strains, including *S. coelicolor* we could not find that motif, at least not using the software (BPROM). Crp, which stands for cAMP receptor protein, is a major regulator widely studied among bacteria. In *E. coli* Crp functions as a major regulator and interestingly *oxyR* transcription at exponential phase is Crp-dependent (Gonzalez-Flecha and Demple 1997), however that was not observed for *S. coelicolor* (Hahn et al. 2002). Crp is highly conserved among *Streptomyces* and it has been recently described as a global regulator of antibiotic production (Gao *et al.* 2012), since it not only influences precursors abundance and supply, but it can also bind and regulate CSRs. Interestingly Crp overexpression in *S. coelicolor* led to changes in transcription of more than 100 genes, including genes

involved in siderophore biosynthesis (Gao *et al.* 2012). Fascinatingly, in *E. coli* AhpC protein has been implicated in the siderophore enterobactin biosynthesis. It was suggested that AhpC could be implicating in the shuttle of chorismate to enterobactin biosynthesis (Ma and Payne 2012). Perhaps in *S. tsukubaensis* AhpC could play a similar role under the regulation of Crp.

Regarding tacrolimus production, both transcriptional and proteomic results provided us with some clues/hypothesis of ways in which our strains could be modulating tacrolimus production. Both Δ*ahpC* and Δ*oxyR* presented an overproducing phenotype while in Δ*sigG* a delay on the onset of tacrolimus production was detected.

Proteomic results of our overproducing strains suggest that an early metabolic switch/stringent response could be occurring. It has been demonstrated for several *Streptomyces* a connection between ppGpp intracellular levels and the onset of secondary metabolism, including in *S. coelicolor* where ppGpp overproduction led to an accumulation of both RED and ACT antibiotics (Kang *et al.* 1998). In order to understand if the increase observed in tacrolimus production could be related with an increase of ppGpp intracellular levels, it would be important to study gene expression of *relA*, the ppGpp synthetase encoding gene. Furthermore, and regarding amino acid metabolism, the results indicate a decrease in valine and leucine biosynthesis, which increases pyruvate availability; pyruvate can be converted into: i) PEP and rerouted into the shikimate pathway, consequently providing more chorismate for tacrolimus biosynthesis ii) acetyl-CoA that can either enter the TCA cycle or be converted into malonyl-CoA; iii) oxaloacetate by pyruvate carboxylase, which in turn can be converted by the aspartate aminotransferase AspC into aspartate that will then enter the lysine biosynthetic pathway, another precursor for tacrolimus biosynthesis. Also the identification of an hypothetical protein, with decreased protein levels in both mutant strains, predicted to be involved in fatty acid biosynthesis also suggested increased levels of acetyl-CoA. Moreover the decrease in Δ*ahpC* of both two sequential proteins in the TCA cycle also suggested that more succinate was being accumulated and being converted in succinyl-CoA and consequently in more methylmalonyl-CoA by methylmalonyl-CoA mutase. Interestingly it has

already been reported that rapamycin production was increased through supplementation of sodium succinate (Zhao *et al.* 2013).

Methylmalonyl-CoA along with shikimate are described to be the two main limiting factors in tacrolimus biosynthesis. We believe that a redirection of both precursors towards tacrolimus production is especially fine-tuned in Δ*ahpC* strain. Metabolic profiling analysis has already demonstrated that it is possible to increase tacrolimus production by increasing the carbon flux from the TCA cycle to methylmalonyl-CoA via succynil-CoA, which was achieved in Δ*ahpC* strain (Xia *et al.* 2013). An overexpression of *fkbO* was also achieved in Δ*ahpC*. In fact, it has been described an increase of 30% in tacrolimus production in a *S. tsukubaensis fkbO* overexpressing strain. Moreover, in this *fkbO*-overexpressing strain, after chorismate supply, the increase in tacrolimus production was even higher (Huang *et al.* 2013), which could suggest that in our mutant strain an increase of chorismate availability towards tacrolimus production could be occurring. From an applied point of view this strain proves to be of extreme importance especially since shikimic acid supplementation cannot be applied to large-scale fermentations due to its high costs (Zhu *et al.* 2010).

In order to have a better knowledge regarding the metabolic route(s) that are being redirected towards tacrolimus production, it would be important to analyse either by transcriptional analysis or enzymatic assays some of the genes/proteins involved in these metabolic pathways in our mutant strains.

All these changes observed in cell physiology, transcription and protein expression profiles points out to a balanced and very intricate communication between different metabolic pathways, which culminate, especially in the case of the Δ*ahpC* strain, with an increase of precursors supply towards an improvement on tacrolimus production.

In Δ*sigG* strain, the deregulation of iron uptake as well as the increased ROS levels during exponential and early stationary phase resulted in a delay in tacrolimus production. Even though the exact role of iron in tacrolimus biosynthesis still remains unknown, it is without a doubt, important. Interestingly, our preliminary data showed that the transcription of genes from the putative siderophore biosynthetic cluster adjacent to tacrolimus biosynthetic gene cluster is increased in our overproducing strain Δ*ahpC* at least in the time-point tested. In

fact, recent work performed in another tacrolimus producing strain, *Streptomyces* sp. strain KCCM 11116P, showed that overexpression of an ECF sigma factor stimulated the expression of tacrolimus biosynthetic genes (Lee *et al.* 2014). Its orthologue in *S. tsukubaensis* (STSU_32110) is present in that putative siderophore biosynthetic cluster.

CHAPTER 5

SODs and catalase role on tacrolimus production

5.1 FUNCTIONAL CHARACTERIZATION OF *S. TSUKUBAENSIS* IRON CONTAINING SUPEROXIDE DISMUTASE: SODA

Superoxide dismutases (SODs) are ubiquitous enzymes responsible for the disproportion of superoxide anion into hydrogen peroxide and molecular oxygen. *S. tsukubaensis* physiological characterization showed that, in tacrolimus producing conditions, both SodA (FeSOD) and SodN (NiSOD) were expressed and displayed SOD activity (Chapter 3; Fig. 3.6). Given the impact that the deletion of *S. natalensis* iron containing SOD, SodF, had in pimaricin production (Beites *et al.* 2011), and in order to functionally characterize *S. tsukubaensis* SodA, a knock-out mutant in *sodA* gene as well as a *sodA* overexpressing strain were generated (see Chapter 3 for further details on mutant strain generation).

5.1.1 Physiological characterization of *S. tsukubaensis* Δ*sodA*

Concerning growth, both *S. tsukubaensis* wild-type and Δ*sodA* strains displayed similar kinetic profiles with no difference in biomass at the end of the culture (192 h). However a slight delay in growth was observed at early exponential phase (72 h), probably due to an extended lag phase in the Δ*sodA* strain (Fig 5.1).

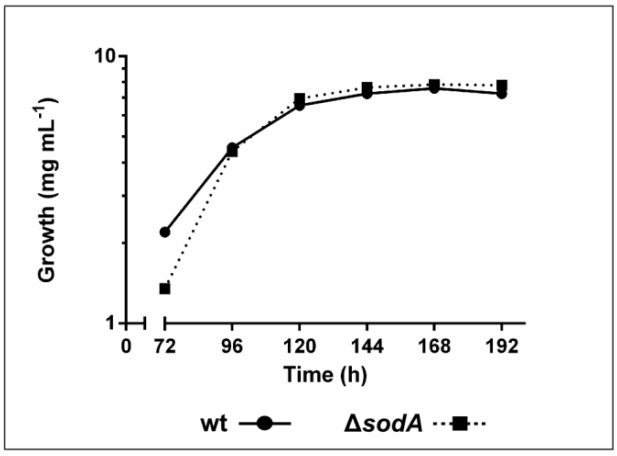

Figure 5.1 – Growth curve of *S. tsukubaensis* wild-**type and Δ***sodA* strains. Both wild-type and Δ*sodA* strains were grown in MGm medium and growth was assessed by dry weight measurements. Vertical bars indicate standard deviation of the mean values. Results (average of triplicates and standard deviation) are representative of three independent experiments.

5.1.1.1 Enzymatic antioxidant defences

Regarding the enzymatic antioxidant defences, characterisation of the SOD activity profile in the wild-type and Δ*sodA* strains was performed throughout

growth (Fig. 5.2). Total SOD activity displayed by Δ*sodA* strain was extremely low, especially during stationary phase where residual activity levels were detected (Fig. 5.2 A). The residual activity detected spectrophotometrically can be ascribed to SodN as verified by native-PAGE analysis (Fig. 5.2 B). As expected, no band corresponding to the iron containing SOD, was detected in the native-PAGE (Fig. 5.2 B). However, a marked decrease in SodN activity was also observed in the Δ*sodA* strain (Fig. 5.2 B).

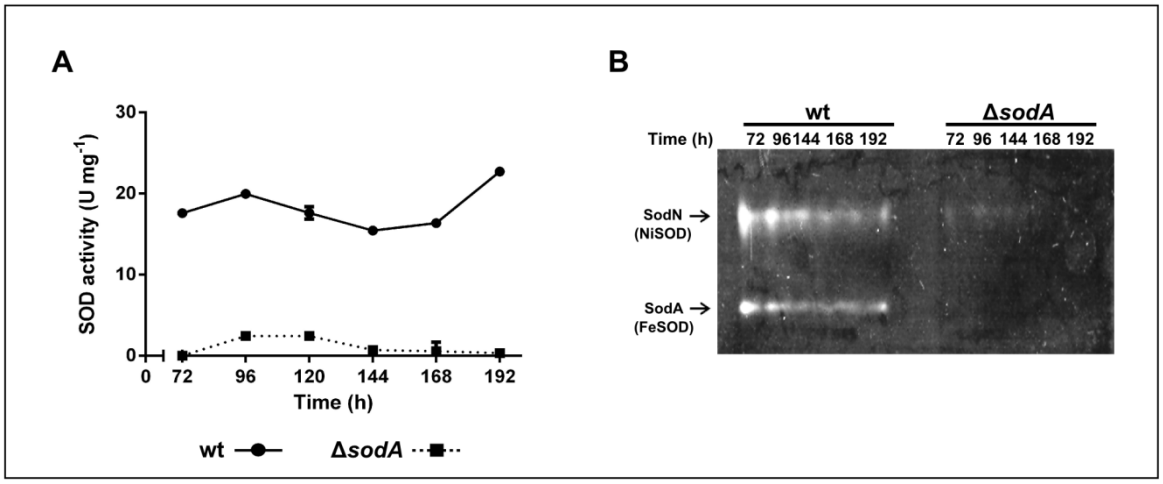

Figure 5.2 – SOD activity profile of *S. tsukubaensis* wild-type and Δ*sodA* strains. (A) Total SOD activity was measured spectrophotometrically in samples collected throughout growth from wild-type and Δ*sodA* cultures. Results (average of triplicates and standard deviation) are representative of three independent experiments. Vertical bars indicate standard deviation of the mean values. (B) Native-PAGE stained for SOD activity with cell-free protein extracts (50 μg of total protein per lane) from samples collected throughout growth from wild-type and Δ*sodA* cultures. Growth conditions were as standard.

In *S. coelicolor* an antagonistic regulation between Fe-containing SOD and Ni-containing SOD has been described (Kim *et al.* 2014). It was shown that a 90 nucleotide small regulatory RNA produced from the 3' UTR of S. *coelicolor sodF* mRNA, matches exactly the 5' UTR of *sodN* mRNA and that by pairing with this region, blocked its translation and induced *sodN* mRNA decay. Furthermore, in the presence of nicke,l *sodN* expression is favoured via an indirect regulatory mechanism, mediated by the transcriptional regulator Nur that represses transcription of the iron containing SOD, *sodF* (An *et al.* 2009). The results for SOD activity suggest a different regulation for *S. tsukubaensis* since in a nickel-containing medium (MGm) the absence of SodA led to a decrease in SodN.

In silico analysis of the SodN amino acid sequence regarding conserved residues important for protein stability, nickel chelation activity or electrostatic guidance system to the active site (Barondeau *et al.* 2004) did not revealed any structural alteration in *S. tsukubaensis* NiSOD that could explain a different regulatory mechanism. Moreover, and contrary to what was observed for *S. natalensis* and *S. coelicolor* (Kim *et al.* 1998, Beites *et al.* 2011), *S. tsukubaensis* grown in YEME medium, a medium described as nickel free (Kim *et al.* 1996), displayed NiSOD activity throughout growth, especially during exponential phase (18 h) (Fig. 5.3).

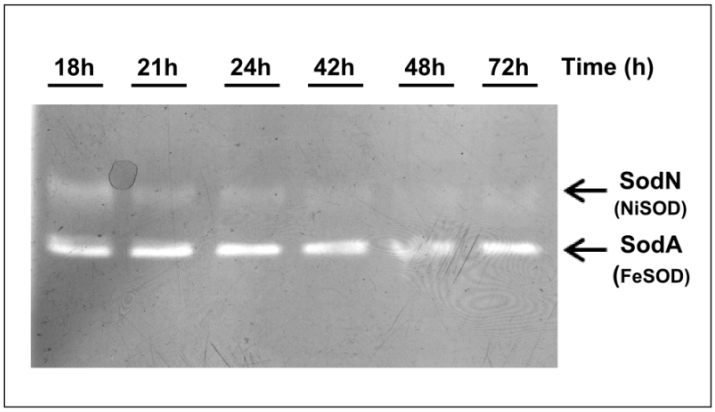

Figure 5.3 – *S. tsukubaensis* SOD activity profile in YEME medium. Native-PAGE stained for SOD activity with cell-free protein extracts (50 µg of total protein per lane) from samples collected throughout growth from *S. tsukubaensis* culture grown in YEME medium.

Characterization of catalase activity profile in *S. tsukubaensis* wild-type and Δ*sodA* strains was also performed throughout growth, both spectrophotometrically and by native-PAGE (Fig. 5.4). *S. tsukubaensis* Δ*sodA* strain displayed higher levels of total catalase activity during growth when compared to the wild-type (Fig. 5.4 A). This increase was also reflected in the native-PAGE analysis (Fig. 5.4 B).

5.1.1.2 Intracellular ROS levels

Intracellular levels of H_2O_2 and $O_2^{\cdot -}$ were monitored throughout growth for both wild-type and Δ*sodA* strains. As expected, due to the absence of *sodA* and the decrease in SodN activity, $O_2^{\cdot -}$ intracellular levels of Δ*sodA* strain were higher than the wild-type. However, this only occurred during early exponential phase (72 h and 96 h) (Fig. 5.5 A). Regarding H_2O_2 intracellular levels, Δ*sodA* strain displayed higher levels when compared to the wild-type at 72 h (Fig. 5.5 B).

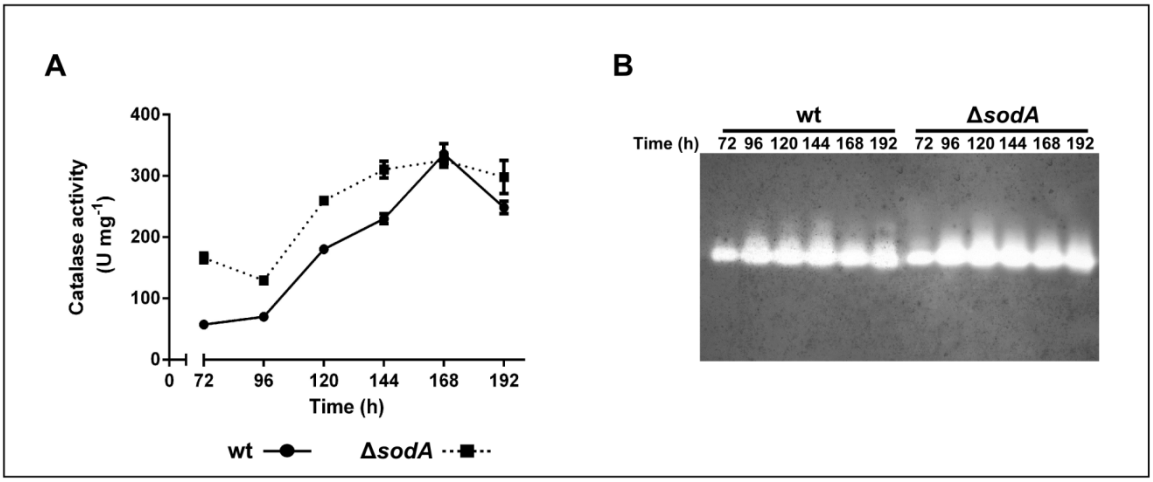

Figure 5.4 –Catalase activity profile of *S. tsukubaensis* wild-**type and Δ***sodA* strains. (A) Total catalase activity was measured spectrophotometrically in samples collected throughout growth from wild-type and Δ*sodA* cultures. Results (average of triplicates and standard deviation) are representative of three independent experiments. Vertical bars indicate standard deviation of the mean values. (B) Native-PAGE stained for catalase activity with cell-free protein extracts (1 μg of total protein per lane) from samples collected throughout growth from wild-type and Δ*sodA* cultures. Growth conditions were as standard.

It was interesting to notice that Δ*sodA* strain presented high intracellular ROS levels at early exponential phase. Although high $O_2^{\cdot-}$ intracellular levels were expected due to the deletion of SodA encoding gene, the increase in H_2O_2 intracellular levels were a surprise, particularly if we take into consideration previous SOD deletions in other studies performed on *Streptomyces* bacteria, that

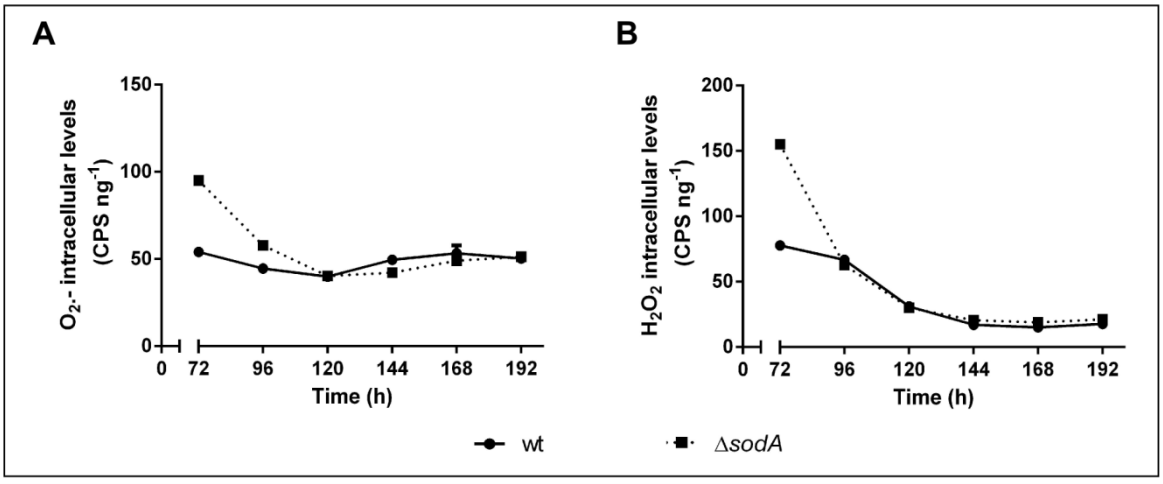

Figure 5.5 – ROS intracellular levels of *S. tsukubaensis* wild-**type and Δ***sodA* strains. (A) DHE oxidation levels were used to measure $O_2^{\cdot-}$ intracellular levels. (B) DHR oxidation levels were used to measure of H_2O_2 intracellular levels. Samples were collected throughout growth curve. Growth conditions were as standard. Vertical bars indicate standard deviation of the mean values. Results (average of triplicates and standard deviation) are representative of three independent experiments.

led to decreased H_2O_2 intracellular levels and growth defects (Beites *et al.* 2011). However, not all H_2O_2 generated in biological systems is derived from $O_2^{\cdot -}$ dismutation. In fact, the auto-oxidation of enzymes involved in the respiratory chain, can also increase H_2O_2 intracellular levels (Imlay 2008).

5.1.1.3 ROS sensitivity

Sensitivity of the mutant strain to induced oxidative stress was tested by evaluating growth inhibition around paper disks containing 9 M H_2O_2 or 1 M of menadione (Fig. 5.6). In both cases, Δ*sodA* strain displayed a slight increased sensitivity towards oxidative stress than the wild-type. Although an increased sensitivity was expected towards menadione, a superoxide anion generator, the increased sensitivity, even if only slightly, to H_2O_2 is not easily explained since total levels of catalase activity in Δ*sodA* strain were higher than the ones observed for the wild-type (Fig. 5.4 A). However, Δ*sodA* strain presented higher intracellular levels of $O_2^{\cdot -}$, which are able to attack iron-sulfur clusters, thus increasing the intracellular pool of iron that react with H_2O_2, generating the hydroxyl radical, and consequently contributing in this way to Δ*sodA* increased sensitivity to H_2O_2.

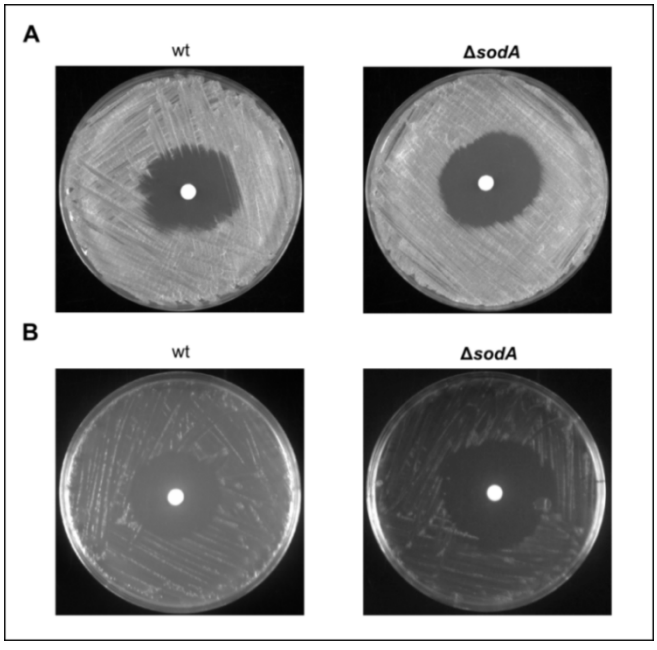

Figure 5.6 – Growth inhibition assays in *S. tsukubaensis* wild-**type and Δ***sodA* strains. For oxidative stress growth inhibition bioassay *S. tsukubaensis* wild-type and Δ*sodA* strains were grown in YED medium. (A) Sensitivity to H_2O_2 was tested with the addition of 9 M of H_2O_2 to sterile discs. (B) Sensitivity to menadione was tested with the addition of 1 M of menadione to sterile discs.

5.1.1.4 Tacrolimus production

Regarding tacrolimus production, Δ*sodA* strain displayed a 17% increase when compared to the wild-type, reaching a production of 27 mg L^{-1} on average (Fig. 5.7). Additionally, an 88% increase in ascomycin production was also observed in the mutant strain, with a change of the ratio tacrolimus/ascomycin from 21, in the wild-type strain, to 12 in Δ*sodA* strain.

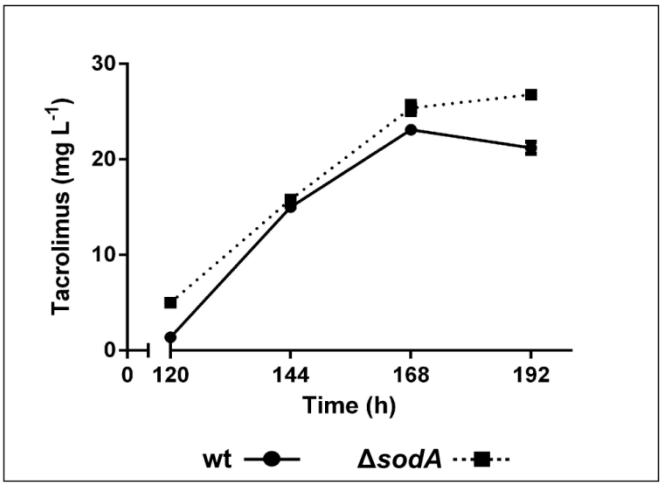

Figure 5.7 –Tacrolimus production in *S. tsukubaensis* wild-**type and Δ***sodA* strains. Tacrolimus production of wild-type and Δ*sodA* strains throughout growth. Tacrolimus production was assessed by HPLC. Vertical bars indicate standard deviation of the mean values. Results (average of triplicates and standard deviation) are representative of three independent experiments.

5.1.2 Transcriptional characterization of *S. tsukubaensis* Δ*sodA*

The transcription of 55 selected genes from different metabolic pathways was assessed by RT-PCR. The most relevant results were observed in the transcription of genes related with oxidative stress, tacrolimus biosynthesis, phosphate metabolism and nitrogen metabolism. The time points selected were 72 h, 96 h and 120 h of growth that covers early exponential phase and late exponential, corresponding to the time-points before and after the onset of tacrolimus production. For transcriptional analysis the RNA polymerase principal sigma factor encoding gene, *hrdB,* was use as reference gene.

5.1.2.1 Oxidative stress related genes

A transcriptional analysis of genes coding for enzymatic defences, as well as their putative regulators was performed for Δ*sodA* strain. Regarding transcription of *sodA*, an increase was observed from 72 h to 120 h in the wild-type strain. As expected no transcription was detected in the mutant strain (Fig.

5.8). In the wild-type strain *sodN* transcription decreased at 120 h of growth, overlapping with the observed increase in *sodA* transcription. Interestingly, and in accordance to native-PAGE analysis (Fig. 5.2), *sodN* transcription in Δ*sodA* strain was down regulated (Fig. 5.8). No apparent differences were observed regarding the transcriptional regulator Nur between the two strains; since Nur regulation of *sodN* transcription is described to be indirect and through *sodA* transcription inhibition this is not surprising (Kim *et al.* 2014). When analysing *ahpC* and *oxyR* transcription, a slight increase in transcription of both genes is observed in Δ*sodA* strain at 72 h. This result can be ascribed to the high H_2O_2 intracellular levels observed in Δ*sodA* strain (Fig. 5.5 B), which can activate transcription of *oxyR* and consequently of *ahpC* (Chapter 4). Both *katA1* and *katA2,* coding for monofunctional catalases, presented increased transcription in the Δ*sodA* strain, when compared to the wild-type. These results were also in agreement to what was observed in the catalase enzymatic assays (Fig. 5.4 A).

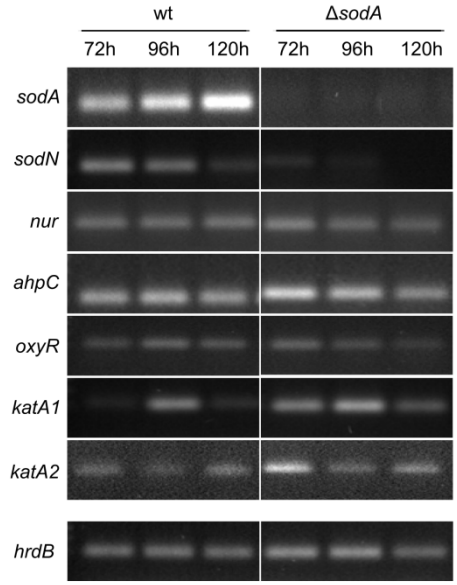

Figure 5.8 – Transcription profile of oxidative stress related genes in *S. tsukubaensis* wild-**type and Δ***sodA* strains. Transcription of *sodA*, *sodN*, *nur*, *ahpC*, *katA1* and *katA2* was analysed in wild-type and Δ*sodA* strains at 72 h, 96 h and 120 h of growth. Growth conditions were as standards. *hrdB* was used as reference gene.

5.1.2.2 Phosphate metabolism

Phosphate (Pi) concentration exerts an important regulatory effect both on primary and secondary metabolism in *Streptomyces* (Martín *et al.* 2012). Phosphate limitation triggers a response, which is mediated by the two-component system PhoRP that directly or indirectly affects *Streptomyces* secondary metabolism. Furthermore, links between phosphate metabolism and oxidative

stress have already been described (Ghorbel *et al.* 2006, Beites *et al.* 2014). RT-PCR results showed an earlier activation of the PhoRP system in Δ*sodA* strain, when compared to the wild-type; an up-regulation of this system sensor and regulator, *phoR* and *phoP* respectively, was observed at 96 h as well as the *phoU* and the high-affinity Pi transporter encoding gene *pstS* (Fig. 5.9) Moreover, transcription of *pitH1* and *pitH2* that codes for low affinity Pi transporters, which transport Pi coupled with divalent metals transport, was also increased in Δ*sodA* strain (Fig. 5.9). These results provide a good indication that in this mutant strain Pi depletion occurs at earlier stages of growth when compared to the wild-type

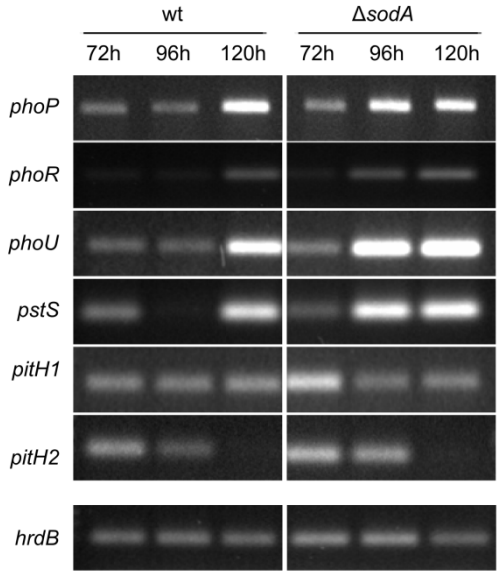

Figure 5.9 – Transcription profile of phosphate metabolism related genes in *S. tsukubaensis* wild-type **and Δ***sodA* strains.. Transcription of *phoP*, *phoR*, *phoU*, *pstS*, *pitH1* and *pitH2* was analysed in wild-type and Δ*sodA* strains at 72 h, 96 h and 120 h of growth. Growth conditions were as standards. *hrdB* was used as reference gene.

strain.

5.1.2.3 Nitrogen metabolism

An up-regulation of the transcription of genes involved in nitrogen metabolism was also observed in the Δ*sodA* strain (Fig. 5.10). GlnR, a global nitrogen regulator, controls the expression of several nitrogen metabolism genes at the transcriptional level including the transcription of glutamine synthetase I (*glnA*), glutamine synthetase II (*glnII*), *glnD* (uridylyltransferase) and *glnK* (PII family protein). RT-PCR analysis showed an earlier (72 h *vs* 120 h) induction of *glnR* transcription in the Δ*sodA* strain. Consequently, transcription of genes regulated by GlnR was also up-regulated in the mutant strain.

Nitrogen control and influence over *Streptomyces* secondary metabolism has been demonstrated. In fact, a role for the global regulator GlnR in secondary metabolism has been reported; the heterologous expression of the GlnR orthologue of *A. mediterranei* led to an anticipation of undecylprodigiosin production and inhibition of actinorhodin production in *S. coelicolor* (Yu *et al.* 2007). Possibly, the increased transcription of *glnR* could also help explain the tacrolimus over-producing phenotype of Δ*sodA* strain.

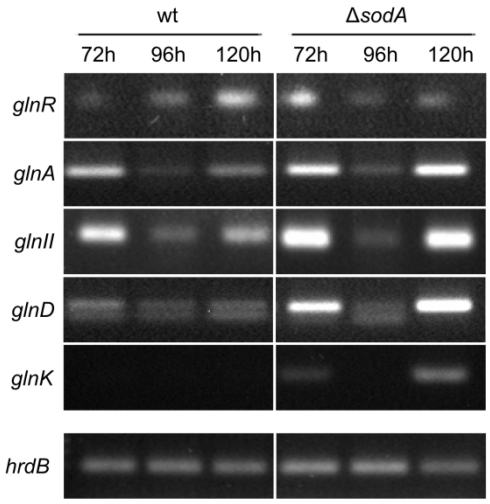

Figure 5.10 – Transcription profile of nitrogen metabolism related genes in in *S. tsukubaensis* **wild-type and Δ***sodA* strains. Transcription of *glnR*, *glnA*, *glnII*, *glnD* and *glnK* was analysed in wild-type and Δ*sodA* strains at 72 h, 96 h and 120 h of growth. Growth conditions were as standards. *hrdB* was used as reference gene.

5.1.2.4 Tacrolimus biosynthetic gene cluster

Transcriptional analysis of genes from the tacrolimus biosynthetic gene cluster revealed that there was an early transcription activation of the cluster in Δ*sodA* strain, when compared to the wild-type (Fig. 5.11). Both transcriptional regulators and structural genes displayed increased transcription at 72 h of growth. The up-regulation was particularly evident for the CSR encoding gene *fkbN* and the genes involved in the supply of biosynthetic precursor units, namely *fkbO* and *fkbL*.

All these results are in accordance with the tacrolimus overproducing profile presented by Δ*sodA* strain (Fig. 5.7).

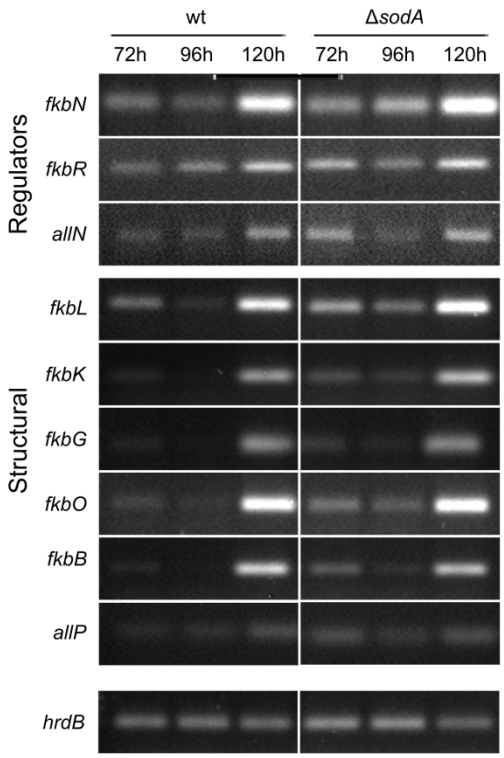

Figure 5.11 – Transcription profile of genes from tacrolimus biosynthetic cluster in *S. tsukubaensis* wild-**type and Δ***sodA* strains. (A) Transcription of the tacrolimus biosynthetic gene cluster regulators: *fkbN*, *fkbR and allN, and* structural genes from tacrolimus biosynthetic cluster: *fkbL*, *fkbK, fkbG, fkbO, fkbB and allP.* Transcription of the genes was analysed in wild-type and Δ*sodA* strains at 72 h, 96 h and 120 h of growth. Growth conditions were as standards. *hrdB* was used as reference gene.

5.1.3 Overexpression of SodA

The integrative vector pIB139 that harbours the strong constitutive promoter *ermE**p was used for *sodA* overexpression. Although it has been reported that pIB139 integration in the chromosome can have detrimental effects on the physiological parameters of several *Streptomyces* strains, especially in secondary metabolism (Vicente *et al.* 2009), pIB139 integration in *S. tsukubaensis* had no apparent effect. In all parameters analysed (growth, tacrolimus production, oxidative stress response and gene transcription of genes from different metabolic pathways) *S. tsukubaensis* [pIB139] strain displayed the same profile as the wild-type, functioning as a good control. See section 3.3.4 for details on the construction of *S. tsukubaensis* [pIB*sodA*] strain.

5.1.3.1 Enzymatic antioxidant defences

Concerning growth, *S. tsukubaensis* [pIB*sodA*] strain presented severe growth defects and was not able to reach the same biomass as the [pIB139] strain (Fig. 5.12).

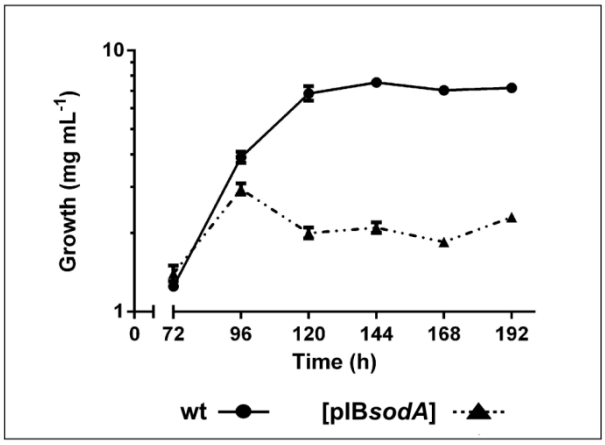

Figure 5.12 – Growth curve of *S. tsukubaensis* [pIB139] and [pIB*sodA*] strains. Strains were grown in MGm medium and growth was assessed by dry weight measurements. Vertical bars indicate standard deviation of the mean values. Results (average of triplicates and standard deviation) are representative of three independent experiments.

Regarding enzymatic antioxidant defences, characterisation of the SOD activity profile in both *S. tsukubaensis* [pIB139] and [pIB*sodA*] strains was performed during stationary phase (120 h, 144 h and 192 h) spectrophotometrically and by native-PAGE. Total SOD activity displayed by [pIB*sodA*] strain was higher than the one presented by the [pIB139] strain, especially at 120 h and 144 h (Fig. 5.13 A), confirming SodA overexpression. The results obtained were in agreement to what was observed in the native-PAGE analysis, which showed that the increase observed in total SOD activity was not only due to an increase in SodA activity but also to an increase of SodN activity (Fig. 5.13 B). These results constitute yet another evidence for the positive cross-regulation between these two superoxide dismutases in *S. tsukubaensis*.

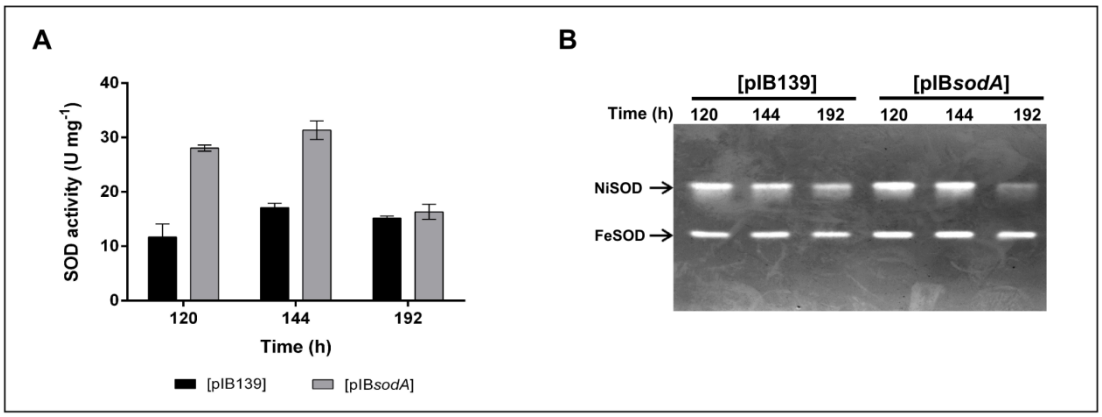

Figure 5.13 –SOD activity profile of *S. tsukubaensis* [pIB139] and [pIB*sodA*] strains. (A) Total SOD activity was measured spectrophotometrically in samples collected at 120 h, 144 h and 192 h of growth from *S. tsukubaensis* [pIB139] and [pIB*sodA*] cultures. Results (average of triplicates and standard deviation) are representative of three independent experiments. Vertical bars indicate standard deviation of the mean values. (B) Native-PAGE stained for SOD activity with cell-free protein extracts (50 μg of total protein per lane) from samples collected at 120 h, 144 h and 192 h of growth form [pIB139] and [pIB*sodA*] cultures. Growth conditions were as standard.

As for catalase activity, [pIBs*odA*] strain presented higher catalase activity levels at 144 h and 192 h when compared to the [pIB139] strain (Fig. 5.14).

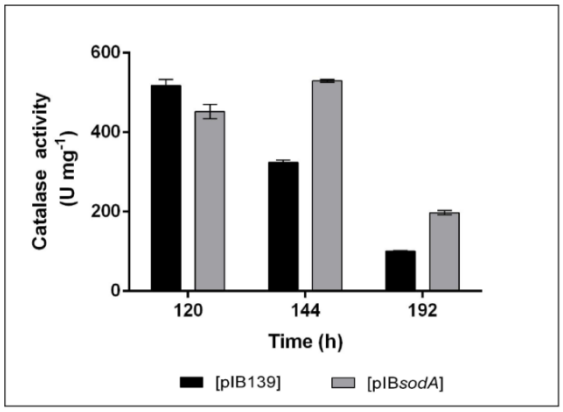

Figure 5.14 – Catalase activity profile of *S. tsukubaensis* [pIB139] and [pIB*sodA*] strains. Total catalase activity was measured spectrophotometrically in samples collected at 120 h, 144 h and 192 h of growth from [pIB139] and [pIB*sodA*] cultures. Growth conditions were as standard. Results (average of triplicates and standard deviation) are representative of three independent experiments. Vertical bars indicate standard deviation of the mean values.

5.1.3.2 Intracellular ROS levels

Intracellular levels of H_2O_2 and $O_2^{\cdot -}$ were monitored and determined at 120 h and 144 h of growth. As expected, and given the increase observed for SodA and also SodN activities in [pIB*sodA*] strain, $O_2^{\cdot -}$ intracellular levels were lower than those presented by [pIB139] strain (Fig. 5.15 A). Conversely, [pIB*sodA*] presented a 5-fold and 9-fold increase in H_2O_2 intracellular levels at 120 h and 144 h, respectively (Fig. 5.15 B).

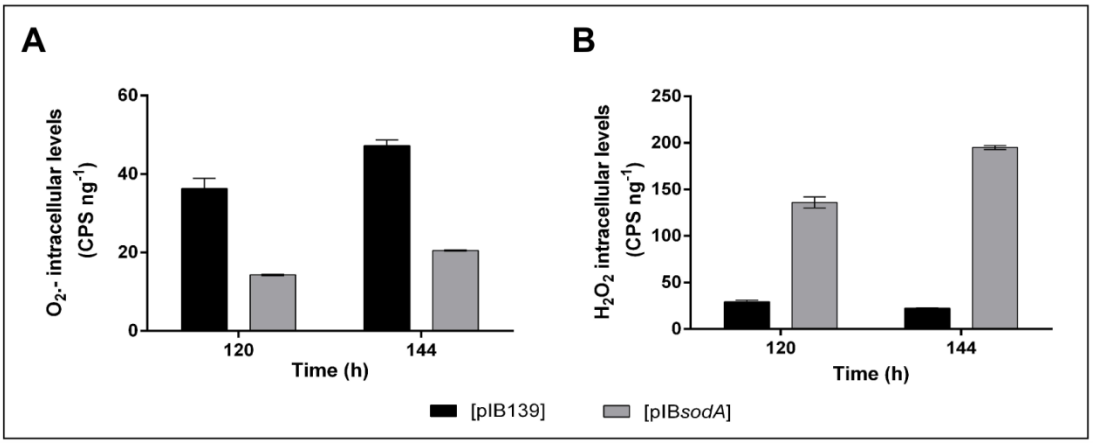

Figure 5.15 –ROS intracellular levels of *S. tsukubaensis* [pIB139] and [pIB*sodA*] strains. (A) DHE oxidation levels were used as a measure of $O_2^{\cdot -}$ intracellular levels. (B) DHR oxidation levels were used as a measure of H_2O_2 intracellular levels. Samples were collected at 120 h and 144 h of growth. Growth conditions were as standard. Vertical bars indicate standard deviation of the mean values. Results (average of triplicates and standard deviation) are representative of three independent experiments.

In fact, the increased H_2O_2 intracellular levels probably contributed to the extremely high sensitivity to H_2O_2 presented by [pIB*sodA*] strain (Fig. 5.16).

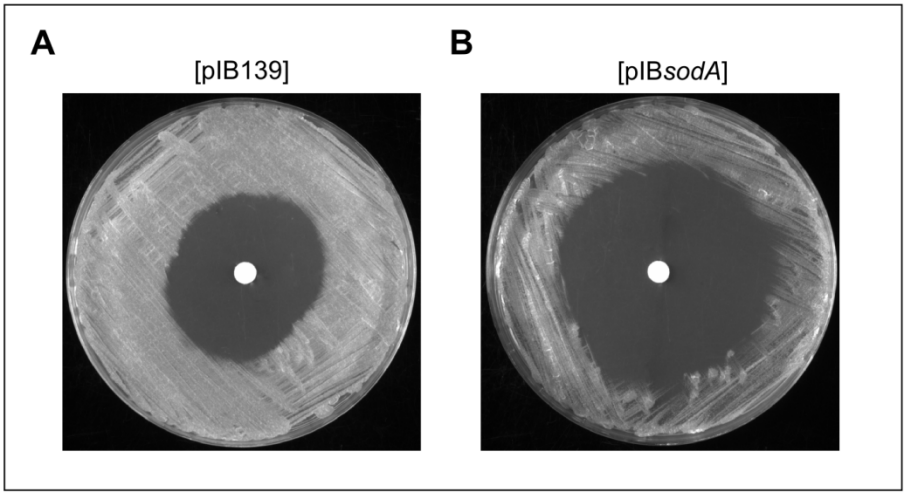

Figure 5.16 – Growth inhibitions assays in *S. tsukubaensis* [pIB139] and [pIB*sodA*] strains. (A) H_2O_2 growth inhibition bioassay in [pIB139] strain. (B) H_2O_2 growth inhibition bioassay in [pIB*sodA*]. [pIB139] and [pIB*sodA*] strains were grown in YED medium. Sensitivity to H_2O_2 was tested with the addition of 9 M of H_2O_2 to sterile discs.

5.1.3.4 Tacrolimus production

Tacrolimus production was followed throughout growth in both strains, however for [pIB*sodA*] we could not detect tacrolimus at any time-point (Fig. 5.17), making of [pIB*sodA*] a tacrolimus non-producing strain.

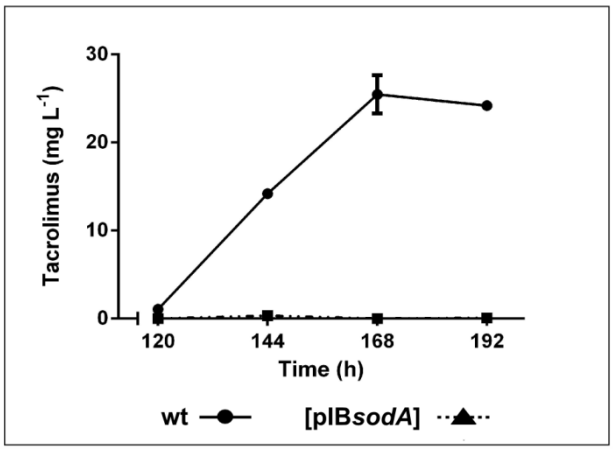

Figure 5.17 – Tacrolimus production profile *S. tsukubaensis* [pIB139] and [pIB*sodA*] strains. Tacrolimus production of [pIB139] and [pIB*sodA*] strains throughout growth. Tacrolimus production was assessed by HPLC. Vertical bars indicate standard deviation of the mean values. Results (average of triplicates and standard deviation) are representative of three independent experiments.

5.2 FUNCTIONAL CHARACTERIZATION OF *S. TSUKUBAENSIS* [PIBS*ODN*]

Considering the cross-regulation between superoxide dismutases in *S. coelicolor* and the positive effect that *sodA*/SodA exerted, both on activity as well as on transcription of *sodN* in *S. tsukubaensis*, a strain overexpressing SodN was constructed in order to further characterize this cross-regulation between SODs in *S. tsukubaensis*. Gene overexpression was performed by cloning *sodN* in pIB139 vector under the control of the constitutive *ermEp** promoter from *Saccharopolyspora erythraea* (Bibb *et al.* 1985). See section 3.3.4 for details on the construction of *S. tsukubaensis* [pIB*sodN*] strain.

Concerning growth, [pIB*sodN*] strain presented the same growth kinetics profile and biomass as the one observed for the control strain, *S. tsukubaensis* [pIB139] (Fig. 5.18 A). Catalase and SOD activity were monitored throughout growth (Fig 5.18 A and B). A similar catalase activity profile was displayed by [pIB*sodN*] strain when compared to [pIB139] strain (Fig. 5.18 B); surprisingly no significant variations were observed in total SOD activity of [pIB*sodN*] strain when compared to [pIB139] strain (Fig. 5.18 C). However native-PAGE analysis of protein extracts suggested a slight increase in SodN activity (Fig. 5.18 D).

ROS intracellular levels were also assessed at exponential phase (120 h) and stationary phase (144 h) and similarly to what was observed for the enzymatic activities, no significant changes were observed between the two strains regarding H_2O_2 intracellular levels nor $O_2^{\cdot -}$ intracellular levels (Fig. 5.18 E and F). Finally, [pIB*sodN*] strain displayed a tacrolimus under-producing profile with an average final yield of 17 mg L^{-1} at 192 h (Fig. 5.18 G).

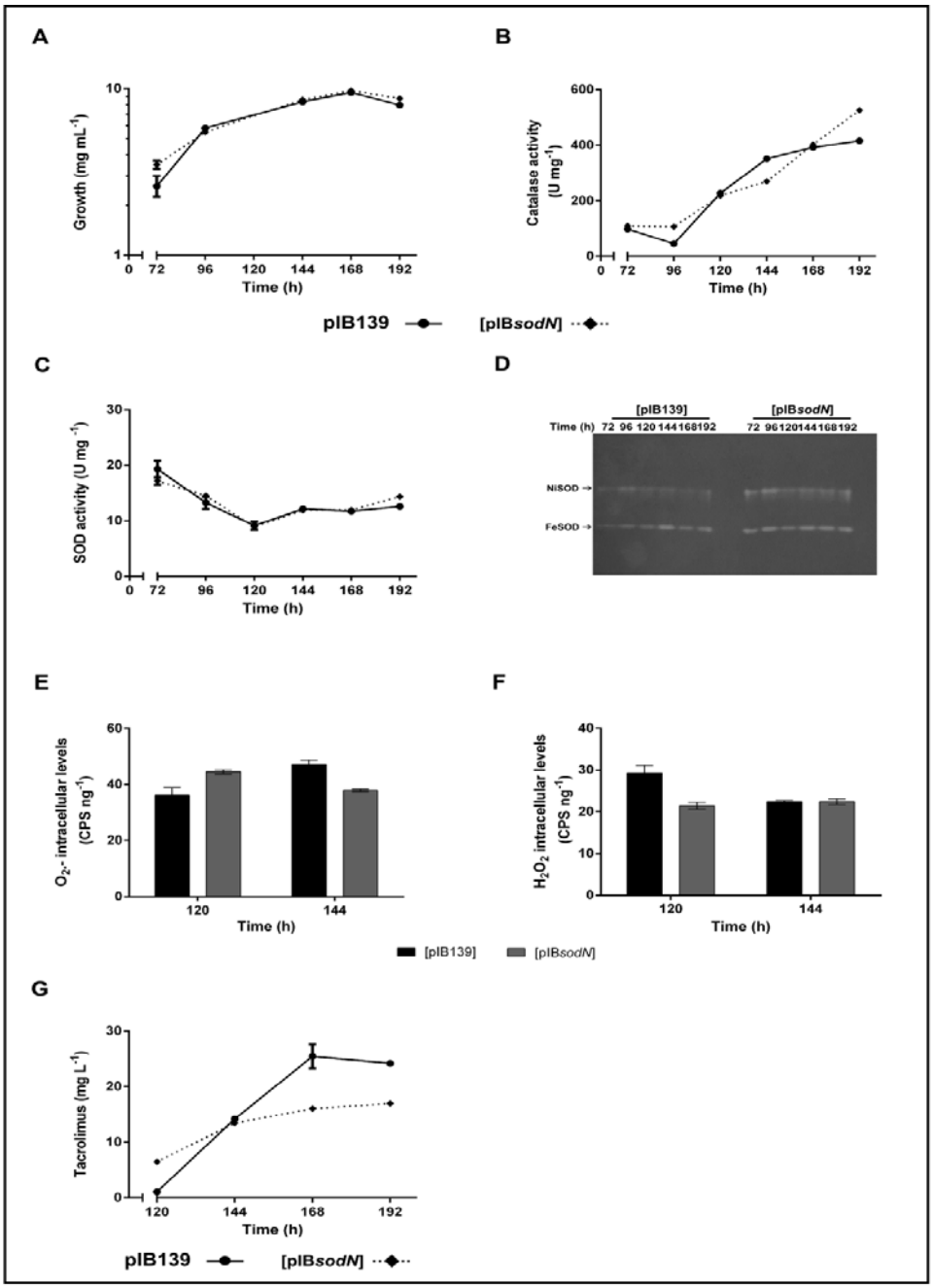

Figure 5.18 – *S. tsukubaensis* [pIB139] and [pIB*sodN*] strains physiological characterization. (A) Growth curve of pIB139 and pIB*sodN* strains. Growth was assessed by dry weight measurements. (B) Total catalase activity was measured spectrophotometrically. (C) Total SOD activity was measured spectrophotometrically. (D) Native-PAGE for SOD activity with cell-free protein extracts (50µg of total protein per lane). Samples were collected throughout growth from pIB139 and pIB*sodN* cultures. (E) DHE oxidation levels were used as a measure of $O_2^{\cdot-}$ intracellular levels. (F) DHR oxidation levels were used as a measure of H_2O_2 intracellular levels. Samples were collected at 120h and 144h of growth. (G) Tacrolimus production profile of pIB139 and pIB*sodN* strains throughout growth. Tacrolimus production was assessed by HPLC. Growth conditions were as standards. Results (average of triplicates and standard deviation) are representative of three independent experiments. Vertical bars indicate standard deviation of the mean values.

A transcriptional analysis was performed in order to investigate whether the tacrolimus under-producing profile could be a reflection of changes at the transcriptional level in genes from the tacrolimus biosynthetic cluster. Additionally, the transcription of oxidative stress related genes was also assessed to verify if SodN overexpression could have exerted any effect on their transcription. Transcription of the selected genes from tacrolimus biosynthetic was down-regulated in [pIB*sodN*] strain (Fig. 5.19); surprisingly, *sodN* transcription was also down-regulated in [pIB*sodN*] strain when comparing to [pIB139], suggesting that *sodN* was not being overexpressed in [pIB*sodN*]. Noteworthy that *nur* transcription profile was similar for both strains (Fig. 5.19).

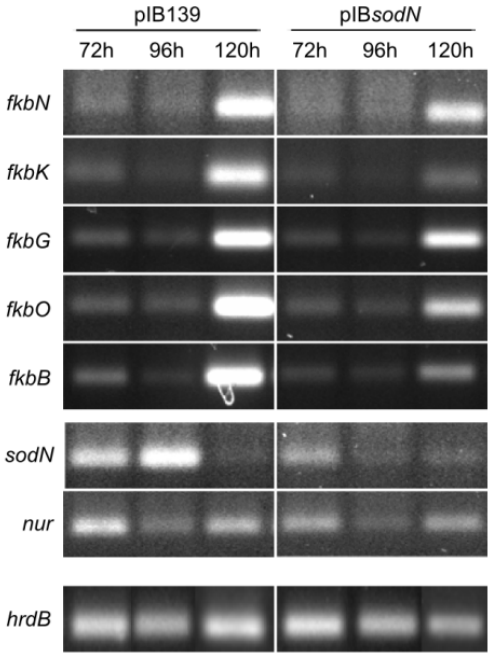

Figure 5.19 – Transcription profile of genes from tacrolimus biosynthetic cluster and oxidative-stress related in *S. tsukubaensis* [pIB139] and [pIB*sodN*]. Transcription of *fkbN*, *fkbK, fkbG, fkbO, fkbB.* Transcription of *sodN* and *nur*. Transcription of *hrdB*. Transcription of these genes was analysed in [pIB139] and [pIB*sodN*] strains at 72 h, 96 h and 120 h of growth. Growth conditions were as standards. *hrdB* was used as reference gene.

Even though [pIB*sodN*] strain identity was confirmed by PCR and both the promoter and the target gene were correctly integrated in *S. tsukubaensis* chromosome (Section 3.3.4; Fig. 3.18,), RT-PCR analysis clearly showed that *sodN* overexpression was not achieved. pIB139 integrates in the *Streptomyces* genome through the site-specific recombination between the vector *attP* site and the host genome *attB loci*. Although this interaction is highly specific, it has been reported vector integration in pseudo-*attB* sites present in the host genome (Combes *et al.* 2002), which may contribute to enhanced phenotype variability. To further confirm the integration of pIB139 and pIB*sodN* in *S. tsukubaensis* genome *attB* site (located within *STSU_17107* gene), we amplified by PCR and sequenced

the integration site in *S. tsukubaensis* [pIB139] and [pIB*sodN*] strains. The results showed that both plasmids integrated in the *S. tsukubaensis attB* site and not in pseudo-*attB* sites; however sequence analysis revealed that during the pIB*sodN* integration process, part of the integrase encoding gene from pIB139 vector suffered a deletion. *In silico* analysis has shown that this deletion should not have affected the overexpression of *sodN*.

In addition to the tacrolimus under-producing phenotype, the culture broth of *sodN* overexpressing strain also presented a greenish colour, contrasting with the dark orange presented by the [pIB139] and wild-type strains (Fig. 5.20 A). The different colour could suggest the production of a novel metabolite/pigment, therefore methanol extracts of the culture broths, spiked with tacrolimus and ascomycin were analysed by HPLC coupled with a diode array detector (Fig. 5.20 B). Two peaks (peak 3 and 4, Fig. 5.20 B) that presented a maximum of absorbance at 300 nm and 262 nm and a relative retention time (RTT) to tacrolimus of 1.05 and 0.68, respectively, were present in both *S. tsukubaensis* wild-type and [pIB139] strains and were absent in [pIB*sodN*] strain. On the other hand, peak 5 (peak 5, Fig. 5.20 B) with a maximum absorbance at 247 nm and a RRT to tacrolimus of 1.32 was only present in the [pIB*sodN*] strain.

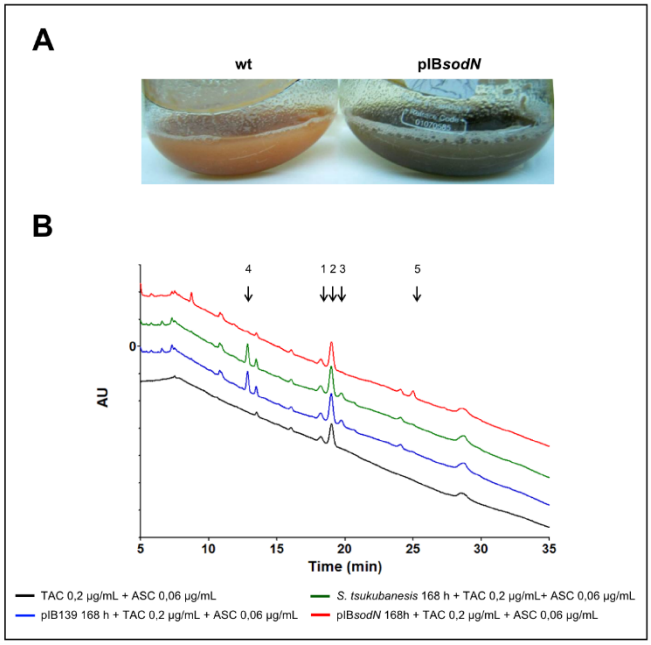

Figure 5.20 – *S. tsukubaensis* [pIB139] and [pIB*sodN*] characterization. (A) Culture broth of *S. tsukubaensis* [pIB139] and [pIB*sodN*] strains at 168 h of growth. (B) Chromatogram at 210 nm of *S. tsukubaensis* wild-type (green), [pIB139] (blue) and [pIB*sodN*] (red) culture broth methanol extracts spiked with tacrolimus and ascomycin. Peak 1 RRT of 0.96 (ascomycin); peak 2 RRT of 1 (tacrolimus); peak 3 RTT of 1.05; peak 4 RTT of 0.68; peak 5 RTT of 1.32. A mixture (3:1) of purified tacrolimus (0.2 µg/mL) and ascomycin (0.06 µg/mL) was used as control.

Further studies on [pIB*sodN*] strain will be needed in order to characterize the putative new compound being produced.

5.3 THE ROLE OF MONOFUNCTIONAL CATALASE IN *S. TSUKUBAENSIS*

5.3.1 Functional characterization of *S. tsukubaensis* [pIB*katA1*]

The results presented in Chapter 3 suggested a key role of catalase activity on tacrolimus production in *S. tsukubaensis*. In order to functionally characterize the monofunctional catalase KatA1 from *S. tsukubaensis*, a *katA1* knock-out mutant was originally planned. However, the double recombination to replace the *katA1* gene by the apramycin resistance cassette proved to be impossible to obtain until the moment. Alternatively, we decided to overexpress *katA1* by cloning it in the pIB139 vector under the control of the constitutive *ermEp** promoter (Bibb *et al.* 1985). See section 3.3.4 for details on the construction of *S. tsukubaensis* [pIB*katA1*] strain.

Concerning growth, *S. tsukubaensis* [pIB*katA1*] strain presented the same growth kinetics profile and biomass as the one observed for the control strain (Fig. 5.21 A). Likewise, total SOD activity on the *katA1* overexpressing strain presented a similar profile as the control strain except for early exponential phase (72 h) where [pIB*katA1*] strain presented significant lower levels (Fig. 5.21 C,D).

Regarding total catalase activity, both native-PAGE analysis and spectrophotometric quantification (Fig. 5.21 E, F) of protein extracts, showed a significant increase in catalase activity at all time points in *S. tsukubaensis* [pIB*katA1*] strain. These results, combined with the RT-PCR analysis of *katA1* gene expression (Fig. 5.22), showed that *katA1* overexpression was successfully achieved. Compared to the control strain, a 3.5-fold average increase in catalase activity in the *katA1* overexpressing strain was reached (Fig. 5.21 F). Simultaneously, the [pIB*katA1*] strain displayed a tacrolimus overproducing profile, presenting at 168 h of growth an increase of 34% in production, when compared to the [pIB139] strain (Fig. 5.21 B).

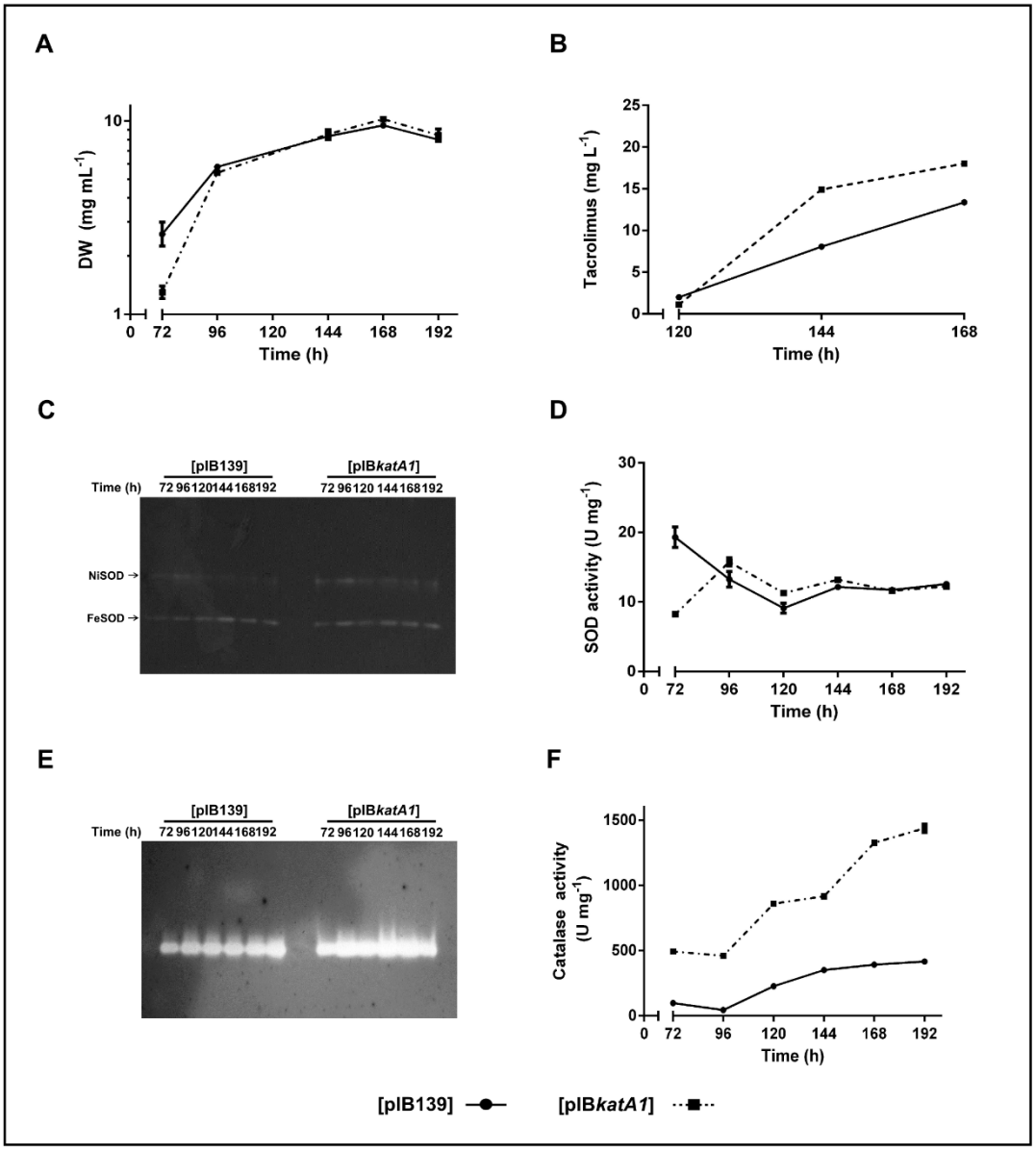

Figure 5.21 – *S. tsukubaensis* [pIB139] and [pIB*katA1*] strains physiological characterization. (A) Growth curve of [pIB139] and [pIB*katA1*] strains. Growth was assessed by dry weight (B) Total SOD activity was measured spectrophotometrically. (C) Native-PAGE stained for SOD activity with cell-free protein extracts (50 μg of total protein per lane). (D) Total catalase activity was measured spectrophotometrically. (E) Native-PAGE stained for catalase activity with cell-free protein extracts (1 μg of total protein per lane). (F) Tacrolimus production profile of [pIB139] and [pIB*katA1*] strains throughout growth. Growth conditions were as standards. Results (average of triplicates and standard deviation) are representative of three independent experiments. Vertical bars indicate standard deviation of the mean values.

Gene expression analysis of selected genes involved in the biosynthesis of tacrolimus suggested that the transcription of the tacrolimus biosynthetic cluster in [pIB*katA1*] strain was increased at earlier time points (72 h and 96 h). Regarding oxidative stress related genes, it should be emphasized the decrease in *ahpC*

transcription observed at 72 h in pIB*katA1* (Fig. 5.22), which suggests a compensatory effect with catalase, i.e., the overexpression of catalase during early exponential phase is compensated by a decrease in *ahpC* transcription.

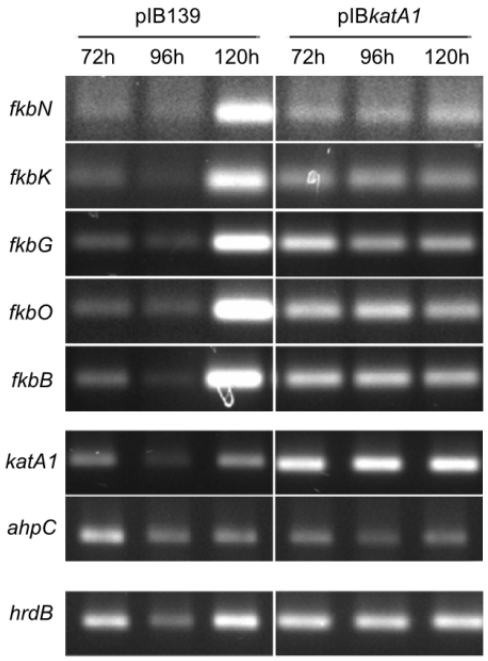

Figure 5.22 – Transcription profile of genes from tacrolimus biosynthetic cluster and oxidative-stress related. (A) Transcription of *fkbN*, *fkbK, fkbG, fkbO, fkbB, katA1* and *ahpC*. Transcription of these genes was analysed in pIB139 and pIB*katA1* strains at 72 h, 96 h and 120 h of growth. Growth conditions were as standards. *hrdB* was used as reference gene.

5.3.2 Catalase activity and tacrolimus production

In *S. tsukubaensis,* total catalase activity profile showed a growth-dependent behaviour with an induction of activity observed during the transition from early to late exponential phase that overlaps with the onset of tacrolimus production. Moreover, a common feature observed in all our overproducing strains was both an increase in catalase activity as well as a decrease in H_2O_2 intracellular levels, when compared to the wild-type. To further understand this link between tacrolimus production, catalase activity and H_2O_2 intracellular levels, we analysed both catalase activity profile and H_2O_2 intracellular levels in *S. tsukubaensis* wild-type strain grown in YEME, a non-producing tacrolimus medium, and compared it with tacrolimus producing conditions.

Although the growth kinetic is similar in both mediums, the lag phases differed considerably (Fig. 5.23). For simplification, instead of growth curve time-points, we will refer to growth phases, namely early exponential (EE), late exponential (LE), stationary phase (S) and late stationary phase (LS). In YEME

medium, *S. tsukubaensis* presented a different catalase activity profile, particularly during late exponential and stationary phase where the typical catalase induction observed in the transition from EE to LE in tacrolimus producing conditions was not observed. In addition, total catalase activity levels were different, with 70-80 U mg^{-1} of catalase activity presented by *S. tsukubaensis* in YEME *vs* the 200-300 U mg^{-1} normally obtained on average in MGm medium (Fig.5.23 A). Moreover, native-PAGE analysis revealed only one band displaying catalase activity in YEME medium, in contrast with the two bands observed in MGm medium (Fig. 5.23 B).

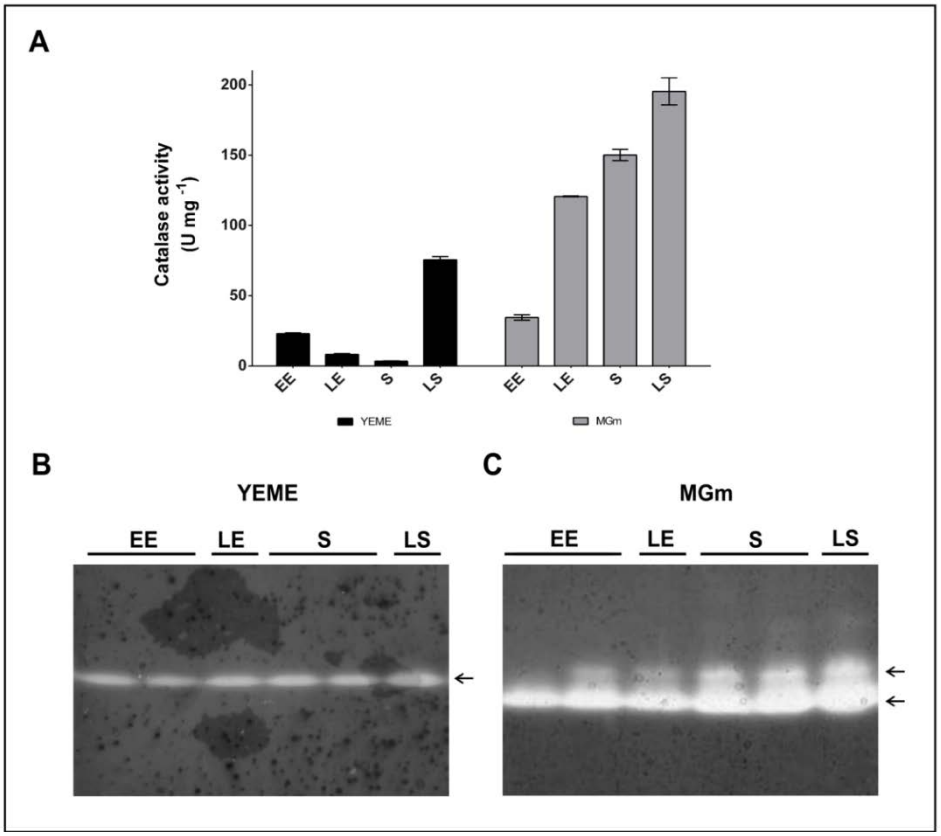

Figure 5.23 – *S. tsukubaensis* catalase activity profile in YEME and MGm medium. (A) Total catalase activity was measured spectrophotometrically. Results (average of triplicates and standard deviation) are representative of three independent experiments. Vertical bars indicate standard deviation of the mean values. (B) Native-PAGE stained for catalase activity with cell-free protein extracts from *S. tsukubaensis* cultures grown in YEME medium (50 μg of total protein per lane) and in MGm medium (1 μg of total protein per lane). Samples were collected throughout growth in the previously defined growth phases.

In accordance to the total catalase levels, H_2O_2 intracellular levels were significant higher in YEME medium than the ones observed for *S. tsukubaensis* cultures grown in MGm (Fig. 5.24).

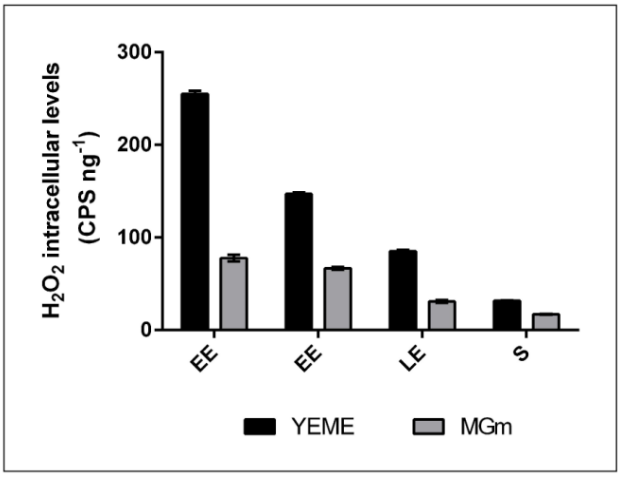

Figure 5.24 – ROS intracellular levels of *S. tsukubaensis* in YEME and MGm medium. DHR oxidation levels were used as a measure of H_2O_2 intracellular levels. Samples were collected from *S. tsukubaensis* cultures grown in YEME and MGm mediums, throughout growth curve in the previously defined growth phases. Vertical bars indicate standard deviation of the mean values. Results (average of triplicates and standard deviation) are representative of three independent experiments.

5.4 DISCUSSION

Functional characterization of *S. tsukubaensis* Δ*sodA* and [pIB*katA1*] strains reinforced the importance of catalase activity (and consequently of H_2O_2 intracellular levels) on tacrolimus biosynthesis in *S. tsukubaensis*. In both strains the increased total catalase activity levels were accompanied by an increase in tacrolimus production: 17 % in Δ*sodA* strain and 34% in [pIB*katA1*] strain, which was also in accordance with the increased transcription of genes from tacrolimus biosynthetic cluster presented by both strains.

Moreover, a 30-fold decrease in catalase activity, and conversely a higher intracellular H_2O_2 levels were observed, in tacrolimus non-production conditions, i.e., when *S. tsukubaensis* was grown in YEME medium. All these results stressed the importance of a very controlled redox homeostasis for tacrolimus production. In fact, [pIB*sodA*] strain constituted another evidence of the redox homeostasis requirement. Although this strain was able to increase catalase activity it was not enough to keep a balanced intracellular redox environment given the high H_2O_2 intracellular levels. One can assume that the oxidative stress present in [pIB*sodA*] had as consequence the absence of tacrolimus production and unlike what it was previously described for other *Streptomyces* strains, where the overexpression of

sodF and *sodN* led to an increase not only in life span but also in secondary metabolite production (Kanth *et al.* 2011), an opposite response was observed for *S. tsukubaensis* [pIB*sodA*].

Transcriptional analysis of Δ*sodA* showed that this mutant strain presented an activation of nitrogen metabolism related genes. *S. coelicolor* GlnR orthologue is described as an activator of *glnA* and *glnII* when in nitrogen limiting conditions. Considering the transcription profile presented by the mutant strain, one can assume that the same response is present in *S. tsukubaensis.* In nitrogen limiting conditions GlnR can also repress transcription of several genes, including *gdhA,* which is involved in the NADPH dependent conversion of 2-oxoglutarate in glutamate (Tiffert *et al.* 2008). Remarkably, deletion of *gdhA* in *S. tsukubaensis* led to a tacrolimus over-producing profile, probably due to an increase of the intracellular pool NADPH, a co-factor required for tacrolimus biosynthesis (Huang *et al.* 2013). Perhaps the presented Δ*sodA* over-producing profile could also be partially assigned to *glnR* repression of *gdhA*. Besides nitrogen metabolism, the PhoRP regulon activation was also anticipated in Δ*sodA*, indicating that Pi was exhausted earlier in the mutant strain. This earlier activation of the regulon could also be related with the onset of tacrolimus production since our over-producing strain Δ*ahpC* presented the same response; furthermore this regulon activation is intrinsically connected with *Streptomyces* secondary metabolism. Moreover, phosphate limitation has also been linked with increased oxidative stress, which can be the case for Δ*sodA* strain. In fact, it has been suggested that PhoU, a metalloprotein containing multinuclear iron clusters, could sense/respond to oxidative stress, given the high susceptibility to oxidative stress presented by the deletion of *phoU* in *S. lividans* (Liu *et al.* 2005, Darbon *et al.* 2012).

Interestingly, the up-regulation of tacrolimus biosynthesis in *S. tsukubaensis* Δ*sodA* strain was accompanied by an increase in ascomycin production suggesting that the ethylmalonyl-CoA unit is more available than in the wild-type strain. The biosynthesis of the allylmalonylCoA or ethylmalonyl-CoA precursor units represents the determining point between tacrolimus and ascomycin biosynthesis respectively. Further studies on this strain could unveil the molecular mechanisms governing the biosynthesis of these precursors in order to decrease the production of the by-product ascomycin in industrial strains.

Surprisingly, both transcriptional and native-PAGE analysis showed that deletion of *sodA* led to a decrease of *sodN* transcription and SodN activity, respectively, and that overexpression of *sodA* resulted in an increase of SodN activity. The functional characterization of SodA revealed an interesting regulatory cross-talk between *sodA* and *sodN*. In 2009, an *in silico* study performed on *Streptomyces* NiSODs showed that not only all *Streptomyces* NiSOD encoding genes presented the proteolytic cleavage site required for SOD activation, but also, while analysing the surrounding regions, it was found a conserved motif of 19 nucleotides (nt) length in all *Streptomyces* genomes (TGAGAAGACGATCACGAGG), located at the transcription start site (–1) of all *sodN* genes. The same exact sequence can be found, in inverse orientation, downstream of all known *sodF* genes with a distance of 14 to 25 nucleotides to the translational stop codon. This study showed that this sequence was present in all messengers encoding superoxide dismutases regardless of their prosthetic group, i.e, nickel or iron. Given this findings it was raised the possibility that these elements could function as translational regulatory elements since they were present within the transcription product (Schmidt *et al.* 2009). While analysing the promoter region of *S. tsukubaensis sodA* and *sodN* the 19 nt motif was found, however, a mutation on the first nucleotide is present in *sodA* (Fig. 5.25).

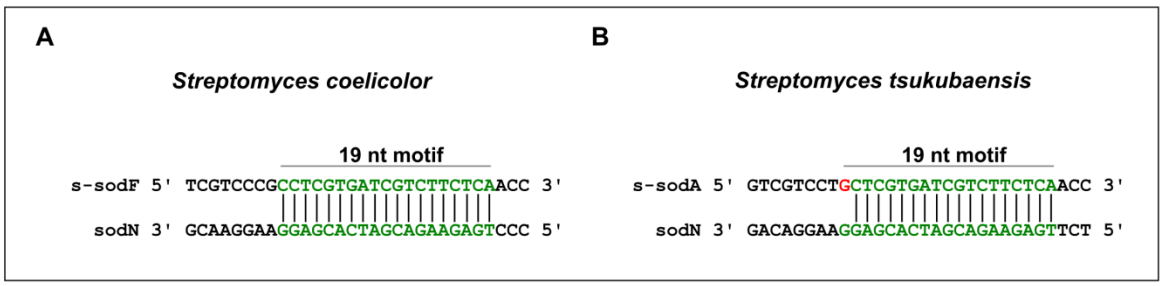

Figure 5.25 – Sequence information of *S. coelicolor* and *S. tsukubaensis* superoxide dismutases encoding genes surrounding region. (A) Sequence information of *S. coelicolor* s-sodF and *sodN* region containing the 19 nt conserved motif (marked in green). (B) Sequence information of *S. tsukubaensis sodA* and *sodN* region containing the 19 nt conserved motif (marked in green). The point mutation present in *S. tsukubaensis sodA* is marked in red.

A recent work performed in *S. coelicolor* confirmed that this region presents a regulatory role with a small regulatory RNA of about 90 nt being produced from *sodF* mRNA 3' UTR (s-sodF), matching exactly the 5' UTR of *sodN* mRNA. Pairing of s-sodF with this region, blocks its translation and decreases *sodN* mRNA half-

life (Kim *et al.* 2014). Moreover, it was demonstrated a sequence-specificity of the 19 nt motif. By generating point mutations in some of these 19 nucleotides a decrease in binding and consequently an increase in *sodN* mRNA half-life occurred, thus alleviating the antagonistic regulatory effect (Kim *et al.* 2014). The antagonist regulation between *sodF* and *sodN* described for *S. coelicolor* is not observed in *S. tsukubaensis.* In fact, our results point to an opposite behaviour, with *sodA* displaying a positive effect in *sodN* transcription. The naturally occurring mutation present in *S. tsukubaensis* anti-*sodN* sequence of *sodF* (Fig. 2. 25) is also present in *S. coelicolor sodF2*, *S. avermitilis sodF*, *S. bingchenggensis sodF* and *sodF2*, *S. scabiei sodF* and *S. venezuelae sodF.* In the future, it would be interesting to understand if a different regulatory mechanism is present in these *Streptomyces* strains and to determine whether this point mutation could be playing a role in the observed change on regulation in *S. tsukubaensis*

.

CHAPTER 6

General Discussion and future perspectives

6.1 GENERAL DISCUSSION AND FUTURE PERSPECTIVES

One of the most notable features of *Streptomyces* bacteria, and the reason they have great industrial interest, is their ability to produce a wide range of valuable specialized metabolites (Hopwood 2007). *Streptomyces* secondary metabolism is under the regulation of a plethora of signals and factors that interplay with each other to have as an outcome the production of specialized metabolites. The onset of production is commonly associated with different stresses, which is understandable, since they are considered to function in their natural environment as a way to provide bacteria an advantage and/or improvement of cell fitness and survival. Among those factors and stresses that influences secondary metabolism one can find oxygen and oxidative stress (Singh and Behera 2009, Wei *et al.* 2011). Oxygen is a key factor on *Streptomyces* physiology as well as in the fermentation processes, so in order to have a rational-based approach to increase production yields we believe to be important to unveil the molecular mechanisms related with oxidative-stress response and redox homeostasis regulation.

S. natalensis work provided us strong evidences that the oxidative stress response/regulation is tightly connected with secondary metabolism. We have shown that H_2O_2 intracellular levels modulated pimaricin production, i.e., generation of *S. natalensis* mutant strains defective on antioxidant related encoding genes and that presented increased levels of intracellular H_2O_2 had a pimaricin overproduction profile when compared to the wild-type (Beites *et al.* 2011). This effect of the oxidative stress response on pimaricin biosynthesis in *S. natalensis* led us to question whether the modulation effect observed in *S. natalensis* knock-out mutants was a general effect of *Streptomyces* secondary metabolism or a strain- or even metabolite-specific phenomena. The opportunity to work with *S. tsukubaensis* allowed us to study the interplay between oxidative stress response and secondary metabolism in another *Streptomyces* strain.

Similar to *S. natalensis*, a growth-dependent catalase activity profile that temporally overlapped with the production of the secondary metabolite was observed for *S. tsukubaensis*. However, contrary to *S. natalensis* where an inhibition of catalase activity was observed during the production of pimaricin, in *S. tsukubaensis* we observed a perfect overlap of catalase induction, and the

concomitant decrease of H_2O_2 intracellular levels, with the onset of tacrolimus production. Throughout this work, the link between catalase activity and tacrolimus production became evident. Several results suggested that catalase activity above a certain threshold is needed for the production of tacrolimus. In tacrolimus non-producing medium (YEME), catalase activity levels were much lower than in MGm medium and by native-PAGE analysis we were able to observe that only one monofunctional catalase was being activated. As a consequence, H_2O_2 intracellular levels were higher when compared to the ones presented in MGm, i.e., tacrolimus producing conditions. Conversely, in producing conditions the two monofunctional catalases were induced, total catalase activity levels were higher and H_2O_2 intracellular levels were kept low during tacrolimus production. Moreover, strains and/or conditions that displayed/led to higher catalase activity levels presented a tacrolimus overproducing phenotype. That was the case for the *S. tsukubaensis* [pIB*katA1*] strain, overexpressing the monofunctional catalase KatA1, the *S. tsukubaensis* ∆*ahpC* strain or the wild-type strains through the increase of DO levels or by the addition of H_2O_2 to the culture broth. Due to its enzymatic activity, catalase activity is inversely correlated with the H_2O_2 intracellular levels. However, in both *S: tsukubaensis* Δ*sigG* and [pIB*sodA*] strains catalase activity induction was not sufficient to efficiently decrease H_2O_2 intracellular levels, especially in the case of [pIB*sodA*] strain. In fact, these strains that presented throughout growth higher H_2O_2 intracellular levels also presented a down-regulated tacrolimus production: Δ*sigG* strain presented a delay in the onset of tacrolimus production and [pIB*sodA*] strain presented total abolishment of production. Noteworthy that these strains were very sensitivity towards H_2O_2 induced stress.

Excitingly, tacrolimus presented antioxidant properties and our results suggest that it can be oxidized by H_2O_2. This, together with the induction of catalase activity as well as the need to maintain low H_2O_2 intracellular levels during tacrolimus production, indicated that a reduced environment is required to produce tacrolimus. The study of the oxidative stress response in *S. natalensis* and *S. tsukubaensis* and its correlation with the production of secondary metabolites indicates that each strain adapts its oxidative response in face of the requirements for the production of each metabolite. In the case of pimaricin, a

macrolide with antifungal properties, H_2O_2 that is generated as a by-product of pimaricin action, also functions as an elicitor on pimaricin production in *S. natalensis* (Mendes *et al.* 2007, Beites *et al.* 2011). As for tacrolimus, and given its antioxidant properties and degradation by H_2O_2, catalase is induced during its production in order to maintain low H_2O_2 intracellular levels. Perhaps the antioxidant role of tacrolimus could be related with its biological role in their natural habitat. Moreover, its biosynthesis induction seems to be a response to stress, which they face on a daily basis in the soil.

S. tsukubaensis Δ*ahpC* strain presented an increased resistance to H_2O_2 that could be partially explained by the induction of catalase, but also by the fact that this strain is a tacrolimus over-producing strain, which can contribute to increase resistance due to its antioxidant properties. However, the increased H_2O_2 intracellular levels displayed by this strain at 72 h and 96 h suggest that the induction of catalase activity was not enough to decrease H_2O_2 intracellular levels, pointing out to an important role of AhpC in H_2O_2 detoxification during exponential phase. However, proteomic results demonstrated that *ahpC* deletion led to a fine tuned redirection of the primary metabolism towards tacrolimus production indicating that AhpC could have other roles inside the cells. A role for AhpC in iron metabolism has been suggested in *E. coli*, more specifically in re-routing chorismate towards the biosynthesis of the siderophore enterobactin (Ma and Payne 2012). Since Δ*ahpC* strain presented a 40% increase in production and that strain characterization results suggested a very effective redirection of precursors, including chorismate, towards tacrolimus production, perhaps AhpC could also be involved in chorismate pool and/or siderophore biosynthesis. Furthermore, an OxyR-independent *ahpC* transcription is also present in *S. tsukubaensis*. Since a Crp binding motif was found in *ahpC* promoter region and it has been shown that Crp is a major regulator in *Streptomyces*, which influences secondary metabolism including siderophore biosynthesis (Gao *et al.* 2012), it would be interesting to assess if another metabolic role could be ascribed to AhpC and if *ahpC* transcription is under the control of the global regulator Crp.

During evolution, genes can be rearranged, gained, lost and duplicated however, evolutionary analysis between close and related species demonstrate that genomic synteny is extremely stable. In fact when analyzing the *oxyR-ahpCD*

genomic region in more than 70 *Streptomyces* strains, one could only found 9 exceptions to the common organization, which raises the question to why is this genomic region different in *S. tsukubaensis*: more specifically what could be the biological role of *S. tsukubaensis oxyR* genomic re-organization. Curiously, in this novel and unique organization a novel ECF sigma factor is present. ECF sigma factors are a common mode of adaptation to different stresses in bacteria (Helmann 2002), and in the case of *S. tsukubaensis,* SigG seems to be regulating iron metabolism, more specifically ferrous iron uptake. In order to understand how SigG achieves this iron metabolism modulation and which are its cognate targets a thorough study will have to be pursued in the future.

OxyR in several bacteria not only regulates the oxidative stress response but also iron metabolism, commonly via the regulation of Fur regulator (Zheng *et al.* 1999). However, in *S. tsukubaensis* iron regulation is under SigG control and even though there is a cross-talk between SigG and OxyR, *S. tsukubaensis* physically separated iron uptake and oxidative stress response regulation in two distinct regulators. Putting our results in perspective this “division” in regulation is quite attention-grabbing given oxidative stress regulation and iron metabolism crucial role on tacrolimus biosynthesis. Iron role on tacrolimus production was well patent in Δ*sigG* strain. The hampered ferrous iron uptake had as a consequence a delay in tacrolimus production. In fact Δ*sigG* strain begins to actively produced tacrolimus when both H_2O_2 intracellular levels and iron extracellular levels decrease. Additionally, this connection was also clearly shown when the wild-type strain was grown in MGm medium without iron supplementation and the same delay in tacrolimus production was observed. Furthermore, one can assume that Δ*sodA* strain tacrolimus overproducing profile can also be related with the strain predicted increased iron intracellular availability, given the increased intracellular levels of the superoxide anion, known to attack iron-sulfur clusters. Fascinatingly, our preliminary results showed that transcription of genes from the putative siderophore cluster downstream of tacrolimus biosynthetic cluster were increased in our overproducing strain, Δ*ahpC*, however with no concomitant production of siderophores (at least not detectable with CAS assay). Study of the putative siderophore role on tacrolimus production could be a good strategy to understand iron role on tacrolimus production.

One also have to point out that both OxyR and iron metabolism are intrinsically related with bacterial pathogenicity (Lau *et al.* 2005, Flores-Cruz and Allen 2011), so it would be interesting to understand if the OxyR point mutation found in *S. tsukubaensis* as well as in other *Streptomyces* strains whose pathogenicity has been described, could have a role in pathogenicity and if this novel ECF sigma factor SigG could also be involved through the regulation of iron uptake.

6.2 ACHIEVEMENTS OF THIS WORK

Specific ones: Through characterization of *S. tsukubaensis* oxidative stress response, we identified that both catalase activity and H_2O_2 intracellular levels are crucial for tacrolimus production. Moreover, with the deletion of *ahpC* we were also able to obtain a robust strain that not only presents a fine-tuned metabolic redirection of precursors towards tacrolimus production, but is also more resistant to stress, constituting a good strain to be used in future scale-up fermentation processes. Additionally, a novel ECF sigma factor, SigG, was also discovered and in our opinion, represents a good model to study iron metabolism in *Streptomyces.*

Broader ones: With this work it was demonstrated a regulatory interplay between intracellular redox status/ROS homeostasis and the onset/biosynthesis of specialized metabolites in *Streptomyces*. However, different strains presented different responses to oxidative stress, which seemed to be metabolite specific and perhaps dependent on the specialized metabolite biological role on the producing strain natural habitat. This rational-based approach could be applied to other *Streptomyces* strains in order to increase production yields.

REFERENCES

Abreu, I. A. and D. E. Cabelli (2010). "Superoxide dismutases-a review of the metal-associated mechanistic variations." Biochim Biophys Acta **1804**(2): 263-274.

Aharonowitz, Y. (1980). "Nitrogen metabolite regulation of antibiotic biosynthesis." Annu Rev Microbiol **34**: 209-233.

Ahn, B.-E., J. Cha, E.-J. Lee, A.-R. Han, C. J. Thompson and J.-H. Roe (2006). "Nur, a nickel-responsive regulator of the Fur family, regulates superoxide dismutases and nickel transport in Streptomyces coelicolor." Molecular Microbiology **59**(6): 1848-1858.

Akimoto, K., Y. Kusunoki, S. Nishio, K. Takagi and S. Kawai (2008). "Safety profile of tacrolimus in patients with rheumatoid arthritis." Clin Rheumatol **27**(11): 1393-1397.

Allenby, N. E., E. Laing, G. Bucca, A. M. Kierzek and C. P. Smith (2012). "Diverse control of metabolism and other cellular processes in Streptomyces coelicolor by the PhoP transcription factor: genome-wide identification of in vivo targets." Nucleic Acids Res **40**(19): 9543-9556.

Almiron, M., A. J. Link, D. Furlong and R. Kolter (1992). "A novel DNA-binding protein with regulatory and protective roles in starved Escherichia coli." Genes Dev **6**(12B): 2646-2654.

Altuvia, S., M. Almiron, G. Huisman, R. Kolter and G. Storz (1994). "The dps promoter is activated by OxyR during growth and by IHF and sigma S in stationary phase." Mol Microbiol **13**(2): 265-272.

An, Y. J., B. E. Ahn, A. R. Han, H. M. Kim, K. M. Chung, J. H. Shin, Y. B. Cho, J. H. Roe and S. S. Cha (2009). "Structural basis for the specialization of Nur, a nickel-specific Fur homolog, in metal sensing and DNA recognition." Nucleic Acids Res **37**(10): 3442-3451.

Andexer, J. N., S. G. Kendrew, M. Nur-e-Alam, O. Lazos, T. A. Foster, A. S. Zimmermann, T. D. Warneck, D. Suthar, N. J. Coates, F. E. Koehn, J. S. Skotnicki, G. T. Carter, M. A. Gregory, C. J. Martin, S. J. Moss, P. F. Leadlay and B. Wilkinson (2011). "Biosynthesis of the immunosuppressants FK506, FK520, and rapamycin involves a previously undescribed family of enzymes acting on chorismate." Proc Natl Acad Sci U S A **108**(12): 4776-4781.

Andrews, S. C., A. K. Robinson and F. Rodriguez-Quinones (2003). "Bacterial iron homeostasis." FEMS Microbiol Rev **27**(2-3): 215-237.

Anjem, A. and J. A. Imlay (2012). "Mononuclear iron enzymes are primary targets of hydrogen peroxide stress." J Biol Chem **287**(19): 15544-15556.

Aparicio, J. F., A. J. Colina, E. Ceballos and J. F. Martin (1999). "The biosynthetic gene cluster for the 26-membered ring polyene macrolide pimaricin. A new polyketide synthase organization encoded by two subclusters separated by functionalization genes." J Biol Chem **274**(15): 10133-10139.

Aparicio, J. F., R. Fouces, M. V. Mendes, N. Olivera and J. F. Martin (2000). "A complex multienzyme system encoded by five polyketide synthase genes is involved in the biosynthesis of the 26-membered polyene macrolide pimaricin in *Streptomyces natalensis*." Chem Biol **7**(11): 895-905.

Aparicio, J. F., M. V. Mendes, N. Antón and J. F. Martin (2002). Biosynthetic rules for macrolide construction. Microbial secondary metabolites: biosynthesis, genetics and regulation. F. Fierro and J. F. Martin. Kerala, Research Signpost**:** 85-98.

Asad, L. M., N. R. Asad, A. B. Silva, C. E. de Almeida and A. C. Leitao (1997). "Role of SOS and OxyR systems in the repair of Escherichia coli submitted to hydrogen peroxide under low iron conditions." Biochimie **79**(6): 359-364.

Aslund, F., M. Zheng, J. Beckwith and G. Storz (1999). "Regulation of the OxyR transcription factor by hydrogen peroxide and the cellular thiol-disulfide status." Proc Natl Acad Sci U S A **96**(11): 6161-6165.

Bagg, A. and J. B. Neilands (1987). "Molecular mechanism of regulation of siderophore-mediated iron assimilation." Microbiol Rev **51**(4): 509-518.

Bailey, T. L., M. Boden, F. A. Buske, M. Frith, C. E. Grant, L. Clementi, J. Ren, W. W. Li and W. S. Noble (2009). "MEME SUITE: tools for motif discovery and searching." Nucleic Acids Res **37**(Web Server issue): W202-208.

Barondeau, D. P., C. J. Kassmann, C. K. Bruns, J. A. Tainer and E. D. Getzoff (2004). "Nickel superoxide dismutase structure and mechanism." Biochemistry **43**(25): 8038-8047.

Barreiro, C. and M. Martinez-Castro (2014). "Trends in the biosynthesis and production of the immunosuppressant tacrolimus (FK506)." Appl Microbiol Biotechnol **98**(2): 497-507.

Barreiro, C., C. Prieto, A. Sola-Landa, E. Solera, M. Martinez-Castro, R. Perez-Redondo, C. Garcia-Estrada, J. F. Aparicio, L. T. Fernandez-Martinez, J. Santos-Aberturas, Z. Salehi-Najafabadi, A. Rodriguez-Garcia, A. Tauch and J. F. Martin (2012). "Draft genome of Streptomyces tsukubaensis NRRL 18488, the producer of the clinically important immunosuppressant tacrolimus (FK506)." J Bacteriol **194**(14): 3756-3757.

Barry, S. M. and G. L. Challis (2009). "Recent advances in siderophore biosynthesis." Curr Opin Chem Biol **13**(2): 205-215.

Beauchamp, C. and I. Fridovich (1971). "Superoxide dismutase: improved assays and an assay applicable to acrylamide gels." Anal Biochem **44**(1): 276-287.

Becker-Hapak, M., E. Troxtel, J. Hoerter and A. Eisenstark (1997). "RpoS dependent overexpression of carotenoids from Erwinia herbicola in OXYR deficient Escherichia coli." Biochem Biophys Res Commun **239**(1): 305-309.

Beers, R. F., Jr. and I. W. Sizer (1952). "A spectrophotometric method for measuring the breakdown of hydrogen peroxide by catalase." J Biol Chem **195**(1): 133-140.

Beites, T., S. D. Pires, C. L. Santos, H. Osorio, P. Moradas-Ferreira and M. V. Mendes (2011). "Crosstalk between ROS homeostasis and secondary metabolism in S. natalensis ATCC 27448: modulation of pimaricin production by intracellular ROS." PloS one **6**(11): e27472.

Beites, T., A. Rodriguez-Garcia, F. Santos-Beneit, P. Moradas-Ferreira, J. F. Aparicio and M. V. Mendes (2014). "Genome-wide analysis of the regulation of pimaricin production in Streptomyces natalensis by reactive oxygen species." Appl Microbiol Biotechnol **98**(5): 2231-2241.

Benov, L. and I. Fridovich (1999). "Why superoxide imposes an aromatic amino acid auxotrophy on Escherichia coli. The transketolase connection." J Biol Chem **274**(7): 4202-4206.

Benson, A., T. Barrett, M. Sparberg and A. L. Buchman (2008). "Efficacy and safety of tacrolimus in refractory ulcerative colitis and Crohn's disease: a single-center experience." Inflamm Bowel Dis **14**(1): 7-12.

Bentley, S. D., K. F. Chater, A. M. Cerdeno-Tarraga, G. L. Challis, N. R. Thomson, K. D. James, D. E. Harris, M. A. Quail, H. Kieser, D. Harper, A. Bateman, S. Brown, G. Chandra, C. W. Chen, M. Collins, A. Cronin, A. Fraser, A. Goble, J. Hidalgo, T. Hornsby, S. Howarth, C. H. Huang, T. Kieser, L. Larke, L. Murphy, K. Oliver, S. O'Neil, E. Rabbinowitsch, M. A. Rajandream, K. Rutherford, S. Rutter, K. Seeger, D. Saunders, S. Sharp, R. Squares, S. Squares, K. Taylor, T. Warren, A. Wietzorrek, J. Woodward, B. G. Barrell, J. Parkhill and D. A. Hopwood (2002). "Complete genome sequence of the model actinomycete Streptomyces coelicolor A3(2)." Nature **417**(6885): 141-147.

Bibb, M. J. (2005). "Regulation of secondary metabolism in streptomycetes." Current Opinion in Microbiology **8**: 208 - 215.

Bibb, M. J., G. R. Janssen and J. M. Ward (1985). "Cloning and analysis of the promoter region of the erythromycin resistance gene (ermE) of Streptomyces erythraeus." Gene **38**(1-3): 215-226.

Bierman, M., R. Logan, K. O'Brien, E. T. Seno, R. N. Rao and B. E. Schoner (1992). "Plasmid cloning vectors for the conjugal transfer of DNA from *Escherichia coli* to *Streptomyces* spp." Gene **116**: 43-49.

Borodina, I., J. Siebring, J. Zhang, C. P. Smith, G. van Keulen, L. Dijkhuizen and J. Nielsen (2008). "Antibiotic overproduction in *Streptomyces coelicolor* A3(2) mediated by phosphofructokinase deletion." J Biol Chem **283**(37): 25186-25199.

Bourn, W. R. and B. Babb (1995). "Computer assisted identification and classification of streptomycete promoters." Nucleic Acids Res **23**(18): 3696-3703.

Breuder, T., C. S. Hemenway, N. R. Movva, M. E. Cardenas and J. Heitman (1994). "Calcineurin is essential in cyclosporin A- and FK506-sensitive yeast strains." Proc Natl Acad Sci U S A **91**(12): 5372-5376.

Bsat, N., A. Herbig, L. Casillas-Martinez, P. Setlow and J. D. Helmann (1998). "Bacillus subtilis contains multiple Fur homologues: identification of the iron uptake (Fur) and peroxide regulon (PerR) repressors." Mol Microbiol **29**(1): 189-198.

Burg, R. W., B. M. Miller, E. E. Baker, J. Birnbaum, S. A. Currie, R. Hartman, Y. L. Kong, R. L. Monaghan, G. Olson, I. Putter, J. B. Tunac, H. Wallick, E. O. Stapley, R. Oiwa and S. Omura (1979). "Avermectins, new family of potent anthelmintic agents: producing organism and fermentation." Antimicrob Agents Chemother **15**(3): 361-367.

Calugay, R. J., H. Miyashita, Y. Okamura and T. Matsunaga (2003). "Siderophore production by the magnetic bacterium Magnetospirillum magneticum AMB-1." FEMS Microbiol Lett **218**(2): 371-375.

Chakraburtty, R. and M. Bibb (1997). "The ppGpp synthetase gene (relA) of Streptomyces coelicolor A3(2) plays a conditional role in antibiotic production and morphological differentiation." J Bacteriol **179**(18): 5854-5861.

Chary, P. and D. O. Natvig (1989). "Evidence for three differentially regulated catalase genes in Neurospora crassa: effects of oxidative stress, heat shock, and development." J Bacteriol **171**(5): 2646-2652.

Chater, K. F. (1993). "Genetics of differentiation in Streptomyces." Annu Rev Microbiol **47**: 685-713.

Chater, K. F. and G. Chandra (2006). "The evolution of development in Streptomyces analysed by genome comparisons." FEMS microbiology reviews **30**(5): 651-672.

Chater, K. F., D. A. Hopwood, T. Kieser and C. J. Thompson (1982). "Gene cloning in Streptomyces." Curr Top Microbiol Immunol **96**: 69-95.

Chelikani, P., I. Fita and P. C. Loewen (2004). "Diversity of structures and properties among catalases." Cellular and Molecular Life Sciences (CMLS) **61**(2): 192-208.

Chen, D., L. Zhang, B. Pang, J. Chen, Z. Xu, I. Abe and W. Liu (2013). "FK506 maturation involves a cytochrome p450 protein-catalyzed four-electron C-9 oxidation in parallel with a C-31 O-methylation." J Bacteriol **195**(9): 1931-1939.

Cheng, Y. R., L. Hauck and A. L. Demain (1995). "Phosphate, ammonium, magnesium and iron nutrition of Streptomyces hygroscopicus with respect to rapamycin biosynthesis." J Ind Microbiol **14**(5): 424-427.

Chiang, S. M. and H. E. Schellhorn (2012). "Regulators of oxidative stress response genes in *Escherichia coli* and their functional conservation in bacteria." Arch Biochem Biophys **525**(2): 161-169.

Cho, Y. H. and J. H. Roe (1997). "Isolation and expression of the catA gene encoding the major vegetative catalase in *Streptomyces coelicolor* Muller." J Bacteriol **179**(12): 4049-4052.

Cho, Y.-H., E.-J. Lee, B.-E. Ahn and J.-H. Roe (2001). "SigB, an RNA polymerase sigma factor required for osmoprotection and proper differentiation of Streptomyces coelicolor." Molecular Microbiology **42**(1): 205-214.

Cho, Y.-H., E.-J. Lee and J.-H. Roe (2000). "A developmentally regulated catalase required for proper differentiation and osmoprotection of Streptomyces coelicolor." Molecular Microbiology **35**(1): 150-160.

Chung, H. J., J. H. Choi, E. J. Kim, Y. H. Cho and J. H. Roe (1999). "Negative regulation of the gene for Fe-containing superoxide dismutase by an Ni-responsive factor in Streptomyces coelicolor." J Bacteriol **181**(23): 7381-7384.

Chung, H. J., E. J. Kim, B. Suh, J. H. Choi and J. H. Roe (1999). "Duplicate genes for Fe-containing superoxide dismutase in Streptomyces coelicolor A3(2)." Gene **231**(1-2): 87-93.

Claessen, D., W. de Jong, L. Dijkhuizen and H. A. Wosten (2006). "Regulation of Streptomyces development: reach for the sky!" Trends Microbiol **14**(7): 313-319.

Clare, D. A., M. N. Duong, D. Darr, F. Archibald and I. Fridovich (1984). "Effects of molecular oxygen on detection of superoxide radical with nitroblue tetrazolium and on activity stains for catalase." Anal Biochem **140**(2): 532-537.

Cohen, G., M. Yanko, M. Mislovati, A. Argaman, R. Schreiber, Y. Av-Gay and Y. Aharonowitz (1993). "Thioredoxin-thioredoxin reductase system of Streptomyces clavuligerus: sequences, expression, and organization of the genes." J Bacteriol **175**(16): 5159-5167.

Combes, P., R. Till, S. Bee and M. C. Smith (2002). "The streptomyces genome contains multiple pseudo-attB sites for the (phi)C31-encoded site-specific recombination system." J Bacteriol **184**(20): 5746-5752.

Cornelis, P., Q. Wei, S. C. Andrews and T. Vinckx (2011). "Iron homeostasis and management of oxidative stress response in bacteria." Metallomics : integrated biometal science **3**(6): 540-549.

Cornelissen, C. N. (2008). "Identification and characterization of gonococcal iron transport systems as potential vaccine antigens." Future Microbiol **3**(3): 287-298.

da Silva Neto, J. F., V. S. Braz, V. C. Italiani and M. V. Marques (2009). "Fur controls iron homeostasis and oxidative stress defense in the oligotrophic alpha-proteobacterium Caulobacter crescentus." Nucleic Acids Res **37**(14): 4812-4825.

Dastoor, Z. and J. L. Dreyer (2001). "Potential role of nuclear translocation of glyceraldehyde-3-phosphate dehydrogenase in apoptosis and oxidative stress." J Cell Sci **114**(Pt 9): 1643-1653.

Datsenko, K. A. and B. L. Wanner (2000). "One-step inactivation of chromosomal genes in Escherichia coli K-12 using PCR products." Proc Natl Acad Sci U S A **97**(12): 6640-6645.

Demain, A. L. (1999). "Pharmaceutically active secondary metabolites of microorganisms." Appl Microbiol Biotechnol **52**(4): 455-463.

Deretic, V., J. Song and E. Pagan-Ramos (1997). "Loss of oxyR in Mycobacterium tuberculosis." Trends Microbiol **5**(9): 367-372.

DeRocco, A. J., M. K. Yost-Daljev, C. D. Kenney and C. N. Cornelissen (2009). "Kinetic analysis of ligand interaction with the gonococcal transferrin-iron acquisition system." Biometals **22**(3): 439-451.

Dhandayuthapani, S., M. Mudd and V. Deretic (1997). "Interactions of OxyR with the promoter region of the oxyR and ahpC genes from Mycobacterium leprae and Mycobacterium tuberculosis." J Bacteriol **179**(7): 2401-2409.

Dick, O., U. Onken, I. Sattler and A. Zeeck (1994). "Influence of increased dissolved oxygen concentration on productivity and selectivity in cultures of a colabomycin-producing strain of Streptomyces griseoflavus." Appl Microbiol Biotechnol **41**(4): 373-377.

Doull, J. L. and L. C. Vining (1989). "Culture conditions promoting dispersed growth and biphasic production of actinorhodin in shaken cultures of Streptomyces coelicolor A3(2)." FEMS microbiology letters **53**(3): 265-268.

Dussurget, O., M. Rodriguez and I. Smith (1996). "An ideR mutant of Mycobacterium smegmatis has derepressed siderophore production and an altered oxidative-stress response." Mol Microbiol **22**(3): 535-544.

Escolar, L., J. Perez-Martin and V. de Lorenzo (1999). "Opening the iron box: transcriptional metalloregulation by the Fur protein." J Bacteriol **181**(20): 6223-6229.

Facey, P. D., M. D. Hitchings, P. Saavedra-Garcia, L. Fernandez-Martinez, P. J. Dyson and R. Del Sol (2009). "Streptomyces coelicolor Dps-like proteins: differential dual roles in response to stress during vegetative growth and in nucleoid condensation during reproductive cell division." Mol Microbiol **73**(6): 1186-1202.

Faulkner, M. J. and J. D. Helmann (2011). "Peroxide stress elicits adaptive changes in bacterial metal ion homeostasis." Antioxid Redox Signal **15**(1): 175-189.

Feng, W. H., X. M. Mao, Z. H. Liu and Y. Q. Li (2011). "The ECF sigma factor SigT regulates actinorhodin production in response to nitrogen stress in Streptomyces coelicolor." Appl Microbiol Biotechnol **92**(5): 1009-1021.

Flardh, K. and M. J. Buttner (2009). "Streptomyces morphogenetics: dissecting differentiation in a filamentous bacterium." Nat Rev Microbiol **7**(1): 36-49.

Flores, F. J., C. Barreiro, J. J. Coque and J. F. Martin (2005). "Functional analysis of two divalent metal-dependent regulatory genes dmdR1 and dmdR2 in Streptomyces coelicolor and proteome changes in deletion mutants." Febs J **272**(3): 725-735.

Flores-Cruz, Z. and C. Allen (2011). "Necessity of OxyR for the hydrogen peroxide stress response and full virulence in Ralstonia solanacearum." Appl Environ Microbiol **77**(18): 6426-6432.

Fujii, T., H. C. Gramajo, E. Takano and M. J. Bibb (1996). "redD and actII-ORF4, pathway-specific regulatory genes for antibiotic production in Streptomyces coelicolor A3(2), are transcribed in vitro by an RNA polymerase holoenzyme containing sigma hrdD." J Bacteriol **178**(11): 3402-3405.

Gaballa, A. and J. D. Helmann (1998). "Identification of a zinc-specific metalloregulatory protein, Zur, controlling zinc transport operons in Bacillus subtilis." J Bacteriol **180**(22): 5815-5821.

Gao, C., Hindra, D. Mulder, C. Yin and M. A. Elliot (2012). "Crp is a global regulator of antibiotic production in streptomyces." MBio **3**(6): e00407-00412.

Garrity, G. M., B. K. Heimbuch, H. Motamedi and A. Shafiee (1993). "Genetic relationships among actinomycetes that produce the immunosuppressant macrolides FK506, FK520/FK523 and rapamycin." J Ind Microbiol **12**(1): 42-47.

Gaudion, A., L. Dawson, E. Davis and K. Smollett (2013). "Characterisation of the Mycobacterium tuberculosis alternative sigma factor SigG: its operon and regulon." Tuberculosis (Edinb) **93**(5): 482-491.

Gerber, N. N. (1979). "Volatile substances from actinomycetes: their role in the odor pollution of water." CRC Crit Rev Microbiol **7**(3): 191-214.

Gil, J. A., G. Naharro, J. R. Villanueva and J. F. Martin (1985). "Characterization and regulation of p-aminobenzoic acid synthase from Streptomyces griseus." J Gen Microbiol **131 (Pt 6)**: 1279-1287.

Godon, C., G. Lagniel, J. Lee, J. M. Buhler, S. Kieffer, M. Perrot, H. Boucherie, M. B. Toledano and J. Labarre (1998). "The H2O2 stimulon in Saccharomyces cerevisiae." J Biol Chem **273**(35): 22480-22489.

Gonzalez-Flecha, B. and B. Demple (1997). "Homeostatic regulation of intracellular hydrogen peroxide concentration in aerobically growing Escherichia coli." J Bacteriol **179**(2): 382-388.

Gonzalez-Flecha, B. and B. Demple (1997). "Transcriptional regulation of the Escherichia coli oxyR gene as a function of cell growth." J Bacteriol **179**(19): 6181-6186.

Goranovic, D., M. Blazic, V. Magdevska, J. Horvat, E. Kuscer, T. Polak, J. Santos-Aberturas, M. Martinez-Castro, C. Barreiro, P. Mrak, G. Kopitar, G. Kosec, S. Fujs, J. F. Martin and H. Petkovic (2012). "FK506 biosynthesis is regulated by two positive regulatory elements in Streptomyces tsukubaensis." BMC microbiology **12**: 238.

Goranovic, D., G. Kosec, P. Mrak, S. Fujs, J. Horvat, E. Kuscer, G. Kopitar and H. Petkovic (2010). "Origin of the allyl group in FK506 biosynthesis." J Biol Chem **285**(19): 14292-14300.

Gort, A. S. and J. A. Imlay (1998). "Balance between endogenous superoxide stress and antioxidant defenses." Journal of Bacteriology **180**(6): 1402-1410.

Gu, M. and J. A. Imlay (2011). "The SoxRS response of Escherichia coli is directly activated by redox-cycling drugs rather than by superoxide." Mol Microbiol **79**(5): 1136-1150.

Guo, X., J. F. Dillman, 3rd, V. L. Dawson and T. M. Dawson (2001). "Neuroimmunophilins: novel neuroprotective and neuroregenerative targets." Ann Neurol **50**(1): 6-16.

Gust, B., G. L. Challis, K. Fowler, T. Kieser and K. F. Chater (2003). "PCR-targeted Streptomyces gene replacement identifies a protein domain needed for biosynthesis of the sesquiterpene soil odor geosmin." Proc Natl Acad Sci U S A **100**(4): 1541-1546.

Haagmans, W. and M. van der Woude (2000). "Phase variation of Ag43 in Escherichia coli: Dam-dependent methylation abrogates OxyR binding and OxyR-mediated repression of transcription." Mol Microbiol **35**(4): 877-887.

Hahn, J. S., S. Y. Oh, K. F. Chater, Y. H. Cho and J. H. Roe (2000). "H_2O_2-sensitive fur-like repressor CatR regulating the major catalase gene in *Streptomyces coelicolor*." J Biol Chem **275**(49): 38254-38260.

Hahn, J. S., S. Y. Oh and J. H. Roe (2000). "Regulation of the furA and catC operon, encoding a ferric uptake regulator homologue and catalase-peroxidase, respectively, in Streptomyces coelicolor A3(2)." J Bacteriol **182**(13): 3767-3774.

Hahn, J. S., S. Y. Oh and J. H. Roe (2002). "Role of OxyR as a peroxide-sensing positive regulator in *Streptomyces coelicolor* A3(2)." J Bacteriol **184**(19): 5214-5222.

Hakenbeck, R. and J. B. Stock (1996). "Analysis of two-component signal transduction systems involved in transcriptional regulation." Methods Enzymol **273**: 281-300.

Hall, A., P. A. Karplus and L. B. Poole (2009). "Typical 2-Cys peroxiredoxins--structures, mechanisms and functions." Febs j **276**(9): 2469-2477.

Hanahan, D. (1983). "Studies on transformation of Escherichia coli with plasmids." J Mol Biol **166**(4): 557-580.

Hantke, K. (1981). "Regulation of ferric iron transport in Escherichia coli K12: isolation of a constitutive mutant." Mol Gen Genet **182**(2): 288-292.

Hardisson, C., M. B. Manzanal, J. A. Salas and J. E. Suarez (1978). "Fine structure, physiology and biochemistry of arthrospore germination in Streptomyces antibioticus." J Gen Microbiol **105**(2): 203-214.

Hassett, D. J., E. Alsabbagh, K. Parvatiyar, M. L. Howell, R. W. Wilmott and U. A. Ochsner (2000). "A protease-resistant catalase, KatA, released upon cell lysis during stationary phase is essential for aerobic survival of a Pseudomonas aeruginosa oxyR mutant at low cell densities." J Bacteriol **182**(16): 4557-4563.

Hatanaka, H., T. Kino, M. Asano, T. Goto, H. Tanaka and M. Okuhara (1989). "FK-506 related compounds produced by Streptomyces tsukubaensis No. 9993." J Antibiot (Tokyo) **42**(4): 620-622.

Hattman, S. and W. Sun (1997). "Escherichia coli OxyR modulation of bacteriophage Mu mom expression in dam+ cells can be attributed to its ability to bind hemimethylated Pmom promoter DNA." Nucleic Acids Res **25**(21): 4385-4388.

Helmann, J. D. (1999). "Anti-sigma factors." Curr Opin Microbiol **2**(2): 135-141.

Helmann, J. D. (2002). "The extracytoplasmic function (ECF) sigma factors." Adv Microb Physiol **46**: 47-110.

Helmann, J. D. and M. J. Chamberlin (1988). "Structure and function of bacterial sigma factors." Annu Rev Biochem **57**: 839-872.

Henderson, I. and P. Owen (1997). "The autoregulatory protein Mor and OxyR are identicial." Microbiology **143 (Pt 5)**: 1482.

Hesketh, A., D. Fink, B. Gust, H. U. Rexer, B. Scheel, K. Chater, W. Wohlleben and A. Engels (2002). "The GlnD and GlnK homologues of Streptomyces coelicolor A3(2) are functionally dissimilar to their nitrogen regulatory system counterparts from enteric bacteria." Mol Microbiol **46**(2): 319-330.

Hesketh, A., C. Hill, J. Mokhtar, G. Novotna, N. Tran, M. Bibb and H. J. Hong (2011). "Genome-wide dynamics of a bacterial response to antibiotics that target the cell envelope." BMC Genomics **12**: 226.

Hidalgo, E., J. M. Bollinger, Jr., T. M. Bradley, C. T. Walsh and B. Demple (1995). "Binuclear [2Fe-2S] clusters in the Escherichia coli SoxR protein and role of the metal centers in transcription." J Biol Chem **270**(36): 20908-20914.

Higgens, C. E., R. L. Hamill, T. H. Sands, M. M. Hoehn and N. E. Davis (1974). "The occurrence of deacetoxycephalosporin C in fungi and streptomycetes." J Antibiot (Tokyo) **27**(4): 298-300.

Higo, A., S. Horinouchi and Y. Ohnishi (2011). "Strict regulation of morphological differentiation and secondary metabolism by a positive feedback loop between two global regulators AdpA and BldA in Streptomyces griseus." Mol Microbiol **81**(6): 1607-1622.

Hillas, P. J., F. S. del Alba, J. Oyarzabal, A. Wilks and P. R. Ortiz De Montellano (2000). "The AhpC and AhpD antioxidant defence system of Mycobacterium tuberculosis." J Biol Chem **275**(25): 18801-18809.

Hopwood, D. A. (2007). "Therapeutic treasures from the deep." Nat Chem Biol **3**(8): 457-458.

Horinouchi, S. (2002). "A microbial hormone, A-factor, as a master switch for morphological differentiation and secondary metabolism in Streptomyces griseus." Front Biosci **7**: d2045-2057.

Horinouchi, S. and T. Beppu (1994). "A-factor as a microbial hormone that controls cellular differentiation and secondary metabolism in Streptomyces griseus." Mol Microbiol **12**(6): 859-864.

Huang, D., S. Li, M. Xia, J. Wen and X. Jia (2013). "Genome-scale metabolic network guided engineering of Streptomyces tsukubaensis for FK506 production improvement." Microb Cell Fact **12**: 52.

Huang, D., M. Xia, S. Li, J. Wen and X. Jia (2013). "Enhancement of FK506 production by engineering secondary pathways of Streptomyces tsukubaensis and exogenous feeding strategies." J Ind Microbiol Biotechnol **40**(9): 1023-1037.

Huang, J., J. Shi, V. Molle, B. Sohlberg, D. Weaver, M. J. Bibb, N. Karoonuthaisiri, C. J. Lih, C. M. Kao, M. J. Buttner and S. N. Cohen (2005). "Cross-regulation among disparate antibiotic biosynthetic pathways of Streptomyces coelicolor." Mol Microbiol **58**(5): 1276-1287.

Imlay, J. A. (2003). "Pathways of oxidative damage." Annu Rev Microbiol **57**: 395-418.

Imlay, J. A. (2008). "Cellular Defenses against Superoxide and Hydrogen Peroxide." Annual Review of Biochemistry **77**(1): 755-776.

Imlay, J. A. (2013). "The molecular mechanisms and physiological consequences of oxidative stress: lessons from a model bacterium." Nat Rev Microbiol **11**(7): 443-454.

Imlay, J. A., S. M. Chin and S. Linn (1988). "Toxic DNA damage by hydrogen peroxide through the Fenton reaction in vivo and in vitro." Science **240**(4852): 640-642.

Ivanova, A. B., G. V. Glinsky and A. Eisenstark (1997). "Role of rpoS regulon in resistance to oxidative stress and near-UV radiation in delta oxyR suppressor mutants of Escherichia coli." Free Radic Biol Med **23**(4): 627-636.

Jiang, L., Y. Liu, P. Wang, Y. Wen, Y. Song, Z. Chen and J. Li (2011). "Inactivation of the extracytoplasmic function sigma factor Sig6 stimulates avermectin production in Streptomyces avermitilis." Biotechnol Lett **33**(10): 1955-1961.

Jones, G. H., M. S. Paget, L. Chamberlin and M. J. Buttner (1997). "Sigma-E is required for the production of the antibiotic actinomycin in Streptomyces antibioticus." Mol Microbiol **23**(1): 169-178.

Julsing, M. K., S. Cornelissen, B. Buhler and A. Schmid (2008). "Heme-iron oxygenases: powerful industrial biocatalysts?" Curr Opin Chem Biol **12**(2): 177-186.

Kang, S. G., W. Jin, M. Bibb and K. J. Lee (1998). "Actinorhodin and undecylprodigiosin production in wild-type and relA mutant strains of Streptomyces coelicolor A3(2) grown in continuous culture." FEMS Microbiol Lett **168**(2): 221-226.

Kelemen, G. H., P. Brian, K. Flardh, L. Chamberlin, K. F. Chater and M. J. Buttner (1998). "Developmental regulation of transcription of whiE, a locus specifying the polyketide spore pigment in Streptomyces coelicolor A3 (2)." J Bacteriol **180**(9): 2515-2521.

Keyer, K. and J. A. Imlay (1996). "Superoxide accelerates DNA damage by elevating free-iron levels." Proc Natl Acad Sci U S A **93**(24): 13635-13640.

Kieser, T., M. Bibb, M. Buttner, K. Chater and D. A. Hopwood (2000). Practical Streptomyces Genetics, John Innes Centre, Norwich, United Kigdom.

Kim, E. J., H. J. Chung, B. Suh, Y. C. Hah and J. H. Roe (1998). "Expression and regulation of the sodF gene encoding iron- and zinc-containing superoxide dismutase in Streptomyces coelicolor Muller." J Bacteriol **180**(8): 2014-2020.

Kim, E. J., H. P. Kim, Y. C. Hah and J. H. Roe (1996). "Differential Expression of Superoxide Dismutases Containing Ni and Fe/Zn in Streptomyces Coelicolor." European Journal of Biochemistry **241**(1): 178-185.

Kim, E. S., H. J. Hong, C. Y. Choi and S. N. Cohen (2001). "Modulation of actinorhodin biosynthesis in Streptomyces lividans by glucose repression of afsR2 gene transcription." J Bacteriol **183**(7): 2198-2203.

Kim, H. M., J. H. Shin, Y. B. Cho and J. H. Roe (2014). "Inverse regulation of Fe- and Ni-containing SOD genes by a Fur family regulator Nur through small RNA processed from 3'UTR of the sodF mRNA." Nucleic Acids Res **42**(3): 2003-2014.

Kim, H. S. and Y. I. Park (2008). "Isolation and identification of a novel microorganism producing the immunosuppressant tacrolimus." J Biosci Bioeng **105**(4): 418-421.

Kim, J. A. and J. Mayfield (2000). "Identification of Brucella abortus OxyR and its role in control of catalase expression." J Bacteriol **182**(19): 5631-5633.

Kim, J. S., S. O. Kang and J. K. Lee (2003). "The protein complex composed of nickel-binding SrnQ and DNA binding motif-bearing SrnR of Streptomyces griseus represses sodF transcription in the presence of nickel." J Biol Chem **278**(20): 18455-18463.

Kinashi, H. and M. Shimaji (1987). "Detection of giant linear plasmids in antibiotic producing strains of Streptomyces by the OFAGE technique." J Antibiot (Tokyo) **40**(6): 913-916.

Kingsley, R. A., R. Reissbrodt, W. Rabsch, J. M. Ketley, R. M. Tsolis, P. Everest, G. Dougan, A. J. Baumler, M. Roberts and P. H. Williams (1999). "Ferrioxamine-mediated Iron(III) utilization by Salmonella enterica." Appl Environ Microbiol **65**(4): 1610-1618.

Kino, T., H. Hatanaka, M. Hashimoto, M. Nishiyama, T. Goto, M. Okuhara, M. Kohsaka, H. Aoki and H. Imanaka (1987). "FK-506, a novel immunosuppressant isolated from a Streptomyces. I. Fermentation, isolation, and physico-chemical and biological characteristics." J Antibiot (Tokyo) **40**(9): 1249-1255.

Kirby, R., V. Sangal, N. P. Tucker, J. Zakrzewska-Czerwinska, K. Wierzbicka, P. R. Herron, C. J. Chu, G. Chandra, A. H. Fahal, M. Goodfellow and P. A. Hoskisson (2012). "Draft genome sequence of the human pathogen Streptomyces somaliensis, a significant cause of actinomycetoma." J Bacteriol **194**(13): 3544-3545.

Kosec, G., D. Goranovic, P. Mrak, S. Fujs, E. Kuscer, J. Horvat, G. Kopitar and H. Petkovic (2012). "Novel chemobiosynthetic approach for exclusive production of FK506." Metab Eng **14**(1): 39-46.

Kuscer, E., N. Coates, I. Challis, M. Gregory, B. Wilkinson, R. Sheridan and H. Petkovic (2007). "Roles of rapH and rapG in positive regulation of rapamycin biosynthesis in Streptomyces hygroscopicus." J Bacteriol **189**(13): 4756-4763.

Lambert, S., M. F. Traxler, M. Craig, M. Maciejewska, M. Ongena, G. P. van Wezel, R. Kolter and S. Rigali (2014). "Altered desferrioxamine-mediated iron utilization is a common trait of bald mutants of Streptomyces coelicolor." Metallomics **6**(8): 1390-1399.

Lau, G. W., B. E. Britigan and D. J. Hassett (2005). "Pseudomonas aeruginosa OxyR is required for full virulence in rodent and insect models of infection and for resistance to human neutrophils." Infect Immun **73**(4): 2550-2553.

Leblond, P., G. Fischer, F. X. Francou, F. Berger, M. Guerineau and B. Decaris (1996). "The unstable region of Streptomyces ambofaciens includes 210 kb terminal inverted repeats flanking the extremities of the linear chromosomal DNA." Mol Microbiol **19**(2): 261-271.

Lechardeur, D., A. Fernandez, B. Robert, P. Gaudu, P. Trieu-Cuot, G. Lamberet and A. Gruss (2010). "The 2-Cys peroxiredoxin alkyl hydroperoxide reductase c binds heme and participates in its intracellular availability in Streptococcus agalactiae." J Biol Chem **285**(21): 16032-16041.

Lee, C., S. M. Lee, P. Mukhopadhyay, S. J. Kim, S. C. Lee, W. S. Ahn, M. H. Yu, G. Storz and S. E. Ryu (2004). "Redox regulation of OxyR requires specific disulfide bond formation involving a rapid kinetic reaction path." Nat Struct Mol Biol **11**(12): 1179-1185.

Lee, S. K., S. H. Yang, C. M. Kang, S. Mo and J. W. Suh (2014). "Overexpression of the putative extracytoplasmic function sigma (sigma) factor FujE enhances FK506 production in Streptomyces sp. strain KCCM 11116P." Can J Microbiol **60**(6): 363-369.

Lerat, S., A. M. Simao-Beaunoir and C. Beaulieu (2009). "Genetic and physiological determinants of Streptomyces scabies pathogenicity." Mol Plant Pathol **10**(5): 579-585.

Lezhava, A., T. Mizukami, T. Kajitani, D. Kameoka, M. Redenbach, H. Shinkawa, O. Nimi and H. Kinashi (1995). "Physical map of the linear chromosome of Streptomyces griseus." J Bacteriol **177**(22): 6492-6498.

Li, W., C. E. Stevenson, N. Burton, P. Jakimowicz, M. S. Paget, M. J. Buttner, D. M. Lawson and C. Kleanthous (2002). "Identification and structure of the anti-sigma factor-binding domain of the disulphide-stress regulated sigma factor sigma(R) from Streptomyces coelicolor." J Mol Biol **323**(2): 225-236.

Lin, Y. S., H. M. Kieser, D. A. Hopwood and C. W. Chen (1993). "The chromosomal DNA of Streptomyces lividans 66 is linear." Mol Microbiol **10**(5): 923-933.

Loewen, P. C. and J. Switala (1988). "Purification and characterization of spore-specific catalase-2 from Bacillus subtilis." Biochem Cell Biol **66**(7): 707-714.

Lonetto, M., M. Gribskov and C. A. Gross (1992). "The sigma 70 family: sequence conservation and evolutionary relationships." J Bacteriol **174**(12): 3843-3849.

Lonetto, M. A., K. L. Brown, K. E. Rudd and M. J. Buttner (1994). "Analysis of the Streptomyces coelicolor sigE gene reveals the existence of a subfamily of eubacterial RNA polymerase sigma factors involved in the regulation of extracytoplasmic functions." Proc Natl Acad Sci U S A **91**(16): 7573-7577.

Loprasert, S., S. Atichartpongkun, W. Whangsuk and S. Mongkolsuk (1997). "Isolation and analysis of the Xanthomonas alkyl hydroperoxide reductase gene and the peroxide sensor regulator genes ahpC and ahpF-oxyR-orfX." J Bacteriol **179**(12): 3944-3949.

Loprasert, S., M. Fuangthong, W. Whangsuk, S. Atichartpongkul and S. Mongkolsuk (2000). "Molecular and physiological analysis of an OxyR-regulated ahpC promoter in Xanthomonas campestris pv. phaseoli." Mol Microbiol **37**(6): 1504-1514.

Lucana, D. O. d. O., T. Schaa and H. Schrempf (2004). "The novel extracellular Streptomyces reticuli haem-binding protein HbpS influences the production of the catalase-peroxidase CpeB." Microbiology **150**(8): 2575-2585.

Lucana, D. O. d. O., M. Troller and H. Schrempf (2003). "Amino acid residues involved in reversible thiol formation and zinc ion binding in the Streptomyces reticuli redox regulator FurS." Mol Genet Genomics **268**(5): 618-627.

Lucana, D. O. d. O., P. Zou, M. Nierhaus and H. Schrempf (2005). "Identification of a novel two-component system SenS/SenR modulating the production of the catalase-peroxidase CpeB and the haem-binding protein HbpS in Streptomyces reticuli." Microbiology **151**(11): 3603-3614.

Luo, Y., J. Xiao, Y. Wang, J. Xu, S. Xie and J. Xu (2011). "Streptomyces indicus sp. nov., an actinomycete isolated from deep-sea sediment." Int J Syst Evol Microbiol **61**(Pt 11): 2712-2716.

Ma, L. and S. M. Payne (2012). "AhpC is required for optimal production of enterobactin by Escherichia coli." J Bacteriol **194**(24): 6748-6757.

Maddocks, S. E. and P. C. Oyston (2008). "Structure and function of the LysR-type transcriptional regulator (LTTR) family proteins." Microbiology **154**(Pt 12): 3609-3623.

Manteca, A., R. Alvarez, N. Salazar, P. Yague and J. Sanchez (2008). "Mycelium differentiation and antibiotic production in submerged cultures of Streptomyces coelicolor." Applied and environmental microbiology **74**(12): 3877-3886.

Manteca, A., D. Claessen, C. Lopez-Iglesias and J. Sanchez (2007). "Aerial hyphae in surface cultures of Streptomyces lividans and Streptomyces coelicolor originate from viable segments surviving an early programmed cell death event." FEMS microbiology letters **274**(1): 118-125.

Martin, J. F. (2004). "Phosphate control of the biosynthesis of antibiotics and other secondary metabolites is mediated by the PhoR-PhoP system: an unfinished story." J Bacteriol **186**(16): 5197-5201.

Martinez, A., A. Urios and M. Blanco (2000). "Mutagenicity of 80 chemicals in Escherichia coli tester strains IC203, deficient in OxyR, and its oxyR(+) parent WP2 uvrA/pKM101: detection of 31 oxidative mutagens." Mutat Res **467**(1): 41-53.

Martinez-Castro, M., C. Barreiro, F. Romero, R. I. Fernandez-Chimeno and J. F. Martin (2011). "Streptomyces tacrolimicus sp. nov., a low producer of the immunosuppressant tacrolimus (FK506)." Int J Syst Evol Microbiol **61**(Pt 5): 1084-1088.

Martinez-Castro, M., E. Solera, J. F. Martin and C. Barreiro (2009). "Efficient pyramidal arrangement of an ordered cosmid library: Rapid screening of genes of the tacrolimus-producer Streptomyces sp. ATCC 55098." J Microbiol Methods **78**(2): 150-154.

Mate, M. J., M. Zamocky, L. M. Nykyri, C. Herzog, P. M. Alzari, C. Betzel, F. Koller and I. Fita (1999). "Structure of catalase-A from Saccharomyces cerevisiae." J Mol Biol **286**(1): 135-149.

Meier, J. L. and M. D. Burkart (2009). "The chemical biology of modular biosynthetic enzymes." Chem Soc Rev **38**(7): 2012-2045.

Melstrom, K. A., Jr., R. Kozlowski, D. J. Hassett, H. Suzuki, D. M. Bates, R. L. Gamelli and R. Shankar (2007). "Cytotoxicity of Pseudomonas secreted exotoxins requires OxyR expression." J Surg Res **143**(1): 50-57.

Mendes, M. V., J. F. Aparicio and J. F. Martin (2000). "Complete nucleotide sequence and characterization of pSNA1 from pimaricin-producing Streptomyces natalensis that replicates by a rolling circle mechanism." Plasmid **43**(2): 159-165.

Mendes, M. V., E. Recio, N. Anton, S. M. Guerra, J. Santos-Aberturas, J. F. Martin and J. F. Aparicio (2007). "Cholesterol oxidases act as signaling proteins for the biosynthesis of the polyene macrolide pimaricin." Chemistry & Biology **14**(3): 279-290.

Mendes, M. V., S. Tunca, N. Anton, E. Recio, A. Sola-Landa, J. F. Aparicio and J. F. Martin (2007). "The two-component phoR-phoP system of Streptomyces natalensis: Inactivation or deletion of phoP reduces the negative phosphate regulation of pimaricin biosynthesis." Metab Eng **9**(2): 217-227.

Messner, K. R. and J. A. Imlay (2002). "Mechanism of superoxide and hydrogen peroxide formation by fumarate reductase, succinate dehydrogenase, and aspartate oxidase." J Biol Chem **277**(45): 42563-42571.

Mikulik, K., I. Janda, J. Weiser, J. Stastna and A. Jiranova (1984). "RNA and ribosomal protein patterns during aerial spore germination in Streptomyces granaticolor." Eur J Biochem **145**(2): 381-388.

Miller, A. F. (2012). "Superoxide dismutases: ancient enzymes and new insights." FEBS Lett **586**(5): 585-595.

Mo, S., D. H. Kim, J. H. Lee, J. W. Park, D. B. Basnet, Y. H. Ban, Y. J. Yoo, S. W. Chen, S. R. Park, E. A. Choi, E. Kim, Y. Y. Jin, S. K. Lee, J. Y. Park, Y. Liu, M. O. Lee, K. S. Lee, S. J. Kim, D. Kim, B. C. Park, S. G. Lee, H. J. Kwon, J. W. Suh, B. S. Moore, S. K. Lim and Y. J. Yoon (2011). "Biosynthesis of the allylmalonyl-CoA extender unit for the FK506 polyketide synthase proceeds through a dedicated polyketide synthase and facilitates the mutasynthesis of analogues." J Am Chem Soc **133**(4): 976-985.

Mo, S., Y. J. Yoo, Y. H. Ban, S. K. Lee, E. Kim, J. W. Suh and Y. J. Yoon (2012). "Roles of fkbN in positive regulation and tcs7 in negative regulation of FK506 biosynthesis in Streptomyces sp. strain KCTC 11604BP." Appl Environ Microbiol **78**(7): 2249-2255.

Mongkolsuk, S., S. Loprasert, W. Whangsuk, M. Fuangthong and S. Atichartpongkun (1997). "Characterization of transcription organization and analysis of unique expression patterns of an alkyl hydroperoxide reductase C gene (ahpC) and the peroxide regulator operon ahpF-oxyR-orfX from Xanthomonas campestris pv. phaseoli." J Bacteriol **179**(12): 3950-3955.

Mongkolsuk, S., W. Whangsuk, M. Fuangthong and S. Loprasert (2000). "Mutations in oxyR resulting in peroxide resistance in Xanthomonas campestris." J Bacteriol **182**(13): 3846-3849.

Motamedi, H. and A. Shafiee (1998). "The biosynthetic gene cluster for the macrolactone ring of the immunosuppressant FK506." Eur J Biochem **256**(3): 528-534.

Motamedi, H., A. Shafiee, S. J. Cai, S. L. Streicher, B. H. Arison and R. R. Miller (1996). "Characterization of methyltransferase and hydroxylase genes involved in the biosynthesis of the immunosuppressants FK506 and FK520." J Bacteriol **178**(17): 5243-5248.

Mukhopadhyay, S. and H. E. Schellhorn (1997). "Identification and characterization of hydrogen peroxide-sensitive mutants of Escherichia coli: genes that require OxyR for expression." J Bacteriol **179**(2): 330-338.

Munch, R., K. Hiller, H. Barg, D. Heldt, S. Linz, E. Wingender and D. Jahn (2003). "PRODORIC: prokaryotic database of gene regulation." Nucleic Acids Res **31**(1): 266-269.

Narva, K. E. and J. S. Feitelson (1990). "Nucleotide Sequence and Transcriptional Analysis of the *redD* Locus of *Streptomyces coelicolor* A3(2)." J. Bacteriol. **172**(1): 326-333.

Newton, G. L., K. Arnold, M. S. Price, C. Sherrill, S. B. Delcardayre, Y. Aharonowitz, G. Cohen, J. Davies, R. C. Fahey and C. Davis (1996). "Distribution of thiols in microorganisms: mycothiol is a major thiol in most actinomycetes." J Bacteriol **178**(7): 1990-1995.

Newton, G. L. and R. C. Fahey (2008). "Regulation of mycothiol metabolism by sigma(R) and the thiol redox sensor anti-sigma factor RsrA." Mol Microbiol **68**(4): 805-809.

Nieselt, K., F. Battke, A. Herbig, P. Bruheim, A. Wentzel, O. Jakobsen, H. Sletta, M. Alam, M. Merlo, J. Moore, W. Omara, E. Morrissey, M. Juarez-Hermosillo, A. Rodriguez-Garcia, M. Nentwich, L. Thomas, M. Iqbal, R. Legaie, W. Gaze, G. Challis, R. Jansen, L. Dijkhuizen, D. Rand, D. Wild, M. Bonin, J. Reuther, W. Wohlleben, M. Smith, N. Burroughs, J. Martin, D. Hodgson, E. Takano, R. Breitling, T. Ellingsen and E. Wellington (2010). "The dynamic architecture of the metabolic switch in Streptomyces coelicolor." BMC Genomics **11**(1): 10.

Noto, J. M. and C. N. Cornelissen (2008). "Identification of TbpA residues required for transferrin-iron utilization by Neisseria gonorrhoeae." Infect Immun **76**(5): 1960-1969.

Nunn, C. M., S. Djordjevic, P. J. Hillas, C. R. Nishida and P. R. Ortiz de Montellano (2002). "The crystal structure of Mycobacterium tuberculosis alkylhydroperoxidase AhpD, a potential target for antitubercular drug design." J Biol Chem **277**(22): 20033-20040.

Ochsner, U. A., M. L. Vasil, E. Alsabbagh, K. Parvatiyar and D. J. Hassett (2000). "Role of the Pseudomonas aeruginosa oxyR-recG operon in oxidative stress defense and DNA repair: OxyR-dependent regulation of katB-ankB, ahpB, and ahpC-ahpF." J Bacteriol **182**(16): 4533-4544.

Ohnishi, Y., J. Ishikawa, H. Hara, H. Suzuki, M. Ikenoya, H. Ikeda, A. Yamashita, M. Hattori and S. Horinouchi (2008). "Genome sequence of the streptomycin-producing microorganism Streptomyces griseus IFO 13350." J Bacteriol **190**(11): 4050-4060.

Ortiz de Orue Lucana, D. and M. R. Groves (2009). "The three-component signalling system HbpS-SenS-SenR as an example of a redox sensing pathway in bacteria." Amino Acids **37**(3): 479-486.

Paget, M. S., L. Chamberlin, A. Atrih, S. J. Foster and M. J. Buttner (1999). "Evidence that the extracytoplasmic function sigma factor sigmaE is required for normal cell wall structure in Streptomyces coelicolor A3(2)." J Bacteriol **181**(1): 204-211.

Paget, M. S., J. G. Kang, J. H. Roe and M. J. Buttner (1998). "sigmaR, an RNA polymerase sigma factor that modulates expression of the thioredoxin system in response to oxidative stress in Streptomyces coelicolor A3(2)." Embo J **17**(19): 5776-5782.

Paget, M. S. B., V. Molle, G. Cohen, Y. Aharonowitz and M. J. Buttner (2001). "Defining the disulphide stress response in Streptomyces coelicolor A3(2): identification of the sigmaR regulon." Molecular Microbiology **42**(4): 1007-1020.

Pandza, K., G. Pfalzer, J. Cullum and D. Hranueli (1997). "Physical mapping shows that the unstable oxytetracycline gene cluster of Streptomyces rimosus lies close to one end of the linear chromosome." Microbiology **143 (Pt 5)**: 1493-1501.

Parker, M. W. and C. C. Blake (1988). "Iron- and manganese-containing superoxide dismutases can be distinguished by analysis of their primary structures." FEBS Lett **229**(2): 377-382.

Parsonage, D., P. A. Karplus and L. B. Poole (2008). "Substrate specificity and redox potential of AhpC, a bacterial peroxiredoxin." Proc Natl Acad Sci U S A **105**(24): 8209-8214.

Paulsen, I. T. (1996). "Carbon metabolism and its regulation in Streptomyces and other high GC gram-positive bacteria." Res Microbiol **147**(6-7): 535-541.

Perez-Llarena, F. J., P. Liras, A. Rodriguez-Garcia and J. F. Martin (1997). "A regulatory gene (ccaR) required for cephamycin and clavulanic acid production in Streptomyces clavuligerus: amplification results in overproduction of both beta-lactam compounds." J Bacteriol **179**(6): 2053-2059.

Perez-Redondo, R., A. Rodriguez-Garcia, J. F. Martin and P. Liras (1998). "The claR gene of Streptomyces clavuligerus, encoding a LysR-type regulatory protein controlling clavulanic acid biosynthesis, is linked to the clavulanate-9-aldehyde reductase (car) gene." Gene **211**(2): 311-321.

Perkins, D. N., D. J. Pappin, D. M. Creasy and J. S. Cottrell (1999). "Probability-based protein identification by searching sequence databases using mass spectrometry data." Electrophoresis **20**(18): 3551-3567.

Peskin, A. V., F. M. Low, L. N. Paton, G. J. Maghzal, M. B. Hampton and C. C. Winterbourn (2007). "The high reactivity of peroxiredoxin 2 with H(2)O(2) is not reflected in its reaction with other oxidants and thiol reagents." J Biol Chem **282**(16): 11885-11892.

Pfaffl, M. W. (2001). "A new mathematical model for relative quantification in real-time RT-PCR." Nucleic Acids Research **29**(9).

Piette, A., A. Derouaux, P. Gerkens, E. E. Noens, G. Mazzucchelli, S. Vion, H. K. Koerten, F. Titgemeyer, E. De Pauw, P. Leprince, G. P. van Wezel, M. Galleni and S. Rigali (2005). "From dormant to germinating spores of Streptomyces coelicolor A3(2): new perspectives from the crp null mutant." J Proteome Res **4**(5): 1699-1708.

Pimentel-Elardo, S. M., S. Kozytska, T. S. Bugni, C. M. Ireland, H. Moll and U. Hentschel (2010). "Anti-parasitic compounds from Streptomyces sp. strains isolated from Mediterranean sponges." Mar Drugs **8**(2): 373-380.

Pollak, N., C. Dolle and M. Ziegler (2007). "The power to reduce: pyridine nucleotides--small molecules with a multitude of functions." Biochem J **402**(2): 205-218.

Pomposiello, P. J. and B. Demple (2001). "Redox-operated genetic switches: the SoxR and OxyR transcription factors." Trends Biotechnol **19**(3): 109-114.

Poole, L. B. and H. R. Ellis (1996). "Flavin-dependent alkyl hydroperoxide reductase from Salmonella typhimurium. 1. Purification and enzymatic activities of overexpressed AhpF and AhpC proteins." Biochemistry **35**(1): 56-64.

Ralser, M., M. M. Wamelink, A. Kowald, B. Gerisch, G. Heeren, E. A. Struys, E. Klipp, C. Jakobs, M. Breitenbach, H. Lehrach and S. Krobitsch (2007). "Dynamic rerouting of the carbohydrate flux is key to counteracting oxidative stress." J Biol **6**(4): 10.

Ramachandran, S., T. S. Magnuson and D. L. Crawford (2000). "Isolation and analysis of three peroxide sensor regulatory gene homologs ahpC, ahpX and oxyR in Streptomyces viridosporus T7A--a lignocellulose degrading actinomycete." DNA Seq **11**(1-2): 51-60.

Regentin, R., L. Cadapan, S. Ou, S. Zavala and P. Licari (2002). "Production of a novel FK520 analog in Streptomyces hygroscopicus: improving titer while minimizing impurities." J Ind Microbiol Biotechnol **28**(1): 12-16.

Reuther, J. and W. Wohlleben (2007). "Nitrogen metabolism in Streptomyces coelicolor: transcriptional and post-translational regulation." J Mol Microbiol Biotechnol **12**(1-2): 139-146.

Rocha, E. R., G. Owens, Jr. and C. J. Smith (2000). "The redox-sensitive transcriptional activator OxyR regulates the peroxide response regulon in the obligate anaerobe Bacteroides fragilis." J Bacteriol **182**(18): 5059-5069.

Rodriguez, H., S. Rico, M. Diaz and R. I. Santamaria (2013). "Two-component systems in Streptomyces: key regulators of antibiotic complex pathways." Microb Cell Fact **12**: 127.

Rodriguez-Garcia, A., A. Sola-Landa, K. Apel, F. Santos-Beneit and J. F. Martin (2009). "Phosphate control over nitrogen metabolism in Streptomyces coelicolor: direct and indirect negative control of glnR, glnA, glnII and amtB expression by the response regulator PhoP." Nucleic Acids Res **37**(10): 3230-3242.

Rokem, J. S., A. E. Lantz and J. Nielsen (2007). "Systems biology of antibiotic production by microorganisms." Nat Prod Rep **24**(6): 1262-1287.

Ross, R. P. and A. Claiborne (1997). "Evidence for regulation of the NADH peroxidase gene (npr) from Enterococcus faecalis by OxyR." FEMS Microbiol Lett **151**(2): 177-183.

Royall, J. A. and H. Ischiropoulos (1993). "Evaluation of 2',7'-dichlorofluorescin and dihydrorhodamine 123 as fluorescent probes for intracellular H2O2 in cultured endothelial cells." Arch Biochem Biophys **302**(2): 348-355.

Ruiz, B., A. Chavez, A. Forero, Y. Garcia-Huante, A. Romero, M. Sanchez, D. Rocha, B. Sanchez, R. Rodriguez-Sanoja, S. Sanchez and E. Langley (2010). "Production of microbial secondary metabolites: regulation by the carbon source." Crit Rev Microbiol **36**(2): 146-167.

Salehi-Najafabadi, Z., C. Barreiro, A. Rodriguez-Garcia, A. Cruz, G. E. Lopez and J. F. Martin (2014). "The gamma-butyrolactone receptors BulR1 and BulR2 of Streptomyces tsukubaensis: tacrolimus (FK506) and butyrolactone synthetases production control." Appl Microbiol Biotechnol **98**(11): 4919-4936.

Sambrook, J. and D. Russell (2001). Molecular Cloning: a Laboratory Manual. Cold Spring Harbor, NY, Cold Spring Harbor Laboratory Press.

Sanchez, S. and A. L. Demain (2008). "Metabolic regulation and overproduction of primary metabolites." Microb Biotechnol **1**(4): 283-319.

Santos-Beneit, F., L. T. Fernandez-Martinez, A. R. Garcia, S. Martin-Martin, M. Ordonez-Robles, P. Yague, A. Manteca and J. F. Martin (2014). "Transcriptional response to vancomycin in a highly vancomycin-resistant Streptomyces coelicolor mutant." Future Microbiol **9**: 603-622.

Santos-Beneit, F., A. Rodriguez-Garcia, E. Franco-Dominguez and J. F. Martin (2008). "Phosphate-dependent regulation of the low- and high-affinity transport systems in the model actinomycete Streptomyces coelicolor." Microbiology **154**(Pt 8): 2356-2370.

Santos-Beneit, F., A. Rodriguez-Garcia, A. Sola-Landa and J. F. Martin (2009). "Cross-talk between two global regulators in Streptomyces: PhoP and AfsR interact in the control of afsS, pstS and phoRP transcription." Mol Microbiol **72**(1): 53-68.

Schell, M. A. (1993). "Molecular biology of the LysR family of transcriptional regulators." Annu Rev Microbiol **47**: 597-626.

Schmidt, A., M. Gube, A. Schmidt and E. Kothe (2009). "In silico analysis of nickel containing superoxide dismutase evolution and regulation." J Basic Microbiol **49**(1): 109-118.

Seaver, L. C. and J. A. Imlay (2001). "Alkyl Hydroperoxide Reductase Is the Primary Scavenger of Endogenous Hydrogen Peroxide in Escherichia coli." J. Bacteriol. **183**(24): 7173-7181.

Seipke, R. F., E. Patrick and M. I. Hutchings (2014). "Regulation of antimycin biosynthesis by the orphan ECF RNA polymerase sigma factor sigma (AntA.)." PeerJ **2**: e253.

Shin, J. H., A. K. Singh, D. J. Cheon and J. H. Roe (2011). "Activation of the SoxR regulon in Streptomyces coelicolor by the extracellular form of the pigmented antibiotic actinorhodin." J Bacteriol **193**(1): 75-81.

Sigmund, J. M., D. C. Clark, F. A. Rainey and A. S. Anderson (2003). "Detection of eubacterial 3-hydroxy-3-methylglutaryl coenzyme a reductases from natural populations of actinomycetes." Microb Ecol **46**(1): 106-112.

Singh, B. P. and B. K. Behera (2009). "Regulation of tacrolimus production by altering primary source of carbons and amino acids." Lett Appl Microbiol **49**(2): 254-259.

Smollett, K. L., L. F. Dawson and E. O. Davis (2011). "SigG does not control gene expression in response to DNA damage in Mycobacterium tuberculosis H37Rv." J Bacteriol **193**(4): 1007-1011.

Sobota, J. M. and J. A. Imlay (2011). "Iron enzyme ribulose-5-phosphate 3-epimerase in Escherichia coli is rapidly damaged by hydrogen peroxide but can be protected by manganese." Proc Natl Acad Sci U S A **108**(13): 5402-5407.

Sola-Landa, A., R. S. Moura and J. F. Martin (2003). "The two-component PhoR-PhoP system controls both primary metabolism and secondary metabolite biosynthesis in Streptomyces lividans." Proc Natl Acad Sci U S A **100**(10): 6133-6138.

Song, S. K., Y.-S. Jeong, P.-H. Kim and G.-T. Chun (2006). Effects of dissolved oxygen level on avermectin B[1a] production by *Streptomyces avermitilis* in computer-controlled bioreactor cultures, Korean Society for Applied Microbiology.

Sreevatsan, S., X. Pan, Y. Zhang, V. Deretic and J. M. Musser (1997). "Analysis of the oxyR-ahpC region in isoniazid-resistant and -susceptible Mycobacterium tuberculosis complex organisms recovered from diseased humans and animals in diverse localities." Antimicrob Agents Chemother **41**(3): 600-606.

Staron, A., H. J. Sofia, S. Dietrich, L. E. Ulrich, H. Liesegang and T. Mascher (2009). "The third pillar of bacterial signal transduction: classification of the extracytoplasmic function (ECF) sigma factor protein family." Mol Microbiol.

Storz, G. and J. A. Imlay (1999). "Oxidative stress." Curr Opin Microbiol **2**(2): 188-194.

Struyk, A. P., I. Hoette, G. Drost, J. M. Waisvisz, T. Van Eek and J. C. Hoogerheide (1957). "Pimaricin, a new antifungal antibiotic." Antibiot Annu **5**: 878-885.

Tao, K. (1997). "oxyR-dependent induction of Escherichia coli grx gene expression by peroxide stress." J Bacteriol **179**(18): 5967-5970.

Teramoto, H., M. Inui and H. Yukawa (2013). "OxyR acts as a transcriptional repressor of hydrogen peroxide-inducible antioxidant genes in Corynebacterium glutamicum R." FEBS J **280**(14): 3298-3312.

Tietze, D., H. Breitzke, D. Imhof, E. Kothe, J. Weston and G. Buntkowsky (2009). "New insight into the mode of action of nickel superoxide dismutase by investigating metallopeptide substrate models." Chemistry **15**(2): 517-523.

Tiffert, Y., P. Supra, R. Wurm, W. Wohlleben, R. Wagner and J. Reuther (2008). "The Streptomyces coelicolor GlnR regulon: identification of new GlnR targets and evidence for a central role of GlnR in nitrogen metabolism in actinomycetes." Mol Microbiol **67**(4): 861-880.

Toledano, M. B., I. Kullik, F. Trinh, P. T. Baird, T. D. Schneider and G. Storz (1994). "Redox-dependent shift of OxyR-DNA contacts along an extended DNA-binding site: a mechanism for differential promoter selection." Cell **78**(5): 897-909.

Touati, D. (2000). "Iron and oxidative stress in bacteria." Arch Biochem Biophys **373**(1): 1-6.

Toyama, H., E. Hayashi, C. Nojiri, K. Katsumata, A. Miyata and Y. Yamada (1982). "Isolation and characterization of small plasmids from Streptomyces." J Antibiot (Tokyo) **35**(3): 369-373.

Traxler, M. F., J. D. Watrous, T. Alexandrov, P. C. Dorrestein and R. Kolter (2013). "Interspecies interactions stimulate diversification of the Streptomyces coelicolor secreted metabolome." MBio **4**(4).

Tunca, S., C. Barreiro, A. Sola-Landa, J. J. Coque and J. F. Martin (2007). "Transcriptional regulation of the desferrioxamine gene cluster of *Streptomyces coelicolor* is mediated by binding of DmdR1 to an iron box in the promoter of the desA gene." FEBS J **274**(4): 1110-1122.

Tusseau-Vuillemin, M. H., F. Lagarde, C. Chauviere and A. Heduit (2002). "Hydrogen peroxide (H2O2) as a source of dissolved oxygen in COD-degradation respirometric experiments." Water Res **36**(3): 793-798.

Ventura, M., C. Canchaya, A. Tauch, G. Chandra, G. F. Fitzgerald, K. F. Chater and D. van Sinderen (2007). "Genomics of Actinobacteria: tracing the evolutionary history of an ancient phylum." Microbiol Mol Biol Rev **71**(3): 495-548.

Vinckx, T., S. Matthijs and P. Cornelis (2008). "Loss of the oxidative stress regulator OxyR in Pseudomonas aeruginosa PAO1 impairs growth under iron-limited conditions." FEMS Microbiol Lett **288**(2): 258-265.

Vinckx, T., Q. Wei, S. Matthijs, J. P. Noben, R. Daniels and P. Cornelis (2011). "A proteome analysis of the response of a Pseudomonas aeruginosa oxyR mutant to iron limitation." Biometals : an international journal on the role of metal ions in biology, biochemistry, and medicine **24**(3): 523-532.

Visick, J. E. and S. Clarke (1997). "RpoS- and OxyR-independent induction of HPI catalase at stationary phase in Escherichia coli and identification of rpoS mutations in common laboratory strains." J Bacteriol **179**(13): 4158-4163.

Volff, J. N. and J. Altenbuchner (1998). "Genetic instability of the Streptomyces chromosome." Mol Microbiol **27**(2): 239-246.

Waldvogel, E., A. Herbig, F. Battke, R. Amin, M. Nentwich, K. Nieselt, T. E. Ellingsen, A. Wentzel, D. A. Hodgson, W. Wohlleben and Y. Mast (2011). "The PII protein GlnK is a pleiotropic regulator for morphological differentiation and secondary metabolism in Streptomyces coelicolor." Appl Microbiol Biotechnol **92**(6): 1219-1236.

Walker, G. E., B. Dunbar, I. S. Hunter, H. G. Nimmo and J. R. Coggins (1995). "A catalase from Streptomyces coelicolor A3(2)." Microbiology **141**(6): 1377-1383.

Walker, J. E., M. Saraste, M. J. Runswick and N. J. Gay (1982). "Distantly related sequences in the alpha- and beta-subunits of ATP synthase, myosin, kinases and other ATP-requiring enzymes and a common nucleotide binding fold." Embo j **1**(8): 945-951.

Wang, F., X. Xiao, A. Saito and H. Schrempf (2002). "Streptomyces olivaceoviridis possesses a phosphotransferase system that mediates specific, phosphoenolpyruvate-dependent uptake of N-acetylglucosamine." Mol Genet Genomics **268**(3): 344-351.

Wang, R., Y. Mast, J. Wang, W. Zhang, G. Zhao, W. Wohlleben, Y. Lu and W. Jiang (2013). "Identification of two-component system AfsQ1/Q2 regulon and its cross-regulation with GlnR in Streptomyces coelicolor." Mol Microbiol **87**(1): 30-48.

Wei, Z.-H., L. Bai, Z. Deng and J.-J. Zhong (2011). "Enhanced production of validamycin A by H_2O_2-induced reactive oxygen species in fermentation of *Streptomyces hygroscopicus* 5008." Bioresource Technology **102**: 1783-1787.

Wietzorrek, A. and M. Bibb (1997). "A novel family of proteins that regulates antibiotic production in streptomycetes appears to contain an OmpR-like DNA-binding fold." Mol Microbiol **25**(6): 1181-1184.

Wilkinson, C. J., Z. A. Hughes-Thomas, C. J. Martin, I. Bohm, T. Mironenko, M. Deacon, M. Wheatcroft, G. Wirtz, J. Staunton and P. F. Leadlay (2002). "Increasing the efficiency of heterologous promoters in actinomycetes." Journal of molecular microbiology and biotechnology **4**(4): 417-426.

Wilson, D. J., Y. Xue, K. A. Reynolds and D. H. Sherman (2001). "Characterization and analysis of the PikD regulatory factor in the pikromycin biosynthetic pathway of Streptomyces venezuelae." J Bacteriol **183**(11): 3468-3475.

Wray, L. V., Jr. and S. H. Fisher (1993). "The Streptomyces coelicolor glnR gene encodes a protein similar to other bacterial response regulators." Gene **130**(1): 145-150.

Wu, C. H., J. J. Tsai-Wu, Y. T. Huang, C. Y. Lin, G. G. Lioua and F. J. Lee (1998). "Identification and subcellular localization of a novel Cu,Zn superoxide dismutase of Mycobacterium tuberculosis." FEBS Lett **439**(1-2): 192-196.

Wu, K., L. Chung, W. P. Revill, L. Katz and C. D. Reeves (2000). "The FK520 gene cluster of Streptomyces hygroscopicus var. ascomyceticus (ATCC 14891) contains genes for biosynthesis of unusual polyketide extender units." Gene **251**(1): 81-90.

Wuerges, J., J. W. Lee, Y. I. Yim, H. S. Yim, S. O. Kang and K. Djinovic Carugo (2004). "Crystal structure of nickel-containing superoxide dismutase reveals another type of active site." Proc Natl Acad Sci U S A **101**(23): 8569-8574.

Xia, M., D. Huang, S. Li, J. Wen, X. Jia and Y. Chen (2013). "Enhanced FK506 production in Streptomyces tsukubaensis by rational feeding strategies based on comparative metabolic profiling analysis." Biotechnol Bioeng **110**(10): 2717-2730.

Yague, P., M. T. Lopez-Garcia, B. Rioseras, J. Sanchez and A. Manteca (2012). "New insights on the development of and their relationships with secondary metabolite production." Curr Trends Microbiol **8**: 65-73.

Yamamura, E., T. Nunoshiba, M. Kawata and K. Yamamoto (2000). "Characterization of spontaneous mutation in the oxyR strain of Escherichia coli." Biochem Biophys Res Commun **279**(2): 427-432.

Yamanaka, K., H. Oikawa, H. O. Ogawa, K. Hosono, F. Shinmachi, H. Takano, S. Sakuda, T. Beppu and K. Ueda (2005). "Desferrioxamine E produced by Streptomyces griseus stimulates growth and development of Streptomyces tanashiensis." Microbiology **151**(Pt 9): 2899-2905.

Yegneswaran, P. K., M. R. Gray and B. G. Thompson (1991). "Effect of dissolved oxygen control on growth and antibiotic production in *Streptomyces clavuligerus* fermentations." Biotechnology Progress **7**(3): 246-250.

Youn, H. D., E. J. Kim, J. H. Roe, Y. C. Hah and S. O. Kang (1996). "A novel nickel-containing superoxide dismutase from Streptomyces spp." Biochem J **318 (Pt 3)**: 889-896.

Zhao, S., D. Huang, H. Qi, J. Wen and X. Jia (2013). "Comparative metabolic profiling-based improvement of rapamycin production by Streptomyces hygroscopicus." Appl Microbiol Biotechnol **97**(12): 5329-5341.

Zheng, M., F. Aslund and G. Storz (1998). "Activation of the OxyR transcription factor by reversible disulfide bond formation." Science **279**(5357): 1718-1721.

Zheng, M., B. Doan, T. D. Schneider and G. Storz (1999). "OxyR and SoxRS regulation of fur." J Bacteriol **181**(15): 4639-4643.

Zheng, M., X. Wang, L. J. Templeton, D. R. Smulski, R. A. LaRossa and G. Storz (2001). "DNA microarray-mediated transcriptional profiling of the Escherichia coli response to hydrogen peroxide." J Bacteriol **183**(15): 4562-4570.

Zhu, X., W. Zhang, X. Chen, H. Wu, Y. Duan and Z. Xu (2010). "Generation of high rapamycin producing strain via rational metabolic pathway-based mutagenesis and further titer improvement with fed-batch bioprocess optimization." Biotechnol Bioeng **107**(3): 506-515.

Zou, P., I. Borovok, D. Ortiz de Orue Lucana, D. Muller and H. Schrempf (1999). "The mycelium-associated Streptomyces reticuli catalase-peroxidase, its gene and regulation by FurS." Microbiology **145 (Pt 3)**: 549-559.

APPENDIX I

```
LOCUS       STSU_348_349_corrected_IBMC     14355 bp    DNA     linear   UNA
FEATURES             Location/Qualifiers
     source          1..8455
                     /organism="Streptomyces tsukubaensis NRRL18488"
                     /mol_type="genomic DNA"
                     /strain="NRRL18488"
                     /culture_collection="NRRL:18488"
                     /db_xref="taxon:1114943"
                     /label=ctg348
     CDS             193..1644
                     /locus_tag="STSU_11535"
                     /note="COG0753 Catalase"
                     /codon_start=1
                     /transl_table=11
                     /product="catalase"
                     /protein_id="EIF92263.1"
                     /db_xref="GI:385668995"
                     /translation="MSDTPYTTNNAGIPVESDEHSLSVGPDGPVLLQDHYLIEKMAQF
                     NRERVPERVVHAKGSGAYGFFEVTNDVSQFTKADLFQPGKRTEMLARFSTVAGEQGSP
                     DTWRDPRGFALKFYTEHGNYDMVGNNTPIFFVRDAQKFQDFIRSQKRHPATGLRNNDM
                     QWDFWTLSPETAHQVTWLMGDRGIPKSYRFMNGYSSHTYMWVNRGGERFWVKYHFKTD
                     QGVDFLTQAEADELAGSDADRHRRDLYESIASGNAPSWTLYMQIMPFDDAPGYRFNPF
                     DLTKVWPHGDYPLIEVGRMVLDRNPEDYFVHIEQAAFEPSNLVPGIGPSPDKMLLGRL
                     FSYPDTHRYRIGPNYAQLPPNRPHSVVASYAKDGPMRYEPANTARPYAPNSYGGPAAD
                     TAQFGEIAGWASAGEMVREAYALHPEDDDWGQAGTLVRKVLDDAARDRLVSNVSGHLK
                     DGVSRPVLDRAVQYWRNIDKTVGDRIAKEVNGG"
     gene            193..1644
                     /locus_tag="STSU_11535"
     CDS             complement(1759..4038)
                     /locus_tag="STSU_11540"
                     /note="COG0744 Membrane carboxypeptidase
                     (penicillin-binding protein)"
                     /codon_start=1
                     /transl_table=11
                     /product="Peptidoglycan glycosyltransferase"
                     /protein_id="EIF92264.1"
                     /db_xref="GI:385668996"
```

```
                     /translation="MGRAEERRARQRGARRGGKSGRTGIRRFFTWKKMLGTFLGLCLL
                     GMGAFAVIYMMVPVPAANAQAEMESNVYKYADGTVLARTGEVNREIIGLEELSEEVRQ
                     TFVAAENKSFYKDNGIDFKGTARGLLNTVSGKGKQGGSTITQQYVKNYYLNQDQTVSR
                     KLKELVIALKVDREKSKDQILAGYINTSYYGRGAYGIQAAAQAYYGIDASKLNVAQAA
                     YLAALLQAPHQYDWAVASPTGKKLVSDRWAYVLNNMVEMGKLDGSVRDAQKFPVPKAP
                     KAAPGMEGQTGYLVEAANAELARQGIGEEDIKAGGWTITLNIDRARQQELEAAVDKEL
                     ESKLDRKKDKKAATVQAGATSVDPTTGKVVALYGGVGATEHWLSNATRRDYQPASTFK
                     PVVLASALENEARTQSGDPISLNTVYDGTSKRPVVGSDTPFNPENEDDRDYGRQITVQ
                     RATNQSVNSVYAQMIVDVGPGKTKKTALDLGMRDGEGWPERPAMSLGTMGASTWDMAG
                     VYAGFANHGKKVTPSIVGSAEHRARKVALKDPVGGQVISRGTADTVTAAMQGVVKEGS
                     GRRAAGIYDAAGKTGTSENNRSAWFVGYTPTLVTSVALFGEKPDGTGQVTLTDTINQG
                     RANGGGMPARIWKAYTSDALSAADARKRFDLEVEEPARGEPAASPSDSPEPSPSRSEE
                     RREEETEDPRPSNTTSRPPVIDPPASQSTRPTTRPSPSGSQTDGTGPGGPGGEPGNPG
                     TGDPNNPRPQFRPPGSQGF"
gene                 complement(1759..4038)
                     /locus_tag="STSU_11540"
CDS                  4383..5324
                     /locus_tag="STSU_11545"
                     /note="COG0330 Membrane protease subunits,
                     stomatin/prohibitin homologs"
                     /codon_start=1
                     /transl_table=11
                     /product="hypothetical protein"
                     /protein_id="EIF92265.1"
                     /db_xref="GI:385668997"
                     /translation="MNTADTAADTAREQYDGVPAGVREFPARSIGGGLALLLGLAGFA
                     GGAAAVVAGAVAGSAAAQVGLIVGGILLALAAVVAMAGLNMVEPGQARVVQLFGRYRG
                     TVRTDGLRWVNPLTSREEISTRVRNHETAVLKVNDAYGNPIELAAVVVWRVEDTAQAL
                     FEVDDFLEFVSTQTESAVRQIAIEYPYDAHDENGLSLRGNAEEITEKLRVELQARAEA
                     AGVRIIESRFTHLAYAPEIASAMLQRQQAGAVVAARRQIVDGAVGMVEAALTRISEDG
                     FVELDSERKAAMVSNLLVVLCGDRAAQPVVNTGTLYQ"
gene                 4383..5324
                     /locus_tag="STSU_11545"
CDS                  5321..5593
                     /locus_tag="STSU_11550"
                     /note="COG4877 Uncharacterized protein conserved in
                     bacteria"
```

```
                /codon_start=1
                /transl_table=11
                /product="hypothetical protein"
                /protein_id="EIF92266.1"
                /db_xref="GI:385668998"
                /translation="MTPPPPPPPPRKQVLLRLDPAVYDALARWASDELRSANAQIEFL
                LRRALTEAGRLPGAAAPIRRRGRPPKAEPDGPGGPDTEEPTGGGAG"
gene            5321..5593
                /locus_tag="STSU_11550"
CDS             complement(5729..6193)
                /locus_tag="STSU_11555"
                /codon_start=1
                /transl_table=11
                /product="hypothetical protein"
                /protein_id="EIF92267.1"
                /db_xref="GI:385668999"
                /translation="MNDTTAAAPGTAADPGPDAAVRALDRLIGTWRVSGGAEGTVSYR
                GLEGGHFLLQDIALEQFGQPVTGVEVIGRLKEFGAEEPGEDIRSRYYDSRGNTFDYVY
                ELDGDTLTIWGGEKGSPAYYRATFSADGNTLSGAWVYPGGGGYDSVMTRVAV"
gene            complement(5729..6193)
                /locus_tag="STSU_11555"
CDS             complement(6323..7432)
                /locus_tag="STSU_11560"
                /EC_number="2.7.7.6"
                /note="COG1595 DNA-directed RNA polymerase specialized
                sigma subunit, sigma24 homolog"
                /codon_start=1
                /transl_table=11
                /product="RNA polymerase factor sigma-70"
                /protein_id="EIF92268.1"
                /db_xref="GI:385669000"
                /translation="MSDQGGGDSTQTAAPVTAPGGAPEPASRPGRSGLGEPSAETIRT
                GGEEVFAALAERYRHELRVHLYRMLGSFTDAEDLVQETLLKAWRRRETFEGRAGFRAW
                LYRIATNTALDFLGGPARNREVALAVDSAGSPVSSALAEVSWLQPYPDRLLDLAAPGT
                GEPHTAAIARETVELAFLAVIQHLPPRQRAVLILRDIAGWSAQETADALDMTVASVKS
                ALQRARTTLRGRLPERRSEWGAATEPSAAERSLLRRYMAASRDADLSALALLLREDAR
                QAMPPHRLVFDGRDAILDLWRPVLEGDTAWGEWRSVPYAVNRQPAAVSYVRRAGETLF
```

```
                TAVNVDVLTVVDGLIAEITTFDPGLLPGIAPTLAE"
     gene       complement(6323..7432)
                /locus_tag="STSU_11560"
     CDS        7582..8562
                /locus_tag="STSU_11565"
                /note="COG0583 Transcriptional regulator"
                /codon_start=1
                /transl_table=11
                /product="LysR family transcriptional regulator"
                /protein_id="EIF92269.1"
                /db_xref="GI:385669001"
                /translation="MATANRGKQPSLSQLRAFTAVAEHLHFRDAAAAIGMSQPALSGA
                VSALEETLGVQLVERTTRKVLLSPAGERLAARAKAVLDAVGELLEEAAAVRAPFTGVL
                RLGVIPTVAPYLLPDVLRLVHGTYPDLDLQVHEEQTSSLLDGLAAGRLDLLLLAVPLG
                VPGVTEIPLFDEDFVLVTPEGHPLGGRRDLSREVLRELPLLLLDEGHCLRDQALDVCR
                EAGRDERAPVTTTAAGLATLVQLVAGGLGVTLLPRTAVEVETGRGGLLTGCFADPAPA
                RRIALATRTGAARQGEFEEFARSLRGALAGLPVRLRTEAAAPETDSAPGA"
     gene       7582..8562
                /locus_tag="STSU_11565"
     source     8456..14355
                /organism="Streptomyces tsukubaensis NRRL18488"
                /mol_type="genomic DNA"
                /strain="NRRL18488"
                /culture_collection="NRRL:18488"
                /db_xref="taxon:1114943"
                /label=ctg_349
     CDS        complement(8618..10981)
                /locus_tag="STSU_11570"
                /codon_start=1
                /transl_table=11
                /product="hypothetical protein"
                /protein_id="EIF92257.1"
                /db_xref="GI:385668988"
                /translation="MTVRTWARDLALGIRFGASGGREGWTRTLLTALGVGLGVAMLLL
                ASSVPGMIEQRDDRADRRTPAEIKQIGSPEIPPSARTVLWDGVETLYRDRVVKGTLLR
                ADGADPVRPPGVAAFPKPGEMVVSPALGELLRSSEGKLLGERYGGKVIGTIGDEGVLG
                SRELYFYLGSADLTQESGSTRIGSFDAAARTSPPLNPILVVLLVLVCVVLLVPVAVFV
```

```
                ATAVRFGGERRDRRLAALRLVGADTRTVHRIAGGEALFGALLGLAFGIGLFFAVRPLA
                GYIGLYDLSAFPSDVTPAPLLGALIVVAVPVSAVAVTLLALRTVVIEPLGVVRHSATR
                QRRLWWRLLPPALGIALLLTGRLGSGDEDVAVFPIAAGAILVLIGLTALLPWLVDAVV
                GRLRGGSVPWQLAVRRLQLSSDAAARAVSGIMVAVAGAIALQMLFSAVEGDFVRETEQ
                DLARAQLSVTADVTGAGSAERVVTDLRGTEGVRTVTGVTQAQLYSPARTPEEVAAGHG
                EIITLTVADCPTLGELAELPSCKDGDAFVVVGRDTETGALIRQSAALGKPYLTGAPRE
                STAGGKPVKAWSLPEGAPTVTARADAADNEHPGIFATPGAVDLRGFPAASAVAMVSVD
                KGVPDAREHVRNTVARIDPGAHVWQLTNVEEDEQFAKVRIALLIGSLATMALIAASML
                VSQIEQLRERRKLLSVLVAFGTRRATIAWSVLWQTAVPVVIGTVLAIAGGLGLGLVML
                ELVGARVADWWGFLPIAGAGIAVIVVVTVLSLPPLYRMMRPDGLRTE"
gene            complement(8618..10981)
                /locus_tag="STSU_11570"
CDS             complement(10978..11664)
                /locus_tag="STSU_11575"
                /note="COG1136 ABC-type antimicrobial peptide transport
                system, ATPase component"
                /codon_start=1
                /transl_table=11
                /product="ABC transporter ATP-binding protein"
                /protein_id="EIF92258.1"
                /db_xref="GI:385668989"
                /translation="MTTEGALLVAEDLRKAYGPTPALDGAHFSVHAGEVVAVMGPSGS
                GKSTLLHCLAGIVPPDSGSIRYQGRELASLSDKERSKLRRTAFGFVFQFGQLVPELTC
                TENVALPLRLAGTGRKEAETAARQWMERLEVDDIGHKRPGQISGGQGQRVAVARSLVT
                SPRVLFADEPTGALDSLNGERVMELFTEAARSTGAAVVLVTHEARVAAYSDREVVVRD
                GKTRGLEYVA"
gene            complement(10978..11664)
                /locus_tag="STSU_11575"
CDS             complement(11661..12185)
                /locus_tag="STSU_11580"
                /note="COG1695 Predicted transcriptional regulators"
                /codon_start=1
                /transl_table=11
                /product="PadR-family transcriptional regulator"
                /protein_id="EIF92259.1"
                /db_xref="GI:385668990"
                /translation="MSIGHTLLGLLESGPRHGYDLKRAFDEKFGHDKPLHYGQVYSTM
```

```
                SRLLKNGLVEVDGVEPGGGPERKRYAITDAGITDVDAWLARPEAPEPYLQSVLYTKVV
                LALLTGRGAAELLDGQRSEHLRMMRILTDRKRRGDFADQLICDHALFHLEADLRWLEL
                TAARLDRLAREVGA"
     gene       complement(11661..12185)
                /locus_tag="STSU_11580"
     CDS        12452..13006
                /locus_tag="STSU_11585"
                /note="COG0450 Peroxiredoxin"
                /codon_start=1
                /transl_table=11
                /product="alkyl hydroperoxide reductase"
                /protein_id="EIF92260.1"
                /db_xref="GI:385668991"
                /translation="MLTVGDQFPTFELTACVSLESGKEFEVINHKSYEGKWKVVFAWP
                KDFTFVCPTEIAAFGKLNDEFADRDAQVLGFSGDSEFVHHAWRKDHADLRDLPFPMLA
                DSKHELMRDLGIEGADGFAQRAVFIVDPNNEIQFTMVTAGSVGRNPKEVLRVLDALQT
                DELCPCNWTKGEDTLDAATLLAGE"
     gene       12452..13006
                /locus_tag="STSU_11585"
     CDS        13010..13546
                /locus_tag="STSU_11590"
                /note="COG2128 Uncharacterized conserved protein"
                /codon_start=1
                /transl_table=11
                /product="alkyl hydroperoxide reductase AhpD"
                /protein_id="EIF92261.1"
                /db_xref="GI:385668992"
                /translation="MSLDALKSAIPDYAKDLKLNLGSVIGNNDKLTPQQLWGTVLATA
                IASRSPIVLRELEPEAKAQLSPEAYNAAKAAAAIMAMNNVFYRTRHLLSDPEYGTLRA
                GLRMNVIGNPGVEKVDFELWSLAVSAVNGCGQCLDSHEQVLRKAGVDRETVQEAFKIA
                SVVQAVGTTLESEAALAG"
     gene       13010..13546
                /locus_tag="STSU_11590"
     CDS        complement(13618..14232)
                /locus_tag="STSU_11595"
                /codon_start=1
                /transl_table=11
```

```
                     /product="hypothetical protein"
                     /protein_id="EIF92262.1"
                     /db_xref="GI:385668993"
                     /translation="MAASLLWAGGLFAYQATTGGDPDPGPYRAVEDLCAPAAMKELTA
                     VLGKVSSRDPEQFAHPAMDEAQCSLVLGADPAVSSGLTSVDPATGVARKLSIGVRISY
                     TLHRRTDPGPEFDARILARAKRMHIEAEPVPGVGERAYRTAEGQDQVLHVLDGQAVLE
                     LQVYSYWTGEQDAPPPSLEGVEESRGALEADARALLEELRGGRG"
     gene            complement(13618..14232)
                     /locus_tag="STSU_11595"
ORIGIN
        1 CTAGCTAGCT AGCGGCGGAG GGGCGCGGCA CCGTGGCGGG TCGCCGCGCC CGTGGATGCC
       61 CGCGCCGTCG CGCCGTACGC CCGACCGGCC GCAGCGGAGT GGCGAGCAGT TGCCGACAAG
      121 GTGTCGGCGG CGTTGACTGA GGTACACGAC GCCTGTAGCG ACCCAACCAT GTCTCCCGGC
      181 GGGAGGACGC TCGTGTCCGA TACCCCCTAC ACCACCAACA ACGCCGGCAT TCCGGTGGAG
      241 AGCGACGAGC ACTCCCTCTC CGTCGGGCCC GACGGCCCGG TCCTGCTCCA GGACCACTAC
      301 CTGATCGAGA AGATGGCCCA GTTCAATCGC GAACGGGTCC CCGAGCGGGT GGTGCACGCC
      361 AAGGGTTCGG GTGCGTACGG CTTCTTCGAG GTGACGAACG ACGTCAGCCA GTTCACCAAG
      421 GCCGACCTCT TCCAGCCCGG GAAGCGCACC GAGATGCTGG CCCGGTTCTC CACGGTCGCG
      481 GGTGAGCAGG GCTCCCCCGA CACCTGGCGC GATCCGCGCG GTTTCGCCCT GAAGTTCTAC
      541 ACCGAGCACG GCAACTACGA CATGGTCGGC AACAACACGC CGATCTTCTT CGTCCGGGAC
      601 GCGCAGAAGT TCCAGGACTT CATCCGCTCG CAGAAGCGCC ATCCGGCGAC CGGGCTGCGC
      661 AACAACGACA TGCAGTGGGA CTTCTGGACC CTCTCCCCCG AGACGGCGCA CCAGGTGACC
      721 TGGCTGATGG GCGACCGCGG CATCCCGAAG TCGTACCGCT TCATGAACGG CTACAGCTCC
      781 CACACCTATA TGTGGGTCAA CCGCGGCGGC GAGCGGTTCT GGGTGAAGTA CCACTTCAAG
      841 ACCGACCAGG GCGTGGACTT CCTCACCCAG GCCGAGGCGG ACGAGCTGGC CGGGTCGGAC
      901 GCGGACCGGC ACCGCCGGGA TCTGTACGAG TCGATCGCGT CGGGGAACGC CCCGAGCTGG
      961 ACGCTGTACA TGCAGATCAT GCCGTTCGAC GATGCGCCGG GCTACCGCTT CAACCCCTTC
     1021 GACCTGACGA AGGTGTGGCC GCACGGCGAC TATCCGCTGA TCGAAGTCGG CCGGATGGTG
     1081 CTGGACCGCA ATCCGGAGGA CTACTTCGTC CATATCGAAC AGGCCGCGTT CGAGCCGTCG
     1141 AACCTGGTGC CGGGCATCGG GCCGTCGCCG GACAAGATGC TCCTCGGGCG GCTGTTCTCG
     1201 TACCCGGACA CCCACCGGTA CCGGATCGGC CCGAACTATG CGCAGTTGCC GCCGAACCGG
     1261 CCGCACTCGG TGGTCGCCTC GTACGCCAAG GACGGGCCGA TGCGGTACGA GCCGGCGAAC
     1321 ACGGCGCGGC CCTATGCGCC CAACTCCTAC GGCGGGCCCG CGGCGGACAC CGCGCAGTTC
     1381 GGCGAGATCG CGGGCTGGGC GAGCGCGGGC GAGATGGTCC GGGAGGCGTA CGCGCTGCAC
     1441 CCGGAGGACG ACGACTGGGG GCAGGCGGGC ACCCTGGTGC GGAAGGTGCT CGACGACGCC
     1501 GCCCGTGACC GGCTGGTGTC GAACGTGTCC GGGCATCTGA AGGACGGGGT GTCCCGGCCG
     1561 GTGCTCGACC GGGCGGTCCA GTACTGGCGC AATATCGACA AGACGGTCGG CGACCGGATC
```

```
1621 GCCAAGGAGG TCAACGGCGG CTGAGCCCGG AGCACCGGGC GGTACGGCGG CCGGAAACGG
1681 CGGTGCCCGC GGCGCCTCCC CCGAAGGGAG CGCGCCGCGG GCACCGCCGT ACCGGCATAT
1741 CGGCTGGGGA CGCCGGGCTC AGAAACCCTG GGAGCCGGGC GGCCGGAACT GCGGGCGGGG
1801 GTTGTTCGGA TCGCCCGTAC CCGGGTTCCC GGGTTCGCCG CCCGGACCGC CCGGTCCGGT
1861 GCCGTCGGTC TGACTCCCGG ACGGCGAGGG GCGTGTGGTG GGGCGGGTGC TCTGCGAGGC
1921 GGGCGGGTCG ATCACCGGCG GCCGGGACGT GGTGTTCGAC GGCCGCGGGT CCTCCGTCTC
1981 CTCCTCGCGC CGCTCCTCGC TCCGGCTGGG GGACGGCTCC GGGGAGTCCG ACGGGGAGGC
2041 GGCGGGCTCG CCGCGGGCGG GTTCCTCGAC CTCCAGGTCG AACCGCTTGC GGGCGTCGGC
2101 CGCGCTCAGC GCGTCGGAGG TGTACGCCTT CCAGATCCGG GCCGGCATAC CGCCGCCGTT
2161 GGCCCGGCCC TGGTTGATGG TGTCGGTGAG GGTGACCTGG CCGGTGCCGT CCGGCTTCTC
2221 GCCGAACAGG GCGACCGAGG TGACCAGGGT GGGCGTATAG CCGACGAACC AGGCGGAACG
2281 GTTGTTCTCG GAGGTGCCGG TCTTGCCCGC CGCGTCGTAG ATGCCCGCGG CCCGGCGGCC
2341 GGAGCCCTCC TTCACAACGC CCTGCATGGC GGCGGTGACG GTGTCGGCCG TACCGCGCGA
2401 GATCACCTGG CCGCCGACGG GGTCCTTCAG CGCGACCTTG CGGGCCCGGT GTTCGGCGGA
2461 GCCCACGATG GAGGGGGTGA CCTTCTTGCC GTGGTTCGCG AATCCGGCGT ACACCCCGGC
2521 CATGTCCCAG GTGGAGGCGC CCATGGTGCC CAGCGACATG GCGGGGCGCT CGGGCCAGCC
2581 TTCGCCGTCG CGCATCCCGA GGTCGAGTGC GGTCTTCTTG GTCTTCCCGG GCCCGACGTC
2641 GACGATCATC TGCGCATAGA CGGAGTTGAC CGACTGGTTG GTCGCCCGCT GCACGGTGAT
2701 CTGCCTGCCG TAGTCCCGGT CGTCCTCGTT CTCCGGGTTG AACGGGGTGT CGCTGCCGAC
2761 GACCGGCCGC TTGCTGGTGC CGTCGTAGAC GGTGTTGAGG CTGATCGGAT CGCCGCTCTG
2821 GGTCCTGGCC TCGTTCTCCA GGGCGGAGGC GAGCACCACC GGCTTGAAGG TGGACGCGGG
2881 CTGGTAGTCG CGGCGGGTGG CGTTGGACAG CCAGTGCTCG GTGGCTCCGA CCCCGCCGTA
2941 CAGCGCGACG ACCTTGCCGG TCGTGGGATC CACGGAGGTG GCCCCGGCCT GGACGGTCGC
3001 GGCCTTCTTG TCCTTCTTCC GGTCGAGCTT GGACTCCAGC TCCTTGTCGA CCGCCGCCTC
3061 CAGCTCCTGC TGCCGGGCGC GGTCGATGTT GAGGGTGATC GTCCAGCCGC CGGCCTTGAT
3121 GTCCTCCTCG CCGATGCCCT GGCGGGCGAG TTCCGCGTTG GCGGCCTCGA CGAGATAGCC
3181 GGTCTGGCCC TCCATACCGG GGGCGGCCTT CGGCGCCTTC GGTACGGGGA ACTTCTGGGC
3241 GTCGCGGACG GACCCGTCGA GCTTGCCCAT CTCGACCATG TTGTTCAGTA CGTAGGCCCA
3301 GCGGTCGGAC ACCAGCTTCT TGCCGGTCGG AGAGGCCACG GCCCAGTCGT ACTGGTGGGG
3361 GGCCTGGAGC AGGGCGGCGA GATAGGCGGC CTGGGCGACG TTCAGCTTCG ACGCGTCGAT
3421 GCCGTAGTAC GCCTGGGCGG CGGCCTGGAT TCCGTAGGCG CCGCGGCCGT AGTAGCTGGT
3481 GTTGATATAG CCCGCGAGGA TCTGGTCCTT GGACTTCTCG CGGTCGACCT TGAGGGCGAT
3541 CACCAGTTCC TTCAGCTTGC GGCTGACCGT CTGGTCCTGG TTGAGGTAGT AGTTCTTGAC
3601 GTACTGCTGG GTGATGGTCG AACCACCCTG CTTGCCCTTG CCGGAGACGG TGTTCAGCAG
3661 ACCCCGGGCG GTGCCCTTGA AGTCGATGCC GTTGTCCTTG TAGAAGCTCT TGTTCTCGGC
3721 GGCGACGAAG GTCTGGCGGA CCTCCTCCGA CAGCTCCTCC AGACCGATGA TCTCGCGGTT
3781 GACCTCACCG GTGCGGGCCA GGACGGTCCC GTCGGCGTAC TTGTAGACGT TGGACTCCAT
```

3841 CTCGGCCTGC GCATTCGCCG CCGGAACCGG AACCATCATG TAGATCACCG CGAAGGCGCC
3901 CATACCGAGC AGGCAGAGAC CGAGGAAGGT GCCCAGCATC TTCTTCCAGG TGAAGAAGCG
3961 GCGTATGCCC GTGCGCCCGC TCTTCCCGCC CCGGCGCGCA CCGCGCTGCC GGGCCCGTCG
4021 TTCCTCGGCT CGGCCCATCG CCCGCCCCGC TCCGCTCTTC CCCGAAAGGT CTGTGTTCTT
4081 GTCGGTCTGG TCGGTCCTGG TTGGTTCTGC TTGATCCAGG TTGGTCCAGG TTGGTCCAGG
4141 TGGACTCTGC TTGGTTCAGG TCGCCGCCGA CCAAAGCGGC TTAGAAAACT AACACCGTTC
4201 GCCCTGAAAA ATTCGGACTA GTACGACGAA TCCGGACGTG AGAATCAGCA CCCCGTCCAC
4261 AGAAGACGAC TCGGCTCTTG CCCAAACGGT TGCCGCATCC ATTAATGTGT AATCACATTG
4321 CTAGCAGCGA GCCGTAGCGG TGGTGAACTC CGCCACCGTC GGCCCTGATC CCTGGGGGGC
4381 CCATGAACAC CGCCGACACC GCAGCCGACA CCGCAAGAGA GCAGTACGAC GGGGTTCCGG
4441 CCGGGGTACG GGAGTTCCCG GCCCGCAGCA TCGGCGGCGG GCTGGCCCTG CTGCTCGGCC
4501 TGGCCGGCTT CGCCGGGGGC GCGGCAGCCG TCGTGGCCGG AGCGGTCGCC GGGTCCGCCG
4561 CGGCCCAGGT CGGCCTGATC GTCGGAGGCA TCCTGCTGGC CCTCGCCGCC GTCGTCGCGA
4621 TGGCCGGGCT GAACATGGTG GAGCCCGGCC AGGCCCGGGT GGTCCAGCTG TTCGGCCGCT
4681 ACCGGGGTAC GGTCCGCACC GACGGGCTGC GCTGGGTCAA TCCGCTGACC TCGCGCGAGG
4741 AGATCTCCAC CCGGGTCCGC AACCACGAGA CCGCGGTCCT GAAGGTCAAC GACGCCTACG
4801 GCAATCCGAT CGAACTGGCC GCCGTGGTGG TGTGGCGGGT CGAGGACACC GCGCAGGCCC
4861 TGTTCGAAGT CGACGACTTC CTGGAGTTCG TCTCCACCCA GACGGAGTCC GCGGTGCGCC
4921 AGATCGCCAT CGAGTACCCC TACGACGCCC ATGACGAGAA CGGCCTCTCG CTGCGCGGGA
4981 ACGCCGAGGA GATCACCGAG AAGCTCCGCG TCGAACTACA GGCCCGCGCC GAGGCGGCGG
5041 GGGTGCGGAT CATCGAGTCG CGCTTCACGC ATCTCGCGTA CGCCCCCGAA ATCGCCTCGG
5101 CGATGCTCCA GCGCCAGCAG GCCGGTGCGG TGGTGGCGGC ACGCCGGCAG ATCGTGGACG
5161 GGGCGGTCGG TATGGTCGAG GCCGCACTGA CCCGGATCAG CGAGGACGGG TTCGTCGAAC
5221 TGGACTCCGA GCGGAAGGCC GCGATGGTCT CGAATCTGCT GGTCGTGCTC TGCGGCGACC
5281 GCGCCGCCCA GCCCGTCGTC AACACCGGCA CGCTCTACCA GTGACGCCCC CGCCGCCCCC
5341 GCCGCCGCCA CGCAAGCAGG TCCTGCTCCG GCTGGACCCC GCGGTCTACG ACGCCCTGGC
5401 CCGCTGGGCC TCGGACGAAC TGCGCAGCGC CAACGCCCAG ATCGAGTTCC TGCTGCGGCG
5461 GGCGCTGACG GAGGCGGGGC GGCTGCCGGG CGCCGCCGCG CCGATCCGCC GGAGGGGCCG
5521 CCCGCCGAAG GCCGAGCCGG ACGGCCCCGG GGGTCCGGAC ACGGAGGAGC CCACGGGCGG
5581 CGGGGCGGGC TGAGCCCGTA CCGGACACCC GTCGAGAGCG GTTCACCTCA TGACGGAGAC
5641 GATCACGGGG TGATCGGGAC TCCGGGTCCG TGGGAGCCGT GCTGCGGCTC CCACGGGACG
5701 TCCGGGCCGC CGTCGCTCCG GCCGGTGTTC ATACCGCGAC CCGGGTCATG ACGGAGTCGT
5761 AGCCGCCGCC CCCGGGGTAG ACCCAGGCGC CGGAGAGCGT ATTGCCGTCG GCGCTGAAAG
5821 TCGCCCGGTA GTAGGCCGGG GACCCCTTCT CGCCGCCCCA GATGGTGAGG GTGTCGCCGT
5881 CGAGTTCGTA GACGTAGTCG AAGGTGTTGC CCCGGCTGTC GTAGTAGCGG GAGCGGATGT
5941 CCTCGCCGGG CTCCTCGGCG CCGAACTCCT TGAGCCGCCC GATGACCTCG ACACCGGTGA
6001 CGGGCTGCCC GAACTGCTCC AGGGCGATGT CCTGGAGGAG GAAGTGGCCG CCCTCCAGCC

6061 CGCGGTAGCT GACAGTGCCC TCGGCGCCGC CGCTGACCCG CCAGGTGCCG ATCAGCCTGT
6121 CCAGCGCGCG CACGGCGGCG TCGGGGCCGG GGTCCGCGGC GGTCCCGGGG GCGGCTGCGG
6181 TGGTGTCGTT CATGGTTCTG CGTCCTTTGC CGTGGTGGTG AGGGTGCGCG GCCGTACGGC
6241 GGGCTCGTGC CGCGCTGCCG CGGTGGTGCC CGTATGACGG GCCGCTCACG GGAAAGGAAT
6301 CGGCGGACTG TTGTGACCCG GGTCACTCCG CCAGGGTGGG GGCGATTCCG GGCAGCAGTC
6361 CGGGGTCGAA GGTGGTGATC TCGGCGATCA GACCGTCCAC GACCGTCAGT ACGTCGACGT
6421 TGACCGCGGT GAAGAGGGTC TCGCCCGCCC GGCGGACATA GCTCACGGCC GCGGGCTGCC
6481 GGTTCACCGC GTACGGCACC GAACGCCACT CGCCCCACGC CGTATCGCCC TCCAGCACCG
6541 GACGCCAGAG GTCGAGGATC GCGTCCCGCC CGTCGAAGAC CAGCCGGTGC GGGGGCATGG
6601 CCTGGCGGGC GTCCTCGCGC AGCAGCAGGG CGAGTGCGGA CAGGTCCGCA TCCCGGGACG
6661 CGGCCATATA GCGCCGGAGC AGCGACCGCT CGGCGGCGCT GGGCTCGGTG GCCGCACCCC
6721 ACTCCGAGCG CCGCTCGGGG AGCCGGCCGC GGAGCGTGGT ACGGGCCCGC TGGAGGGCGC
6781 TCTTGACCGA GGCGACGGTC ATATCGAGGG CGTCCGCGGT CTCCTGGGCG GACCAGCCGG
6841 CGATATCGCG GAGGATCAGG ACCGCGCGCT GGCGGGGCGG CAGATGCTGG ATCACGGCGA
6901 GGAAGGCGAG TTCGACGGTC TCCCGGGCGA TCGCGGCGGT GTGCGGTTCG CCGGTGCCGG
6961 GGGCGGCGAG GTCGAGCAGC CGGTCGGGGT AGGGCTGGAG CCAGCTGACC TCCGCGAGGG
7021 CCGAGGAGAC GGGGGATCCG GCGCTGTCGA CGGCGAGCGC CACCTCGCGG TTCCGGGCGG
7081 GTCCGCCGAG GAAGTCGAGC GCCGTGTTGG TGGCGATCCG GTACAGCCAG GCCCGGAAGC
7141 CGGCGCGCCC TTCGAAGGTC TCGCGCCGCC GCCAGGCCTT CAGCAGGGTC TCCTGGACCA
7201 GGTCCTCGGC GTCGGTGAAG GAGCCGAGCA TCCGGTAGAG GTGCACGCGC AGCTCGTGGC
7261 GGTAGCGCTC GGCGAGCGCG GCGAAGACCT CTTCCCCGCC GGTGCGGATC GTCTCGGCGG
7321 ACGGCTCGCC CAGGCCGCTG CGCCCGGGGC GGGACGCCGG TTCCGGGGCT CCGCCGGGCG
7381 CCGTCACCGG CGCCGCCGTC TGCGTGCTGT CTCCGCCACC CTGGTCGCTC ATACCTCTCT
7441 TCGTATCAGC AGCACCACCG GGAAACACCT GCTCCGGTGA TCACGGCCGC CCCGGGCACC
7501 GGGACCGGCA GTCGGCACCC CTCGCCGACC CCATGGGAAC AACCGATTAA CATCAAGGGG
7561 AACGATAGGG AGAAGGAATC AATGGCTACG GCGAACCGGG GCAAGCAGCC CAGCCTGTCG
7621 CAACTGCGGG CCTTCACTGC GGTGGCCGAG CATCTGCACT TCCGGGACGC AGCCGCGGCC
7681 ATCGGCATGA GTCAGCCCGC GCTCTCCGGG GCCGTATCGG CGCTGGAGGA GACCCTCGGG
7741 GTGCAGCTCG TGGAGCGGAC CACCCGGAAG GTGCTGCTCT CCCCCGCGGG CGAGCGGCTC
7801 GCGGCCCGCG CCAAGGCGGT CCTGGACGCC GTCGGGGAGC TGCTGGAGGA GGCGGCGGCG
7861 GTACGGGCCC CGTTCACCGG CGTCCTGCGG CTCGGCGTAA TCCCGACGGT CGCCCCCTAT
7921 CTGCTGCCGG ATGTGCTGAG GCTGGTCCAC GGCACCTATC CCGACCTCGA CCTCCAGGTC
7981 CACGAGGAAC AGACCTCGTC GCTGCTGGAC GGGCTGGCGG CCGGACGGCT CGACCTGCTG
8041 CTGCTCGCGG TGCCGCTGGG GGTGCCGGGG GTCACCGAGA TCCCGCTGTT CGACGAGGAC
8101 TTCGTCCTGG TGACCCCGGA GGGCCATCCC CTCGGCGGGC GCCGCGATCT CTCCCGCGAG
8161 GTGCTGCGCG AACTGCCGCT GCTGCTCCTC GACGAGGGGC ACTGCCTGCG CGACCAGGCC
8221 CTGGACGTCT GCCGGGAGGC GGGGCGCGAC GAGCGGGCGC CGGTGACGAC GACCGCCGCG

```
 8281 GGTCTGGCGA CGCTGGTGCA GCTGGTGGCG GGCGGCCTCG GGGTGACGCT GCTGCCGCGG
 8341 ACCGCGGTCG AGGTGGAGAC CGGCCGGGGC GGGCTGCTGA CCGGCTGCTT CGCGGACCCC
 8401 GCGCCGGCGC GCCGGATCGC CCTGGCGACC CGCACCGGGG CGGCCCGCCA GGGCGAGTTC
 8461 GAGGAGTTCG CGCGGTCGCT GCGGGGCGCG CTGGCGGGCC TGCCGGTACG GCTGCGCACC
 8521 GAGGCCGCGG CTCCGGAGAC GGATTCCGCC CCCGGAGCCT GACCTTCCGG CGCAGTGCCG
 8581 CCCGATGCCA TTCCGCGCTG TTCGCGGCTA CTCGGTGCTA CTCGGTGCGG AGGCCGTCCG
 8641 GGCGCATCAT CCGGTAGAGC GGCGGCAGGC TGAGCACCGT CACCACCACG ATCACCGCGA
 8701 TGCCCGCCCC GGCGATCGGC AGGAAGCCCC ACCAGTCGGC CACCCGCGCC CCGACCAGTT
 8761 CGAGCATCAC CAGGCCGAGA CCGAGACCGC CGGCGATCGC CAGGACCGTG CCGATGACCA
 8821 CCGGGACCGC GGTCTGCCAC AGGACCGACC AGGCGATGGT GGCTCGGCGG GTGCCGAAGG
 8881 CGACGAGCAC CGAGAGCAGC TTGCGCCGTT CCCGCAGCTG TTCGATCTGG GAGACCAGCA
 8941 TGGAGGCGGC GATCAGCGCC ATGGTCGCGA GGGAACCGAT CAGCAGCGCA ATGCGGACTT
 9001 TGGCGAACTG CTCGTCCTCC TCGACGTTGG TCAGCTGCCA GACGTGCGCG CCGGGGTCGA
 9061 TCCGGGCCAC GGTGTTGCGG ACGTGCTCCC GCGCGTCGGG CACCCCCTTG TCGACGGAGA
 9121 CCATCGCCAC GGCGCTCGCG GCGGGGAAAC CCCGGAGGTC GACGGCGCCC GGGGTGGCGA
 9181 AGATCCCGGG GTGTTCGTTG TCCGCCGCGT CGGCCCGGGC GGTCACGGTC GGCGCGCCCT
 9241 CGGGCAGGCT CCAGGCCTTG ACGGGCTTGC CGCCGGCGGT GCTCTCCCGG GGGGCTCCCG
 9301 TCAGATACGG CTTGCCGAGG GCGGCGGACT GCCTGATCAG CGCGCCCGTT TCGGTGTCCC
 9361 TGCCGACGAC GACGAACGCG TCGCCGTCCT TGCAGGAGGG GAGCTCGGCG AGTTCACCCA
 9421 GGGTGGGGCA GTCGGCGACG GTCAGCGTGA TGATCTCGCC GTGACCGGCC GCCACCTCCT
 9481 CCGGGGTGCG GGCGGGGCTG TAGAGCTGCG CCTGGGTCAC TCCGGTGACC GTGCGGACCC
 9541 CTTCCGTCCC CCGGAGGTCG GTGACCACCC GCTCGGCGGA CCCGGCACCG GTGACGTCCG
 9601 CCGTGACGCT CAGCTGGGCC CGGGCCAGGT CCTGCTCGGT CTCGCGGACG AAGTCCCCCT
 9661 CGACCGCGGA GAACAGCATC TGGAGCGCGA TCGCCCCGGC GACCGCGACC ATGATGCCGC
 9721 TGACTGCCCG GGCGGCCGCA TCGCTGCTCA GCTGCAGCCG CCGGACCGCC AGTTGCCAGG
 9781 GGACGGAACC GCCGCGCAGC CGTCCGACGA CGGCGTCGAC CAGCCACGGC AGCAGGGCCG
 9841 TGAGCCCGAT GAGTACCAGG ATCGCCCCGG CCGCTATCGG GAAGACCGCG ACGTCCTCGT
 9901 CGCCGGAGCC GAGCCGGCCG GTGAGCAGCA GGGCGATTCC GAGAGCCGGG GGCAGCAGCC
 9961 GCCACCACAG ACGGCGCTGC CTGGTGGCGG AGTGCCGTAC GACGCCGAGC GGTTCGATCA
10021 CGACCGTACG CAGGGCGAGA AGGGTGACCG CGACGGCGGA GACGGGTACG GCGACCACGA
10081 TCAGCGCGCC GAGCAGCGGC GCCGGTGTCA CATCGGAGGG GAAGGCGCTC AGGTCGTACA
10141 GTCCGATGTA CCCGGCGAGG GGCCGGACCG CGAAGAACAG GCCGATGCCG AAGGCGAGTC
10201 CGAGCAGGGC GCCGAAGAGC GCCTCGCCGC CCGCGATCCG GTGGACCGTC CGGGTGTCGG
10261 CGCCGACCAG GCGGAGTGCG GCGAGCCGCC GGTCGCGCCG CTCGCCGCCG AAGCGGACGG
10321 CGGTGGCGAC GAAGACGGCC ACCGGCACCA GCAGCACCAC GCAGACCAGT ACGAGGAGGA
10381 CGACGAGGAT GGGGTTGAGC GGTGGGGACG TTCTGGCGGC GGCGTCGAAG CTGCCGATCC
10441 GGGTGCTGCC GGACTCCTGG GTGAGGTCCG CGCTGCCGAG GTAGAAGTAC AGCTCGCGCG
```

10501 AGCCGAGGAC GCCCTCGTCG CCGATGGTGC CGATGACCTT TCCCCCGTAG CGCTCGCCGA
10561 GGAGCTTGCC CTCGGAGGAG CGCAGGAGTT CGCCGAGGGC GGGTGAGACG ACCATCTCGC
10621 CGGGCTTCGG GAAGGCGGCG ACACCGGGCG GCCGTACGGG GTCGGCGCCG TCCGCCCGCA
10681 GCAGGGTGCC CTTGACGACC CGGTCGCGGT AGAGGGTTTC GACGCCGTCC CAGAGCACGG
10741 TGCGGGCACT GGGCGGAATC TCCGGCGAGC CGATCTGCTT GATCTCCGCC GGGGTCCGGC
10801 GGTCGGCGCG GTCGTCCCGC TGTTCGATCA TGCCGGGGAC GGAGGACGCC AGCAGCAGCA
10861 TGGCGACGCC GAGGCCGACG CCGAGTGCGG TGAGGAGGGT ACGGGTCCAG CCCTCGCGCC
10921 CGCCGGAGGC GCCGAAGCGG ATACCGAGGG CGAGGTCGCG GGCCCAGGTG CGGACGGTCA
10981 TGCGACGTAC TCCAGGCCCC GGGTCTTTCC GTCGCGGACG ACGACTTCCC GGTCCGAGTA
11041 GGCCGCGACC CGGGCCTCGT GGGTGACGAG GACGACGGCC GCGCCGGTCG ACCGGGCGGC
11101 TTCGGTGAAC AGCTCCATCA CCCGCTCACC GTTGAGGGAG TCGAGGGCGC CGGTGGGTTC
11161 GTCGGCGAAG AGCACCCGGG GCGAGGTGAC CAGGGAGCGG GCGACGGCGA CCCGCTGCCC
11221 CTGCCCGCCG GATATCTGGC CGGGGCGCTT GTGCCCGATG TCGTCGACTT CCAGCCGCTC
11281 CATCCACTGC CGGGCGGCCG TCTCGGCCTC CTTCCGGCCG GTCCCGGCGA GGCGGAGCGG
11341 CAGGGCGACG TTCTCCGTGC AGGTCAGCTC GGGCACCAGC TGGCCGAACT GGAAGACGAA
11401 GCCGAAGGCG GTACGGCGGA GTTTGCTGCG CTCCTTGTCG GAGAGCGAGG CCAGTTCGCG
11461 GCCCTGGTAG CGGATGGATC CGGAGTCGGG CGGCACGATG CCGGCGAGGC AGTGCAGCAG
11521 GGTCGACTTG CCGGAGCCGG AGGGCCCCAT GACAGCGACG ACCTCACCGG CGTGGACGGA
11581 GAAGTGGGCG CCGTCCAGGG CGGGGGTGGG GCCGTACGCC TTGCGCAGGT CCTCGGCGAC
11641 GAGCAGGGCT CCTTCGGTGG TCATGCGCCT ACCTCCCGGG CGAGACGGTC CAGCCGGGCC
11701 GCGGTCAGTT CCAGCCAGCG CAGATCGGCC TCCAGATGGA ACAGCGCGTG GTCGCAGATC
11761 AGCTGGTCGG CGAAGTCGCC GCGGCGCTTG CGGTCGGTCA GGATCCGCAT CATCCGCAGA
11821 TGCTCGGAGC GCTGACCGTC GAGCAGCTCC GCCGCGCCTC GTCCGGTGAG CAGGGCGAGG
11881 ACGACCTTGG TGTAGAGCAC GGACTGGAGG TACGGCTCCG GGGCCTCGGG CCGGGCGAGC
11941 CACGCGTCGA CGTCGGTGAT CCCGGCGTCG GTGATCGCGT ACCGCTTCCG CTCGGGTCCG
12001 CCGCCGGGCT CGACGCCGTC GACCTCGACG AGTCCGTTCT TCAGGAGCCG GGACATGGTC
12061 GAGTAGACCT GCCCGTAGTG GAGGGGCTTG TCGTGGCCGA ACTTCTCGTC GAAGGCACGT
12121 TTGAGGTCGT AGCCGTGACG AGGGCCGGAT TCGAGGAGCC CGAGAAGGGT GTGACCGATG
12181 GACATGGTCC GACTATACAC ACGAGGTATA CATGGAGTGC ATACGCAGGT GGGAGCAGTA
12241 CGCCCGCCGA GCACCCGCAC AACGCCCGAC GCCTGGCAGA ATCGGCACGG CCGCCGCACC
12301 CGGTCCGCAC AGCGCGGAGC GCCCGCCCGG AAGAGTGCCC TCCGATTGAT TGAAGGATCG
12361 GATCACACTG ACCTGATTGA TCAATTTCAC CGGCGATCGC GGGTATGACA GGGTGGATTT
12421 GTCCAACCCC TCAGCACCAT GGAGTGACAC TGTGCTCACT GTCGGCGACC AGTTCCCCAC
12481 CTTCGAACTG ACGGCCTGCG TCTCGCTCGA GAGCGGCAAG GAGTTCGAGG TCATCAACCA
12541 CAAGTCCTAC GAGGGCAAGT GGAAGGTCGT CTTCGCCTGG CCGAAGGACT TCACCTTCGT
12601 CTGCCCGACC GAGATCGCCG CCTTCGGCAA GCTGAACGAC GAGTTCGCCG ACCGCGACGC
12661 CCAGGTCCTC GGCTTCTCCG GCGACTCGGA GTTCGTCCAC CACGCCTGGC GCAAGGACCA

```
12721 CGCCGACCTG CGTGACCTGC CCTTCCCGAT GCTGGCCGAC TCCAAGCACG AGCTGATGCG
12781 CGACCTCGGC ATCGAGGGCG CCGACGGCTT CGCCCAGCGC GCCGTCTTCA TCGTCGACCC
12841 GAACAACGAG ATCCAGTTCA CGATGGTGAC CGCGGGCTCC GTCGGCCGTA ACCCGAAGGA
12901 GGTCCTCCGG GTCCTCGACG CCCTCCAGAC GGACGAGCTG TGCCCGTGCA ACTGGACCAA
12961 GGGCGAGGAC ACCCTGGACG CCGCCACGCT GCTGGCCGGT GAGTGACCCG TGTCGCTCGA
13021 CGCGCTGAAG TCCGCCATAC CGGACTACGC CAAGGACCTG AAGCTCAACC TGGGCTCGGT
13081 CATCGGCAAC AACGACAAGC TCACCCCGCA GCAGCTCTGG GGCACCGTGC TGGCCACCGC
13141 GATCGCCTCG CGCAGCCCGA TCGTCCTGCG TGAGCTGGAG CCGGAGGCCA AGGCGCAGCT
13201 GTCGCCCGAG GCGTACAACG CCGCCAAGGC CGCCGCCGCG ATCATGGCGA TGAACAACGT
13261 CTTCTACCGC ACCCGGCACC TGCTCTCCGA CCCGGAGTAC GGCACGCTCC GCGCCGGTCT
13321 GCGGATGAAC GTCATCGGCA ACCCGGGCGT GGAGAAGGTC GACTTCGAGC TCTGGTCGCT
13381 CGCCGTCTCC GCCGTCAACG GCTGCGGCCA GTGCCTCGAC TCGCACGAGC AGGTGCTCCG
13441 CAAGGCGGGC GTGGACCGCG AGACGGTCCA GGAGGCGTTC AAGATCGCCT CCGTCGTCCA
13501 GGCCGTGGGC ACCACGCTGG AGTCCGAGGC CGCGCTCGCG GGCTGACCGC CGGAACGCAT
13561 GGCAGGGCCC GTACGGCACA CGTCGTACGG GCCCTGTTCA TACCCGGGGG TACGGGATCA
13621 GCCCCGGCCG CCGCGCAACT CCTCCAGCAG CGCCCGCGCA TCCGCCTCCA GGGCGCCCCG
13681 GCTCTCCTCG ACCCCCTCCA GGGACGGCGG CGGCGCGTCC TGCTCGCCCG TCCAGTAGGA
13741 GTAGACCTGC AGCTCCAGTA CGGCCTGCCC GTCGAGGACA TGGAGCACCT GGTCCTGGCC
13801 CTCGGCCGTA CGGTACGCGC GCTCACCGAC CCCCGGCACC GGCTCGGCCT CGATGTGCAT
13861 CCGCTTCGCC CGGGCCAGGA TCCGTGCGTC GAACTCGGGC CCCGGATCGG TCCTGCGGTG
13921 CAGCGTGTAG CTGATCCGGA CCCCGATGCT CAGCTTGCGC GCCACTCCCG TCGCCGGATC
13981 GACGGACGTC AGCCCGCTGC TGACCGCCGG ATCCGCGCCG AGGACGAGGC TGCACTGCGC
14041 CTCGTCCATC GCCGGGTGCG CGAACTGCTC GGGGTCCCGC GACGACACCT TGCCGAGGAC
14101 GGCGGTCAGC TCCTTCATGG CGGCCGGTGC GCACAGATCC TCGACCGCGC GGTACGGGCC
14161 GGGATCCGGG TCCCCGCCGG TGGTGGCCTG GTACGCGAAC AGCCCGCCCG CCCAGAGCAG
14221 CGAAGCCGCC ACCGCTCCGG CGACACCCCA CTGCCAGGGC TTCAGCGGCG GCCGGCGCCC
14281 CTCGCGGCCC GACTCCAGCC GCTCGCCCCG GCCGCCGTCC GGGTCGCCGT CCCGGTCGCG
14341 GTGCTAGCTA GCTAG
//
```

APPENDIX II

Table A. 1 –OxyR$_{STSUK}$ orthologues (30 best BLASTp hits) in *Streptomyces*.

Strain	E value	Acession ID
S. clavuligerus	7e-165	WP_003955233
Streptomyces sp.CNT372	2e-163	WP_018845711
S. venezuelae ATCC 10712	3e-162	WP_015035888
S. scopuliridis	6e-161	WP_030352997
Streptomyces sp. NRRL S-1824	1e-160	WP_030969361
S. flavochromogenes	1e-160	WP_030320547
S. exfoliatus	5e-160	WP_030548723
S. pristinaespiralis ATCC 25486	1e-158	WP_005312619
Streptomyces sp. SirexAA-E	3e-158	WP_014048080
Streptomyces sp. AW19M42	8e-158	WP_024492147
Streptomyces sp. NRRL S-15	1e-157	WP_031091729
S. griseus XylebKG-1	1e-157	WP_003966617
Streptomyces sp. MspMP-M5	2e-157	WP_018536445
S. roseosporus NRRL 11379	2e-157	EFE77248
S. griseus subsp. *griseus* NBRC 13350	4e-157	WP_012379247
Streptomyces sp. NRRL S-118	4e-157	WP_031069144
S. pratensis ATCC 33331	7e-157	WP_014154321
Streptomyces sp. FxanaC1	1e-156	WP_026169576
S. auratus AGR0001	2e-156	WP_006603398
Streptomyces sp. NRRL F-5135	2e-156	WP_030749851
S. albulus CCRC 11814	7e-156	WP_016570300
S. flavidovirens	1e-154	WP_028813085
Streptomyces sp. NRRL B-1347	2e-154	WP_030668274
Streptomyces sp. CNB091	3e-154	WP_026290224
S. ruber	4e-154	WP_030358043
S. albulus NK660	1e-153	AIA05660
S. decoyicus NRRL ISP-5087	2e-153	WP_030084283
S. mediolani NRRL WC-3934	5e-153	WP_030808275
S. anulatus NRRL B-2873	7e-153	WP_030579994
S. catenulae NRRL B-2342	1e-152	WP_030287970